CHARACTERIZATION OF $GABA_A$ RECEPTOR SUBUNIT MUTATIONS ASSOCIATED WITH EPILEPTIC ENCEPHALOPATHIES

By

Dingding Shen

Dissertation

Submitted to the Faculty of the

Graduate School of Vanderbilt University

In partial fulfillment of the requirements

for the degree of

DOCTOR OF PHILOSOPHY

in

Neuroscience

October 31, 2017

Nashville, Tennessee

Approved:

Douglas G. McMahon, Ph.D.

Kevin C. Ess, M.D., Ph.D.

Martin J. Gallagher, M.D., Ph.D.

Robert L. Macdonald, M.D., Ph.D.

To my parents, for their endless support

and

To my husband, who fulfills my life

Table of Contents

List of Figures

Page

List of Tables

Page

List of Abbreviations

3'-UTR: three prime untranslated region

aCGH: array comparative genomic hybridization

ACTH: adrenocorticotropic hormone

ADHD: attention-deficit/hyperactivity disorder

AED: antiepileptic drugs

APC: adenomatous polyposis coli gene

ARX: aristaless related homeobox gene

ASA: accessible surface area

BAC: bacterial artificial chromosome

CAE: childhood absence epilepsy

CF: cystic fibrosis

CNS: central nervous system

CNV: copy number variation

CRH: corticotrophin-releasing hormone

DMD: Duchenne muscular dystrophy

DRG: dorsal root ganglion

ECD: extracellular domain

EE: epileptic encephalopathy

EEG: electroencephalography

EOEE: early-onset epileptic encephalopathy

EPSP: excitatory postsynaptic potential

ER: endoplasmic reticulum

ERAD: ER-associated degradation

FS: febrile seizures

GABA: γ-aminobutyric acid

$GABA_ARs$: type-A GABA receptors

GABARAP: $GABA_AR$ associated protein

GABR: $GABA_A$ receptor gene

GAT: GABA transporter

GE: genetic epilepsy

GEF: guanine nucleotide exchange factor

GEFS+: generalized epilepsy with febrile seizures plus

GGE: genetic generalized epilepsy syndromes

GTCS: generalized tonic-clonic seizures

HAP: Huntington-associated protein

HEK: human embryonic kidney

IGE: idiopathic generalized epilepsies

IBE: international bureau for epilepsy

ILAE: international league against epilepsy

IPSC: inhibitory post-synaptic current

IS: infantile spasms

JME: juvenile myoclonic epilepsy

LGIC: ligand-gated ion channel

LGS: Lennox-Gastaut syndrome

LTD: long term depression

LTP: long term potentiation

MAE: myoclonic-astatic epilepsy

MRI: magnetic resonance imaging

NGS: next-generation sequencing technology

NMD: nonsense-mediated mRNA decay

NMDA: N-Methyl-D-Aspartate

PEI: polyethylenimine

PSD: postsynaptic density

PTC: premature translation-termination codon

PTZ: pentylenetetrazol

SNP: single nucleotide polymorphism

SUDEP: sudden unexpected death in epilepsy

SWDs: spike-wave-discharges

TTX: tetrodotoxin

UPR: unfolded protein response

VB: ventrobasal

WES: whole exome sequencing

WGS: whole genome sequencing

Chapter 1: Introduction

Seizures and epilepsy

1. Definitions of epileptic seizure and epilepsy

Epilepsy is one of the most common neurologic disorders, affecting more than 65 million people worldwide and 2.2 million people in the United states (*1*). Approximately 4% of individuals will develop epilepsy during their lifetime (*2*). Although epilepsy may affect people of all ages, it has a bimodal onset, most often occurring in childhood and older adulthood. Epilepsy is associated with a wide spectrum of devastating neuropsychiatric comorbidities including depression, bipolar disorder, attention-deficit/hyperactivity disorder (ADHD), movement disorders and cognitive deficits (*3*). Compared to the general population, individuals with epilepsy are at substantially increased risk for premature death, and sudden unexpected death in epilepsy (SUDEP) is the most frequent cause of this mortality. In addition, individuals with epilepsy suffer from social discrimination (*4*). Given the relatively high prevalence and adverse effects on quality of life, the epilepsies represent a substantial health and economic burden on patients, their families, the community, and society as a whole (*5*).

In 2005, the International League Against Epilepsy (ILAE) and the International Bureau for Epilepsy (IBE) proposed a definition for an epileptic seizure as "a transient occurrence of signs and/or symptoms due to abnormal, excessive or synchronous neuronal activity in the brain" (*6*). Epilepsy is a pathological state characterized by recurrent, unprovoked epileptic seizures (*7*). Epilepsy syndromes imply a persistent epileptogenic abnormality of the brain itself that is able to spontaneously generate paroxysmal activity, independent of any acute insult or condition (*8*). The traditional definition of epilepsy requires at least two unprovoked seizures. In 2014, an ILAE task force revised the definition of epilepsy as a disease of the brain defined by any of the following conditions: 1) At least two unprovoked (or reflex) seizures occurring >24 h apart; 2) one unprovoked (or reflex) seizure and a probability of further seizures similar to the general

recurrence risk (at least 60%) after two unprovoked seizures, occurring over the next 10 years; 3) diagnosis of an epilepsy syndrome (*9*).

2. Classification of seizures and epilepsies

Classification of seizures and epilepsies plays a critical role not only in guiding clinical management, but also in epilepsy research and in development of new treatments for this disorder. Recently, the ILAE released a 2017 version of the classification of epileptic seizures (*10, 11*) and epilepsies (*12*) in an effort to have concepts and terminology that reflected the advances in understanding and knowledge of these disorders.

The 2017 seizure classification is based mostly on signs and symptoms of seizures (*13*) and presents both basic and expanded versions. The basic version maintained the overall frame work of the 1981 seizure classification (*14*) and the revision in 2010 (*15*), with minor modifications (Figure 1-1). Based on the type of onset, seizures are first divided into three categories: focal onset (formerly called partial), generalized onset, and unknown onset seizures (*10, 11*). Focal onset epileptic seizures are defined as "originating within networks limited to one hemisphere". A seizure can begin focally and later generalize. For focal seizures, level of awareness is the next (optional) classifier. Focal aware or impaired awareness seizures may be further classified into motor or non-motor onset subdivisions. Generalized onset seizures are conceptualized as "originating at some point within, and rapidly engaging, bilaterally distributed networks", which do not necessarily include the entire cortex and can be asymmetrical (*15, 16*). Generalized seizures are divided into motor and nonmotor (absence) seizures. Level of consciousness is not a classifier for generalized seizures since awareness is almost always impaired. The third category of unknown onset may later be reclassified into focal or generalized categories with further information. In this regard, unknown onset is a placeholder rather than a characteristic of the seizure. It is useful to describe certain commonly encountered entities (*13*). The most important seizures of unknown onset include tonic-clonic seizures, epileptic spasms, and nonmotor

seizures with behavioral arrest. The expanded seizure classification is built on the framework of the basic classification with more details (Figure 1-2).

In addition to the new classification of seizures, the ILAE also released a new classification of the epilepsies (*12*). The 1989 classification (*17*) has been used widely for research and clinical management. Revisions to these classifications have been recommended based on advances made in the last 3 decades, and a proposal was published in 2010 (*15*). The new 2017 classification of the epilepsies provides a framework of three levels (Figure 1-3). The classification process starts with diagnosis of the seizure type, which is outlined in the accompanying paper mentioned above (*11*). In some cases, it may not possible for the clinician to progress past the classification of seizure type, either due to inadequate information available or limited clinical testing resources. Otherwise, the next step is to assume that the patient has a diagnosis of epilepsy based on the 2014 definition (*9*) and determine the epilepsy type. The epilepsy types include focal, generalized, combined generalized and focal, and also an unknown epilepsy group. As a new category in the 2017 classification, the "combined generalized and focal" type was added to capture patients who have both types of seizures, such as those with Dravet syndrome and Lennox-Gastaut syndrome. The third step in classification is a diagnosis of the epilepsy syndrome, which refers to a cluster of features incorporating seizure types, EEG, and imaging features that tend to occur together. Certain syndromes are associated with distinct age-related feature, comorbidities and EEG or imaging findings, as well as specific implications regarding etiology, prognosis and treatment. Identification of epilepsy syndromes is a rapidly growing field and there has been no official classification of epilepsy syndromes by ILAE. Idiopathic generalized epilepsies (IGE) is a well-recognized subgroup of generalized epilepsies, but the clinician has the option of using "genetic generalized epilepsy (GGE)" when appropriate.

It is recommended that as soon as patients present with their first epileptic seizure, clinicians should begin considering its etiology. In accordance, the revised classification includes six etiologic subgroups with

implications for treatment: structural (genetic or acquired or both), genetic, infectious, metabolic, immune, as well as an unknown group (Figure 1-3). More than one etiological category can apply to a patient's epilepsy, and the clinical importance of each may vary depending on the circumstance.

The ILAE 2017 seizure and epilepsy classification will not be a final classification and some aspects of the new classification still need to be clarified (*18*). New classification schemes will continue to evolve as knowledge about epilepsy pathophysiology and genetics grows.

Genetic epilepsy syndromes

In approximately 20–30% of epilepsy cases, acquired factors are thought to contribute to epileptogenesis, such as trauma, viral infection, stroke, tumor, inborn brain malformations, etc. (*9*). However, the remaining 70–80 % of cases have no obvious causes and are usually believed to have a genetic basis, referred to as genetic epilepsies (GEs) (*19*). There is substantial evidence for a genetic contribution in epilepsies through twin and family studies. Twin studies demonstrated that the concordance of epilepsy in monozygotic twins exceeds that in dizygotic twins (*20, 21*). Epidemiologic studies have estimated that the cumulative incidence of epilepsy to age 40 was 4.7% among relatives of all probands, and risk was increased 3.3-fold (95% confidence interval 2.75–5.99) compared with population incidence (*22*).

The concept of a GE is that it results directly from a known or presumed genetic mutation in which seizures are a core symptom of the disorder (*12*). GEs consist of multiple epilepsy syndromes that vary in severity from the relatively benign febrile seizures (FS) and childhood absence epilepsy (CAE) to the more severe generalized epilepsy with febrile seizures (GEFS+). A subpopulation of GEs is associated with severe recurrent seizures and neurodevelopmental impairment that has been referred to as an epileptic encephalopathy (EE). It should be noted that there is no widely accepted list of GE syndromes. Some

syndromes can be produced by either genetic or acquired factors. For example, the majority (60%-75%) of cases of Infantile Spasms (IS) result from acquired factors such as hypoxic ischemic encephalopathies, cerebral malformations, or neonatal infections. However, the remaining 25%-40% have no known acquired source and their syndrome is thought to have a genetic etiology.

1. Genetic architecture of epilepsies - the range of variants predisposing to human epilepsy

Epilepsy genetics can be conceptualized under two broad headings: monogenic epilepsies in which a single variant of large effect (either inherited or *de novo*) is considered causative and complex genetic epilepsies in which a presumed combinatorial effect of multiple susceptibility variants is thought to underlie the disease (*23*).

1) Size

Genetic risk factors predisposing to human epilepsies may span a continuum of scale, ranging from changes in single base pairs to chromosomal rearrangements (*24*). Between both extremes are copy number variations (CNVs), which are small deletions or duplications of segments of DNA larger than 1 kB (typically *de novo*). CNVs in the form of microdeletions or microduplications are important molecular causes of GE, with ~10% of studied individuals with complex epilepsy phenotypes showing a causative or potentially contributing CNV (*25, 26*).

2) Inheritance pattern

Genetic risk factors for GEs may occur in familial epilepsies in large pedigrees that can be inherited in a dominant or recessive fashion or can arise *de novo* in the affected patient (Figure 1-4).

Monogenic epilepsies or Mendelian epilepsies, which are often “monogenic, simple, and rare” epilepsies, account for about 2% of all epilepsy cases. Monogenic epilepsies may show variable penetrance and variable

degrees of severity of the epilepsy. For dominant transmission, a genetic change in a single copy of the gene is sufficient to cause epilepsy through a dominant mechanism (such as gain of function, dominant negative, or haploinsufficiency). This is the case in many familial epilepsy syndromes such as GEFS+ that are associated with mutations in *GABRG2* or *SCN1A*. Recessive epilepsies are caused by mutations in both disease alleles. They tend to be severe and progressive, often associated with deficiency of an enzyme or cofactor. The above examples affect the autosomes. However, GEs can be transmitted through the X chromosome in a dominant (e.g., *CDLK5*) or recessive (e.g., *ARX*) fashion, displaying a variety of sex-related phenotypic patterns. Mutations in the mitochondria can follow autosomal recessive or maternal inheritance (*27*). An increasing number of epilepsies are found to be due to *de novo* mutations. In these cases, the mutation is found in the affected proband, but is absent in both unaffected parents. These mutations can be conceptualized as dominant mutations, which probably occur in the gamete or early in embryogenesis. However, in most cases, there is no transmission in families, as the patients are severely affected and do not have children. In the severe EEs, there is an increasing focus on *de novo* mutations, as recent studies suggest that this mechanism explains a significant number of cases (*28*).

However, the vast majority of GEs are complex genetic diseases exhibiting a polygenic inheritance, in which both common and rare variants of susceptibility genes, possibly in combination with environmental factors contribute to the penetrance and expressivity in affected individuals. This genetic complexity is consistent with the report that many deleterious mutations in ion channel genes can be found in healthy individuals without epilepsy (*29*). The identification of genetic risk factors in complex GEs occurs through association studies, and the recruitment of large patient cohorts having sufficient power for reliable results has been a long-standing weakness of the field (*30*). Attempts to identify variants that confer susceptibility to complex epilepsy using GWAS have identified few contributory variants, most likely because of small sample sizes in the epilepsy GWAS to date (*31*). Thus, the complex inheritance of GEs is poorly understood at present (*24*).

3) Human Epilepsy (hEP) Genes – the synaptopathy era

Human GEs have been associated with mutations of many genes, referred to as human epilepsy (hEP) genes. In the majority of the monogenic epilepsies, the mutated genes encode ion channel subunits (voltage-gated and ligand-gated ion channels) that determine neuronal excitability and whose gain or loss of function result in abnormal generation and propagation of action potentials. This led to the "channelopathy" concept, which postulates ion channel dysfunction as the key pathological mechanism underlying GEs (*32, 33*). Mutations of ion channel subunit genes that either increase excitatory or reduce inhibitory neurotransmission would produce neuronal hyperexcitability, thereby predisposing individuals harboring the mutant gene to experience seizures.

In addition to ion channels, recent genetic studies identified additional epilepsy-related synaptic proteins, such as K^+–Cl^- cotransporter KCC2 (*SLC12A5*) (*34*), synaptic Ras-GTPase-activating protein (*SYNGAP1) (35)*, and synaptic adhesion molecule Caspr2 *(CNTNAP2) (36)*. This accumulating evidence has expanded the epileptogenesis of GEs from channelopathy to synaptopathy (*37*) .

I will summarize mutations in inhibitory $GABA_A$ receptor subunit genes that have been associated with GEs later in this thesis.

2. Genetic approaches for mutation discovery

Genetic testing in epilepsy patients is important for precise genetic diagnosis that can guide clinical management, providing accurate prognosis and direct genetic counseling for families (*38*). More importantly, clinical discovery of epilepsy mutations can inform basic research regarding mechanisms of epileptogenesis that will direct precision medicine based on an individual's underlying genetic etiology in the future (*39*). Fortunately, the ability to identify genetic causes of epilepsy is improving as testing approaches are becoming more sophisticated and more widely available (*40*). A summary of these methods is given in Table 1-1.

1) Targeted single gene sequencing

Sanger sequencing has been the dominant gene sequencing technology for the past 30 years and is still the gold standard for validating genetic variants. In addition, there are a few epilepsy syndromes with very characteristic phenotypes, which could trigger testing a specific gene. Under these conditions, candidate gene testing is the most direct route and may be instrumental and prudent due to issues related to treatment or prognosis (*41*). The best example is testing for *SCN1A* mutations. In Dravet syndrome, over 80% of cases are associated with mutations in *SCN1A*, the gene encoding the α1 subunit of the voltage-gated sodium channel (*42, 43*). Recurrent prolonged febrile hemiconvulsive or generalized seizures in the first year of life should prompt consideration of Dravet syndrome (*44*). Testing for a mutation in *SCN1A* could provide definitive confirmation before the child's plateau in development in the second year of life and inform counseling on prognosis and risks to siblings (*21*). Definitive diagnosis avoids further unnecessary investigation in these severely ill children, allows optimization of antiepileptic therapy such as avoiding carbamazepine and lamotrigine (*45*), and thus minimizes negative impact on development. However, in a small proportion of Dravet syndrome patients, no pathogenic variant can be found in SCN1A, and there may be mutations in other genes including *GABRG2(46, 47)*, *GABRA1(48), STXB1(48)*, and *HCN1(48)* as well as other genes. Screening of one gene after another at one time is labor-intensive and time consuming. The genetic heterogeneity of epilepsy makes Sanger-sequencing for individual genes often impractical as hundreds of epilepsy genes have been already identified (*49*) .

2) Chromosomal analysis

Molecular karyotyping approaches, such as array comparative genomic hybridization (aCGH) techniques, have been informative as a first-line test in identifying common CNVs associated with various forms of epilepsy including EEs (*50*). Use of aCGH is indicated in drug-resistant epilepsy, especially when associated with congenital anomalies or developmental delay. Depending on case series and criteria for inclusion, about

12% of people with complex epilepsy might have a CNV considered relevant, making aCGH important and relevant in current practice (*51*).

3) Next generation sequencing (NGS)

In contrast to Sanger sequencing, in which single DNA fragments are sequenced, next generation sequencing (NGS) allows for rapid parallel sequencing of large numbers of DNA segments that are broken into smaller pieces, sequenced, and then realigned and analyzed computationally. Faster and less expensive, NGS can be used to sequence a set of candidate genes (targeted epilepsy gene panel analysis), the exome consisting of the coding regions (whole exome sequencing, WES) and/or the entire genome including its noncoding regions (whole genome sequencing, WGS). During the last decade, the advent of NGS technologies has advanced the identifications of genetic factors in GEs (*52, 53*).

i. Epilepsy Gene Panels

Given incomplete penetrance, variable expressivity, multigenic interactions, and lack of an informative family history, targeted single gene sequencing is not practical in most cases. These issues drove development of epilepsy-related gene panels, replacing the Sanger single-gene approach with a parallel-sequencing approach of various targeted genes simultaneously. The epilepsy gene panel can either be commercially developed or custom-designed. The composition of custom-designed gene panels varies significantly, both in the number of genes and in the choice of candidate genes, according to whether they are developed to investigate broader or more specific epilepsy syndromes (*54*). Gene panels have been increasingly used in diagnostic settings for testing a genetic etiology in various epilepsies (*53, 55*). In 2012, Lemke et al. demonstrated for the first time the utility of gene panel study by using a panel of 265 genes on a cohort of 33 index patients with various types of epilepsies (*56*). Using a NGS-based approach, the authors identified presumed disease-causing mutations in 16 of 33 patients, demonstrating that gene panel approaches are useful diagnostic tools. Another report in 2014 documented a diagnostic yield of 47% of a 67 epilepsy gene-sequencing platform (*57*). The

genotype–phenotype interpretation is a key step in the NGS analysis and guidelines have been published that provide uniform criteria for interpreting sequence variants (*58*). However, panels have their limitations; they include only the selected candidate genes. There may be a gene not yet suspected to be related to a particular type of epilepsy that is actually the cause of the syndrome in question; if that gene is not included in the epilepsy panel, a genetic cause will be missed (*51*).

ii. WES and WGS

The clinical application of WES has recently emerged as a powerful and unbiased method to investigate the genetic basis of rare and genetically heterogeneous sporadic epilepsies not amenable to traditional genetic investigation techniques (*59*). The advantage of WES is that this technique does not predefine the set of genes to be studied, enabling the identification of a multitude of new confirmed or putative epilepsy candidate genes (*23*). The application of WES in parent–offspring trios has been successful in identifying *de novo* mutations in a large fraction of patients with sporadic EEs, and the advance in technology has made it possible to undertake large-scale WES studies that allow for a global assessment of the genetic architecture of these conditions (*53*). These studies demonstrate the great genetic heterogeneity of EEs, with recurrent mutations occurring in only a minority of identified genes. For instance, a large-scale WES study led by the EPI4K study group identified 329 *de novo* mutations in a cohort of 264 trios with EEs. However, in only 9 genes, *de novo* mutations were observed in at least two probands (*60*). In addition, exome sequencing studies have expanded the phenotypic spectrum associated with some of the well-known hEP genes. For instance, *KNCQ2* mutations that are most commonly associated with benign familial myoclonic epilepsy (*61*) were subsequently identified in patients with Ohtahara syndrome using WES (*62*). Ongoing studies are also starting to concentrate on WGS, because this may identify possible contribution of mutations in noncoding DNA to the occurrence of epilepsy. WES or WGS is unquestionably a powerful tool for dissecting the genetic basis of GEs not completely tractable to previous gene discovery strategies. However, WES and WGS are currently only available on a clinical basis in a very few centers. We anticipate that they are likely

to become more widely available and supersede candidate and panel testing in the future, with major impacts on epilepsy management (*63*).

$GABA_A$ receptors

γ-Aminobutyric acid (GABA) is the predominant inhibitory neurotransmitter in the adult mammalian central nervous system (CNS). After release from GABAergic presynaptic terminals, GABA exerts its inhibitory effects via two classes of receptors with distinct electrophysiological and pharmacological properties: ionotropic $GABA_A$ and metabotropic $GABA_B$ receptors. $GABA_A$ receptors ($GABA_ARs$) are fast-activating chloride ion channels, while $GABA_B$ receptors produce slow and prolonged inhibitory responses (*64*). As members of the Cys-loop super family of ligand-gated ion channels (LGICs) that includes nicotinic acetylcholine (nACh), glycine, and 5-hydroxytryptamine type 3 ($5\text{-}HT_3$) receptors (*65*), $GABA_ARs$ mediate fast phasic inhibition at postsynaptic sites and also tonic inhibition by producing currents in peri- and extra-synaptic locations (*66*). Widely distributed throughout the CNS, $GABA_ARs$ play a major role in maintaining excitation/inhibition balance and are essential for virtually all aspects of brain function including sleep–wakefulness, cognition, sensory and motor processing, emotions, etc. (*67*). In addition, it is now well recognized that $GABA_AR$-mediated synaptic transmission regulates neuronal development and maturation during ontogenesis and adult neurogenesis (*68*). As such, $GABA_ARs$ serve as important targets in the treatment of a wide range of neurological and psychiatric disorders (e.g. epilepsy, sleep disorders, and anxiety) (*69, 70*) and for the induction and maintenance of general anesthesia (*71*).

1. Structure of $GABA_ARs$

1) Topology and function domains of $GABA_AR$ subunits

Functional Cys-loop receptor ion channels require assembly of homologous channel subunit proteins pseudo-symmetrically into a pentameric complex. $GABA_AR$ heteropentamers are assembled from a large family of subunit subtypes that confer diverse functional properties but share a common topological organization

(Figure 1-5). Mature subunits are approximately 450 amino acids in length and are comprised of a ~200 residue N-terminal extracellular ligand-binding domain and four α-helical transmembrane domains (M1–M4) of approximately 20 amino acids in length. The highly conserved M2 segment contributes to the formation of the pore region of the $GABA_AR$ channel. Between M3 and M4 there is a large cytoplasmic loop serving as the site for various post-translational modulations through interactions with many receptor-associated proteins. These proteins have been shown to play important roles in regulating receptor trafficking and synaptic clustering (*72, 73*).

In addition to major structural elements of $GABA_ARs$, a more detailed description of receptor structure is necessary to understand the mechanisms of ligand binding and channel gating. Although not gated by GABA, the only available three-dimensional crystal structure of a $GABA_AR$, the human β3 subunit homopentamer, was crystallized with a bound synthetic agonist benzamidine in 2014 (*74*), providing important insights into its architectural elements. Each extracellular domain (ECD) is composed of an α-helix followed by ten β-strands folded into a curled β-sandwich. These β-strands contain six major loops that are important for GABA binding. Loops A-C are located on the "principal" or "(+)" side of subunits, while loops D-F are located on the "complementary" or "(-)" side. The GABA binding site is located at the interface between the principal side of the β subunit and the complementary side of the α subunit. However, conformational variability cannot be studied based on this engineered $GABA_AR$ since only the structure of a single conformation is available. $GABA_ARs$ share a similar structural basis for ligand binding-channel gating coupling mechanism with the glutamate-gated chloride channel (GluCL) and the glycine receptor (GlyR) α1 subunit. Thus, recent x-ray structure of the GluCL (*75*) and cryoelectron microscopy studies of GlyR (*76*) have demonstrated many features of structural rearrangements during conformational transitions. GABA binding stabilizes a quaternary twisting/un-blooming reorganization of the ECD triggering $GABA_AR$ channel activation. The M2-M3 loop acts as a key coupling-element. It interacts with the bottom of the ECD interface and undergoes a large outward translation that is concerted with gate opening (*77*) .

2) Subunit composition and heterogeneity of $GABA_A$Rs

$GABA_A$Rs are remarkable for their diversity among neurotransmitter receptors. To date, eight families with nineteen $GABA_A$R subunit subtypes (α1-6, β1-3, γ1-3, δ, ε, θ, π, and ρ1-3) have been cloned and sequenced from mammalian CNS. Given the notion that the $GABA_A$R is a heteropentamer and the diversity of known subunits subtypes, there is a potential for an enormous number of unique $GABA_A$Rs if one assumes random assembly. However, only a limited number of subunit combinations are in fact expressed on the neuronal plasma membrane and form functional receptors (*78*). The overwhelming majority of native receptors are composed of ternary subunit combinations (*79*), and the most abundantly expressed are the α1β2γ2 receptors, which account for about 40% of all $GABA_A$Rs (*80*). αβ receptors are the most prominent binary receptors in which the γ subunit is replaced by a β subunit (*81*). Receptors comprised of four and even five different subunits have also been reported, such as α1α5 subunit-containing receptors (*82*). In addition, β3 and ρ1 subunits may form homopentamers as well as heteropentamers (*83, 84*). For synaptic αβγ receptors, a stoichiometry of 2α:2β:1γ with a β-α-γ-β-α counterclockwise configuration when viewed from the synaptic cleft has been proposed (*85*). It is generally accepted that the β-α-β-α portion of the pentamers is conserved within ternary receptors, whereas the γ subunit position could sometimes be replaced by other subunit subtypes such as δ or ε. In addition to canonical β-α-γ/δ-β-α receptors, receptors with other subunit arrangements including β-α-γ/δ-α-α receptors at lower levels of γ2/δ expression, and β-α-γ/δ-α-γ/δ receptors at higher levels of expression have been proposed (*86*). However, the existence of these α1β2γ2 unconventional receptors in neurons is controversial due to their low expression levels in oocytes and unusual functional properties (*87*).

Although not all subunit combinations can form functional receptors, there is consensus that more than twenty different $GABA_A$R subtypes still exist in CNS neurons (*88*). $GABA_A$R subtypes represent distinct entities with unique spatial and temporal expression patterns in the mammalian CNS (*89*), and with specific physiological and pharmacological profiles including GABA affinity, kinetics, conductance, probability of

channel opening, allosteric modulation, and interaction with modulatory proteins. For instance, while $\alpha_{1\text{-}3}\beta\gamma$ receptors are localized to synapses where they produce large extensively desensitizing currents and mediate phasic inhibition, α_{4-6} and δ subunit-containing receptors are mainly localized to peri- and extrasynaptic compartments where they produce small, slowly desensitizing currents and mediate tonic inhibition (*66*).

2. Biogenesis of $GABA_A$Rs

Neurons maintain and modulate their inhibitory tone by regulating $GABA_A$R biosynthesis and cell surface expression, endocytosis, and recycling. Under normal physiological conditions, the CNS tunes GABAergic networks by exerting strict spatial and temporal control over the number and composition of $GABA_A$R receptors. In addition, with CNS pathology, $GABA_A$R expression is often altered.

As with all membrane proteins, once translated $GABA_A$R subunit proteins enter the secretory pathway in the endoplasmic reticulum (ER), resulting in processing of individual immature subunits to immature multimeric ion channels. These immature ion channels are trafficked through the Golgi apparatus to become mature pentameric ion channels on the surface membrane of neurons (Figure 1-6). All the mechanisms contributing to $GABA_A$R biogenesis and intracellular trafficking, including post-translational modification of the receptors, are critical for the modulation of inhibitory synaptic plasticity (*90*).

1) Transcription and translation of $GABA_A$R subunit genes

Human $GABA_A$R subunit messenger RNAs (mRNAs) contain 9-10 coding exons (9-13 total exons), and several subunits undergo alternative splicing, further increasing the potential for heterogeneity. For example, the $\gamma2$ subunit exists in short ($\gamma2S$) and long ($\gamma2L$) forms, which differ by an eight-amino acid insertion in the intracellular domain (*91*). Additionally, $\alpha3$ subunits undergo developmentally regulated adenosine-to-inosine RNA editing (*92, 93*).

The CNS modulates $GABA_AR$ mRNA expression in different brain regions and cell types throughout development and in different physiological and pathological conditions including epilepsy (*94*). High levels of variability in the expression of mRNAs encoding the 19 $GABA_AR$ subunits has been found to be under the control of multiple gene regulatory mechanisms (*95*). In the first step of biogenesis, multiexon $GABA_AR$ subunit genes are transcribed in the nucleus to produce premature mRNAs that then interact with the mRNA-splicing machinery to remove introns and to produce mature mRNAs that are translocated to the ER.

2) $GABA_AR$ assembly in the endoplasmic reticulum (ER)

All immature $GABA_AR$ subunits are predicted to contain signal peptides (*96*). During the translation of $GABA_AR$ subunit mRNA, the signal peptides target the nascent polypeptides to the ER, where they fold and oligomerize in a process that depends heavily upon luminal molecular chaperones such as immunoglobulin heavy-chain binding protein (BiP) and calnexin (*96*). There have been reports of multiple amino acid sequences that are important for subunit oligomerization and receptor assembly. Such sequences were found primarily in in the large N-terminal domain of α, β and γ subunits (*97*). $GABA_AR$ assembly in the ER is a rather slow and inefficient process (*98*). The subunits exit the ER and enter the secretory pathway only when they are properly folded and assembled, whereas the misfolded and unoligomerized subunits are rapidly targeted for ER-associated degradation (*99*).

3) Exit from the ER and traffic through the Golgi apparatus

When successfully folded and assembled, the immature $GABA_AR$ subunits are trafficked from the ER to the Golgi apparatus where ER core glycans are trimmed and mature glycans are attached, whereas the subunits inside the ER remain core-glycosylated or unglycosylated (*100*). ER-to-Golgi translocation can be facilitated by the ubiquitin-like protein Plic-1 (proteins that link integrin-associated protein with the cytoskeleton), which binds directly to intracellular loops of α and β subunits. Plic-1 inhibits ubiquitin-dependent degradation of subunits and increases stability of $GABA_AR$ within the ER, thus contributing to an up-

regulation of $GABA_AR$ surface expression in neurons (*101, 102*). Within the Golgi apparatus, $GABA_AR$ subunits undergo many post-translational modifications facilitated by associated proteins. Golgi-specific palmitoyltransferase DHHC zinc finger domain protein (GODZ) interacts with a cysteine-rich domain in the M3-M4 loop of γ1-3 subunits and palmitoylates γ subunits in assembled receptors. This palmitoylation is essential for normal clustering and membrane insertion of γ subunit-containing $GABA_ARs$ (*103, 104*).

4) Trans-Golgi network and beyond

The assembled $GABA_ARs$ are incorporated into vesicles and inserted into the plasma membrane (*105*). The translocation of $GABA_AR$ from the trans-Golgi apparatus to the plasma membrane is regulated by a list of proteins including $GABA_AR$ associated protein (GABARAP) *(106,107)*, phospholipase-C-related catalytically inactive proteins 1 and 2 (PRIP1/2) (*108*), brefeldin-A-inhibited GDP/GTP exchange factor 2 (BIG2) (*109*) and N-ethylmaleimide-sensitive factor (NSF) (*110*). GABARAP, a membrane-associated protein, interacts with the intracellular domains of $GABA_AR$ γ subunits and microtubules (*111*). Overexpression of GABARAP in heterologous cells (*112*) and cultured hippocampal neurons (*113*) increases the surface expression of γ2 subunit-containing $GABA_ARs$, suggesting that GABARAP may enhance the exit of $GABA_ARs$ from the Golgi apparatus and vesicular transport toward the plasma membrane. PRIP-1 and -2 competitively inhibit γ2 subunit binding to GABARAP (*114*). In addition, PRIP-1 has been shown to bind to intracellular domains of β subunits as well as protein phosphatase 1α (PP1α), and as such serves as a scaffold protein that regulates the phosphorylation state of $GABA_ARs$ (*115*). Therefore, PRIPs have complex effects on the delivery of $GABA_ARs$ receptors to the membrane and can act both through and independent of their association with GABARAP. BIG2 is a guanine nucleotide exchange factor (GEF) that catalyzes GDP/GTP exchange on the small G-protein ADP-ribosylation factor (*116*). Activation of these G-proteins regulates coated vesicle budding from the Golgi apparatus and facilitates cargo translocation from trans-Golgi network to plasma membrane. In addition to its GEF function, BIG2 was also identified to interact with the intracellular domains of $GABA_AR$ β subunits in a yeast-two hybrid assay (*109*). Although BIG2 is concentrated mainly in

the Golgi apparatus, $GABA_AR$/BIG2 colocalization also occurs in vesicle-like structures along dendrites. Thus, BIG2 enhances the transport of newly assembled $GABA_ARs$ to the postsynaptic plasma membrane and may also influence endocytic recycling of receptors. NSF, a hexameric ATPase, interacts with GABARAP within the Golgi apparatus, where it is proposed to modulate the intracellular trafficking of $GABA_ARs$ (*117*). In addition, NSF directly binds to the intracellular loops of $GABA_AR$ β subunits and decreases receptor cell surface expression level by regulating receptor insertion rather than endocytosis (*110*).

5) Postsynaptic targeting and clustering of $GABA_ARs$

$GABA_AR$ surface expression is very dynamic and regulated. The accumulation of $GABA_ARs$ at inhibitory synapses involves a number of receptor-associated proteins and cytoskeletal elements that are concentrated at postsynaptic densities (PSDs). Once in the membrane they can reach the postsynaptic region through lateral diffusion, and the synaptic receptors may be stabilized by interacting with their scaffold proteins. Gephyrin is considered to be the most important scaffold protein for both GABAergic and glycinergic synapses (*118*). Gephyrin, a 93-kDa polypeptide, oligomerizes and forms clusters at postsynaptic sites through interaction of the N-terminal domain of the protein (G-gephyrin) that assumes a trimeric structure and the C-terminal E domain that forms a dimer (*119*). A direct interaction between $GABA_ARs$ and gephyrin was first observed for the α2 subunit (*120, 121*). Additional studies reported the identification of gephyrin interaction motifs in the homologous regions of α1 and α3 subunits and a novel gephyrin-binding motif in β2 and β3 subunit large cytoplasmic loops (*122*). Although the $GABA_AR$ γ2 subunit is required for recruiting gephyrin to the surface membrane (*123*), the γ2 subunit binding site in gephyrin is still unknown. Alternatively, and depending on their molecular composition, $GABA_ARs$ may remain at extrasynaptic sites. The clustering of $GABA_ARs$ at extrasynaptic sites is mediated by the 81-kDa actin-binding protein radixin, an ezrin/radixin/moesin(ERM)-family member (*124*). Radixin is an α5 subunit-interacting protein and is essential for extrasynaptic anchoring of α5β3γ2 receptors (*125, 126*).

6) Endocytosis of $GABA_A$Rs from the plasma membrane

Most neuronal $GABA_A$Rs are internalized via clathrin-mediated endocytosis, and the clathrin-Adaptor Protein 2 (AP2) plays a key role in targeting receptors to clathrin-coated pits (*127*). Phosphorylation impairs AP2-$GABA_A$R association, thereby reducing receptor endocytosis and increasing inhibitory transmission (*128*). After endocytosis, $GABA_A$Rs are targeted for lysosomal degradation or are rapidly recycled back to the cell surface (*129*). A direct interaction of $GABA_A$Rs and Huntington-Associated Protein 1 (HAP1) plays an important role in this decision. HAP1 inhibits the degradation of $GABA_A$Rs and facilitates receptor recycling. HAP1 overexpression was shown to increase $GABA_A$R surface expression and GABAergic IPSC amplitudes in cultured neurons (*130*).

GEs and $GABA_A$R mutations

1. Overview

Dysfunctional GABAergic transmission had long been considered to contribute to epilepsy. This view was eventually confirmed at the molecular level in 2001 when the first two GE-associated $GABA_A$R subunit gene (*GABR)* mutations *GABRG2(K328M)* and *GABRG2(R82Q)* were reported in a family with GEFS + (*131*) and a family with CAE and FS, respectively (*132*). Since these important discoveries, dozens of additional mutations in *GABRs* encoding the α1, β2, β3, γ2, or δ subunits (*GABRA1*, *GABRB2*, *GABRB3*, *GABRG2*, and *GABRD*, respectively) have been associated with monogenic GE subtypes over the last 16 years (Table 1-2). These GEs range from mild generalized absence epilepsy to severe EEs such as Dravet syndrome, Infantile Spasms, and Lennox-Gastaut syndrome.

Most of these *GABR* mutations have autosomal dominant inheritance or are sporadic *de novo* mutations. Based on the location and the impact on protein sequence, these epilepsy mutations can be divided broadly into four classes: (1) missense mutations in coding regions, (2) nonsense mutations in coding regions, (3)

insertion/deletion mutations in coding regions, and (4) promoter and splice donor site mutations in noncoding regions (*133*). Missense mutations encode a different amino acid in the subunit, insertions/deletions can lead to subunit truncation due to a frame shift that leads to a premature translation-termination codon (PTC) in the new reading frame or to degradation of the coding mRNA by nonsense mediated mRNA decay (NMD), and splice donor site mutations alter splicing that also generates a PTC and protein truncation or NMD. In the coding regions, mutations occur in different functional substructures including the N-terminus, transmembrane domain, and intracellular or extracellular loops. The numbering of all *GABR* mutations in this thesis will be designated in the DNA sequence coding for the immature subunit that includes the signal sequence and the mature subunit.

2. Pathophysiological mechanisms of GE-associated *GABR* subunit mutations

All of the GE-associated *GABR* mutations have been shown to impair GABAergic function but to different extents and by diverse mechanisms, including reducing subunit mRNA transcription or stability, impairing subunit oligomerization and receptor trafficking, dominant negative effects, mutant subunit aggregation causing cell stress and cell death, and gating defects. A comprehensive understanding of the molecular deficits and epileptogenesis mechanisms underlying these mutations would benefit the diagnosis, prognosis and treatment design.

1) GE-associated *GABR* mutations generally impaired $GABA_AR$ biogenesis

Transcription of mutant *GABRs* produce mutant mRNAs and translation of mutant mRNA produces mutant subunits. Biogenesis of mutant $GABA_AR$ receptors are subject to cellular quality control at both mRNA and protein levels, including NMD, ER retention, and ER-associated degradation (ERAD). These quality control checkpoints prevent nonfunctioning or malfunctioning $GABA_AR$ subunits from assembling into receptors and trafficking to the cell surface and ensure that $GABA_ARs$ at synapses or at extrasynaptic sites are mature and functional. The majority of *GABR* mutations produce mutant subunits with impaired biogenesis and

trafficking. Therefore, reduction or loss of mutant subunit protein on the cell surface is a common defect for many PTC-generating nonsense and missense *GABR* mutations. This can lead to a subsequent reduction of inhibitory inputs in neurons and therefore increased excitability.

2) GE-associated *GABR* mutations that produce PTCs may be subject to incomplete NMD

NMD is a posttranscriptional, but translation dependent, cellular mRNA quality surveillance mechanism. It recognizes and initiates degradation of abnormal transcripts with PTCs, thus reducing intracellular levels of potentially deleterious truncated proteins (*134*). As a general rule, mRNAs with an aberrantly configured 3' untranslated region (*135*) or with a PTC that is at least 50–55 nucleotides upstream from an exon–exon junction (*136*) elicit NMD. However, NMD efficiency is often not complete, and the levels of intact, undegraded mRNAs vary among different cell types (*137*).

At least seven mutations in human *GABR* genes have been shown to produce mRNAs that activate NMD. These mutations are in *GABRG2* and *GABRA1* and include nonsense mutations (*GABRG2(Q40X), GABRG2(R136X)* and *GABRG2(Q390X)*), frameshift mutations (*GABRG2(S443delC)*, *GABRA1(975delC, S326fs328X)*, and *GABRA1(K353delins18X))* and an intron 6 splice donor site mutation (*GABRG2(IVS6 + 2T→G)*.

For instance, the *GABRA1(975delC, S326fs328X)* mutation associated with CAE (*138*) caused a shift in the reading frame, resulting in a PTC 74 nucleotides upstream of the last exon-exon junction. Using intron-inclusion minigene constructs that support mRNA splicing and editing, it was demonstrated that the *GABRA1(975delC, S326fs328X)* mutation activated NMD, resulting a substantial reduction but not complete loss of mRNA in heterologous cells and rat cortical neurons, which could be reversed by silencing the NMD essential factor UPF1 (*139*). However, it was also shown that the extent of mutant mRNA reduction was variable among different cell systems and different transfection methods. This might imply a variation in

NMD efficiency among neurons in different regions of the brain and during different developmental time windows that could contribute to regional and developmental differences in the pathophysiological effects of mutant PTC-containing $GABA_AR$ subunits (*140*). Similarly, *GABRG2(Q40X)* (*141*) and *GABRG2(R136X) (142)* are two nonsense mutations located in the second exon of the *GABRG2* gene and both PTCs activate the NMD machinery. *GABRG2(IVS6 + 2T→G)* is an intronic splice donor site mutation that segregated with CAE and FS in a small pedigree (*143*). When the mutation is made in the *GABRG2* intron 6 cloned in a bacterial artificial chromosome, a cryptic splice donor site was activated resulting in partial intron 6 retention and a frame shift that resulted in a PTC in exon 7. This exon 7 PTC had an exon-exon junction downstream and thus activated NMD and reduced mutant *GABRG2* transcript level (*144*).

All of these mutations produce mRNAs that are partially degraded by NMD, and likely cause epilepsy due to *GABRA1* or *GABRG2* haploinsufficiency. However, mutant mRNAs escaping NMD could still result in translation of a certain amount of truncated proteins. These truncated proteins are subject to cellular quality control mechanism at protein level, a topic that I will elaborate on later. Studies have demonstrated that GEs associated with PTCs are caused by a combination of degradation of unstable subunit mRNA and of unstable truncated subunit protein (*139, 140*).

3) GE-associated *GABR* mutations that do not activate NMD may cause ER retention and activate ERAD at different rates

Newly synthesized $GABA_AR$ subunits must properly fold before being transported and inserted into the membrane. Similar to mRNA surveillance at the mRNA level, at the protein level, trafficking deficient mutant subunits that do not fold properly within a certain time are targeted for ER protein quality control, leading to ER retention and ERAD after translation (*145*). ERAD efficiently dislocates trafficking deficient mutant subunits from the ER lumen into the cytosol for degradation via the ubiquitin-proteasome system (*146*)

or chaperone-mediated autophagy (*147*). When expressed with partnering subunits in HEK 293T cells, all the mutant subunits had reduced expression on the cell surface compared with wild-type subunits.

According to the 50-nucleotide boundary rule, PTCs in the last exon of a multi-exon gene or less than 50–55 nucleotides upstream of the last exon–exon junction do not activate NMD; thus their mRNAs are not degraded and they generate truncated subunits. Two nonsense mutations in the last exon of *GABRG2* (*Q390X* and *W429X*) have been reported to be associated with GEFS+ (*46, 148*). They both were located in the large M3-M4 intracellular loop of γ2 subunits and generated a PTC in the last exon. As expected, both of the mutations produce mRNAs that are stable and not degraded by NMD. Translation of mutant mRNAs resulted in production of truncated proteins that were incompletely degraded by ERAD (*149, 150*). Consistent with this, significantly reduced peak currents were recorded from homozygous mutant receptors (*151*) .

In addition to nonsense mutations, missense *GABR* mutations that significantly alter protein structure often result in misfolding or impaired oligomerization of subunits and thus disrupt $GABA_AR$ biogenesis. These trafficking-deficient missense mutations include *GABRA1(A322D), GABRA1(D219N)*, *GABRG2(R82Q)*, *GABRG2(P83S)*, *GABRG2(R177G)*, *GABRB3(G32R)* and *GABRB2(T287P)*.

Cell surface $GABA_AR$ subunits are more mature and have a higher molecular mass compared with immature subunits inside the ER. When coexpressed with the wild-type partnering subunits, the mutant subunits displayed only ER glycosylation that is the core glycosylation for the immature subunits, while the wild-type subunits had mature glycosylation, suggesting subunit trafficking beyond the trans-Golgi to the cell surface. The glucosidase Endo-H removes high-mannose N-linked glycans attached in the ER, but not those attached in the trans-Golgi region. By contrast, the glucosidase PNGase F removes glycans attached in both ER and trans-Golgi regions. Glycosylation studies have demonstrated that some mutant subunits have arrested glycosylation, confirming that they are retained in the ER and have impaired forward trafficking. For instance,

the *GABRG2(R177G)* mutation was identified in a family of complex FS (*152*). On western blots of transfected HEK 293T whole cell lysates, Endo-H digestion shifted the subunit protein main bands to the same levels obtained with PNGase F digestion, suggesting that when coexpressed with partnering subunits, γ2(R177G) subunits underwent ER, but not Golgi, glycosylation (*23*).

These mutant subunits to varying extent were reported to have impaired folding and impaired oligomerization with other subunits and to be subject to ER retention and subsequent degradation by ERAD. However, the degradation rate of different subunits harboring different mutations may differ. The relative stability of mutant subunits may vary with the stability of different subunit subtypes and with the nature and location of the mutation. For instance, the three *GABRG2* mutations R82Q, P83S and N79S were all located in the N-terminus that contributes to the γ+/β- subunit interface. R82Q and P83S produced severely impaired subunit surface expression, while the N79S mutation had mildly impaired surface expression (*153*).

4) *GABR* mutations may cause dominant negative suppression of the remaining $GABA_AR$ function

While some mutations cause only simple haploinsufficiency, some *GABR* mutations generate mutant subunits that cause dominant negative suppression of wild-type $GABA_AR$ subunits.

Using the nonsense *GABRG2* mutations as an example, despite minimal cell surface expression for all the truncated subunits, mutant γ2 subunits imposed different levels of dominant negative effects (γ2(Q390X)> γ2(W429X)> γ2(R136X)) to reduce the surface expression of partnering α and β subunits and wild-type γ2 subunits (*150*). *GABRA1(A322D)* and *GABRG2(R82Q)* represent the group of missense mutations with slight dominant negative effects. More than 80% of the α1(A322D) subunits were degraded in the ER (*154*), but the mutant subunits still oligomerized with wildtype subunits and decreased surface α1β2γ2 and α3β2γ2 receptor levels (*155*). Interestingly, endogenous expression of α5 subunits in cultured hippocampal neurons was

reduced when coexpressed with γ2(R82Q) subunits, indicating that γ2(R82Q) subunits conferred a dominant negative effect (*156*).

The degree of dominant negative suppression variation likely correlated with the specific structural disturbance and degradation rate of mutant $GABA_AR$ subunits. A detailed comparison of γ2 subunit metabolism with the radiolabeled pulse-chase assay has been done with *GABRG2* nonsense mutations *GABRG2(Q390X)* and *GABRG2(W429X)*. The γ2(Q390X) subunits were more stable than wild-type subunits and thus imposed strong dominant negative effects. In contrast, the *GABRG2(W429X)* mutation produced γ2 subunits with mild dominant negative effects and had slightly enhanced degradation compared with the wild-type γ2 subunits (*150*).

5) *GABR* mutations could induce epilepsy by inducing ER stress, UPR and gain of cellular toxicity

It has been previously demonstrated that several GE-associated trafficking deficient mutant $GABA_AR$ subunits were subject to ERAD and were removed from the cells. However, the build-up of an overwhelming load of mutant subunits in the ER may cause ER stress and activate corrective intracellular signal transduction pathways, cumulatively referred to as the unfolded protein response (UPR) (*157*). The UPR copes with ER stress through a broad transcriptional upregulation of ER folding chaperones, lipid biosynthesis, and ERAD components with a reduction in the biosynthetic burden of protein load that flux into the ER through selective translational repression and mRNA degradation (*158*). The UPR allows cells to restore normal function of the ER and is therefore critical for cellular homeostasis. In settings of severe and sustained ER stress, however, the UPR can become cytotoxic, rather than cytoprotective, and commits the cell to various pathways of cell death (apoptosis) (*159*).

Neurodegenerative diseases such as Alzheimer's disease and Huntington's disease are often associated with ER stress-induced apoptosis caused by mutant proteins. However, the chronic cellular toxicity resulting from

GE-associated *GABR* mutations has seldom been addressed. The *GABRG2(IVS6 + 2T→G)* mutation significantly increased the UPR-induced ER stress marker BIP level *in vitro*. The γ2(Q390X) subunit also substantially increased BIP levels in HEK 293T cells, but to a level slightly less than that the increase produced by the *GABRG2(IVS6 + 2T→G)* mutation. Thus, ER responses may contribute to the pathogenic mechanism of both *GABRG2(Q390X)* and *GABRG2(IVS6 + 2T→G)* mutations. However, *GABRG2(IVS6 + 2T→G)* subunit transfected cells did not induce apoptosis, suggesting that the *GABRG2(IVS6 + 2T→G)* subunit induced mild, chronic stress in the cell (*144*).

Recently, our laboratory generated a heterozygous *Gabrg2*$^{+/\ Q390X}$ KI mouse and compared it with the heterozygous *Gabrg2*$^{+/-}$ knockout (KO) mouse that has reduction of functional γ2 subunits without accumulation of the mutant subunits. *Gabrg2*$^{+/\ Q390X}$ KI mice had spontaneous GTCs and sudden death after seizures while *Gabrg2*$^{+/-}$ KO mice only displayed mild absence epilepsy. KI mice also had more severe neurobehavioral comorbidities than KO mice including hyperactivity, impaired social interactions as well as cognitive deficits (*160*). In addition to impairing inhibitory neurotransmission, it was demonstrated that mutant γ2(Q390X) subunits progressively formed intraneuronal detergent-resistant, high molecular-mass protein complexes containing γ2 subunits in old, but not young, heterozygous *Gabrg2*$^{+/Q390X}$ KI mice. The γ2(Q390X) subunits activated caspase 3 and caused widespread neurodegeneration that increased in severity with aging (*161*). A study using brain magnetic resonance imaging (MRI) found substantial cortical atrophy and possible neuronal loss in a large group of GE patients (*162*). These results provide evidence that in addition to the disinhibition produced by substantial loss of functional γ2 subunits leading to epilepsy, the worsening epilepsy and progressive behavioral changes caused by the *GABRG2(Q390X)* mutation may also be a result of the accumulation and aggregation of truncated γ2(Q390X) subunits that increases cell stress and leads to chronic neurodegeneration *in vivo*.

6) Altered channel kinetics as a rare molecular defect for *GABR* mutations

Several $GABA_AR$ subunit mutations/variants associated with GEs alter receptor channel gating. For instance, a lysine to methionine mutation *GABRG2(K328M)* in the M2–M3 loop of the γ2 subunit is associated with the epilepsy syndrome GEFS+. Mutant γ2(K328M) subunits assemble into $GABA_ARs$ and traffick to the postsynaptic membrane at normal efficiency. However, patch-clamp electrophysiological experiments in transfected HEK293T cells demonstrated that the α1β2γ2(K328M) receptors had reduced single-channel open time, and GABA-evoked currents from homozygous mutant receptors deactivated significantly faster than wild type receptor currents (*163*). In addition, miniature inhibitory post synaptic currents (mIPSCs) recorded from hippocampal neurons transfected with γ2(K328M) subunits had reduced deactivation times relative to mIPSCs recorded from untransfected neurons or from neurons transfected with wild type γ2 subunits (*156*). LGS-associated *GABRB3(D120N, E180G, Y302C)* mutations located at β subunit $^+$ interfaces reduced whole cell currents by decreasing single channel open probability without loss of surface receptors. In contrast, the IS associated *GABRB3(N110D)* and *GABRB1(F246S)* mutations at β subunit $^-$ interfaces produced minor changes in whole cell current peak amplitudes but altered current deactivation by decreasing or increasing single channel burst duration, respectively (*164*). Recently, a *de novo* missense mutation, *GABRG2(P302L)*, was identified in a patient with Dravet syndrome using targeted NGS. The mutation faces the pore lumen in the γ2 subunit and caused ~90% loss of whole-cell current by altering the conduction pathway of the receptor during gating transitions among closed, open, and desensitized states (*165*).

3. Model systems for studying physiological mechanisms associated with *GABR* mutations

The functional characterization of GE-associated $GABA_AR$ subunit mutations has been performed in heterologous cells, cultured neurons, and genetically modified mice as model systems (*133*). The basic cell quality control machineries such as mRNA surveillance, ER retention, and ERAD should be conserved from heterologous cell system to neurons and from mice to humans. In general, *in vitro* studies permit direct investigation of the effects of the mutation on $GABA_AR$ biogenesis and function in a relatively simple system

without the impact of complex neuronal development or network activities. They allow a relatively fast screening of mutants and thus are usually the methods of first choice, but they do not fully recapitulate the situations *in vivo*. Compared with them, genetically modified KI mice have the advantage of allowing evaluation of the impact of the mutant $GABA_A$Rs in the complex context of an intact living organism. It is important that results of functional studies should be interpreted carefully considering the characteristics of the experimental systems used (*166*). Because each model system has its own advantages and limitations, combining the findings from multiple model systems and identifying the common mechanisms will be important in unraveling the complicated cellular mechanisms contributing to the GABR-related epilepsies and in identifying new treatments.

1) Heterologous expression systems

Heterologous cells are non-neuronal cells that have minimal endogenous currents and are relatively easy to use. To confirm genetic data, screening for channel defects affecting ion channel genes and studying the involvement of impaired $GABA_A$R function in the pathogenesis of epilepsy, heterologous expression is a necessary first step. As a relatively fast and efficient approach, heterologous expression systems enable selection of a mutation for further studies in complex neural cellular and animal models.

i. Xenopus oocytes

The oocytes of the clawed African frog Xenopus laevis have been widely used for many years as a heterologous expression system for studying ion channels (*167*). These huge cells (1 - 1.3 mm in diameter) with few endogenous channels are cheap and easy to handle. Furthermore, they can efficiently translate exogenous mRNAs and allow subsequent long and stable electrophysiological recordings of ion channel currents. Initial functional characterizations of several $GABA_A$R mutations were first studied by using this expression system (*131, 132*).

However, use of the Xenopus oocytes expression system requires consideration of several limitations (*166*); the most serious of which is its non-mammalian cell background. It has been shown that $GABA_AR$ assembly in Xenopus oocytes is more promiscuous than in mammalian cells. Furthermore, the oocyte system has relatively slow temporal resolution, which makes it difficult to explore the rapid kinetic properties most relevant to the time scale of synaptic transmission, such as activation, desensitization, and deactivation. Therefore, Xenopus oocytes are now used less often for studies of $GABA_AR$ mutations.

ii. Cultured mammalian cell lines

The use of cultured mammalian cell lines has now become the first line experimental approach for studying the cellular consequences of *GABR* mutations. The most commonly used cells are human embryonic kidney (HEK) cells. The principle characteristics that have made the HEK cell a robust and reliable platform in which to express mutant $GABA_ARs$ are: easy maintenance and quick growth, high efficiency of transfection and protein production using inexpensive methods, small endogenous currents, and small cell size with minimal processes appropriate for voltage-clamp recordings (*168*). Other popular cell lines include COS-7 cells and HeLa cells. The evaluation of *GABR* mutations based on the combination of traditional electrophysiological methods and biochemical methods by overexpressing them in heterologous mammalian cell lines has provided substantial knowledge of the cellular and molecular mechanisms underlying GE epileptogenesis.

The results from these studies are relevant to effects of the mutations *in vivo* because fundamental features of subunit translation, folding and oligomerization, and receptor assembly and trafficking are highly conserved between heterologous cells and neurons (*169*). However, $GABA_AR$ expression and function in heterologous cells and *in vivo* could differ (*133*). Heterologous cells do not provide a neuronal background, in that they don't have endogenous $GABA_AR$ subunits and also lack many neuron specific $GABA_AR$-associated proteins that play important roles in $GABA_AR$ biogenesis, trafficking and cell surface clustering and stabilization (*72,*

73). In addition, it is impossible to study the effect of mutations on GABAergic synaptic transmission in heterologous cells because they do not form synapses. Moreover, mutations may alter the subcellular distribution of $GABA_A$Rs, but this effect cannot be observed in non-polarized heterologous cells.

Additionally, it should also be noted that functional studies in heterologous expression systems have provided inconsistent and ambiguous results. For example, regarding whether there is altered diazepam sensitivity associated with the *GABRG2(R82Q)* mutation, some studies revealed altered benzodiazepine binding (*170*) while other groups reported intact benzodiazepine binding to mutant $GABA_A$Rs (*163, 171-173*). This discrepancy may have arisen from differences in transfection methods or culturing conditions that may have altered the functional consequences of mutant $GABA_A$R subunits.

2) Cultured neurons

Cultured neurons can overcome most, if not all, of the limitations of heterologous cells mentioned above. In addition to expressing neuronal specific proteins, their polarity and subcellular specialization allow for investigation of the targeting of mutant $GABA_A$Rs to synaptic, perisynaptic or extrasynaptic sites. Moreover, they can form active GABAergic synapses and functional neuronal networks which obviate the need for exogenous applications of GABA (*133*).

Several GE-associated *GABR* mutations including *GABRA1(A322D)* (*155*), *GABRG2(R82Q)* (*156*), *GABRG2(K328M)* (*156*), *GABRG2(Q390X)*(*149-151*) and *GABRG2(P302L)(165)* have been studied in cultured neurons. Unsurprisingly, these studies confirmed some of the initial observations obtained in the heterologous cells. For example, studies in HEK cells revealed that mutant γ2(Q390X) subunits were immature and retained in the ER, resulting in loss of function of the γ2 subunit. In addition, γ2(Q390X) subunits exhibited a dominant negative effect by impairing assembly and trafficking of wild type partnering subunits. Similarly, when coexpressed with α1 and β2 subunits, γ2(Q390X) subunits were haploinsufficient

with minimal expression on the surface of hippocampal neurons. Electrophysiological experiments in neurons demonstrated that heterozygous α1β2γ2(Q390X) receptor current amplitudes were less than half of wild type peak current amplitudes, confirming the dominant negative effect of mutant γ2(Q390X) subunits.

Studies in cultured neurons also revealed partially different or completely new findings that could not have been predicted from the heterologous expression system alone. For instance, expression of the γ2(R82Q) subunit in hippocampal neurons selectively reduced extrasynaptic tonic GABAergic currents but had no effect on synaptic phasic inhibition, whereas in transfected HEK cells only a general deficit in GABAergic signaling was detected. In addition, observations made in hippocampal neurons revealed that mutant γ2(R82Q) subunits reduced α5 surface expression (*156*). This finding would not have been observed in heterologous cell lines that do not express either endogenous $GABA_AR$ subunits or neuron-specific proteins such as radixin, which associates with the α5 subunit (*126*).

Transfected neurons in primary cultures can be a better experimental model in comparison with heterologous cells and a step forward in studying physiological effects of mutant $GABA_AR$ subunits. However, it must be highlighted that they still do not complete reproduce *in vivo* conditions because with transfection, the exogenous $GABA_ARs$ are overexpressed at non-physiological levels.

Although expression of mutant $GABA_AR$ subunits in cultured neurons has been useful, it is still likely that the details of the pathophysiology are incomplete using this approach. With transfection, it is not possible to regulate the levels of subunit transcription and translation and therefore the relative amounts of wild type and mutant subunits and assembly partners will not be physiologically correct. In addition, the epilepsy mutations may have different actions in different brain regions or in different neuronal cell types and thus could modify neuronal network function differently in different nervous system locations. Ultimately, many of these

questions must be answered by studying genetically modified animals as well as human patients who possess these mutations.

3) Genetically modified mouse models

Epilepsy is a complex disease of neuronal networks involving the interaction of many cell types in different brain regions that can be influenced by *GABR* mutations. Although there is no doubt that *in vitro* studies have and will continue to shed light on the cellular and molecular effects of various mutant $GABA_AR$ subunits on GABAergic physiology, building a complete understanding of epileptogenesis in GEs requires models that enable investigation at different organization levels and temporal scales. Genetically modified KI mice harboring homologous human *GABR* mutations preserve the complexity of the nervous system and better recapitulate real pathophysiological conditions. Therefore, they are one of the best available systems to investigate epileptogenesis of GEs. In addition, they will aid in the identification and validation of novel targets for the treatment and prevention of epilepsy.

Currently, the availability of KI mice that mimic human GEs arising from *GABR* mutations is extremely poor because they are costly and time-consuming to generate. To date, only heterozygous *Gabrg2*$^{+/R82Q}$ (*174-178*), *Gabrg2*$^{+/Q390X}$ (*160, 161, 179*), and *Gabra1*$^{+/A322D}$ (*180, 181*) KI mice have been made and studied. Advances in CRISPR (clustered regularly interspaced short palindromic repeats)-mediated genome editing have made it easier to produce KI mice. Our laboratory has successfully generated *Gabrb3*$^{+/P11S}$ KI mice as a model of CAE (unpublished).

Here I will take the heterozygous *Gabrg2*$^{+/R82Q}$ KI mouse model as an example. Heterozygous mice harboring the *GABRG2(R82Q)* mutation recapitulate the two major seizure types seen in human patients, including CAE and FS. Consistent with the findings in heterologous cells and in cultured neurons, the mutation substantially reduced γ2 subunit surface expression in the mouse brain (*174*). However, in contrast

to the dominant negative effect of mutant γ2(R82Q) subunits observed in cell-culture experiments, no change of α1 subunit expression was detected in embryonic neuron cultures from *Gabrg2*$^{+/R82Q}$ KI mice. This finding highlights the caution required when interpreting data from *in vitro* findings to explain the pathophysiological mechanisms of mutant $GABA_AR$ subunits (*182*).

Moreover, investigations in this mouse model also revealed some important findings that could not be predicted *in vitro*. Analysis of synaptic inhibition demonstrated significantly reduced miniature IPSC amplitudes in the somatosensory cortex (layer 2/3 pyramidal cortical neurons), with no change in the thalamic reticular nucleus or ventrobasal thalamus (*174*). This generated the hypothesis that a reduction in cortical $GABA_AR$-mediated inhibition may underlie CAE epileptogenesis. Furthermore, it was demonstrated that the *GABRG2(R82Q)* mutation causes CAE and FS through distinct molecular mechanisms, and these two epilepsy phenotypes have different sensitivity to genetic background (*178*). To investigate the developmental impact of the *GABRG2(R82Q)* mutation, a tetracycline-based conditional *Gabrg2*$^{+/R82Q}$ KI model that enabled a forebrain-specific activation of the R82Q allele at specific times during development was created (*175*). Seizure susceptibility was significantly reduced in mice where the R82Q allele was suppressed during development, suggesting that *GABRG2(R82Q)* mutation impacts network stability during a critical developmental period and triggers a cascade of events (morphological and transcriptional changes) that define long-term network stability. These complex series of events can only be fully expressed and studied in mouse models.

The *Gabrg2*$^{+/R82Q}$ KI mouse has provided important insights into how a human *GABR* mutation can impact GABAergic inhibition in small time scales, and impact neurodevelopment and consequently increases seizure susceptibility in longer time scales (*183*). Future work with more genetically modified mice carrying *GABR* mutations will better enable us to determine the functional effect of these mutations and develop therapeutic strategies.

Rationale for experimental chapters

1. The genetics of EEs-the *de novo* revolution

As previously discussed, genetic factors in EEs have been increasingly recognized in the past few years. In the genomic era, the major breakthrough in the field was the recent discovery that a substantial proportion of the genetic architecture of the EEs is due to *de novo* mutations. Large-scale studies, most prominently the Epi4K project and the EuroEpinomics project (*60, 184*), assessed genetic epilepsies by applying family-based exome sequencing, focusing on the identification of *de novo* mutations. Currently it is estimated that in 75% of pediatric patients with genetically identified EEs, the disease is due to a heterozygous *de novo* mutation, with smaller subsets due to familial autosomal recessive or X-linked inheritance (*185*). Through advances in NGS technologies, which enable systematic assessment of large parts of the coding region in each individual, the epilepsy field has made great strides in identifying genes associated with EE. As of 2017, more than 30 genes have been securely established as causative genes for genetic EEs (*186*).

Previous studies linking *GABRG2* variants to EE have largely focused on nonsense mutations such as *GABRG2(Q390X)* and *GABRG2(Q40X)*, which lead to truncated protein products with no surface expression. The γ2 missense variants have only been linked to less severe epilepsy syndromes, such as FS, CAE, as well as GEFS+. Our research laboratory collaborated with clinical teams from several hospitals and performed NGS (targeted gene panels or WES) on trios with early-onset EEs. Six *de novo GABRG2* variants (A106T, I107T, P282S, R323Q, R323W, and F343L) were identified in eight independent patients. We provided for the first genetic evidence of the contribution of missense *GABRG2* variants in EEs.

2. Functional and structural characterizations of EE-associated *GABRG2* mutations *in vitro*

However, the *de novo GABRG2* variants identified in our study do not necessarily prove that the respective gene is causative. A large amount of genetic variation is found in the general population. With every affected

and unaffected individual found to carry on average at least one *de novo* variant in their exome sequence (*53*); the challenge in our study shifts from identifying *de novo GABRG2* variants to understanding their role and being able to discriminate them from random genomic noise. Therefore, to determine if these *de novo GABRG2* variants were causative, we performed additional functional and structural studies. Using a combination of molecular modeling, biochemistry, and electrophysiology, we demonstrated meaningful functional changes in a recombinant expression system for all the *GABRG2* mutations identified in this cohort of patients with severe EEs (*187*).

The second part of this dissertation takes a few small steps toward addressing the correlations between the structural disturbances and the biochemical and electrophysiological properties of the mutant γ2 subunits and $GABA_AR$ channels (*188*). We extensively characterized three nonsense *GABRG2* mutations associated with different epilepsy syndromes, *GABRG2(R136X), GABRG2(Q390X)* and *GABRG2(W429X)*. We demonstrated that despite having loss-of-function in common, different nonsense *GABRG2* mutations result in different structural disturbance and different suppression of wild-type partnering subunits, leading to different epilepsy severities. The characterization of the structural basis for the different mutant γ2 subunits in this study may provide novel insights into epilepsy phenotype heterogeneity. To our knowledge, this is the first attempt to correlate mutant protein structural disturbances, biochemical properties and function of the mutant proteins resulting from different mutations associated with a spectrum of disease phenotypes in the same gene.

3. Neurobehavioral phenotyping of *Gabrb3*$^{+/N110D}$ KI mouse model of infantile spasms

For studies of disease pathophysiology of genetic EEs, the most useful models are rodent models harboring mutations corresponding to the ones detected in patients. Even though the procedures for generation of the genetic mouse models have significantly improved in recent years due to advances in novel genome-editing techniques, the number of reported EE mouse lines in literature is still small (*189*). Recently, out laboratory generated a novel KI mouse carrying a human IS mutation, the heterozygous *Gabrb3*$^{+/N110D}$ KI mouse.

In addition to spontaneous spasms, a characteristic feature of IS is developmental stagnation or cognitive plateauing/regression during periods of excessive epileptic activity that often manifests as continuous discharges on the EEG. To determine whether the KI mice have the behavioral comorbidities present in IS patients, I performed a suite of behavioral tests in adult *Gabrb3*$^{+/N110D}$ KI mice. They displayed several abnormal behavioral phenotypes including hyperactivity, increased anxiety, social interaction deficits, and impaired spatial learning and memory, which phenocopy major neurobehavioral comorbidities of IS. However, it is unclear if the neurobehavioral impairment is primarily due to the *GABRB3(N110D)* mutation itself or secondary to the persistent epileptic activity. Further studies are required to address this question.

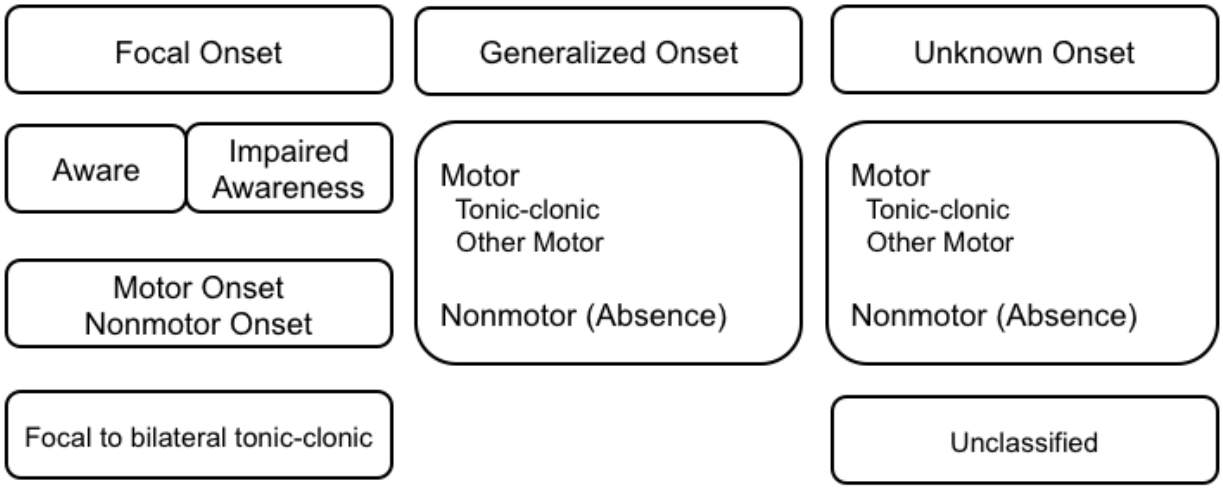

Figure 1-1: Classification of seizure types, basic version. Adapted from (11)

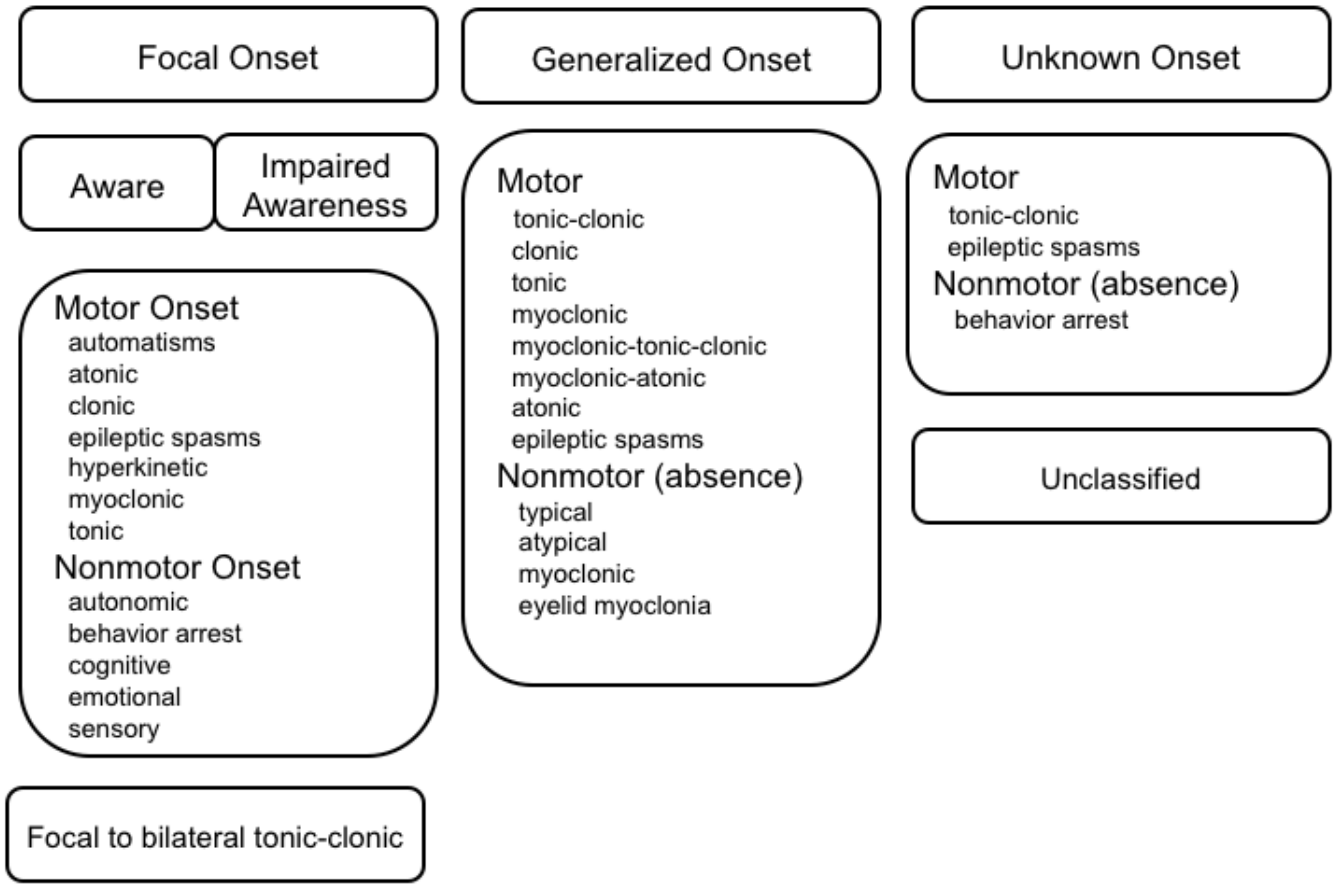

Figure 1-2: Classification of seizure types, expanded version. Adapted from (*11*)

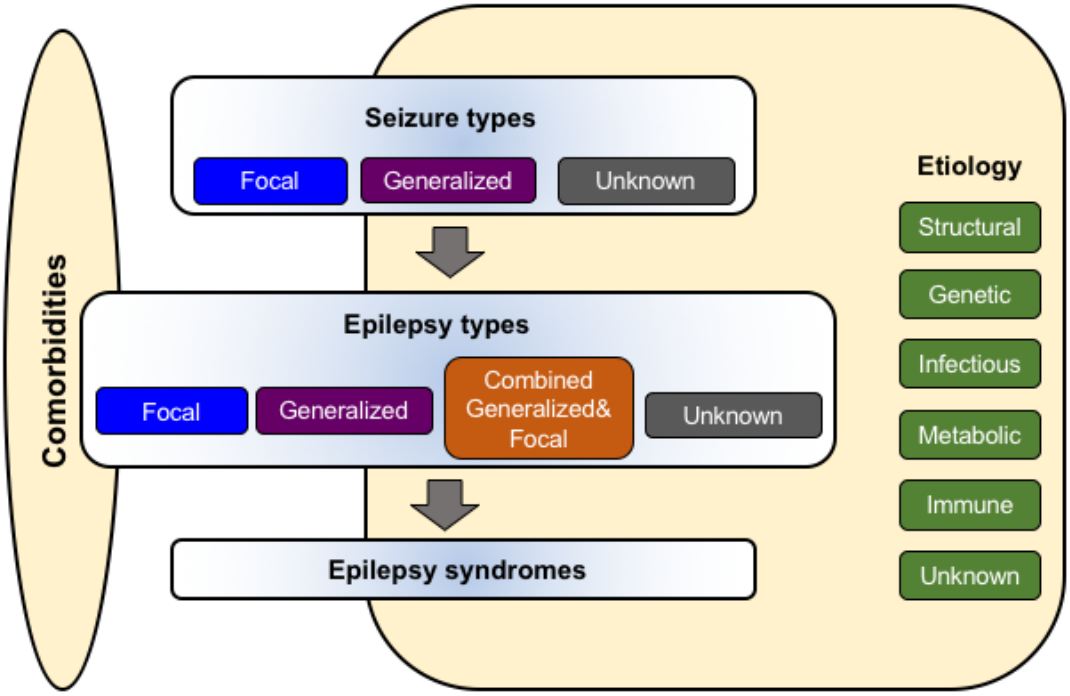

Figure 1-3: Classification of the epilepsies. Adapted from (*12*)

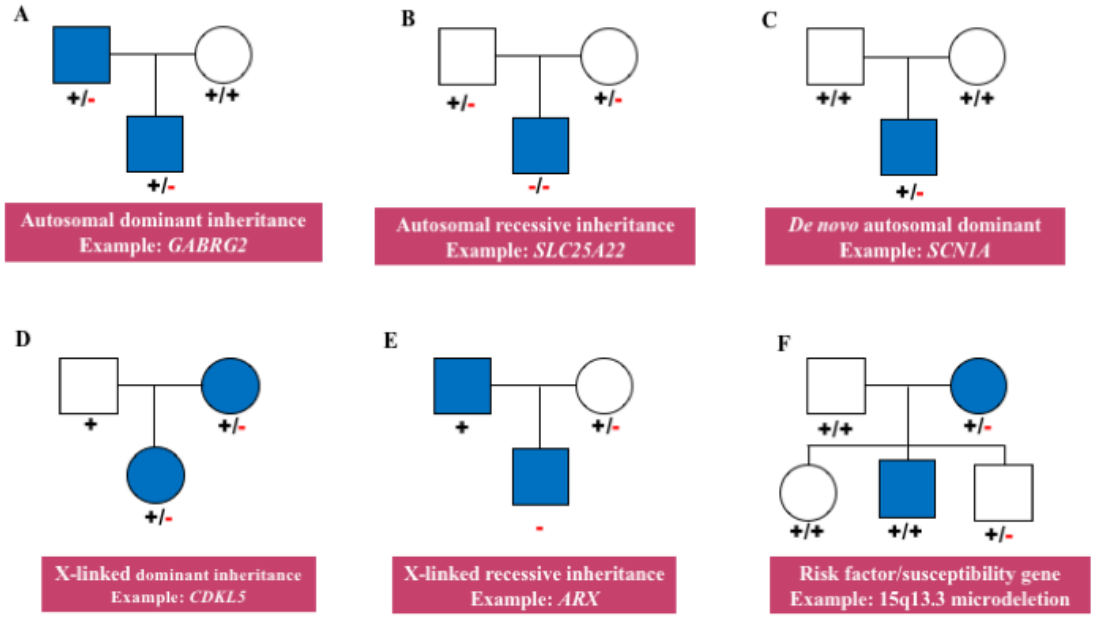

Figure 1-4: Various inheritance patterns in human GEs

A. Autosomal dominant inheritance is the most common inheritance pattern in monogenic GEs, such as in *GABRG2*-related GEFS+ phenotype.
B. Much less frequently, epilepsy syndromes can be can be inherited in an autosomal recessive pattern. For instance, homozygous mutations in *SLC25A22* are associated with migrating partial seizures in infancy.
C. Mutations associated with EEs typically arise *de novo.* For example, SCN1A mutations can lead to Dravet syndrome.
D. For X-linked dominant epilepsies such as *CDKL5* encephalopathy, the vast majority of patients are females. Male patients are rare and typically more severely affected than females.
E. For X-linked recessive epilepsies such as *ARX*-related epilepsy, the vast majority of patients are males. Female carriers are generally asymptomatic or very mildly affected.
F. Gene variant can be a risk factor/susceptibility gene of epilepsy: not all affected individuals have the variant, and some unaffected individuals are carriers of it, such as 15q13.3 deletion.

Blue represents individuals with epilepsy.

Table 1-1: An overview of the advantages and limitations across different types of genetic tests in patients with epilepsy

Genetic test	Variations that may be detected	Typical condition for which test may be appropriate	Advantages	Disadvantages
Targeted single gene sequencing	Point mutations, small CNVs	A diagnosed epilepsy type in which there is a suspected candidate gene that explains the vast majority of cases	Results typically highly reliable, with low false positive and false negative rates	• Gene must be known and suspected by clinician • Cost per gene often considerable • Turnaround time typically long
aCGH	CNVs	Epilepsy syndromes with features in addition to seizures, such as dysmorphism, intellectual disability or autism	• Higher resolution coverage of genome than karyotyping • Can detect chromosome imbalances when there are no clues to what the chromosome anomaly might be	• Will not identify balanced chromosome rearrangements, such as balanced translocations and inversions • The significance of specific CNVs can be difficult to interpret without knowing whether or not a parent carries the same imbalance • Results require confirmation with other tests, such as fluorescent in situ hybridization
Epilepsy gene panels	Point mutations in a broad range of possible candidate genes	Nonspecific epilepsy phenotype in which family history is uninformative	• Excellent read depth, efficient and sensitive look if causal gene is in the panel • Cost less than WES and WGS	• Only evaluate prespecified genes: a risk of missing the causative variant if the panel does not include the responsible gene • Cannot identify CNV • Results require confirmation with Sanger sequencing
WES or WGS	Point mutations or CNVs in coding regions (WES) or the entire genome with its noncoding regions (WGS)	No suspected candidate genes, or above tests do not yield positive results	• Coverage of entire exome/genome • Unbiased approach with potential capacity to detect a variety of different types of change, all in one test	• Relatively more expensive, not commonly available at a clinical level • Uneven coverage: a risk of missing the causative variant if the responsible gene is poorly covered • Turnaround time typically long • Interpretation may be challenging, with both false positives and false negatives • Results require confirmation with Sanger sequencing

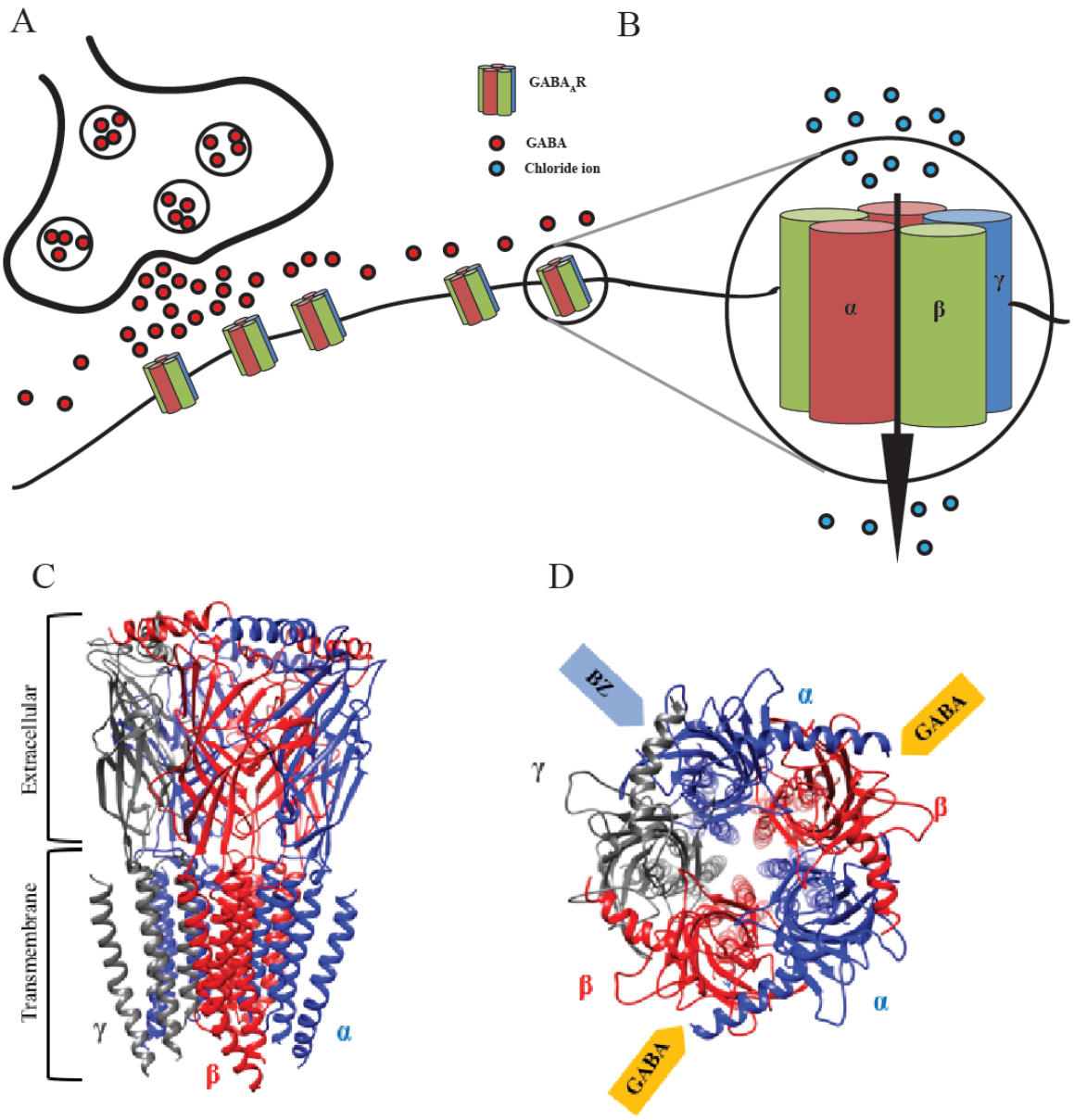

Figure 1-5: Schematics of GABA$_A$Rs

A. GABA$_A$Rs are localized at both synaptic and extrasynaptic sites.
B. Schematic of a heteropentameric GABA$_A$R composed of two α, two β and one γ subunits. Binding of GABA triggers the opening of the channel, allowing the rapid influx of chloride ions.
C. A 3D structural model of the αβγ GABA$_A$R was displayed with α subunits in blue, β subunits in red, and the γ subunit in gray.
D. Top view of the structural model of the αβγ GABA$_A$R from the synapse cleft. The subunit interfaces at which benzodiazepines (BZ) and GABA bind are labeled with arrows.

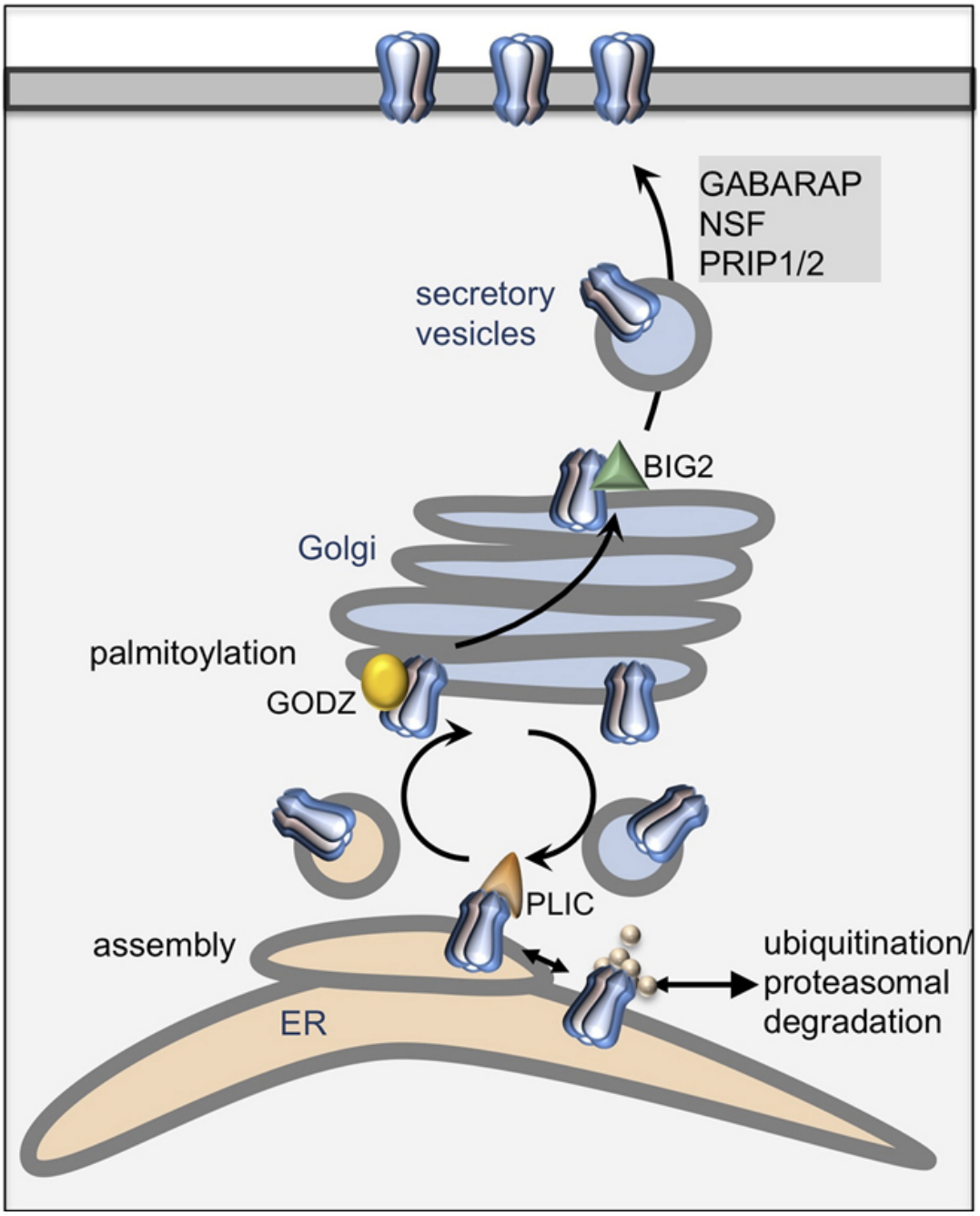

Figure 1-6: Biogenesis of $GABA_A$Rs. Adapted from (*78*)

Table 1-2. GEs-associated *GABR* mutations

Subunit gene	Mutation	Type	Location	Inheritance	Epilepsy syndrome	Reference
GABRA1	V74I	missense	N-terminus	AD	GEFS+	*(190)*
	S76R	missense	N-terminus	*De novo*	DS-like/ EE	*(190)*
	F104C	missense	N-terminus	AD	JME	*(190)*
	R112Q	missense	N-terminus	*De novo*	DS	*(48, 190)*
				De novo	IS	*(191)*
	N115D	missense	N-terminus	*De novo*	Mild EE	*(190)*
	L146M	missense	N-terminus	*De novo*	DS	*(190)*
	R214H	missense	N-terminus	*De novo*	DS/EE	*(190)*
	D219N	missense	N-terminus	AD	GGE	*(192)*
	G251D	missense	N-terminus	*De novo*	Mild EE	*(190)*
	G251S	missense	N-terminus	*De novo*	DS	*(48)*
	P260L	missense	TM1	*De novo*	OS to WS, WS	*(191)*
	M263T	missense	TM1	*De novo*	WS	*(191)*
	M263I	missense	TM1	De novo	WS	*(191)*
	V287L	missense	TM2	*De novo*	EOEE	*(191)*
	T289P	missense	TM2	*De novo*	EIEE	*(190)*
	T289A	missense	TM2	unknown	EIEE	*(190)*
	T292I	missense	TM2	*De novo*	IS	*(60)*
	K306T	missense	TM2-TM3 loop	*De novo*	DS	*(48)*
				De novo	MAE-like	*(190)*
	A322D	missense	TM3	AD	JME	*(193)*
	S326fs328X	frameshift	TM3	AD	CAE	*(138)*
	K353delins18X	splite site	TM3-TM4 loop	*De novo*	CAE	*(192)*
GABRB1	F246S	missense	TM1	*De novo*	IS	*(60)*
	T287I	missense	TM2	*De novo*	EE	*(194)*
GABRB2	M79T	missense	N-terminus	*De novo*	GGE	*(195)*
	T287P	missense	TM2	*De novo*	EME	*(196)*
GABRB3	-897T/C	promoter	Exon 1a promoter	AD	CAE	*(197)*
	P11S	missense	signal peptide	AD	CAE	*(198)*
	S15F	missense	signal peptide	AD	CAE	*(198)*
	G32R	missense	N-terminus	AD	CAE	*(198)*
	V37G	missense	N-terminus	AD	GEFS+	*(199)*
	N110D	missense	N-terminus	*De novo*	IS	*(60)*
	R111X	nonsese	N-terminus	*De novo*	MAE	*(199)*
	D120N	missense	N-terminus	De novo	LGS	(60)
	T157M	missense	N-terminus	AD	GEFS+	(199)
	L170R	missense	N-terminus	*De novo*	EOEE	*(200)*

	E180G	missense	N-terminus	*De novo*	LGS	*(60)*
	Y182F	missense	N-terminus	*De novo*	EE	*(201)*
	Y184H	missense	N-terminus	*De novo*	MAE	*(199)*
	Q249K	missense	TM1	*De novo*	EE	*(201)*
	L256Q	missense	TM1	*De novo*	EE/WS	*(199)*
	T287I	missense	TM2	*De novo*	EOEE	*(202)*
	Y302C	missense	TM2-TM3 loop	*De novo*	LGS	*(60)*
	A305V	missense	TM2-TM3 loop	*De novo*	EOEE	*(200)*
	A305T	missense	TM2-TM3 loop	*De novo*	LGS	*(201)*
	R429Q	missense	TM3-TM4 loop	AD	GEFS+	*(60)*
GABRG2	Q40X	nonsense	N-terminus	*De novo*	DS	*(203)*
	P59fsX12	frame shift	N-terminus	AD	FS	*(204)*
	R82Q	missense	N-terminus	AD	CAE/FS	*(132)*
	P83S	missense	N-terminus	AD	GGE	*(192)*
	A106T	missense	N-terminus	*De novo*	EE	*(187)*
	I107T	missense	N-terminus	*De novo*	EE	*(187)*
	R136X	nonsense	N-terminus	AD	GEFS+	*(142)*
	R177G	missense	N-terminus	AD	FS	*(152)*
	IVS6+2T->G	splice site	Intron 6	AD	CAE/FS	*(143)*
	M199V	missense	N-terminus	AD	GEFS+	*(204)*
	c.549-3T>G	splice site	N-terminus	AD	RE	*(205)*
	G257R	missense	N-terminus	AD	RE	*(205)*
	P282S	missense	TM1	*De novo*	EE	*(187)*
	P302L	missense	TM2	*De novo*	DS	*(165)*
	R323Q	missense	TM2	*De novo*	MAE	*(35)*
				De novo	RE	*(205)*
	R323W	missense	TM2	*De novo*	EE	*(187)*
	K328M	missense	TM2-TM3 loop	AD	GEFS+	*(131)*
	F343L	missense	TM3	*De novo*	EE	*(187)*
	Q390X	nonsense	TM3-TM4 loop	AD	GEFS+/DS	*(46)*
	E402fsX3	frame shift	TM3-TM4 loop	AD	FS/TLE	*(204)*
	W429X	nonsense	TM3-TM4 loop	AD	GEFS+	*(148)*
	S443delC	frame shift	TM4	AD	GEFS+	*(206)*
	V462fsX33	frame shift	TM4	AD	FS	*(204)*
GABRD	E117A	missense	N-terminus	AD	GEFS+	*(207)*
	R220H	missense	N-terminus	AD	GEFS+	*(207)*

Abbreviations: IGE, idiopathic generalized epilepsy; JME, juvenile myoclonic epilepsy; CAE, childhood absence epilepsy; DS, Dravet syndrome (severe myoclonic epilepsy of infancy); EE, epileptic encephalopathy; EOEE, early-onset epileptic encephalopathy; OS, Ohtahara syndrome; WS, west syndrome; FS, febrile seizures; GEFS+, generalized epilepsy with febrile seizures plus; EME, early myoclonic encephalopathy; IS, Infantile spasms; LGS, Lennox-Gastaut syndrome; MAE, myoclonic absence epilepsy; RE, rolandic epilepsy; TLE, temporal lobe epilepsy

References

1. M. J. England, C. T. Liverman, A. M. Schultz, L. M. Strawbridge, Epilepsy across the spectrum: promoting health and understanding. A summary of the Institute of Medicine report. *Epilepsy Behav* 25, 266-276 (2012).

2. D. C. Hesdorffer, G. Logroscino, E. K. Benn, N. Katri, G. Cascino, W. A. Hauser, Estimating risk for developing epilepsy: a population-based study in Rochester, Minnesota. *Neurology* 76, 23-27 (2011).

3. R. Ottman, R. B. Lipton, A. B. Ettinger, J. A. Cramer, M. L. Reed, A. Morrison, G. J. Wan, Comorbidities of epilepsy: results from the Epilepsy Comorbidities and Health (EPIC) survey. *Epilepsia* 52, 308-315 (2011).

4. H. M. de Boer, M. Mula, J. W. Sander, The global burden and stigma of epilepsy. *Epilepsy Behav* 12, 540-546 (2008).

5. W. J. Cardarelli, B. J. Smith, The burden of epilepsy to patients and payers. *Am J Manag Care* 16, S331-336 (2010).

6. R. S. Fisher, W. van Emde Boas, W. Blume, C. Elger, P. Genton, P. Lee, J. Engel, Jr., Epileptic seizures and epilepsy: definitions proposed by the International League Against Epilepsy (ILAE) and the International Bureau for Epilepsy (IBE). *Epilepsia* 46, 470-472 (2005).

7. C. E. Stafstrom, L. Carmant, Seizures and epilepsy: an overview for neuroscientists. *Cold Spring Harb Perspect Med* 5, (2015).

8. J. Engel, Jr., Report of the ILAE classification core group. *Epilepsia* 47, 1558-1568 (2006).

9. R. S. Fisher, C. Acevedo, A. Arzimanoglou, A. Bogacz, J. H. Cross, C. E. Elger, J. Engel, Jr., L. Forsgren, J. A. French, M. Glynn, D. C. Hesdorffer, B. I. Lee, G. W. Mathern, S. L. Moshe, E. Perucca, I. E. Scheffer, T. Tomson, M. Watanabe, S. Wiebe, ILAE official report: a practical clinical definition of epilepsy. *Epilepsia* 55, 475-482 (2014).

10. R. S. Fisher, J. H. Cross, C. D'Souza, J. A. French, S. R. Haut, N. Higurashi, E. Hirsch, F. E. Jansen, L. Lagae, S. L. Moshe, J. Peltola, E. Roulet Perez, I. E. Scheffer, A. Schulze-Bonhage, E. Somerville, M. Sperling, E. M. Yacubian, S. M. Zuberi, Instruction manual for the ILAE 2017 operational classification of seizure types. *Epilepsia* 58, 531-542 (2017).

11. R. S. Fisher, J. H. Cross, J. A. French, N. Higurashi, E. Hirsch, F. E. Jansen, L. Lagae, S. L. Moshe, J. Peltola, E. Roulet Perez, I. E. Scheffer, S. M. Zuberi, Operational classification of seizure types by the International League Against Epilepsy: Position Paper of the ILAE Commission for Classification and Terminology. *Epilepsia* 58, 522-530 (2017).

12. I. E. Scheffer, S. Berkovic, G. Capovilla, M. B. Connolly, J. French, L. Guilhoto, E. Hirsch, S. Jain, G. W. Mathern, S. L. Moshe, D. R. Nordli, E. Perucca, T. Tomson, S. Wiebe, Y. H. Zhang, S. M. Zuberi, ILAE classification of the epilepsies: Position paper of the ILAE Commission for Classification and Terminology. *Epilepsia* 58, 512-521 (2017).

13. R. S. Fisher, An overview of the 2017 ILAE operational classification of seizure types. *Epilepsy Behav*, (2017).

14. Proposal for revised clinical and electroencephalographic classification of epileptic seizures. From the Commission on Classification and Terminology of the International League Against Epilepsy. *Epilepsia* 22, 489-501 (1981).

15. A. T. Berg, S. F. Berkovic, M. J. Brodie, J. Buchhalter, J. H. Cross, W. van Emde Boas, J. Engel, J. French, T. A. Glauser, G. W. Mathern, S. L. Moshe, D. Nordli, P. Plouin, I. E. Scheffer, Revised terminology and concepts for organization of seizures and epilepsies: report of the ILAE Commission on Classification and Terminology, 2005-2009. *Epilepsia* 51, 676-685 (2010).

16. A. T. Berg, J. J. Millichap, The 2010 revised classification of seizures and epilepsy. Continuum (Minneap Minn) 19, 571-597 (2013).

17. Proposal for revised classification of epilepsies and epileptic syndromes. Commission on Classification and Terminology of the International League Against Epilepsy. *Epilepsia* 30, 389-399 (1989).

18. E. Beghi, Epilepsy: New classification of seizures and epilepsies - an advance? *Nat Rev Neuro*l, (2017).

19. M. S. Hildebrand, H. H. Dahl, J. A. Damiano, R. J. Smith, I. E. Scheffer, S. F. Berkovic, Recent advances in the molecular genetics of epilepsy. J Med Genet 50, 271-279 (2013).

20. L. Vadlamudi, E. Andermann, C. T. Lombroso, S. C. Schachter, R. L. Milne, J. L. Hopper, F. Andermann, S. F. Berkovic, Epilepsy in twins: insights from unique historical data of William Lennox. *Neurology* 62, 1127-1133 (2004).

21. I. Helbig, I. E. Scheffer, J. C. Mulley, S. F. Berkovic, Navigating the channels and beyond: unravelling the genetics of the epilepsies. Lancet Neurol 7, 231-245 (2008).

22. A. L. Peljto, C. Barker-Cummings, V. M. Vasoli, C. L. Leibson, W. A. Hauser, J. R. Buchhalter, R. Ottman, Familial risk of epilepsy: a population-based study. *Brain* 137, 795-805 (2014).

23. R. H. Thomas, S. F. Berkovic, The hidden genetics of epilepsy-a clinically important new paradigm. *Nat Rev Neurol* 10, 283-292 (2014).

24. I. Helbig, E. L. Heinzen, H. C. Mefford, I. G. Commission, Primer Part 1-The building blocks of epilepsy genetics. *Epilepsia* 57, 861-868 (2016).

25. I. Helbig, M. E. Swinkels, E. Aten, A. Caliebe, R. van 't Slot, R. Boor, S. von Spiczak, H. Muhle, J. A. Jahn, E. van Binsbergen, O. van Nieuwenhuizen, F. E. Jansen, K. P. Braun, G. J. de Haan, N. Tommerup, U. Stephani, H. Hjalgrim, M. Poot, D. Lindhout, E. H. Brilstra, R. S. Moller, B. P. Koeleman, Structural genomic variation in childhood epilepsies with complex phenotypes. *Eur J Hum Genet* 22, 896-901 (2014).

26. J. Wincent, S. Kolbjer, D. Martin, A. Luthman, P. Amark, M. Dahlin, B. M. Anderlid, Copy number variations in children with brain malformations and refractory epilepsy. *Am J Med Genet* A 167A, 512-523 (2015).

27. S. Rahman, Mitochondrial disease and epilepsy. *Dev Med Child Neuro*l 54, 397-406 (2012).

28. A. McTague, K. B. Howell, J. H. Cross, M. A. Kurian, I. E. Scheffer, The genetic landscape of the epileptic encephalopathies of infancy and childhood. *Lancet Neurol* 15, 304-316 (2016).

29. T. Klassen, C. Davis, A. Goldman, D. Burgess, T. Chen, D. Wheeler, J. McPherson, T. Bourquin, L. Lewis, D. Villasana, M. Morgan, D. Muzny, R. Gibbs, J. Noebels, Exome sequencing of ion channel genes reveals complex profiles confounding personal risk assessment in epilepsy. *Cell* 145, 1036-1048 (2011).

30. I. Helbig, D. H. Lowenstein, Genetics of the epilepsies: where are we and where are we going? *Curr Opin Neurol* 26, 179-185 (2013).

31. e.-a. u. e. a. International League Against Epilepsy Consortium on Complex Epilepsies. Electronic address, Genetic determinants of common epilepsies: a meta-analysis of genome-wide association studies. *Lancet Neurol* 13, 893-903 (2014).

32. I. Helbig, Genetic Causes of Generalized Epilepsies. *Semin Neurol* 35, 288-292 (2015).

33. O. K. Steinlein, Genetic mechanisms that underlie epilepsy. *Nat Rev Neurosci* 5, 400-408 (2004).

34. M. Puskarjov, P. Seja, S. E. Heron, T. C. Williams, F. Ahmad, X. Iona, K. L. Oliver, B. E. Grinton, L. Vutskits, I. E. Scheffer, S. Petrou, P. Blaesse, L. M. Dibbens, S. F. Berkovic, K. Kaila, A variant of KCC2 from patients with febrile seizures impairs neuronal Cl- extrusion and dendritic spine formation. *EMBO Rep* 15, 723-729 (2014).

35. G. L. Carvill, S. B. Heavin, S. C. Yendle, J. M. McMahon, B. J. O'Roak, J. Cook, A. Khan, M. O. Dorschner, M. Weaver, S. Calvert, S. Malone, G. Wallace, T. Stanley, A. M. Bye, A. Bleasel, K. B. Howell, S. Kivity, M. T. Mackay, V. Rodriguez-Casero, R. Webster, A. Korczyn, Z. Afawi, N. Zelnick, T. Lerman-Sagie, D. Lev, R. S. Moller, D. Gill, D. M. Andrade, J. L. Freeman, L. G. Sadleir, J. Shendure, S. F. Berkovic, I. E. Scheffer, H. C. Mefford, Targeted resequencing in epileptic encephalopathies identifies de novo mutations in CHD2 and SYNGAP1. *Nat Genet* 45, 825-830 (2013).

36. P. Rodenas-Cuadrado, N. Pietrafusa, T. Francavilla, A. La Neve, P. Striano, S. C. Vernes, Characterisation of CASPR2 deficiency disorder--a syndrome involving autism, epilepsy and language impairment. *BMC Med Genet* 17, 8 (2016).

37. Y. Fukata, M. Fukata, Epilepsy and synaptic proteins. *Curr Opin Neurobiol* 45, 1-8 (2017).

38. A. Poduri, When Should Genetic Testing Be Performed in Epilepsy Patients? *Epilepsy Curr* 17, 16-22 (2017).

39. L. A. Smith, J. F. Ullmann, H. E. Olson, C. M. Achkar, G. Truglio, M. Kelly, B. Rosen-Sheidley, A. Poduri, A Model Program for Translational Medicine in Epilepsy Genetics. *J Child Neurol* 32, 429-436 (2017).

40. T. T. Sands, H. Choi, Genetic Testing in Pediatric Epilepsy. *Curr Neurol Neurosci Rep* 17, 45 (2017).

41. M. A. Ream, A. D. Patel, Obtaining genetic testing in pediatric epilepsy. *Epilepsia* 56, 1505-1514 (2015).

42. L. A. Harkin, J. M. McMahon, X. Iona, L. Dibbens, J. T. Pelekanos, S. M. Zuberi, L. G. Sadleir, E. Andermann, D. Gill, K. Farrell, M. Connolly, T. Stanley, M. Harbord, F. Andermann, J. Wang, S. D. Batish, J. G. Jones, W. K. Seltzer, A. Gardner, C. Infantile Epileptic Encephalopathy Referral, G. Sutherland, S. F. Berkovic, J. C. Mulley, I. E. Scheffer, The spectrum of SCN1A-related infantile epileptic encephalopathies. *Brain* 130, 843-852 (2007).

43. S. M. Zuberi, A. Brunklaus, R. Birch, E. Reavey, J. Duncan, G. H. Forbes, Genotype-phenotype associations in SCN1A-related epilepsies. *Neurology* 76, 594-600 (2011).

44. C. Dravet, Dravet syndrome history. *Dev Med Child Neurol* 53 Suppl 2, 1-6 (2011).

45. C. Chiron, O. Dulac, The pharmacologic treatment of Dravet syndrome. *Epilepsia* 52 Suppl 2, 72-75 (2011).

46. L. A. Harkin, D. N. Bowser, L. M. Dibbens, R. Singh, F. Phillips, R. H. Wallace, M. C. Richards, D. A. Williams, J. C. Mulley, S. F. Berkovic, I. E. Scheffer, S. Petrou, Truncation of the GABA(A)-receptor gamma2 subunit in a family with generalized epilepsy with febrile seizures plus. *Am J Hum Genet* 70, 530-536 (2002).

47. A. Ishii, T. Kanaumi, M. Sohda, Y. Misumi, B. Zhang, N. Kakinuma, Y. Haga, K. Watanabe, S. Takeda, M. Okada, S. Ueno, S. Kaneko, S. Takashima, S. Hirose, Association of nonsense mutation in GABRG2 with abnormal trafficking of GABAA receptors in severe epilepsy. *Epilepsy Res* 108, 420-432 (2014).

48. G. L. Carvill, S. Weckhuysen, J. M. McMahon, C. Hartmann, R. S. Moller, H. Hjalgrim, J. Cook, E. Geraghty, B. J. O'Roak, S. Petrou, A. Clarke, D. Gill, L. G. Sadleir, H. Muhle, S. von Spiczak, M. Nikanorova, B. L. Hodgson, E. V. Gazina, A. Suls, J. Shendure, L. M. Dibbens, P. De Jonghe, I. Helbig, S. F. Berkovic, I. E. Scheffer, H. C. Mefford, GABRA1 and STXBP1: novel genetic causes of Dravet syndrome. *Neurology* 82, 1245-1253 (2014).

49. G. L. Holmes, J. L. Noebels, The Epilepsy Spectrum: Targeting Future Research Challenges. *Cold Spring Harb Perspect Med* 6, (2016).

50. H. C. Mefford, CNVs in Epilepsy. *Curr Genet Med Rep* 2, 162-167 (2014).

51. S. M. Sisodiya, Genetic screening and diagnosis in epilepsy? *Curr Opin Neurol* 28, 136-142 (2015).

52. C. T. Myers, H. C. Mefford, Advancing epilepsy genetics in the genomic era. *Genome Med* 7, 91 (2015).

53. R. S. Moller, H. A. Dahl, I. Helbig, The contribution of next generation sequencing to epilepsy genetics. *Expert Rev Mol Diagn* 15, 1531-1538 (2015).

54. D. Mei, E. Parrini, C. Marini, R. Guerrini, The Impact of Next-Generation Sequencing on the Diagnosis and Treatment of Epilepsy in Paediatric Patients. *Mol Diagn Ther,* (2017).

55. C. Chambers, L. A. Jansen, R. Dhamija, Review of Commercially Available Epilepsy Genetic Panels. *J Genet Couns* 25, 213-217 (2016).

56. J. R. Lemke, E. Riesch, T. Scheurenbrand, M. Schubach, C. Wilhelm, I. Steiner, J. Hansen, C. Courage, S. Gallati, S. Burki, S. Strozzi, B. G. Simonetti, S. Grunt, M. Steinlin, M. Alber, M. Wolff, T. Klopstock, E. C. Prott, R. Lorenz, C. Spaich, S. Rona, M. Lakshminarasimhan, J. Kroll, T. Dorn, G. Kramer, M. Synofzik, F. Becker, Y. G. Weber, H. Lerche, D. Bohm, S. Biskup, Targeted next generation sequencing as a diagnostic tool in epileptic disorders. *Epilepsia* 53, 1387-1398 (2012).

57. E. Della Mina, R. Ciccone, F. Brustia, B. Bayindir, I. Limongelli, A. Vetro, M. Iascone, L. Pezzoli, R. Bellazzi, G. Perotti, V. De Giorgis, S. Lunghi, G. Coppola, S. Orcesi, P. Merli, S. Savasta, P. Veggiotti, O. Zuffardi, Improving molecular diagnosis in epilepsy by a dedicated high-throughput sequencing platform. *Eur J Hum Genet* 23, 354-362 (2015).

58. S. Richards, N. Aziz, S. Bale, D. Bick, S. Das, J. Gastier-Foster, W. W. Grody, M. Hegde, E. Lyon, E. Spector, K. Voelkerding, H. L. Rehm, A. L. Q. A. Committee, Standards and guidelines for the interpretation of sequence variants: a joint consensus recommendation of the American College of Medical Genetics and Genomics and the Association for Molecular Pathology. *Genet Med* 17, 405-424 (2015).

59. E. Rossignol, K. Kobow, M. Simonato, J. A. Loeb, T. Grisar, K. L. Gilby, J. Vinet, S. D. Kadam, A. J. Becker, WONOEP appraisal: new genetic approaches to study epilepsy. *Epilepsia* 55, 1170-1186 (2014).

60. K. C. Epi, P. Epilepsy Phenome/Genome, A. S. Allen, S. F. Berkovic, P. Cossette, N. Delanty, D. Dlugos, E. E. Eichler, M. P. Epstein, T. Glauser, D. B. Goldstein, Y. Han, E. L. Heinzen, Y. Hitomi, K. B. Howell, M. R. Johnson, R. Kuzniecky, D. H. Lowenstein, Y. F. Lu, M. R. Madou, A. G. Marson, H. C. Mefford, S. Esmaeeli Nieh, T. J. O'Brien, R. Ottman, S. Petrovski, A. Poduri, E. K. Ruzzo, I. E. Scheffer, E. H. Sherr, C. J. Yuskaitis, B. Abou-Khalil, B. K. Alldredge, J. F. Bautista, S. F. Berkovic, A. Boro, G. D. Cascino, D. Consalvo, P. Crumrine, O. Devinsky, D. Dlugos, M. P. Epstein, M. Fiol, N. B. Fountain, J. French, D. Friedman, E. B. Geller, T. Glauser, S. Glynn, S. R. Haut, J. Hayward, S. L. Helmers, S. Joshi, A. Kanner, H. E. Kirsch, R. C. Knowlton, E. H. Kossoff, R. Kuperman, R. Kuzniecky, D. H. Lowenstein, S. M. McGuire, P. V. Motika, E. J. Novotny, R. Ottman, J. M. Paolicchi, J. M. Parent, K. Park, A. Poduri, I. E. Scheffer, R. A. Shellhaas, E. H. Sherr, J. J. Shih, R. Singh, J. Sirven, M. C. Smith, J. Sullivan, L. Lin Thio, A. Venkat, E. P. Vining, G. K. Von Allmen, J. L. Weisenberg, P. Widdess-Walsh, M. R. Winawer, De novo mutations in epileptic encephalopathies. *Nature* 501, 217-221 (2013).

61. C. Biervert, B. C. Schroeder, C. Kubisch, S. F. Berkovic, P. Propping, T. J. Jentsch, O. K. Steinlein, A potassium channel mutation in neonatal human epilepsy. *Science* 279, 403-406 (1998).

62. H. Saitsu, M. Kato, A. Koide, T. Goto, T. Fujita, K. Nishiyama, Y. Tsurusaki, H. Doi, N. Miyake, K. Hayasaka, N. Matsumoto, Whole exome sequencing identifies KCNQ2 mutations in Ohtahara syndrome. *Ann Neurol* 72, 298-300 (2012).

63. H. C. Martin, G. E. Kim, A. T. Pagnamenta, Y. Murakami, G. L. Carvill, E. Meyer, R. R. Copley, A. Rimmer, G. Barcia, M. R. Fleming, J. Kronengold, M. R. Brown, K. A. Hudspith, J. Broxholme, A. Kanapin, J. B. Cazier, T. Kinoshita, R. Nabbout, W. G. S. Consortium, D. Bentley, G. McVean, S. Heavin, Z. Zaiwalla, T. McShane, H. C. Mefford, D. Shears, H. Stewart, M. A. Kurian, I. E. Scheffer, E. Blair, P. Donnelly, L. K. Kaczmarek, J. C. Taylor, Clinical whole-genome sequencing in severe early-onset epilepsy reveals new genes and improves molecular diagnosis. *Hum Mol Genet* 23, 3200-3211 (2014).

64. D. Ulrich, B. Bettler, GABA(B) receptors: synaptic functions and mechanisms of diversity. *Curr Opin Neurobiol* 17, 298-303 (2007).

65. C. N. Connolly, K. A. Wafford, The Cys-loop superfamily of ligand-gated ion channels: the impact of receptor structure on function. *Biochem Soc Trans* 32, 529-534 (2004).

66. M. Farrant, Z. Nusser, Variations on an inhibitory theme: phasic and tonic activation of GABA(A) receptors. *Nat Rev Neurosci* 6, 215-229 (2005).

67. J. M. Fritschy, P. Panzanelli, GABAA receptors and plasticity of inhibitory neurotransmission in the central nervous system. *Eur J Neurosci* 39, 1845-1865 (2014).

68. J. C. Platel, B. Lacar, A. Bordey, GABA and glutamate signaling: homeostatic control of adult forebrain neurogenesis. *J Mol Histo*l 38, 303-311 (2007).

69. U. Rudolph, H. Mohler, GABA-based therapeutic approaches: GABAA receptor subtype functions. *Curr Opin Pharmacol* 6, 18-23 (2006).

70. S. Braat, R. F. Kooy, The GABAA Receptor as a Therapeutic Target for Neurodevelopmental Disorders. *Neuron* 86, 1119-1130 (2015).

71. R. W. Olsen, G. D. Li, M. Wallner, J. R. Trudell, E. J. Bertaccini, E. Lindahl, K. W. Miller, R. L. Alkana, D. L. Davies, Structural models of ligand-gated ion channels: sites of action for anesthetics and ethanol. *Alcohol Clin Exp Res* 38, 595-603 (2014).

72. Z. W. Chen, R. W. Olsen, GABAA receptor associated proteins: a key factor regulating $GABA_A$ receptor function. *J Neurochem* 100, 279-294 (2007).

73. T. C. Jacob, S. J. Moss, R. Jurd, GABA(A) receptor trafficking and its role in the dynamic modulation of neuronal inhibition. *Nat Rev Neurosci* 9, 331-343 (2008).

74. P. S. Miller, A. R. Aricescu, Crystal structure of a human $GABA_A$ receptor. *Nature* 512, 270-275 (2014).

75. R. E. Hibbs, E. Gouaux, Principles of activation and permeation in an anion-selective Cys-loop receptor. *Nature* 474, 54-60 (2011).

76. J. Du, W. Lu, S. Wu, Y. Cheng, E. Gouaux, Glycine receptor mechanism elucidated by electron cryo-microscopy. *Nature* 526, 224-229 (2015).

77. A. Nemecz, M. S. Prevost, A. Menny, P. J. Corringer, Emerging Molecular Mechanisms of Signal Transduction in Pentameric Ligand-Gated Ion Channels. *Neuron* 90, 452-470 (2016).

78. M. Vithlani, M. Terunuma, S. J. Moss, The dynamic modulation of GABA(A) receptor trafficking and its role in regulating the plasticity of inhibitory synapses. *Physiol Rev* 91, 1009-1022 (2011).

79. R. W. Olsen, W. Sieghart, $GABA_A$ receptors: subtypes provide diversity of function and pharmacology. *Neuropharmacology* 56, 141-148 (2009).

80. R. M. McKernan, P. J. Whiting, Which $GABA_A$-receptor subtypes really occur in the brain? *Trends Neurosci* 19, 139-143 (1996).

81. M. Mortensen, T. G. Smart, Extrasynaptic alphabeta subunit $GABA_A$ receptors on rat hippocampal pyramidal neurons. *J Physiol* 577, 841-856 (2006).

82. F. Araujo, D. Ruano, J. Vitorica, Native gamma-aminobutyric acid type A receptors from rat hippocampus, containing both alpha 1 and alpha 5 subunits, exhibit a single benzodiazepine binding site with alpha 5 pharmacological properties. *J Pharmacol Exp Ther* 290, 989-997 (1999).

83. P. M. Taylor, P. Thomas, G. H. Gorrie, C. N. Connolly, T. G. Smart, S. J. Moss, Identification of amino acid residues within GABA(A) receptor beta subunits that mediate both homomeric and heteromeric receptor expression. *J Neurosci* 19, 6360-6371 (1999).

84. Y. Pan, H. Ripps, H. Qian, Random assembly of GABA rho1 and rho2 subunits in the formation of heteromeric GABA(C) receptors. *Cell Mol Neurobiol* 26, 289-305 (2006).

85. S. W. Baumann, R. Baur, E. Sigel, Subunit arrangement of gamma-aminobutyric acid type A receptors. *J Biol Chem* 276, 36275-36280 (2001).

86. E. J. Botzolakis, K. N. Gurba, A. H. Lagrange, H. J. Feng, A. K. Stanic, N. Hu, R. L. Macdonald, Comparison of gamma-Aminobutyric Acid, Type A (GABAA), Receptor alphabetagamma and alphabetadelta Expression Using Flow Cytometry and Electrophysiology: EVIDENCE FOR ALTERNATIVE SUBUNIT STOICHIOMETRIES AND ARRANGEMENTS. *J Biol Chem* 291, 20440-20461 (2016).

87. R. Baur, E. Sigel, Low Expression in Xenopus Oocytes and Unusual Functional Properties of alpha1beta2gamma2 $GABA_A$ Receptors with Non-Conventional Subunit Arrangement. *PLoS One* 12, e0170572 (2017).

88. R. W. Olsen, W. Sieghart, International Union of Pharmacology. LXX. Subtypes of gamma-aminobutyric acid(A) receptors: classification on the basis of subunit composition, pharmacology, and function. Update. *Pharmacol Rev* 60, 243-260 (2008).

89. S. Pirker, C. Schwarzer, A. Wieselthaler, W. Sieghart, G. Sperk, GABA(A) receptors: immunocytochemical distribution of 13 subunits in the adult rat brain. *Neuroscience* 101, 815-850 (2000).

90. M. Mele, G. Leal, C. B. Duarte, Role of $GABA_AR$ trafficking in the plasticity of inhibitory synapses. *J Neurochem* 139, 997-1018 (2016).

91. P. Kofuji, J. B. Wang, S. J. Moss, R. L. Huganir, D. R. Burt, Generation of two forms of the gamma-aminobutyric acidA receptor gamma 2-subunit in mice by alternative splicing. *J Neurochem* 56, 713-715 (1991).

92. C. Daniel, H. Wahlstedt, J. Ohlson, P. Bjork, M. Ohman, Adenosine-to-inosine RNA editing affects trafficking of the gamma-aminobutyric acid type A (GABA(A)) receptor. *J Biol Chem* 286, 2031-2040 (2011).

93. E. Y. Rula, A. H. Lagrange, M. M. Jacobs, N. Hu, R. L. Macdonald, R. B. Emeson, Developmental modulation of GABA(A) receptor function by RNA editing. *J Neurosci* 28, 6196-6201 (2008).

94. H. L. Grabenstatter, S. J. Russek, A. R. Brooks-Kayal, Molecular pathways controlling inhibitory receptor expression. *Epilepsia* 53 Suppl 9, 71-78 (2012).

95. M. K. Mulligan, X. Wang, A. L. Adler, K. Mozhui, L. Lu, R. W. Williams, Complex control of GABA(A) receptor subunit mRNA expression: variation, covariation, and genetic regulation. *PLoS One* 7, e34586 (2012).

96. C. N. Connolly, B. J. Krishek, B. J. McDonald, T. G. Smart, S. J. Moss, Assembly and cell surface expression of heteromeric and homomeric gamma-aminobutyric acid type A receptors. *J Biol Chem* 271, 89-96 (1996).

97. I. Sarto-Jackson, W. Sieghart, Assembly of GABA(A) receptors (Review). *Mol Membr Biol* 25, 302-310 (2008).

98. W. N. Green, N. S. Millar, Ion-channel assembly. *Trends Neurosci* 18, 280-287 (1995).

99. J. T. Kittler, K. McAinsh, S. J. Moss, Mechanisms of $GABA_A$ receptor assembly and trafficking: implications for the modulation of inhibitory neurotransmission. *Mol Neurobiol* 26, 251-268 (2002).

100. W. Y. Lo, A. H. Lagrange, C. C. Hernandez, R. Harrison, A. Dell, S. M. Haslam, J. H. Sheehan, R. L. Macdonald, Glycosylation of {beta}2 subunits regulates $GABA_A$ receptor biogenesis and channel gating. *J Biol Chem* 285, 31348-31361 (2010).

101. F. K. Bedford, J. T. Kittler, E. Muller, P. Thomas, J. M. Uren, D. Merlo, W. Wisden, A. Triller, T. G. Smart, S. J. Moss, GABA(A) receptor cell surface number and subunit stability are regulated by the ubiquitin-like protein Plic-1. *Nat Neurosc*i 4, 908-916 (2001).

102. R. S. Saliba, M. Pangalos, S. J. Moss, The ubiquitin-like protein Plic-1 enhances the membrane insertion of $GABA_A$ receptors by increasing their stability within the endoplasmic reticulum. *J Biol Chem* 283, 18538-18544 (2008).

103. C. Fang, L. Deng, C. A. Keller, M. Fukata, Y. Fukata, G. Chen, B. Luscher, GODZ-mediated palmitoylation of GABA(A) receptors is required for normal assembly and function of GABAergic inhibitory synapses. *J Neurosci* 26, 12758-12768 (2006).

104. C. A. Keller, X. Yuan, P. Panzanelli, M. L. Martin, M. Alldred, M. Sassoe-Pognetto, B. Luscher, The gamma2 subunit of GABA(A) receptors is a substrate for palmitoylation by GODZ. *J Neurosci* 24, 5881-5891 (2004).

105. Y. Gu, S. L. Chiu, B. Liu, P. H. Wu, M. Delannoy, D. T. Lin, D. Wirtz, R. L. Huganir, Differential vesicular sorting of AMPA and $GABA_A$ receptors. *Proc Natl Acad Sci U S A* 113, E922-931 (2016).

106. A. J. Boileau, R. A. Pearce, C. Czajkowski, Tandem subunits effectively constrain $GABA_A$ receptor stoichiometry and recapitulate receptor kinetics but are insensitive to GABAA receptor-associated protein. *J Neurosci* 25, 11219-11230 (2005).

107. J. Mohrluder, M. Schwarten, D. Willbold, Structure and potential function of gamma-aminobutyrate type A receptor-associated protein. *FEBS J* 276, 4989-5005 (2009).

108. A. Mizokami, T. Kanematsu, H. Ishibashi, T. Yamaguchi, I. Tanida, K. Takenaka, K. I. Nakayama, K. Fukami, T. Takenawa, E. Kominami, S. J. Moss, T. Yamamoto, J. Nabekura, M. Hirata, Phospholipase C-related inactive protein is involved in trafficking of gamma2 subunit-containing GABA(A) receptors to the cell surface. *J Neurosci* 27, 1692-1701 (2007).

109. E. I. Charych, W. Yu, C. P. Miralles, D. R. Serwanski, X. Li, M. Rubio, A. L. De Blas, The brefeldin A-inhibited GDP/GTP exchange factor 2, a protein involved in vesicular trafficking, interacts with the beta subunits of the GABA receptors. *J Neurochem* 90, 173-189 (2004).

110. H. Goto, M. Terunuma, T. Kanematsu, Y. Misumi, S. J. Moss, M. Hirata, Direct interaction of N-ethylmaleimide-sensitive factor with GABA(A) receptor beta subunits. *Mol Cell Neurosci* 30, 197-206 (2005).

111. H. Wang, F. K. Bedford, N. J. Brandon, S. J. Moss, R. W. Olsen, GABA(A)-receptor-associated protein links GABA(A) receptors and the cytoskeleton. *Nature* 397, 69-72 (1999).

112. L. Chen, H. Wang, S. Vicini, R. W. Olsen, The gamma-aminobutyric acid type A ($GABA_A$) receptor-associated protein (GABARAP) promotes GABAA receptor clustering and modulates the channel kinetics. *Proc Natl Acad Sci U S A* 97, 11557-11562 (2000).

113. T. A. Leil, Z. W. Chen, C. S. Chang, R. W. Olsen, $GABA_A$ receptor-associated protein traffics $GABA_A$ receptors to the plasma membrane in neurons. *J Neurosci* 24, 11429-11438 (2004).

114. T. Kanematsu, I. S. Jang, T. Yamaguchi, H. Nagahama, K. Yoshimura, K. Hidaka, M. Matsuda, H. Takeuchi, Y. Misumi, K. Nakayama, T. Yamamoto, N. Akaike, M. Hirata, K. Nakayama, Role of the PLC-related, catalytically inactive protein p130 in GABA(A) receptor function. *EMBO J* 21, 1004-1011 (2002).

115. M. Terunuma, I. S. Jang, S. H. Ha, J. T. Kittler, T. Kanematsu, J. N. Jovanovic, K. I. Nakayama, N. Akaike, S. H. Ryu, S. J. Moss, M. Hirata, GABAA receptor phospho-dependent modulation is regulated by phospholipase C-related inactive protein type 1, a novel protein phosphatase 1 anchoring protein. *J Neurosci* 24, 7074-7084 (2004).

116. A. Togawa, N. Morinaga, M. Ogasawara, J. Moss, M. Vaughan, Purification and cloning of a brefeldin A-inhibited guanine nucleotide-exchange protein for ADP-ribosylation factors. *J Biol Chem* 274, 12308-12315 (1999).

117. J. T. Kittler, P. Rostaing, G. Schiavo, J. M. Fritschy, R. Olsen, A. Triller, S. J. Moss, The subcellular distribution of GABARAP and its ability to interact with NSF suggest a role for this protein in the intracellular transport of GABA(A) receptors. *Mol Cell Neurosci* 18, 13-25 (2001).

118. J. M. Fritschy, R. J. Harvey, G. Schwarz, Gephyrin: where do we stand, where do we go? *Trends Neurosci* 31, 257-264 (2008).

119. T. Saiyed, I. Paarmann, B. Schmitt, S. Haeger, M. Sola, G. Schmalzing, W. Weissenhorn, H. Betz, Molecular basis of gephyrin clustering at inhibitory synapses: role of G- and E-domain interactions. *J Biol Chem* 282, 5625-5632 (2007).

120. L. Saiepour, C. Fuchs, A. Patrizi, M. Sassoe-Pognetto, R. J. Harvey, K. Harvey, Complex role of collybistin and gephyrin in GABAA receptor clustering. *J Biol Chem* 285, 29623-29631 (2010).

121. Y. Nakamura, D. H. Morrow, A. Modgil, D. Huyghe, T. Z. Deeb, M. J. Lumb, P. A. Davies, S. J. Moss, Proteomic Characterization of Inhibitory Synapses Using a Novel pHluorin-tagged gamma-Aminobutyric Acid Receptor, Type A (GABAA), alpha2 Subunit Knock-in Mouse. *J Biol Chem* 291, 12394-12407 (2016).

122. S. Kowalczyk, A. Winkelmann, B. Smolinsky, B. Forstera, I. Neundorf, G. Schwarz, J. C. Meier, Direct binding of GABAA receptor beta2 and beta3 subunits to gephyrin. *Eur J Neurosci* 37, 544-554 (2013).

123. M. J. Alldred, J. Mulder-Rosi, S. E. Lingenfelter, G. Chen, B. Luscher, Distinct gamma2 subunit domains mediate clustering and synaptic function of postsynaptic GABAA receptors and gephyrin. *J Neurosci* 25, 594-603 (2005).

124. R. G. Fehon, A. I. McClatchey, A. Bretscher, Organizing the cell cortex: the role of ERM proteins. *Nat Rev Mol Cell Biol* 11, 276-287 (2010).

125. T. J. Hausrat, M. Muhia, K. Gerrow, P. Thomas, W. Hirdes, S. Tsukita, F. F. Heisler, L. Herich, S. Dubroqua, P. Breiden, J. Feldon, J. R. Schwarz, B. K. Yee, T. G. Smart, A. Triller, M. Kneussel, Radixin

regulates synaptic GABAA receptor density and is essential for reversal learning and short-term memory. *Nat Commun* 6, 6872 (2015).

126. S. Loebrich, R. Bahring, T. Katsuno, S. Tsukita, M. Kneussel, Activated radixin is essential for GABAA receptor alpha5 subunit anchoring at the actin cytoskeleton. *EMBO J* 25, 987-999 (2006).

127. J. T. Kittler, P. Delmas, J. N. Jovanovic, D. A. Brown, T. G. Smart, S. J. Moss, Constitutive endocytosis of GABAA receptors by an association with the adaptin AP2 complex modulates inhibitory synaptic currents in hippocampal neurons. *J Neurosci* 20, 7972-7977 (2000).

128. K. R. Smith, J. Muir, Y. Rao, M. Browarski, M. C. Gruenig, D. F. Sheehan, V. Haucke, J. T. Kittler, Stabilization of GABA(A) receptors at endocytic zones is mediated by an AP2 binding motif within the GABA(A) receptor beta3 subunit. *J Neurosci* 32, 2485-2498 (2012).

129. I. L. Arancibia-Carcamo, E. Y. Yuen, J. Muir, M. J. Lumb, G. Michels, R. S. Saliba, T. G. Smart, Z. Yan, J. T. Kittler, S. J. Moss, Ubiquitin-dependent lysosomal targeting of GABA(A) receptors regulates neuronal inhibition. *Proc Natl Acad Sci U S A* 106, 17552-17557 (2009).

130. J. T. Kittler, P. Thomas, V. Tretter, Y. D. Bogdanov, V. Haucke, T. G. Smart, S. J. Moss, Huntingtin-associated protein 1 regulates inhibitory synaptic transmission by modulating gamma-aminobutyric acid type A receptor membrane trafficking. *Proc Natl Acad Sci U S A* 101, 12736-12741 (2004).

131. S. Baulac, G. Huberfeld, I. Gourfinkel-An, G. Mitropoulou, A. Beranger, J. F. Prud'homme, M. Baulac, A. Brice, R. Bruzzone, E. LeGuern, First genetic evidence of GABA(A) receptor dysfunction in epilepsy: a mutation in the gamma2-subunit gene. *Nat Genet* 28, 46-48 (2001).

132. R. H. Wallace, C. Marini, S. Petrou, L. A. Harkin, D. N. Bowser, R. G. Panchal, D. A. Williams, G. R. Sutherland, J. C. Mulley, I. E. Scheffer, S. F. Berkovic, Mutant GABA(A) receptor gamma2-subunit in childhood absence epilepsy and febrile seizures. *Nat Genet* 28, 49-52 (2001).

133. R. L. Macdonald, J. Q. Kang, M. J. Gallagher, Mutations in $GABA_A$ receptor subunits associated with genetic epilepsies. *J Physiol* 588, 1861-1869 (2010).

134. H. A. Kuzmiak, L. E. Maquat, Applying nonsense-mediated mRNA decay research to the clinic: progress and challenges. *Trends Mol Med* 12, 306-316 (2006).

135. N. Amrani, R. Ganesan, S. Kervestin, D. A. Mangus, S. Ghosh, A. Jacobson, A faux 3'-UTR promotes aberrant termination and triggers nonsense-mediated mRNA decay. *Nature* 432, 112-118 (2004).

136. O. Isken, L. E. Maquat, Quality control of eukaryotic mRNA: safeguarding cells from abnormal mRNA function. *Genes Dev* 21, 1833-1856 (2007).

137. L. Linde, S. Boelz, G. Neu-Yilik, A. E. Kulozik, B. Kerem, The efficiency of nonsense-mediated mRNA decay is an inherent character and varies among different cells. *Eur J Hum Genet* 15, 1156-1162 (2007).

138. S. Maljevic, K. Krampfl, J. Cobilanschi, N. Tilgen, S. Beyer, Y. G. Weber, F. Schlesinger, D. Ursu, W. Melzer, P. Cossette, J. Bufler, H. Lerche, A. Heils, A mutation in the GABA(A) receptor alpha(1)-subunit is associated with absence epilepsy. *Ann Neurol* 59, 983-987 (2006).

139. J. Q. Kang, W. Shen, R. L. Macdonald, Two molecular pathways (NMD and ERAD) contribute to a genetic epilepsy associated with the GABA(A) receptor GABRA1 PTC mutation, 975delC, S326fs328X. *J Neurosci* 29, 2833-2844 (2009).

140. J. Q. Kang, R. L. Macdonald, Making sense of nonsense GABA(A) receptor mutations associated with genetic epilepsies. *Trends Mol Med* 15, 430-438 (2009).

141. X. Huang, M. Tian, C. C. Hernandez, N. Hu, R. L. Macdonald, The *GABRG2* nonsense mutation, Q40X, associated with Dravet syndrome activated NMD and generated a truncated subunit that was partially rescued by aminoglycoside-induced stop codon read-through. *Neurobiol Dis* 48, 115-123 (2012).

142. A. J. Johnston, J. Q. Kang, W. Shen, W. O. Pickrell, T. D. Cushion, J. S. Davies, K. Baer, J. G. Mullins, C. L. Hammond, S. K. Chung, R. H. Thomas, C. White, P. E. Smith, R. L. Macdonald, M. I. Rees, A novel GABRG2 mutation, p.R136*, in a family with GEFS+ and extended phenotypes. *Neurobiol Dis* 64, 131-141 (2014).

143. C. Kananura, K. Haug, T. Sander, U. Runge, W. Gu, K. Hallmann, J. Rebstock, A. Heils, O. K. Steinlein, A splice-site mutation in *GABRG2* associated with childhood absence epilepsy and febrile convulsions. *Arch Neurol* 59, 1137-1141 (2002).

144. M. Tian, R. L. Macdonald, The intronic *GABRG2* mutation, IVS6+2T->G, associated with childhood absence epilepsy altered subunit mRNA intron splicing, activated nonsense-mediated decay, and produced a stable truncated gamma2 subunit. *J Neurosci* 32, 5937-5952 (2012).

145. M. H. Smith, H. L. Ploegh, J. S. Weissman, Road to ruin: targeting proteins for degradation in the endoplasmic reticulum. *Science* 334, 1086-1090 (2011).

146. J. H. Claessen, L. Kundrat, H. L. Ploegh, Protein quality control in the ER: balancing the ubiquitin checkbook. *Trends Cell Biol* 22, 22-32 (2012).

147. M. Martinez-Vicente, A. M. Cuervo, Autophagy and neurodegeneration: when the cleaning crew goes on strike. *Lancet Neurol* 6, 352-361 (2007).

148. H. Sun, Y. Zhang, J. Liang, X. Liu, X. Ma, H. Wu, K. Xu, J. Qin, Y. Qi, X. Wu, SCN1A, SCN1B, and GABRG2 gene mutation analysis in Chinese families with generalized epilepsy with febrile seizures plus. *J Hum Genet* 53, 769-774 (2008).

149. J. Q. Kang, W. Shen, M. Lee, M. J. Gallagher, R. L. Macdonald, Slow degradation and aggregation in vitro of mutant $GABA_A$ receptor gamma2(Q351X) subunits associated with epilepsy. *J Neurosci* 30, 13895-13905 (2010).

150. J. Q. Kang, W. Shen, R. L. Macdonald, Trafficking-deficient mutant *GABRG2* subunit amount may modify epilepsy phenotype. *Ann Neurol* 74, 547-559 (2013).

151. J. Q. Kang, W. Shen, R. L. Macdonald, The GABRG2 mutation, Q351X, associated with generalized epilepsy with febrile seizures plus, has both loss of function and dominant-negative suppression. *J Neurosci* 29, 2845-2856 (2009).

152. D. Audenaert, E. Schwartz, K. G. Claeys, L. Claes, L. Deprez, A. Suls, T. Van Dyck, L. Lagae, C. Van Broeckhoven, R. L. Macdonald, P. De Jonghe, A novel GABRG2 mutation associated with febrile seizures. *Neurology* 67, 687-690 (2006).

153. X. Huang, C. C. Hernandez, N. Hu, R. L. Macdonald, Three epilepsy-associated GABRG2 missense mutations at the gamma+/beta- interface disrupt GABAA receptor assembly and trafficking by similar mechanisms but to different extents. *Neurobiol Dis* 68, 167-179 (2014).

154. M. J. Gallagher, L. Ding, A. Maheshwari, R. L. Macdonald, The GABAA receptor alpha1 subunit epilepsy mutation A322D inhibits transmembrane helix formation and causes proteasomal degradation. *Proc Natl Acad Sci* U S A 104, 12999-13004 (2007).

155. L. Ding, H. J. Feng, R. L. Macdonald, E. J. Botzolakis, N. Hu, M. J. Gallagher, GABA(A) receptor alpha1 subunit mutation A322D associated with autosomal dominant juvenile myoclonic epilepsy reduces the expression and alters the composition of wild type GABA(A) receptors. *J Biol Chem* 285, 26390-26405 (2010).

156.E. Eugene, C. Depienne, S. Baulac, M. Baulac, J. M. Fritschy, E. Le Guern, R. Miles, J. C. Poncer, GABA(A) receptor gamma 2 subunit mutations linked to human epileptic syndromes differentially affect phasic and tonic inhibition. *J Neurosci* 27, 14108-14116 (2007).

157. D. Ron, P. Walter, Signal integration in the endoplasmic reticulum unfolded protein response. *Nat Rev Mol Cell Biol* 8, 519-529 (2007).

158. B. M. Gardner, D. Pincus, K. Gotthardt, C. M. Gallagher, P. Walter, Endoplasmic reticulum stress sensing in the unfolded protein response. *Cold Spring Harb Perspect Biol* 5, a013169 (2013).

159. I. Tabas, D. Ron, Integrating the mechanisms of apoptosis induced by endoplasmic reticulum stress. *Nat Cell Biol* 13, 184-190 (2011).

160. T. A. Warner, W. Shen, X. Huang, Z. Liu, R. L. Macdonald, J. Q. Kang, Differential molecular and behavioural alterations in mouse models of GABRG2 haploinsufficiency versus dominant negative mutations associated with human epilepsy. *Hum Mol Genet* 25, 3192-3207 (2016).

161. J. Q. Kang, W. Shen, C. Zhou, D. Xu, R. L. Macdonald, The human epilepsy mutation GABRG2(Q390X) causes chronic subunit accumulation and neurodegeneration. *Nat Neurosci* 18, 988-996 (2015).

162. L. E. Betting, S. B. Mory, I. Lopes-Cendes, L. M. Li, M. M. Guerreiro, C. A. Guerreiro, F. Cendes, MRI reveals structural abnormalities in patients with idiopathic generalized epilepsy. *Neurology* 67, 848-852 (2006).

163. M. T. Bianchi, L. Song, H. Zhang, R. L. Macdonald, Two different mechanisms of disinhibition produced by GABAA receptor mutations linked to epilepsy in humans. *J Neurosci* 22, 5321-5327 (2002).

164. V. S. Janve, C. C. Hernandez, K. M. Verdier, N. Hu, R. L. Macdonald, Epileptic encephalopathy de novo GABRB mutations impair GABAA receptor function. *Ann Neurol*, (2016).

165. C. C. Hernandez, W. Kong, N. Hu, Y. Zhang, W. Shen, L. Jackson, X. Liu, Y. Jiang, R. L. Macdonald, Altered Channel Conductance States and Gating of GABAA Receptors by a Pore Mutation Linked to Dravet Syndrome. *eNeuro* 4, (2017).

166. M. Mantegazza, R. Rusconi, P. Scalmani, G. Avanzini, S. Franceschetti, Epileptogenic ion channel mutations: from bedside to bench and, hopefully, back again. *Epilepsy Res* 92, 1-29 (2010).

167. C. A. Wagner, B. Friedrich, I. Setiawan, F. Lang, S. Broer, The use of Xenopus laevis oocytes for the functional characterization of heterologously expressed membrane proteins. *Cell Physiol Biochem* 10, 1-12 (2000).

168. P. Thomas, T. G. Smart, HEK293 cell line: a vehicle for the expression of recombinant proteins. *J Pharmacol Toxicol Methods* 51, 187-200 (2005).

169. R. L. Macdonald, J. Q. Kang, M. J. Gallagher, in Jasper's Basic Mechanisms of the Epilepsies, J. L. Noebels, M. Avoli, M. A. Rogawski, R. W. Olsen, A. V. Delgado-Escueta, Eds. (Bethesda (MD), 2012).

170. M. P. Goldschen-Ohm, D. A. Wagner, S. Petrou, M. V. Jones, An epilepsy-related region in the GABA(A) receptor mediates long-distance effects on GABA and benzodiazepine binding sites. *Mol Pharmacol* 77, 35-45 (2010).

171. J. Q. Kang, R. L. Macdonald, The $GABA_A$ receptor gamma2 subunit R43Q mutation linked to childhood absence epilepsy and febrile seizures causes retention of alpha1beta2gamma2S receptors in the endoplasmic reticulum. *J Neurosci* 24, 8672-8677 (2004).

172. F. Sancar, C. Czajkowski, A $GABA_A$ receptor mutation linked to human epilepsy (gamma2R43Q) impairs cell surface expression of alphabetagamma receptors. *J Biol Chem* 279, 47034-47039 (2004).

173. T. G. Hales, H. Tang, K. A. Bollan, S. J. Johnson, D. P. King, N. A. McDonald, A. Cheng, C. N. Connolly, The epilepsy mutation, gamma2(R43Q) disrupts a highly conserved inter-subunit contact site, perturbing the biogenesis of $GABA_A$ receptors. *Mol Cell Neurosci* 29, 120-127 (2005).

174. H. O. Tan, C. A. Reid, F. N. Single, P. J. Davies, C. Chiu, S. Murphy, A. L. Clarke, L. Dibbens, H. Krestel, J. C. Mulley, M. V. Jones, P. H. Seeburg, B. Sakmann, S. F. Berkovic, R. Sprengel, S. Petrou, Reduced cortical inhibition in a mouse model of familial childhood absence epilepsy. *Proc Natl Acad Sci U SA* 104, 17536-17541 (2007).

175. C. Chiu, C. A. Reid, H. O. Tan, P. J. Davies, F. N. Single, I. Koukoulas, S. F. Berkovic, S. S. Tan, R. Sprengel, M. V. Jones, S. Petrou, Developmental impact of a familial $GABA_A$ receptor epilepsy mutation. *Ann Neuro*l 64, 284-293 (2008).

176. E. L. Hill, S. Hosie, R. S. Mulligan, K. L. Richards, P. J. Davies, C. M. Dube, T. Z. Baram, C. A. Reid, M. V. Jones, S. Petrou, Temperature elevation increases GABA(A) -mediated cortical inhibition in a mouse model of genetic epilepsy. Epilepsia 52, 179-184 (2011).

177. C. A. Reid, T. H. Kim, S. F. Berkovic, S. Petrou, Low blood glucose precipitates spike-and-wave activity in genetically predisposed animals. Epilepsia 52, 115-120 (2011).

178. C. A. Reid, T. Kim, A. M. Phillips, J. Low, S. F. Berkovic, B. Luscher, S. Petrou, Multiple molecular mechanisms for a single $GABA_A$ mutation in epilepsy. *Neurology* 80, 1003-1008 (2013).

179. G. Xia, P. P. S, T. A. Warner, C. Q. Zhang, L. M. R, J. Q. Kang, Altered $GABA_A$ receptor expression in brainstem nuclei and SUDEP in Gabrg2(+/Q390X) mice associated with epileptic encephalopathy. *Epilepsy Res* 123, 50-54 (2016).

180. F. Arain, C. Zhou, L. Ding, S. Zaidi, M. J. Gallagher, The developmental evolution of the seizure phenotype and cortical inhibition in mouse models of juvenile myoclonic epilepsy. *Neurobiol Dis* 82, 164-175 (2015).

181. L. Ding, M. J. Gallagher, Dynamics of sensorimotor cortex activation during absence and myoclonic seizures in a mouse model of juvenile myoclonic epilepsy. *Epilepsia* 57, 1568-1580 (2016).

182. C. A. Reid, S. F. Berkovic, S. Petrou, Mechanisms of human inherited epilepsies. *Prog Neurobiol 87, 41-57 (2009).*

183. S. Petrou, C. A. Reid, in Jasper's Basic Mechanisms of the Epilepsies, J. L. Noebels, M. Avoli, M. A. Rogawski, R. W. Olsen, A. V. Delgado-Escueta, Eds. (Bethesda (MD), 2012).

184. E.-R. E. S. C. Euro, P. Epilepsy Phenome/Genome, K. C. Epi, De novo mutations in synaptic transmission genes including DNM1 cause epileptic encephalopathies. *Am J Hum Genet* 95, 360-370 (2014).

185. K. L. Helbig, K. D. Farwell Hagman, D. N. Shinde, C. Mroske, Z. Powis, S. Li, S. Tang, I. Helbig, Diagnostic exome sequencing provides a molecular diagnosis for a significant proportion of patients with epilepsy. *Genet Med* 18, 898-905 (2016).

186. I. Helbig, M. von Deimling, E. D. Marsh, Epileptic Encephalopathies as Neurodegenerative Disorders. *Adv Neurobiol* 15, 295-315 (2017).

187. D. Shen, C. C. Hernandez, W. Shen, N. Hu, A. Poduri, B. Shiedley, A. Rotenberg, A. N. Datta, S. Leiz, S. Patzer, R. Boor, K. Ramsey, E. Goldberg, I. Helbig, X. R. Ortiz-Gonzalez, J. R. Lemke, E. D. Marsh, R. L. Macdonald, De novo *GABRG2* mutations associated with epileptic encephalopathies. *Brain* 140, 49-67 (2017).

188. J. Wang, D. Shen, G. Xia, W. Shen, R. L. Macdonald, D. Xu, J. Q. Kang, Differential protein structural disturbances and suppression of assembly partners produced by nonsense *GABRG2* epilepsy mutations: implications for disease phenotypic heterogeneity. *Sci Rep* 6, 35294 (2016).

189. S. Maljevic, C. A. Reid, S. Petrou, Models for discovery of targeted therapy in genetic epileptic encephalopathies. *J Neurochem*, (2017).

190. K. Johannesen, C. Marini, S. Pfeffer, R. S. Moller, T. Dorn, C. E. Niturad, E. Gardella, Y. Weber, M. Sondergard, H. Hjalgrim, M. Nikanorova, F. Becker, L. H. Larsen, H. A. Dahl, O. Maier, D. Mei, S. Biskup, K. M. Klein, P. S. Reif, F. Rosenow, A. F. Elias, C. Hudson, K. L. Helbig, S. Schubert-Bast, M. R. Scordo, D. Craiu, T. Djemie, D. Hoffman-Zacharska, H. Caglayan, I. Helbig, J. Serratosa, P. Striano, P. De Jonghe, S. Weckhuysen, A. Suls, K. Muru, I. Talvik, T. Talvik, H. Muhle, I. Borggraefe, I. Rost, R. Guerrini, H. Lerche, J. R. Lemke, G. Rubboli, S. Maljevic, Phenotypic spectrum of *GABRA1*: From generalized epilepsies to severe epileptic encephalopathies. *Neurology* 87, 1140-1151 (2016).

191. H. Kodera, C. Ohba, M. Kato, T. Maeda, K. Araki, D. Tajima, M. Matsuo, N. Hino-Fukuyo, K. Kohashi, A. Ishiyama, S. Takeshita, H. Motoi, T. Kitamura, A. Kikuchi, Y. Tsurusaki, M. Nakashima, N. Miyake, M. Sasaki, S. Kure, K. Haginoya, H. Saitsu, N. Matsumoto, De novo *GABRA1* mutations in Ohtahara and West syndromes. *Epilepsia* 57, 566-573 (2016).

192. P. Lachance-Touchette, P. Brown, C. Meloche, P. Kinirons, L. Lapointe, H. Lacasse, A. Lortie, L. Carmant, F. Bedford, D. Bowie, P. Cossette, Novel alpha1 and gamma2 $GABA_A$ receptor subunit mutations in families with idiopathic generalized epilepsy. *Eur J Neurosci* 34, 237-249 (2011).

193. P. Cossette, L. Liu, K. Brisebois, H. Dong, A. Lortie, M. Vanasse, J. M. Saint-Hilaire, L. Carmant, A. Verner, W. Y. Lu, Y. T. Wang, G. A. Rouleau, Mutation of *GABRA1* in an autosomal dominant form of juvenile myoclonic epilepsy. *Nat Genet* 31, 184-189 (2002).

194. E. Lien, A. K. Vatevik, R. Ostern, B. I. Haukanes, G. Houge, A second patient with a De Novo *GABRB1* mutation and epileptic encephalopathy. *Ann Neurol* 80, 311-312 (2016).

195. S. Srivastava, J. Cohen, J. Pevsner, S. Aradhya, D. McKnight, E. Butler, M. Johnston, A. Fatemi, A novel variant in GABRB2 associated with intellectual disability and epilepsy. *Am J Med Genet* A 164A, 2914-2921 (2014).

196. A. Ishii, J. Q. Kang, C. C. Schornak, C. C. Hernandez, W. Shen, J. C. Watkins, R. L. Macdonald, S. Hirose, A de novo missense mutation of GABRB2 causes early myoclonic encephalopathy. *J Med Genet* 54, 202-211 (2017).

197. L. Urak, M. Feucht, N. Fathi, K. Hornik, K. Fuchs, A GABRB3 promoter haplotype associated with childhood absence epilepsy impairs transcriptional activity. *Human molecular genetics* 15, 2533-2541 (2006).

198. M. Tanaka, R. W. Olsen, M. T. Medina, E. Schwartz, M. E. Alonso, R. M. Duron, R. Castro-Ortega, I. E. Martinez-Juarez, I. Pascual-Castroviejo, J. Machado-Salas, R. Silva, J. N. Bailey, D. Bai, A. Ochoa, A. Jara-Prado, G. Pineda, R. L. Macdonald, A. V. Delgado-Escueta, Hyperglycosylation and reduced GABA currents of mutated GABRB3 polypeptide in remitting childhood absence epilepsy. *Am J Hum Genet* 82, 1249-1261 (2008).

199. R. S. Moller, T. V. Wuttke, I. Helbig, C. Marini, K. M. Johannesen, E. H. Brilstra, U. Vaher, I. Borggraefe, I. Talvik, T. Talvik, G. Kluger, L. L. Francois, G. Lesca, J. de Bellescize, S. Blichfeldt, N. Chatron, N. Holert, J. Jacobs, M. Swinkels, C. Betzler, S. Syrbe, M. Nikanorova, C. T. Myers, L. H. Larsen, S. Vejzovic, M. Pendziwiat, S. von Spiczak, S. Hopkins, H. Dubbs, Y. Mang, K. Mukhin, H. Holthausen, K. L. van Gassen, H. A. Dahl, N. Tommerup, H. C. Mefford, G. Rubboli, R. Guerrini, J. R. Lemke, H. Lerche, H. Muhle, S. Maljevic, Mutations in GABRB3: From febrile seizures to epileptic encephalopathies. *Neurology* 88, 483-492 (2017).

200. Y. Zhang, W. Kong, Y. Gao, X. Liu, K. Gao, H. Xie, Y. Wu, Y. Zhang, J. Wang, F. Gao, X. Wu, Y. Jiang, Gene Mutation Analysis in 253 Chinese Children with Unexplained Epilepsy and Intellectual/Developmental Disabilities. *PLoS One* 10, e0141782 (2015).

201. K. C. E. a. e. k. c. e. Epi, K. C. Epi, De Novo Mutations in SLC1A2 and CACNA1A Are Important Causes of Epileptic Encephalopathies. *Am J Hum Genet* 99, 287-298 (2016).

202. A. Papandreou, A. McTague, N. Trump, G. Ambegaonkar, A. Ngoh, E. Meyer, R. H. Scott, M. A. Kurian, GABRB3 mutations: a new and emerging cause of early infantile epileptic encephalopathy. *Dev Med Child Neurol* 58, 416-420 (2016).

203. S. Hirose, A new paradigm of channelopathy in epilepsy syndromes: intracellular trafficking abnormality of channel molecules. *Epilepsy Res* 70 Suppl 1, S206-217 (2006).

204. M. Boillot, M. Morin-Brureau, F. Picard, S. Weckhuysen, V. Lambrecq, C. Minetti, P. Striano, F. Zara, M. Iacomino, S. Ishida, I. An-Gourfinkel, M. Daniau, K. Hardies, M. Baulac, O. Dulac, E. Leguern, R. Nabbout, S. Baulac, Novel *GABRG2* mutations cause familial febrile seizures. *Neurol Genet* 1, e35 (2015).

205. E. M. Reinthaler, B. Dejanovic, D. Lal, M. Semtner, Y. Merkler, A. Reinhold, D. A. Pittrich, C. Hotzy, M. Feucht, H. Steinbock, U. Gruber-Sedlmayr, G. M. Ronen, B. Neophytou, J. Geldner, E. Haberlandt, H. Muhle, M. A. Ikram, C. M. van Duijn, A. G. Uitterlinden, A. Hofman, J. Altmuller, A. Kawalia, M. R. Toliat, E. C. Euro, P. Nurnberg, H. Lerche, M. Nothnagel, H. Thiele, T. Sander, J. C. Meier, G. Schwarz, B. A. Neubauer, F. Zimprich, Rare variants in gamma-aminobutyric acid type A receptor genes in rolandic epilepsy and related syndromes. *Ann Neurol* 77, 972-986 (2015).

206. M. Tian, D. Mei, E. Freri, C. C. Hernandez, T. Granata, W. Shen, R. L. Macdonald, R. Guerrini, Impaired surface alphabetagamma GABA(A) receptor expression in familial epilepsy due to a *GABRG2* frameshift mutation. *Neurobiol Dis* 50, 135-141 (2013).

207. L. M. Dibbens, H. J. Feng, M. C. Richards, L. A. Harkin, B. L. Hodgson, D. Scott, M. Jenkins, S. Petrou, G. R. Sutherland, I. E. Scheffer, S. F. Berkovic, R. L. Macdonald, J. C. Mulley, *GABRD* encoding a protein for extra- or peri-synaptic $GABA_A$ receptors is a susceptibility locus for generalized epilepsies. *Human molecular genetics* 13, 1315-1319 (2004).

Chapter 2: *De novo GABRG2* mutations associated with epileptic encephalopathies

Dingding Shen,[*] Ciria C. Hernandez,[*] Wangzhen Shen, Ningning Hu, Annapurna Poduri, Beth Shiedley, Alex Rotenberg, Alexandre N. Datta, Steffen Leiz, Steffi Patzer, Rainer Boor, Kerri Ramsey, Ethan Goldberg, Ingo Helbig, Xilma R. Ortiz-Gonzalez, Johannes R. Lemke, Eric D. Marsh, and Robert L. Macdonald

[*]Both authors contributed equally to the manuscript.

This work has been published in Brain. 140:49-67 (2017)

1. Abstract

Epileptic encephalopathies are a devastating group of severe childhood onset epilepsies with medication resistant seizures and poor developmental outcomes. Many epileptic encephalopathies have a genetic etiology and are often associated with *de novo* mutations in genes mediating synaptic transmission, including $GABA_A$ receptor subunit genes. Recently, we performed next generation sequencing on patients with a spectrum of epileptic encephalopathy phenotypes, and we identified five novel (A106T, I107T, P282S, R323W and F343L) and one known (R323Q) *de novo GABRG2* pathogenic variants (mutations) in eight patients. To gain insight into the molecular basis for how these mutations contribute to epileptic encephalopathies, we compared the effects of the mutations on the properties of recombinant α1β2γ2L $GABA_A$ receptors transiently expressed in HEK293T cells. Using a combination of patch clamp recording, immunoblotting, confocal imaging and structural modeling, we characterized the effects of these *GABRG2* mutations on $GABA_A$ receptor biogenesis and channel function. Compared with wild-type α1β2γ2L receptors, $GABA_A$ receptors containing a mutant γ2 subunit had reduced cell surface expression with altered subunit stoichiometry or decreased GABA-evoked whole-cell current amplitudes, but with different levels of reduction. While a causal role of these mutations cannot be established directly from these results, the functional analysis together with the genetic information suggests that these *GABRG2* variants may be major contributors to the epileptic encephalopathy phenotypes.

Our study further expands the *GABRG2* phenotypic spectrum and supports growing evidence that defects in GABAergic neurotransmission participate in the pathogenesis of genetic epilepsies including epileptic encephalopathies.

Keywords: Epileptic encephalopathy; $GABA_A$ receptor*; GABRG2; de novo* mutation; next generation sequencing

Abbreviations: EE = Epileptic encephalopathy, *GABR* = $GABA_A$ receptor subunit gene

2. Introduction

Epileptic encephalopathies (EEs) are a devastating group of severe infantile and childhood onset epilepsies, which are clinically and etiologically heterogeneous and characterized by intractable seizures, neurodevelopmental impairment, and poor prognosis (*1*). Because of the severity of the seizures and the associated intellectual and behavioral disabilities, the children and their families often suffer from substantial economic, social, and emotional burdens (*2*).

Due to developments in massively parallel sequencing technologies, a significant proportion of EE patients' etiologies have been shown to be genetic in nature. EE patients usually have limited or no family history of epilepsy and pathogenic variants typically arise *de novo* (*3*). Trio whole exome sequencing, in which the genomes of the individual with epilepsy and both parents are sequenced, is a powerful tool for dissecting the genetic basis of EEs (*4*). Use of targeted epilepsy-related gene panels for next generation sequencing is an alternative approach for identifying candidate *de novo* variants in sporadic cases of EE (*5*). Increased efficiency and reduced cost of these technologies have enabled discovery of numerous new EE genes with unprecedented success (*6*). The majority of the genes identified, to date, are involved in regulating synaptic transmission (*7*), which is not surprising given the importance of synaptic function in regulating excitability in the brain.

$GABA_A$ receptors mediate the majority of fast inhibitory neurotransmission and control network excitability in the brain. They are heteropentameric GABA-gated chloride ion channels, and the α1β2γ2 receptor is the most abundant $GABA_A$ receptor subtype in the CNS (*8*). The γ2 subunits are abundantly expressed and play important roles in receptor trafficking, clustering, synaptic maintenance (*9, 10*) and current kinetic properties (*11*). Hence, dysfunctions of $GABA_A$ receptor γ2 subunits have been postulated to be involved in the etiology of epilepsy. In fact, among currently known epilepsy-associated mutations identified in $GABA_A$ receptor subunits, over half of them are found in the $GABA_A$ receptor γ2 subunit gene, *GABRG2* (*12*). A substantial number of *GABRG2* mutations have been associated with autosomal dominant genetic epilepsies (GEs), ranging from relatively benign febrile seizures (FS) and childhood absence epilepsy (CAE) to more severe genetic epilepsy with febrile seizures plus (GEFS+) and Dravet Syndrome (*13*). *In vitro* studies have demonstrated that these *GABRG2* mutations exhibited a wide array of functional deficits, including alternation of RNA processing or protein stability, channel kinetic defects, and dominant negative effects (*14*). Moreover, heterozygous knock in (KI) mice bearing human *GABRG2* epilepsy mutations had reduced cortical inhibition and displayed epilepsy phenotypes (*13, 15, 16*).

Given the critical role of γ2 subunits and the reported *GABRG2* mutations in a broad spectrum of epilepsy syndromes, we wondered whether rare pathogenic *GABRG2* variants might also contribute to the etiology of EE. To test this hypothesis, we carried out next-generation sequencing in parent-offspring trios with a wide range of intractable EE phenotypes and searched for *de novo GABRG2* mutations. Six *de novo* missense *GABRG2* mutations (A106T, I107T, P282S, R323Q, R323W and F343L) were discovered in eight isolated patients. We obtained the patients' clinical history and investigated functional effects of these *de novo GABRG2* mutations on $GABA_A$ receptor biogenesis, trafficking and function *in vitro*. $GABA_A$ receptor α1 and β2 subunits were co-expressed with wild-type or mutant γ2 subunits in HEK 293T cells. Using this heterologous expression system, we found that all of these *de novo GABRG2* mutations impaired $GABA_A$

receptor biogenesis and/or channel function, but to different extents. Furthermore, we characterized mutation-induced alternations of secondary and tertiary structures of $GABA_A$ receptors based on structural modeling. Our genetic and functional findings provide strong evidence that *GABRG2* mutations are a genetic risk factor for the development of EE.

3. Materials and methods

Patient phenotypes

Seven patients, (six female/one male) were selected for sequencing due to having an intractable early onset epilepsy. The eighth patient (female) was tested for severe intellectual disability, movement disorder and early onset seizures. The patients were collected from multiple sites, four European clinical programs (University of Basal, University of Leipzig, Clinic for Children and Adolescents Munich, Clinic for Children and Adolescents Halle [IH, JRL, SP, SL, RB, AD]), and three American pediatrics programs (Children's Hospital of Philadelphia [EDM, EG, XOG], Boston Children's Hospital [AP, BS, AR], and Center for Rare Childhood Disorders, TGEN [KR]). De-identified clinical information was collected and compared across all patients as part of a case series. Five patients were identified on comprehensive epilepsy panels as clinical testing, one by clinical whole exome sequencing, and two by research exome sequencing.

Whole exome sequencing and analysis

Whole exome sequencing was performed for one patient at the Duke University Sequencing core (Duke CHGV) using the Illumina Genome Analyzer IIx massively parallel sequencing system (Illumina, Inc., San Diego, CA) as previously published (*17*). Alignment to the human genome (reference build hg18) was conducted with BWA version 0.5.5. Consensus and variant calls were performed using SAMtools version 0.1.7. Annotation, filtering for quality and removal of potential variants present in dbSNP129 or in 220 individuals from a group non-enriched for neuropsychiatric phenotypes, and prediction of functional effects of

potential mutations were performed using Sequent Variant Analyzer (SVA) (http://people.genome.duke.edu). The research laboratory believed the variant was pathogenic.

WES was performed at the TGen research laboratory in another patient using the following protocol. Libraries were prepared using the Illumina's TruSeq DNA sample preparation kit and the TruSeq exome enrichment kit following the manufacturer's protocol. Sequencing was done by 100-bp paired-end sequencing on a Illumina HiSeq2000 instrument. Reads were aligned to the Human Genome (Hg19/GRC37) using Burrows-Wheeler transform alignment (BWA v.0.7.5)1. PCR duplicates were removed using Picard v.1.922, and base quality recalibration, indel realignment and single nucleotide polymorphism (SNP) and indel discovery were performed using the Genome Analysis Toolkit (GATK v.2.5-2)3. Variants were annotated with SnpEff 3.2a and selected (SnpSift) for protein-coding events. Prediction scores were loaded from dbNSFP and used for filtering. This variant was considered probably pathogenic and was validated by GeneDx.

In one patient, the *GABRG2* variant was found on clinical exome sequencing through GeneDx (XomeDX, Gene DX, Gaithersburg MD) as per their clinical protocol (for details see http://www.genedx.com/test-catalog/xomedx/). GeneDx reported the mutation (c.1027T>C) as Variant, Likely Mutation.

Epilepsy panels

One patient was identified on the GeneDx comprehensive epilepsy panel (Infantile Epilepsy Panel, Gene DX, Gaithersburg MD) and reported as a variant of uncertain significance. Subsequent parental testing revealed the mutation to be *de novo*. The panel was performed as per GeneDx available methodology (http://www.genedx.com/test-catalog/available-tests/infantile-epilepsy-panel/).

Four European patients identified through the CeGaT epilepsy panel (CeGaT GmbH, Tübingen, Germany). All were called pathogenic or likely pathogenic based on the recent guideline from the ACMG (*18*). The panel targeted 119 genes (www.cegat.de/diagnostik/panel-diagnostik/epilepsie-und-migraene/) and was performed as previously described (*19*). In brief, the sequencing was performed by enriching for coding regions and exon-intron boundaries using Agilent SureSelect technology (Agilent Technologies, Santa Clara, California, USA) and sequencing on an Illumina HiSeq2500 platform (Illumina, San Diego, California, USA). Annotation was performed using SAMtools (v0.1.18) and VarScan (v2.3). Variants were selected with a minor allele frequency below 5% (according to 1000 Genomes, dbSNP, EVS and in-house database). More than 98% of targets had at least 30x coverage. Validation of suspicious variants as well as segregation analysis in both parents were performed by post-hoc standard Sanger sequencing.

Complementary DNA (cDNA) constructs

The coding sequences of human α1, β2 and γ2L $GABA_A$ receptor subunits and EGFP were cloned into pcDNA3.1 (+) expression vectors (Invitrogen). Mutant γ2L subunit constructs were generated using the QuikChange site-directed mutagenesis kit (Agilent) and confirmed by DNA sequencing. Due to the lack of a highly specific antibody against the extracellular domain of the γ2 subunit, N-terminal HA-tagged ($\gamma2L^{HA}$) subunits were employed. The HA epitope was inserted between the 4th and 5th residue of the mature γ2L subunit, a functionally silent position (*20*). Note that all subunit residues were numbered based on the immature peptide that includes the signal peptide.

Cell culture and transfection

HEK293T cells (ATCC, CRL-11268) were cultured at 37°C in humidified 5% CO_2 incubator and maintained in Dulbecco's modified Eagle's medium (Invitrogen) supplemented with 10% fetal bovine serum (Life technologies), and 100 IU/ml penicillin/ streptomycin (Life technologies). Cells were transfected using polyethylenimine (PEI) reagent (40 kD, Polysciences) at a DNA: transfection reagent ration of 1:2.5, and

harvested 36 hours after transfection. To express wild-type and mutant α1β2γ2 receptors, a total of 3 μg of subunit cDNAs were transfected at a ratio of 1:1:1 into 6 cm dishes for most experiments except for whole-cell recording. For the mock-transfected condition, empty pcDNA3.1 vector was added to make a final cDNA transfection amount to 3 μg.

Western Blot and surface biotinylation

Transfected HEK293T cells were collected in modified RIPA buffer (50 mM Tris (pH = 7.4), 150 mM NaCl, 1% NP-40, 0.2% sodium deoxycholate, 1 mM EDTA) and 1% protease inhibitor cocktail (Sigma). Collected samples were subjected to gel electrophoresis using 4-12% BisTris NuPAGE precast gels (Invitrogen) and transferred to PVDF-FL membranes (Millipore). Polyclonal anti-γ2 antibodies (Alomone or Millipore) were used to detect $GABA_A$ receptor γ2 subunits. Anti-Na^+/K^+ ATPase antibody (Abcam) was used as a loading control. IRDye® (LI-COR Biosciences) conjugated secondary antibody was used at a 1:10,000 dilution in all cases. Membranes were scanned using the Odyssey Infrared Imaging System (LI-COR Biosciences). The integrated intensity value of bands was determined using the Odyssey Image Studio software (LI-COR Biosciences).

Biotinylation protocols have been described previously (*21*). Briefly, transfected cells were incubated in membrane-impermeable reagent sulf-HNS-SS-biotin (1 mg/ml, Thermo Scientific) at 4°C for 40 min. Cells were lysed after being quenched with 0.1 M glycine. Lysates were cleared by after centrifugation and then incubated overnight with High Binding Capacity NeutrAvidin beads (Thermo Scientific Pierce). After incubation, protein was eluted in sampling buffer (Invitrogen) containing 10% beta-mercaptoethanol and subjected to immunoblotting.

Flow cytometry

Flow cytometry was performed to determine surface expression levels of $\gamma 2L^{HA}$ subunits. Cells were collected 36-48 h after transfection in FACS buffer composed of phosphate-buffered saline, 2% fetal bovine serum, and 0.05% sodium azide. Cells were then incubated with monoclonal anti-HA epitope tag. Following primary antibody incubation, cells were stained again with Alexa647-conjugated anti-mouse IgG secondary antibody (Invitrogen) and fixed by 2% paraformaldehyde.

The fluorescence signals were read using a BD LSR II 3/5-laser flow cytometer (BD Biosciences) and analyzed offline using FlowJo 7.5.5 (Tree Star). For each experimental condition, 10,000 cells in the final gate were acquired. Mean fluorescence intensity (FI) of samples was calculated after subtracting the mean FI of the cells in the mock-transfected condition. The relative FI for each condition was calculated by normalizing to the control ($\alpha 1\beta 2\gamma 2L^{HA}$). Flow cytometry experiments were performed in the VMC Flow Cytometry Shared Resource.

Immunocytochemistry and confocal microscopy

For immunofluorescence, cover slip-grown HEK293T cells were washed with PBS and fixed with Prefer (Anatech) to stain surface proteins or permeabilized with 0.5% Triton X-100 to stain total proteins. The fixed/permeabilized cells were blocked for 2 hours with 5% BSA in PBS, and then stained with primary antibodies overnight, followed by incubation in Alexa 488-conjugated donkey anti-rabbit IgG antibodies and Cy3-conjugated donkey anti-mouse IgG antibodies. Primary antibodies used were as the follows: rabbit monoclonal HA antibody (Cell signaling), mouse monoclonal α1 subunit antibody (Millipore), mouse monoclonal anti-calnexin antibody (Abcam). Coverslips were mounted with Prolong Gold antifade reagent (Thermo Fisher Scientific Inc.).

Confocal images were obtained from HEK293T cells using a Zeiss LSM 710 Meta inverted confocal microscope. Stained HEK293T cells were excited with the 488 nm laser for the Alexa 488 fluorophore signal and the 543 nm laser for the Cy3 fluorophore signal. Images were taken with 8 bit, 1024× 1024 pixel resolution. Pinholes were adjusted so that the sample thickness was 0.9 μm. An average of four scans was taken to decrease the background noise. Confocal experiments were performed in part using the VUMC Cell Imaging Shared Resource.

Colocalization analysis was performed using the Coloc2 plugin in the open source image processing program Fiji (*22*). Microscopic image files were imported, and the 2 channels (green and red) were separated. The 2 channels being compared were assigned to channel 1 (green) and channel 2 (red) in a manner consistent across all samples. A region of interest (ROI) surrounding individual cells was selected in the green channel, and its location was set in the Coloc2 panel. Both Pearson's correlation coefficient (R) and Manders' colocalization coefficient (MCC) were calculated.

Electrophysiology

Whole-cell recordings of wild-type and mutant $GABA_A$ receptor currents were obtained at room temperature from lifted HEK293T cells (*23*). The external solution was composed of (in mM): 142 NaCl, 8 KCl, 10 D(+)-glucose, 10 HEPES, 6 $MgCl_2.6H_2O$, and 1 $CaCl_2$ (pH 7.4, ~326 mOsm). The internal solution consisted of (in mM): 153 KCl, 10 HEPES, 5 EGTA 2 Mg-ATP, and 1 $MgCl_2.6H_2O$ (pH 7.3, ~300 mOsm). The Cl^- reversal potential was near 0 mV, and cells were voltage clamped at -20 mV. GABA (1 mM) was applied for 4 s for measurements of current amplitude and zinc inhibition. Zinc (10 μM) was pre-applied for 10 s followed by co-application with GABA. $GABA_A$ receptor current concentration–response curves were fitted using GraphPad Prism version 6.07 for Windows (GraphPad Software, La Jolla, CA). GABA was applied using a four-barrel square glass pipette connected to a SF-77B Perfusion Fast-Step system (Warner Instruments Corporations). The solution exchange time across the open electrode tip was ~200-400 μs, and the exchange

around lifted cells (~8-10 pF) occurred within 800 μs, which was sufficiently fast for these experiments (*24*) and guaranteed rapid solution exchanges and accurate measure of the kinetic properties of the receptor. All experiments were performed at room temperature (22–23°C). Whole cell currents were amplified and low-pass filtered at 2 kHz using an Axopatch 200B amplifier, digitized at 10 kHz using Digidata 1550, and saved using pCLAMP 10.4 (Axon Instruments). Data were analysed offline using Clampfit 10.4 (Axon Instruments). Activation onset and deactivation weight time constants (τ) were measured from currents obtained by application of 1 mM GABA for 10 ms, while peak current amplitude was measured from currents obtained by application of 1 mM GABA for 4 s. Activation and deactivation time constants (τ) were fitted using the Levenberg–Marquardt least squares method with up to four component exponential functions of the form $\sum a_n \exp(-t/\tau_n) + C$, where n is the number of the exponential components, t is time, a is the relative amplitude, τ_n is the time constant, and C is the residual current at the end of GABA application. Additional components were accepted only if they significantly improved the fit, as determined by an F test on the sum of squared residuals. The multiexponential time course of deactivation was presented as a weighted time constant, defined by the following expression: $\sum a_n \tau_n / \sum a_n$

Structural modeling and simulation

$GABA_A$ receptor α1, β2 and γ2 subunit raw sequences in FASTA format were individually loaded into Swiss-PdbViewer 4.10 for template search against the ExPDB database. The structure of the *Caenorhabditis elegans* glutamate-gated chloride channel (GluCl; PDB: 3RHW) was identified as a template using DeepView/Swiss-PdbViewer 4.02 (*25*) . The long cytoplasmic regions of $GABA_A$ receptor subunits were excluded from modeling as they were absent in the solved GluCl structure and separate alignments were generated for the TM4 domains. Full-length multiple alignments were submitted for automated comparative protein modeling incorporated in SWISS-MODEL program suite. The resulting subunit models were energy-optimized using GROMOS96 of the Swiss-PdbViewer. To generate pentameric $GABA_A$ receptor 3D models, α1, β2 and γ2 subunit structural models were assembled in a counter-clockwise β2-α1-β2-α1-γ2 order by

superposition onto the *C. elegans* GluCl channel. Neighborhood structural variability on the 3D $GABA_A$ receptor predicted by the γ2 subunit mutations were implemented using Rosetta 3.1 (*26*) (https://kortemmelab.ucsf.edu/backrub/cgi-bin/rosettaweb.py). Up to twenty of the best-scoring structures were generated for each mutation by choosing parameters recommended by the application. We measured mutation-induced structural differences by analyzing the root mean squared (RMS) deviation between the initial (wild-type) structures and superimposed simulated (mutated) structures. RMS deviation provides carbon-α/carbon-α comparisons between two structurally aligned models; the larger the RMS deviation, the more the mutant structure deviates from the wild-type structure. For each mutation, the average RMS deviation over ten lowest energy structures was computed. We prepared the figures using Chimera 1.7 (*27*).

Statistical analysis

Numerical data were reported as mean ± S.E.M. Statistical analysis was performed using GraphPad Prism version 6.07 for Windows (GraphPad Software, La Jolla, CA). Statistically significant differences were taken as $p < 0.05$ using one-way ANOVA followed by Dunnett's multiple comparison test.

4. Results

Mutation screening and *de novo GABRG2* variants

All eight patients, (seven female/one male) were selected for sequencing due to having an intractable early onset epilepsy. The testing was done at a mean age of 6.4 years (range 3 years to 10 years old). For six patients, sequencing was done as part of clinical evaluation using either epilepsy panels (n = 5) or WES (n = 1) at GeneDx or CeGaT. For the others, research WES sequencing was performed. In all eight patients, the variant was found to occur *de novo* in the child after testing the parental DNA (Fig. 2-1A).

Patient phenotypes

The clinical features of the eight patients with *GABRG2* variants were summarized in Table 2-1, and their representative EEG and brain MRI images were shown in Fig. 2-1. The age of onset of epilepsy was within the first year of life in all eight patients (range day of life 1 to 1 year of age). Seizure semiology at onset was described as tonic-clonic seizures in two patients, tonic seizures in three patients, partial seizures with secondary generalization in one patient, and febrile seizures in combination with myoclonic seizures in two patients. The epilepsy in these patients progressed in all except one patient (patient 8) with development of additional seizure types, which included atonic, generalized tonic clonic, absence and focal seizures. As EEs are a spectrum of disorders that include a number of named syndromes, we asked if any patient fit criteria for a specific electroclinical syndrome diagnosis (i.e. Infantile Spasms syndrome). No patients were given a diagnosis early, but three patients eventually had features of Lennox-Gastaut syndrome. Epilepsy outcome was variable, with two patients eventually becoming seizure free (patients 1 and 7), whereas the six other patients seizures remained intractable as of last follow up despite combination therapy with antiepileptic drugs. Physical and neurological examinations were remarkable for the presence of hypotonia in six patients, abnormal eye movements in four patients, and choreiform movements in four patients. There were no dysmorphic or other pathognomonic features on exam, and two patients (patients 5 and 7) were described as having normal physical and neurological examinations. Developmentally, all eight individuals had severe intellectual disability, were nonverbal, and had severe motor disabilities.

Additional studies of EEG and MRI in this cohort were also variable with no consistent findings. The initial EEG was normal in three patients (patient 1, 2 and 5), but over time all became abnormal. A variety of EEG abnormalities was found in patients with *GABRG2* variants (Fig. 2-1B) including seven of eight with either focal (three patients) or generalized (four patients) interictal epileptiform discharges. Brain MRIs were normal in five patients and showed mild nonspecific findings in three patients (delayed myelination, volume loss, and falx hypoplasia in one patient each) (Fig. 2-1C). These data suggest that *GABRG2* can lead to variable neurodevelopmental outcomes, including EE and abnormal motor development.

***De novo GABRG2* variants identified in patients with EE were located in different structural domains of $GABA_A$ receptor γ2 subunits**

Individual $GABA_A$ receptor γ2 subunits are composed of a large extracellular N-terminal domain, followed by four transmembrane domains (M1-M4) as well as extracellular (M2-M3) and two intracellular (M1-M2; M3-M4) loops (*28, 29*), and the six variants identified here were located in functionally important regions of the receptor channel (Fig. 2-2A). By analyzing the sequence alignment among the *GABRs*, we found that P282 and R323 were invariant residues across all $GABA_A$ receptor subunits, and F343 was a highly conserved residue (Fig. 2-2B). Consistently, *in silico* analysis using Polyphen-2 (*30*) and SIFT (*31*) predicted that the substitutions P282S, R323Q, R323W and F343L would not be tolerated and might damage protein structure. In contrast, the variants A106T and I107T, which were located in the non-conserved residue (Fig. 2-2B), were predicted to be tolerated.

$GABA_A$ receptors are hetero-pentameric proteins assembled with γ-β-α-β-α stoichiometry (Fig. 2-2C). Remarkably, γ2 subunit variants were mapped to locations that were closely connected among structural domains between the interface of the N-terminal (β1-β2 loop) and transmembrane domains (M1, M2 and M3). In the N-terminal domain, γ2(A106T) and γ2(I107T) variants occurred in the β1-β2 loop, whereas γ2(P282S), γ2(R323W), γ2(R323Q) and γ2(F343L) variants occurred in the transmembrane domains M1, M2 and M3 delineating the pore region of the receptor (Fig. 2-2B, C).

***De novo* $GABA_A$ receptor γ2 subunit variants found in EE patients decreased GABA-evoked currents to different extents and altered their Zn^{2+} sensitivity**

We determined the functional consequences of EE-associated γ2 subunit variants by measuring macroscopic GABA-evoked currents in transfected HEK293T cells (Fig. 2-3). All γ2 subunit variants decreased $GABA_A$ currents, but to different extents. While γ2L(A106T), γ2L(I107T), γ2L(P282S), and γ2L(F343L) variants

located at the N-terminal and M1 and M3 domains, decreased currents by ~30 % (Table 2-2), γ2L(R323W) and γ2L(R323Q) variants located in the pore forming M2 domain decreased channel current ~ 50 %, relative to wild-type currents (Table 2-2) (Fig. 2-3A, B). In addition, $GABA_A$ receptors containing γ2L(I107T), γ2L(P282S), γ2L(R323W) and γ2L(R323Q) variants increased by ~25 % the fractional Zn^{2+} inhibition of currents (Table 2-2) of the wild-type receptor (10 ± 1 %, n = 51) (Fig. 2-3C). No changes in Zn^{2+} sensitivity were found for $GABA_A$ receptors containing γ2L(A106T) and γ2L(F343L) variants (Table 2-2).

Decrease of current amplitudes can be produced by impaired biogenesis of receptors leading to decreased or altered expression of surface receptors or to mutation-induced alteration of surface receptor channel gating. Increased sensitivity of $GABA_A$ receptors to Zn^{2+} inhibition may be the result of the variant itself or of alterations in the subunit composition of receptors expressed on the cell surface such as formation of surface αβ receptors.

Mutant γ2 subunits were stable in transfected HEK293T cells, but with different total levels

The *GABRG2* EE-associated variants all decreased $GABA_A$ receptor currents due to impaired biogenesis or channel gating. To determine if these variants affected biogenesis of γ2 subunits, we expressed wild-type and mutant γ2L subunits with α1 and β2 subunits in HEK293T cells. Whole-cell lysates were analyzed by Western blot and immunoblotted using polyclonal γ2 subunit antibodies (Fig. 2-4).

Wild-type γ2L and mutant γ2L(A106T), γ2L(P282S), γ2L(R323Q), γ2L(R323W), and γ2L(F343L) subunits all migrated at the same molecular mass, predicted to be ~45 kD (Fig. 2-4A). The variant γ2L(I107T) introduced a new amino acid threonine two amino acids after asparagine 105, thus creating a new fourth potential glycosylation motif (NXS/T) in the extracellular domain. Unsurprisingly, in cells cotransfected with mutant γ2L(I107T) subunits, a main band with a shift in molecular mass compared with wild-type γ2L was detected, consistent with the increased glycosylation of the mutant protein (Fig. 2-4A). Interestingly and

unexpectedly, mutant γ2L(P282S) and γ2L(I107T) subunits also formed substantial amounts of protein complexes that migrated at a high molecular mass (~75-150 kD). It is very possible that these high-molecular-mass protein complexes are oligomers formed by mutant γ2 subunits as observed in γ2(Q390X) subunits (*13, 32*).

We then quantified the γ2 subunit band intensity of each lane, normalized to the ATPase band intensity of the same lane, and compared the normalized γ2/ATPase ratio among wild-type and mutant subunits (Fig. 2-4B). Total levels of mutant γ2L(A106T), γ2L(R323Q), γ2L(R323W), and γ2L(F343L) subunits did not differ from those of wild-type γ2L subunits (1.00, n = 4). In contrast, the total amount of mutant γ2L(I107T) and γ2L(P282S) subunits were increased to 1.62 ± 0.22 ($p < 0.05$, n = 4) and 1.76 ± 0.23 ($p < 0.05$, n = 4), respectively, suggesting that mutant γ2L(I107T) and γ2L(P282S) subunits were more stable than wild-type subunits and/or were retained in the endoplasmic reticulum (Fig. 2-4B).

The variants all decreased surface levels of γ2 subunits, but to different extents

We asked if mutant γ2 subunits could assemble with α1 and β2 subunits and traffic to cell membranes as functional receptors. To assess surface trafficking of mutant γ2 subunits, we cotransfected HEK293T cells with α1, β2, and wild-type or mutant γ2L subunits at a 1:1:1 α1:β2:γ2 subunit ratio and evaluated surface levels of wild-type and mutant γ2L subunits by surface biotinylation (Fig. 2-4C). Compared to coexpressed wild-type γ2L subunits (1.00, n = 6), surface levels of coexpressed mutant γ2L subunits were reduced to 0.74 ± 0.03 ($p < 0.05$, n = 6) for A106T, 0.76 ± 0.06 ($p < 0.05$, n = 6) for I107T, 0.65 ± 0.02 ($p < 0.05$, n = 4) for P282S, 0.73 ± 0.07 ($p < 0.05$, n = 5) for R323Q, 0.46 ± 0.09 ($p < 0.05$, n = 6) for R323W and 0.53 ± 0.05 ($p < 0.05$, n = 6) for F343L, respectively. These results demonstrated that A106T, I107T, P282S, R323Q, R323W and F343L substitutions all reduced surface levels of γ2L subunits, but to different extents (24 – 54%). The reductions in surface levels of γ2 subunits (Fig. 2-4D) were similar to the reductions in whole cell currents produced by these γ2 subunit variants (Fig. 2-3), suggesting that the variants may reduce biogenesis of

$GABA_A$ receptors. All of these *GABRG2* variants were *de novo* and their pathogenicity was confirmed by our functional characterization. Thus, we will refer to them as mutations instead of variants.

The γ2(I107T) mutation introduced a novel glycosylation site

To this point, we observed two principle effects of the γ2(I107T) mutation. First, it added a fourth glycosylation site to γ2(I107T) subunits, and second, there was decreased γ2(I107T) subunit surface expression. However, it remained unclear whether there was a causal relationship between these two phenomena. We therefore mutated the N-glycosylation site Asn-105 to glutamine in wild-type γ2 and mutant γ2(I107T) subunits, thereby creating glycosylation-defective subunits. The double mutant construct γ2(N105Q/I107T) disrupted the novel glycosylation sequence, although it retained the I107T mutation. We then coexpressed α1 and β2 subunits with wild-type $\gamma2L^{HA}$, wild-type/glycosylation-deficient $\gamma2L(N105Q)^{HA}$, mutant $\gamma2L(I107T)^{HA}$ and mutant/glycosylation-deficient $\gamma2L(N105Q/I107T)^{HA}$ subunits, and measured surface levels of $\gamma2L^{HA}$ subunits in each condition using flow cytometry (Fig. 2-5). With $\alpha1\beta2\gamma2L(N105Q)^{HA}$, $\alpha1\beta2\gamma2L(I107T)^{HA}$, and $\alpha1\beta2\gamma2L(N105Q/I107T)^{HA}$ subunit coexpression, surface HA levels were significantly reduced to 0.60 ± 0.06 ($p < 0.001$, n = 3), 0.48 ± 0.03 ($p < 0.001$, n = 11), and 0.69 ± 0.05 ($p < 0.001$, n = 4), respectively, compared with the wild-type condition. Immunoblotting for γ2 subunit surface protein yielded similar results (Fig. 2-4E). The molecular mass of the double mutant protein γ2(N105Q/I107T) returned to the size of wild-type level, as would be expected since the added glycosylation site was eliminated. Importantly, γ2L(N105Q), γ2L(I107T) and γ2L(N105Q/I107T) subunits all had lower surface expression level relative to wild-type γ2L subunit. Taken together, these results suggested that the I107T mutation itself and not the new glycosylation site at Asn-105 was the mechanism by which the I107T mutation impaired γ2L subunit surface incorporation and, $GABA_A$ receptor function.

Mutant γ2 subunits had different surface and intracellular distribution

We next extended our study to determine and compare the cellular locations of mutant and wild-type γ2 subunits in HEK293T cells using confocal microscopy (Fig. 2-6 and Fig. 2-7). Wild-type and mutant $\gamma2L^{HA}$ subunits were coexpressed in HEK293T cells with α1 and β2 subunits at a 1:1:1 cDNA ratio. We co-labeled cells with anti-α1 subunit (red) and anti-HA (green) antibodies. Without cell permeabilization, wild-type $\gamma2L^{HA}$ subunit signals were present on the surface and were colocalized well with α1 subunit signals, consistent with coassembly with α1 and β2 subunits into receptors that were trafficked to the cell surface (Fig 5A, yellow florescence is colocalization). In contrast, $\gamma2L(A106T)^{HA}$, $\gamma2L(I107T)^{HA}$, $\gamma2L(P282S)^{HA}$, $\gamma2L(R323Q)^{HA}$, $\gamma2L(R323W)^{HA}$ and $\gamma2L(F343L)^{HA}$ subunits all had reduced surface HA signals (lack or reduction of yellow florescence in Fig. 2-6 and Fig. 2-7).

With cell permeabilization and coexpression with α1 and β2 subunits, wild-type $\gamma2L^{HA}$ subunits were well distributed intracellularly (Fig. 2-6B). Coexpressed $\gamma2L(I107T)^{HA}$ and $\gamma2L(P282S)^{HA}$ subunits had more prominent intracellular HA signaling than wild-type $\gamma2L^{HA}$ subunits. This was consistent with the higher total amount of mutant γ2L(I107T) and γ2L(P282S) subunits in whole-cell lysates. However, the total expression of $\gamma2L(A106T)^{HA}$, $\gamma2L(R323Q)^{HA}$, $\gamma2L(R323W)^{HA}$ and $\gamma2L(F343L)^{HA}$ subunits was indistinguishable from that of wild-type $\gamma2L^{HA}$ subunits (Fig. 2-7B).

We observed that wild-type $\gamma2L^{HA}$ subunits were localized primarily to the plasma membrane. In contrast, mutant $\gamma2L(I107T)^{HA}$ and $\gamma2L(P282S)^{HA}$ subunits accumulated in cells and had impaired trafficking to the cell surface when coexpressed with α1 and β2 subunits. Given the previous results, we hypothesized that I107T and P282S mutations resulted in the retention of the mutated $\gamma2L^{HA}$ subunits in the ER. This was confirmed by colabeling permeabilized cells with anti-HA and anti-calnexin antibodies (Fig. 2-6C). Calnexin, a well-established ER marker, exhibits a typical perinuclear and reticular distribution suggestive of its ER

distribution. Wild-type $\gamma2L^{HA}$ subunits spread outside the ER, which presumably represented the newly synthesized subunits that were in transit to the cell surface. In contrast, mutant $\gamma2L(I107T)^{HA}$ and $\gamma2L(P282S)^{HA}$ subunits were found to be predominantly localized to the ER as evidenced by their colocalization with calnexin.

Quantification of the colocalization of mutant $\gamma2L(I107T)^{HA}$ and $\gamma2L(P282S)^{HA}$ subunits with the ER in HEK293T cells was shown in Fig. 2-6D. Correlation between the signal intensities of $\gamma2L^{HA}$ subunits and the ER was significantly stronger for both I107T ($R = 0.70 \pm 0.02$) and P282S ($R = 0.63 \pm 0.02$) mutations relative to the wild-type condition ($R = 0.33 \pm 0.06$), as measured by Pearson's correlation analysis. We also determined the interaction between γ2L subunits and the ER by quantifying the Manders' colocalization coefficient (MCC), which measures co-occurrence of two proteins independent of signal proportionality (*33, 34*). The Manders' coefficient M1 indicated the fraction of γ2L subunits that colocalized with the ER, whereas the Manders' coefficient M2 indicated the fraction of ER that colocalized with the γ2L subunits. In both cases, we observed that mutant $\gamma2L(I107T)^{HA}$ and $\gamma2L(P282S)^{HA}$ subunits had significantly increased colocalization with the ER (M1 of 0.71 ± 0.03 and 0.65 ± 0.02 in I107T and P282S, respectively, M2 of 0.75 ± 0.02 and 0.72 ± 0.01 in I107T and P282S, respectively), in comparison with wild-type γ2L subunits (M1 of 0.37 ± 0.02 and M2 of 0.46 ± 0.02).

De novo $GABA_A$ receptor γ2 subunit mutations found in EE patients altered the kinetic properties of $GABA_A$ receptor currents

Assembly of mutant subunits into surface $GABA_A$ receptors may impair channel gating by causing macroscopic kinetic changes of GABA-evoked currents. To address this possibility, we determined whether the EE-associated mutations altered the kinetic properties of functional $GABA_A$ receptors. Thus, we measured current desensitization, activation and deactivation rates of wild-type and mutant receptor currents.

$GABA_A$ receptor desensitization during 4 s GABA (1 mM) application was variably affected by γ2 subunit mutations (Fig. 2-8A). Thus, only the γ2L(R323Q) mutation significantly increased the extent of current desensitization (Table 2-2), whereas γ2L(A106T) and γ2L(R323W) mutations slowed desensitization (Fig. 2-8B, C). It is noteworthy that all of these mutations occur at the interface between the N-terminal domain and the pore region of the receptor (Fig. 2-2C and 2-8A, B).

We determined current activation and deactivation by measuring the current time constant (τ) at current onset (Fig. 2-8D) and at current offset (Fig. 2-8E) during and following the 10 ms GABA (1 mM) application. While most of the γ2 subunit mutations accelerated (A106T, F343L) or did not affect (I107T, P282S, R323W) receptor activation, the γ2L(R323Q) mutation significantly slowed it (Table 2-2) (Fig. 2-8F). The deactivation of the receptor was also affected but in opposite directions. Most of the γ2 subunit mutations slowed deactivation (A106T, I107T, P282S, F343L) (Fig. 2-8G). The γ2L(F343L) subunit mutation caused the greatest effect about 5 times the value of the wild-type condition (Table 2-2). Only γ2L(R323W) and γ2L(R323Q) subunit mutations accelerated deactivation (Fig. 2-8G).

Taken together, these results demonstrate that the primary effect of the γ2 subunit mutations was to reduce receptor biogenesis but the mutations also have variable, subunit-dependent effects on the kinetic properties that appeared to be correlated with the structural domain of the receptor where the mutation occurs. As a result, γ2 subunit mutations located near the interface between N-terminal domain and channel pore (A106T, I107T, P282S, and F343L) mainly accelerated activation and prolonged deactivation, and those in the pore (R323W and R323Q) accelerated deactivation of the receptor and decreased channel function by ~50 %.

***De novo* γ2 mutations decreased GABA potency by disrupting structural domains important for $GABA_A$ receptor function**

Changes in $GABA_A$ receptor potency appeared to be correlated with well-defined structural domains, which have been described as essential to receptor function (*24, 35-40*). To determine whether predicted changes in channel structure caused by the γ2 subunit mutations are related to changes in the $GABA_A$ receptor potency, we first generated wild-type and mutant pentameric αβγ $GABA_A$ receptor simulations (Fig. 2-9) using solved structures of the *C. Elegans* GluCl channel as template (*39*). We computed rearrangements of the subunit's secondary structure by computing the RMS deviation between the wild-type and mutant structural simulations (*41*) (Fig. 2-9A, C and E). When the perturbations of the secondary structure and side chain residues had RMS deviation values ≥ 0.5 Å, they were shown in rainbow colors on the simulation. Our simulations revealed that more than 1 subunit was affected. Structural changes were propagated through the entire structure, perturbing the Cys-loop, β1-β2 loop, Pre-M1 region, and M2-M3 loop at the extracellular junction between the N-terminal domain and transmembrane domain, which participate in the activation of the receptor. Subsequently, we measured the effects of the γ2 subunit mutations on GABA concentration-response curves (Fig. 2-9B, D and F). Peak $GABA_A$ receptor peak currents were obtained by applying various concentrations of GABA for 4 s to wild-type α1β2γ2L and mutant $GABA_A$ receptors. For wild-type α1β2γ2L $GABA_A$ receptors, the EC_{50} for current stimulation was 8.27 ± 1.16 μM, and the maximal current was 8922 ± 216 pA (n = 5-6). Therefore, we clustered the mutations by their structural location when assessing the disturbances that the mutation caused on the receptor structure and the measurable functional changes in $GABA_A$ receptor potency (see below).

γ2(A106T) and γ2(I107T) subunit mutations: These mutations are located in the β1-β2 inner loop in the N-terminal domain, at the interface between the principal (+) side of the γ2 subunit and the complementary (−) side of the β2 subunit, which delimits the γ+/β- interface (Fig. 2-9A). Mainly the structural perturbations were restricted to the γ2 subunit in the Cys-loop, β1–β2 loop and the M2–M3 loop on the mutant γ2(A106T)

subunit model and were propagated to Loop F of the neighboring β2 subunit on the mutant γ2(I107T) subunit model. It is noteworthy that when γ2L(A106T) and γ2L(I107T) subunits were co-expressed with wild-type α1 and γ2L subunits (Fig. 7B), the EC_{50} was shifted 6- to 2-fold to the right respectively (46.3 ± 1.22 μM; 14.3 ± 1.19 μM), with a reduction of 80-85 % in the maximal response to GABA (7117 ± 296 pA and 7585 ± 233 pA, respectively, n = 5-6).

γ2(R323W) and γ2(R323Q) subunit mutations: These mutations are located at the extracellular interface of the transmembrane α-helices M2 of the γ2 subunit, in the outermost portion of the pore of the receptor at the γ+/β- subunit interface (Fig. 2-9C). These mutations caused mainly rearrangements at α-helices M2, M3 and M2-M3 loop of the γ2 subunit towards the γ+/β- subunit interface of the receptor, and propagated to the α-helix Pre-M1 of the neighboring β2 subunit at the extracellular junction between the N-terminal and the transmembrane domains of the receptor. In contrast to wild-type receptors (Fig. 2-9D), the GABA concentration-response curves of γ2L(R323W) and γ2L(R323Q) subunits was shifted considerably, with EC_{50} right-shifted 13- to 3-fold (108 ± 1.13 μM; 20.2 ± 1.13 μM, respectively) and had substantial reduction of 58-69 % in the maximal response to GABA (5154 ± 165 pA and 6187 ± 129 pA, respectively, n = 5-6).

γ2(P282S) and γ2(F343L) subunit mutations: These mutations are located at the deeper portion of the transmembrane α-helices M1 and M3 of the γ2 subunit, towards the α+/γ- and γ+/β- subunit interfaces, respectively (Fig. 2-9E). While on the γ2(P282S) subunit simulation, structural perturbations occurred mainly at the α-helix M1 of the γ2 subunit, on the γ2(F343L) subunit simulation, structural perturbations occurred in the α-helices M2 and M3 of the γ2 subunit, and in the deeper region of the α-helix M1 of the neighboring β2 subunit. Distinct from the aforementioned γ2 subunit mutations that are located at the at the extracellular junction of the receptor, $GABA_A$ receptors expressing γ2L(R323W) and γ2L(R323Q) subunits had EC_{50}s similar to those of wild-type α1β2γ2L $GABA_A$ receptors (5.35 ± 1.33 μM; 7.82 ± 1.23 μM, respectively). In contrast, receptors with these mutant subunits displayed a similar reduction of 51-78 % in the maximal

response to GABA (4538 ± 198 pA and 6950 ± 220 pA, respectively, n = 5-6) (Fig. 2-9F). Remarkably, these findings clearly demonstrated that mutations that disrupt the structure of the coupling interface of $GABA_A$ receptors decreased GABA potency.

5. Discussion

Mutations in *GABRG2* have been most frequently associated with GEs among all the *GABRs* (*42*). However, clinical evidence implicating *GABRG2* mutations in EEs is still lacking. Here we present both genetic information and functional analysis that for the first time provides strong evidence that mutations in *GABRG2* may contribute to early onset EE.

GABRG2 mutations are associated with early onset EE

There were a few consistent clinical features of this cohort, including infantile onset seizures (less than 1 year) and severe intellectual disability without prominent brain MRI findings. None of these patients were originally diagnosed with a named infantile epilepsy syndrome (Ohtahara syndrome or Infantile Spasms syndrome (West Syndrome)), but three patients did progress to be diagnosed with the electroclinical pattern of Lennox-Gastaut syndrome. From this cohort, there was no distinguishing pathognomonic clinical feature associated with *GABRG2* mutations. This level of phenotypic pleiotropy is increasingly recognized across many epilepsy syndromes, and using the more broad diagnosis of early onset EE is appropriate. While the clinical features may not point to a specific pattern of disease, the genetic data, all patients carrying *de novo* changes with two recurrent variants, provides strong genetic evidence for the importance of *GABRG2* as an EE gene.

Pathophysiological mechanisms of EE-associated *GABRG2* mutations

Our electrophysiological experiments showed significant reductions in current amplitudes for all of these mutations, thus demonstrating directly a clear impairment of $GABA_A$ receptor function. Disease severity might be related to the extent of mutation-induced functional channel impairment, but this cannot be definitively established with this small cohort of patients. In addition, we demonstrated that these mutations reduced channel function to different extents and by diverse mechanisms including impaired surface expression, ER retention, and gating defects (overview in Table 2-3).

All of these γ2 subunit mutations produced significant, but variable, impairment of γ2 subunit surface expression, which is a common abnormality for *GABRG2* missense mutations (*21, 43*). A106T, R323Q, R323W and F343L mutations did not affect the total expression levels of γ2 subunits. In contrast, mutant γ2(I107T) and γ2(P282S) subunits were more stable than wild-type subunits and were retained predominantly within the ER, which is the location where immature $GABA_A$ receptor subunits reside once synthesized. The presence of ER-retained trafficking-deficient γ2 subunits has been demonstrated to produce ER stress (*44*). The sustained ER stress could lead to neurodegeneration, as evidenced by increased caspase 3 activation in older *Gabrg2*$^{+/Q390X}$ mice (*13*). Thus, it is possible that the misfolded mutant γ2(I107T) and γ2(P282S) subunit proteins could progressively accumulate and form aggregates inside neurons, which could affect function and survival of neurons *in vivo.*

Our finding that surface expression of γ2 subunits was reduced by the R323Q substitution was contrary to a previous study that reported that surface expression of γ2(R323Q) subunits was at the wild-type level (*45*). This conflict may have been due to the different γ2 subunit cDNAs used for transfection. In contrast to the PHluorin-tagged mouse γ2 subunit construct used in their study, we used HA-tagged or untagged human γ2 subunits.

EE-associated *GABRG2* mutations altered structural domains that decreased GABA potency

Our results demonstrated a structure-dysfunction correlation with the location of the mutation in the receptor. The substitutions A106T and I107T were located next to each other in the β1-β2 inner loop of the N-terminal extracellular domain that contributes to the γ+/β- subunit interface at the junction of the transmembrane domain that couples the opening of the receptor. The occurrence of these mutations demonstrates the importance of this domain in transducing GABA-binding-coupling once they caused a significant decrease in GABA sensitivity. In addition, the occurrence of the R323W and R323Q mutations in the outermost region of the transmembrane M2 facing the extracellular junction, also substantially decreased the sensitivity for GABA. Thus, the EE-associated *GABRG2* mutations located in the outermost region of the pore-forming domain of the receptor, which is the outer ring region between the N-terminal extracellular domain and the pore, directly altered $GABA_A$ receptor activation (*24, 37, 39*), and may contribute to the pathophysiological mechanism of the disease. In contrast, the P282S and F343L mutations, located in the transmembrane M1 and M3 of the γ2 subunit respectively, seemed not to contribute directly to the activation of the receptor due to lack of altered sensitivity to GABA. Nevertheless, they produced a significant decrease in the maximum response to GABA that might be accounted for by the altered expression and receptor kinetics. Similar decreases in the maximal response to GABA were found for mutations located in the transmembrane M2 with decreased surface expression. No mutations in transmembrane domains M1 and M3 of the γ2 subunit have ever been reported in epilepsy patients. Recently, three *de novo* mutations in the M1 domain of *GABRA1* were identified in patients with Ohtahara and West syndromes (*46*), one of those in a homologous position of the γ2 subunit, supporting the important role of the M1 domain in $GABA_A$ receptor function (*37*).

***GABRG2* mutations in GEs and phenotype/genotype correlations**

The first two GE-associated *GABRG2* mutations (K328M and R82Q) were reported in a family with GEFS+ (*47*) and a family with CAE and FS (*48*) in 2001. Up to now, a total of nineteen *GABRG2* epilepsy mutations have been identified in patients with simple FS and several different epilepsy syndromes (*49*). Before this

present study, it has been generally accepted that missense *GABRG2* mutations are associated with mild phenotypes including CAE and FS (*47, 48, 50, 51*), while nonsense *GABRG2* mutations lead to more severe phenotypes ranging from GEFS+ to Dravet syndromes (*44, 52-54*).

The current data demonstrated that missense *GABRG2* mutations could also lead to severe epilepsy phenotypes. Patients in our cohort showed a broad epilepsy phenotypic spectrum including Lennox-Gastaut syndrome and unclassified EEs. There were loose correlations between mutation type and disease severity. For example, among these *GABRG2* mutations, the I107T mutation had the most striking effect on $GABA_A$ receptor macroscopic current properties and cellular localization (Table 2-3). With respect to age of onset, motor development and, epilepsy outcomes, the most severe disease course was also seen in patient 3 with the I107T mutation. However, since there are only a small number of patients with *GABRG2* mutations and only the cohort in this report with EE, we cannot make a definitive statement about effect of mutation on channel function and EE severity. What is likely is that the clinical and biophysical effects of *GABRG2* mutations can be modified by the genetic background of the individual as evidenced by the difference in epilepsy phenotypes of KI mice with different genetic backgrounds (*16*) and that variants can be found in both an inherited and *de novo* pattern.

Conclusions

Collectively, our study employed a combination of massively parallel sequencing and *in vitro* functional assays and established that mutations of the *GABRG2* gene are genetic risk factors for EEs. This complemented the prevailing GABAergic channelopathy paradigm in epilepsy and broadened the phenotype of EEs associated with *GABRG2*. Our findings are of clinical significance, as $GABA_A$ receptors are known to be targets for epilepsy treatment (*55*). Identification of additional *GABRG2* mutations will no doubt guide further studies of the precise role of γ2 subunits in epileptogenesis and provide new insights into the targeted treatment for EEs. Our present results do not cover the full spectrum of possible mutation-induced channel

dysfunction, and the precise mechanisms by which mutations cause EE in humans remain to be clarified. Future studies in cultured neurons or in animal models will be required to study the downstream effects of these mutations in detail and solidify genotype-phenotype relationships in *GABRG2*-EE.

Acknowledgements: This work was supported by the NIH RO1 NS 33300 grant to RLM. The authors would like to thank Rebecca Kamens for clinical data entry and Dr. Erin Heinzen for access to the Duke Sequencing core.

Funding: The study was supported in part by NIH R01 NS33300 to RLM.

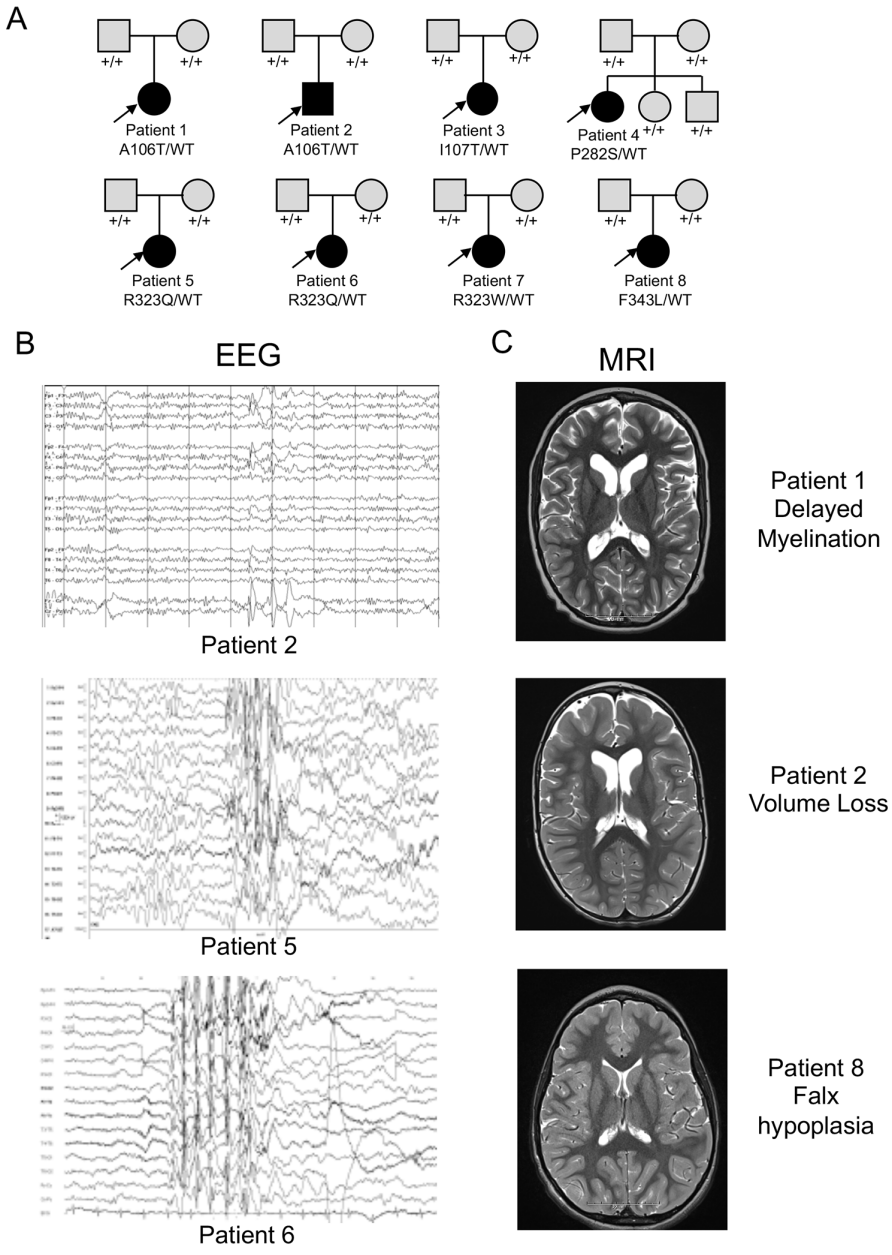

Figure 2-1: De novo *GABRG2* variants were identified in eight individuals with EE.
(A) Pedigrees and segregation analysis of the six *GABRG2* missense variants identified in eight patients. Arrows indicate probands. **(B)** Three representative EEGs are presented. The top EEG demonstrates excessive beta activity and focal discharges over the vertex head region. The lower two EEG traces show more diffuse background slowing and irregularly generalized (middle) and generalized (lower) epileptiform discharges. (**C)** Most of the brain MRIs were normal (not shown), but three patients had non specific findings and are presented (top MRI - delayed myelination of the frontal lobes; middle MRI – hypoplasia of the falx; bottom MRI - enlarged ventricles and extraaxial CSF spaces for age). All MRIs are presented at level of head of caudate.

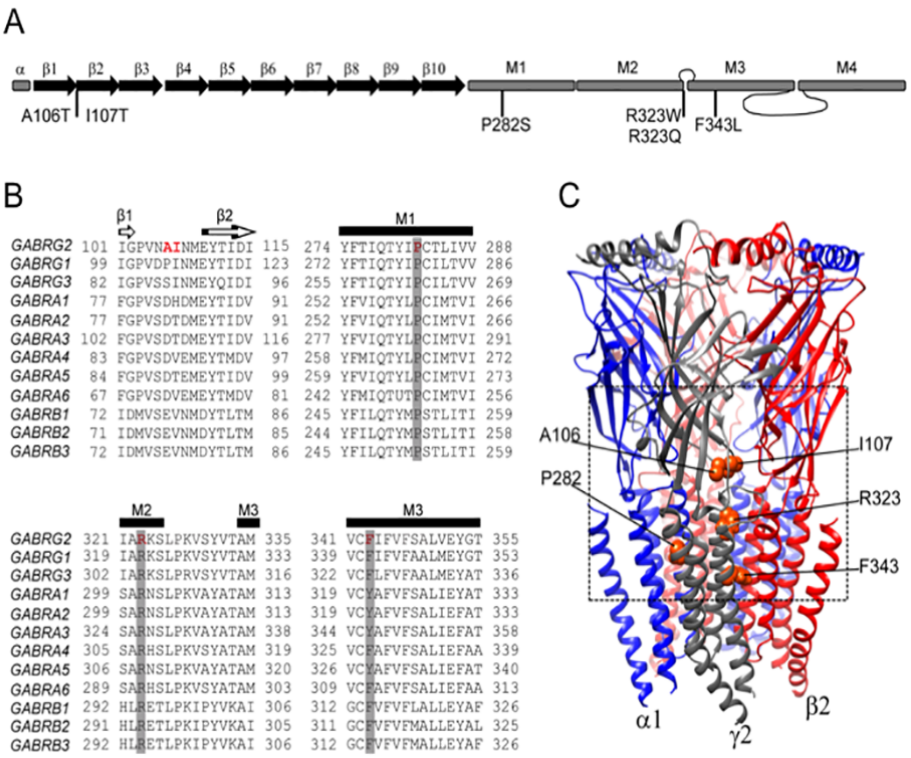

Figure 2-2: *De novo* γ2 variants were located between the interface of the N-terminal and transmembrane domains of the $GABA_A$ Receptor.

(A) A cartoon representation of the linearized secondary structure of a γ2 subunit was made displaying putative locations of the substitutions identified in this study. β-strands were represented as black arrows and α-helices as gray rectangles. **(B)** Alignment of human γ(1-3), α(1-6), and β(1-3) subunits from the $GABA_A$ receptor subunit family were performed. Sites of *de novo* variants in the γ2 subunit were shown in red. A106 and I107 residues were not conserved (shown in red in γ2 subunit only). Across all sequences, P282 and R323 residues were identical (highlighted in dark gray), and the residue F343 was conserved (highlighted in light gray). Secondary structures such as β-strands (β1 and β2) or transmembrane domains (M1, M2 and M3) were also represented across subunits above the alignments. (**C)** A 3D structural model of the $GABA_A$ receptor was constructed. *GABRG2 de novo* variants were mapped onto the γ2 subunit in orange. The dashed box highlights the observation that the variants were closely connected with the structural domains between the interface of the N-terminal (β1-β2 loop, Cys-loop, loop F) and transmembrane domains (M2-M3 loop, M1, M2, M3). See extended details in Fig.2-9.

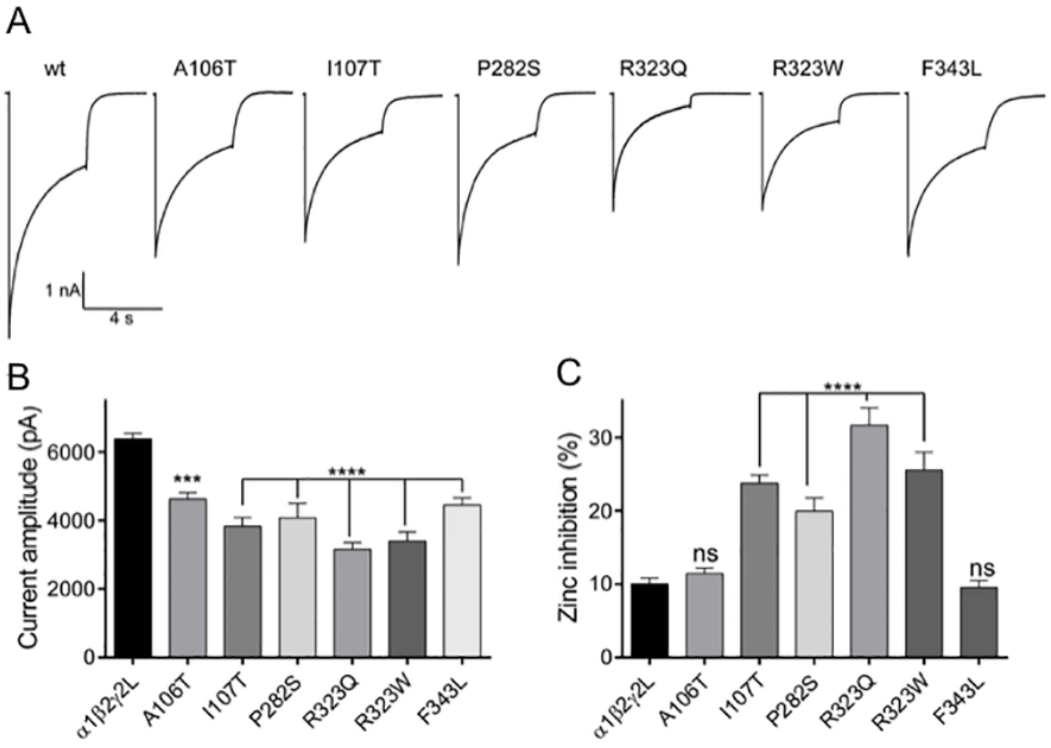

Figure 2-3: Mutant α1β2γ2L receptors showed decreased GABA-evoked whole-cell currents and increased zinc sensitivity.

(A) Representative GABA current traces are shown that were obtained following rapid application of 1 mM GABA for 4s to lifted HEK293T cells voltage clamped at -20 mV. **(B, C)** Bar graphs showing average peak current and zinc inhibition from cells co-expressing α1β2 subunits with wild-type (wt) or mutant γ2 subunits. Values were expressed as mean ± S.E.M (see Table 2-2). One-way ANOVA with Dunnett's post-test was used to determine significance compared to the wt condition. ****$p < 0.0001$, ***$p < 0.001$, and $^{ns}p > 0.05$, respectively.

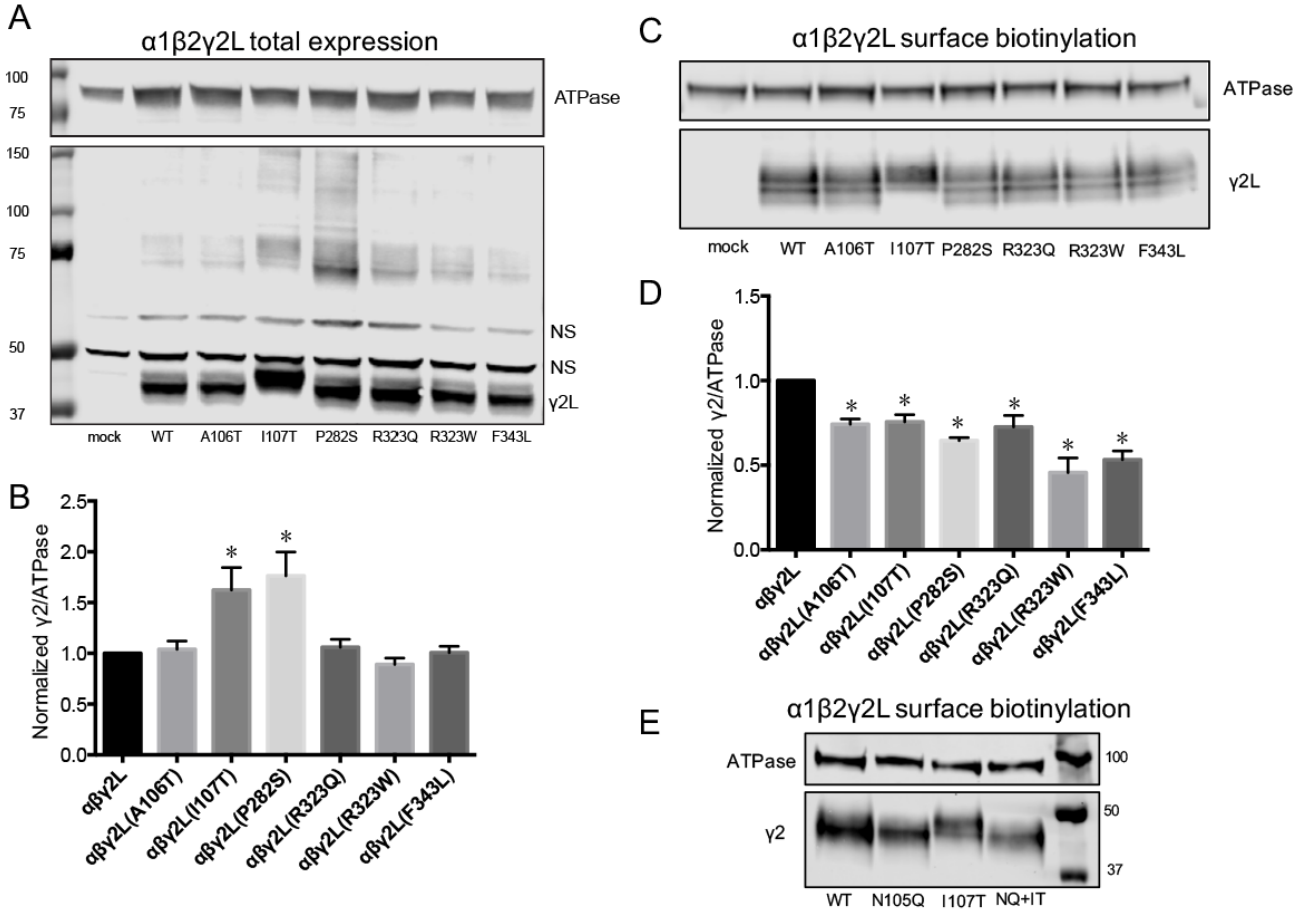

Figure 2-4: Immunoblotting studies were obtained for mutant γ2L subunits.
Wild-type or mutant γ2L subunits were cotransfected with α1β2 subunits into HEK293T cells. **(A)** Total cell lysates were collected, analyzed by SDS-PAGE and blotted by anti-γ2 and anti-ATPase antibodies. In this representative western blot, NS stands for nonspecific control. **(B)** Band intensity of γ2L subunits was normalized to the ATPase signal (n = 4, mean ± S.E.M.). Both the lower and higher-molecular-mass bands were included. **(C)** Surface protein samples were collected through biotinylation and probed by anti-γ2 and anti-ATPase antibodies. A representative western blot was presented. **(D)** Band intensities of γ2L subunits were normalized to the ATPase signal ($n \geq 4$, mean ± S.E.M.). One-way ANOVA followed by Dunnett's multiple comparison test were used to determine significance. (*$p < 0.05$, compared with wild-type condition). **(E)** Surface proteins of HEK293T cells coexpressing α1β2γ2L, α1β2γ2L(N105Q), α1β2γ2L(I107T) or α1β2γ2L(N105Q/I107T) subunits were collected and probed with anti-γ2 and anti-ATPase antibodies. A representative western blot was presented.

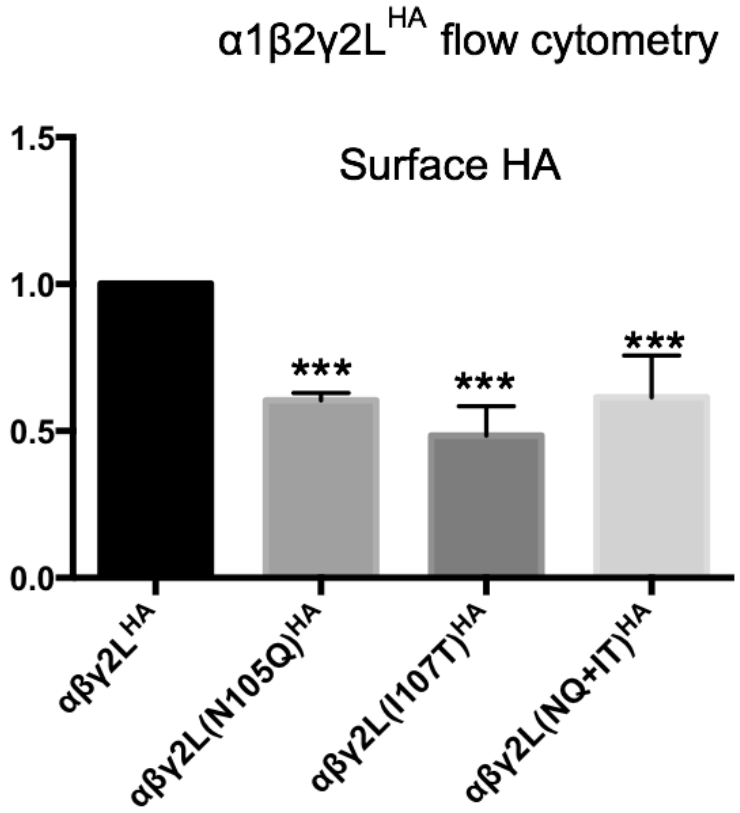

Figure 2-5: γ2L^{HA} subunit surface expression was reduced significantly by the I107T mutation itself rather than by glycosylation of the N105 residue.
Surface γ2L^{HA} subunit levels in HEK293T cells coexpressing α1, β2 and mutated/glycosylation-deficient γ2L^{HA} subunits were evaluated through flow cytometry. The mock-subtracted mean fluorescence intensity of γ2L^{HA} subunit signals under different experimental conditions were normalized to those obtained with cotransfection of wild-type α1β2γ2L^{HA} subunits. Differences compared to wild-type condition were analyzed by the one-way ANOVA test followed by Dunnett's multiple comparison test. (*** $p < 0.001$).

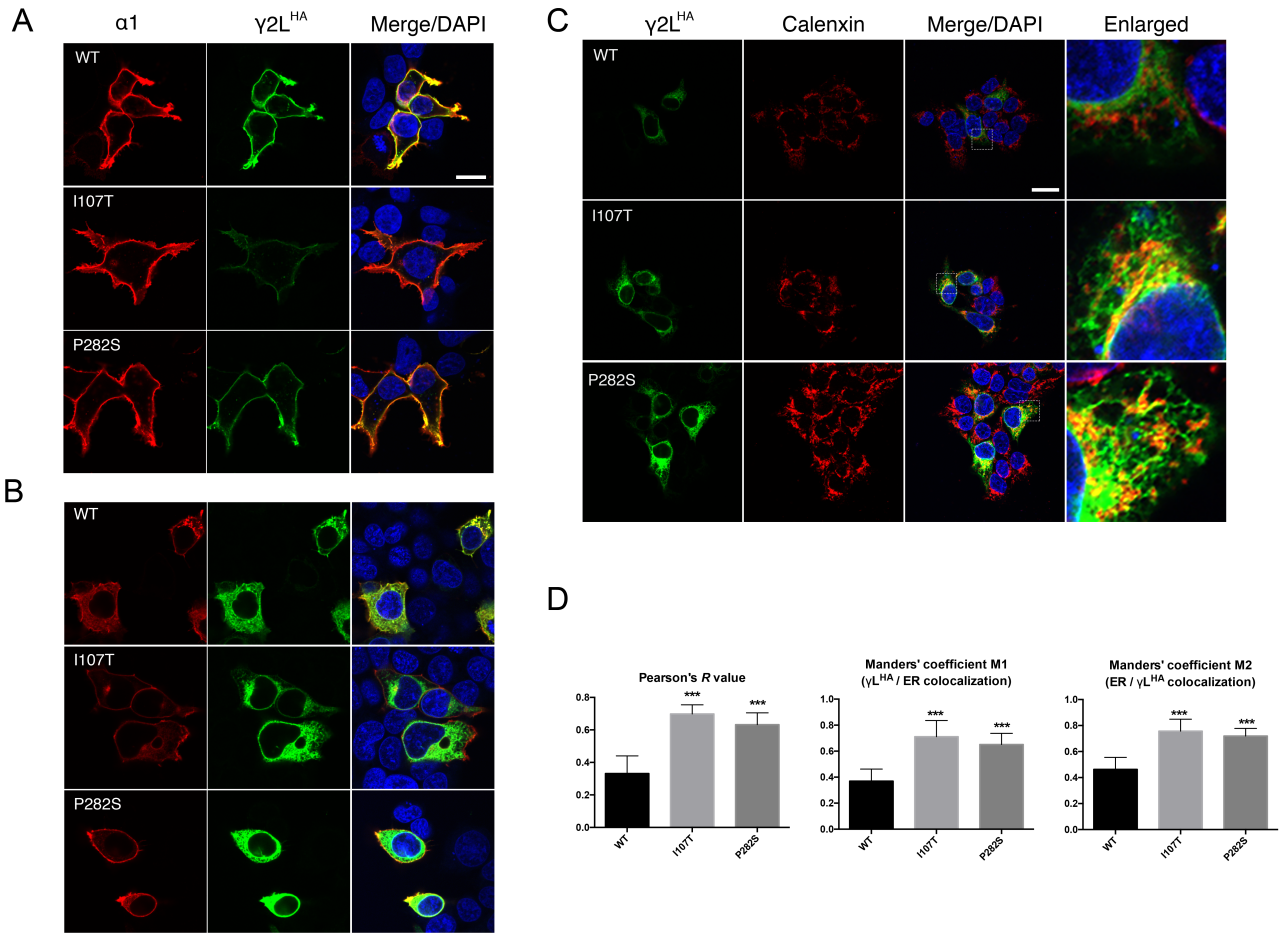

Figure 2-6: γ2L(I107T)^{HA} and γ2L(P282S)^{HA} subunits were retained intracellularly.
Wild-type or mutant γ2L(I107T)^{HA} and γ2L(P282S)^{HA} subunits were coexpressed with α1 and β2 subunits in HEK293T cells. Surface **(A)** and total **(B)** staining patterns were revealed by confocal microscopy. Both permeablized and unpermeablized cells were stained with antibodies against the α1 subunit (red) and the HA tag (green). Also shown was DAPI nuclear counterstaining (blue), and the merge of these stainings. Scale bars, 10 μm. **(C)** The transfected cells were permeablized, and γ2L^{HA} subunits were labeled with anti-HA antibody (green). The ER was visualized with anti-calnexin antibody (red). White boxes on the merged images depict the enlarged area shown in the images to the right. Scale bars, 20 μm. **(D)** Statistical analyses of wild-type or mutant γ2L^{HA} subunits and ER colocalization was performed using Pearson's correlation coefficient (R) and Manders' co-occurrence coefficient (M1 and M2). Results shown are the mean ± S.E.M of 15 cells in 3 independent experiments. (*** $p < 0.001$).

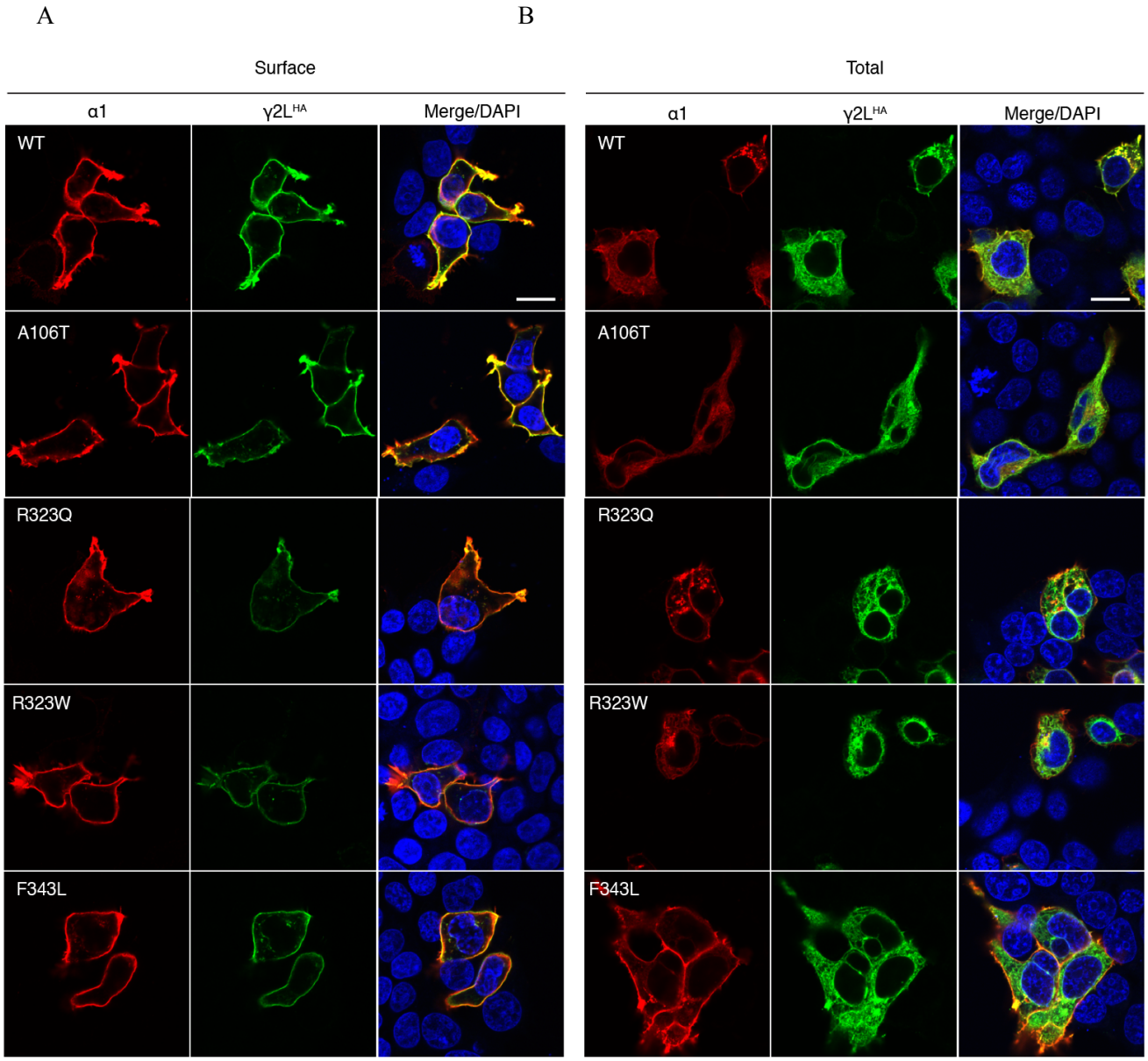

Figure 2-7: Mutant γ2 subunits had different intracellular and surface distributions.
Wild-type or mutant $\gamma 2L^{HA}$ subunits were coexpressed with α1 and β2 subunits in HEK293T cells. Surface **(A)** and total **(B)** staining patterns were determined by confocal microscopy. Both permeabilized and unpermeablized cells were stained with antibodies against the α1 subunit (red) and the HA tag (green). Also shown was DAPI nuclear counterstaining (blue), and the merge of these stainings. Scale bars, 10 μm

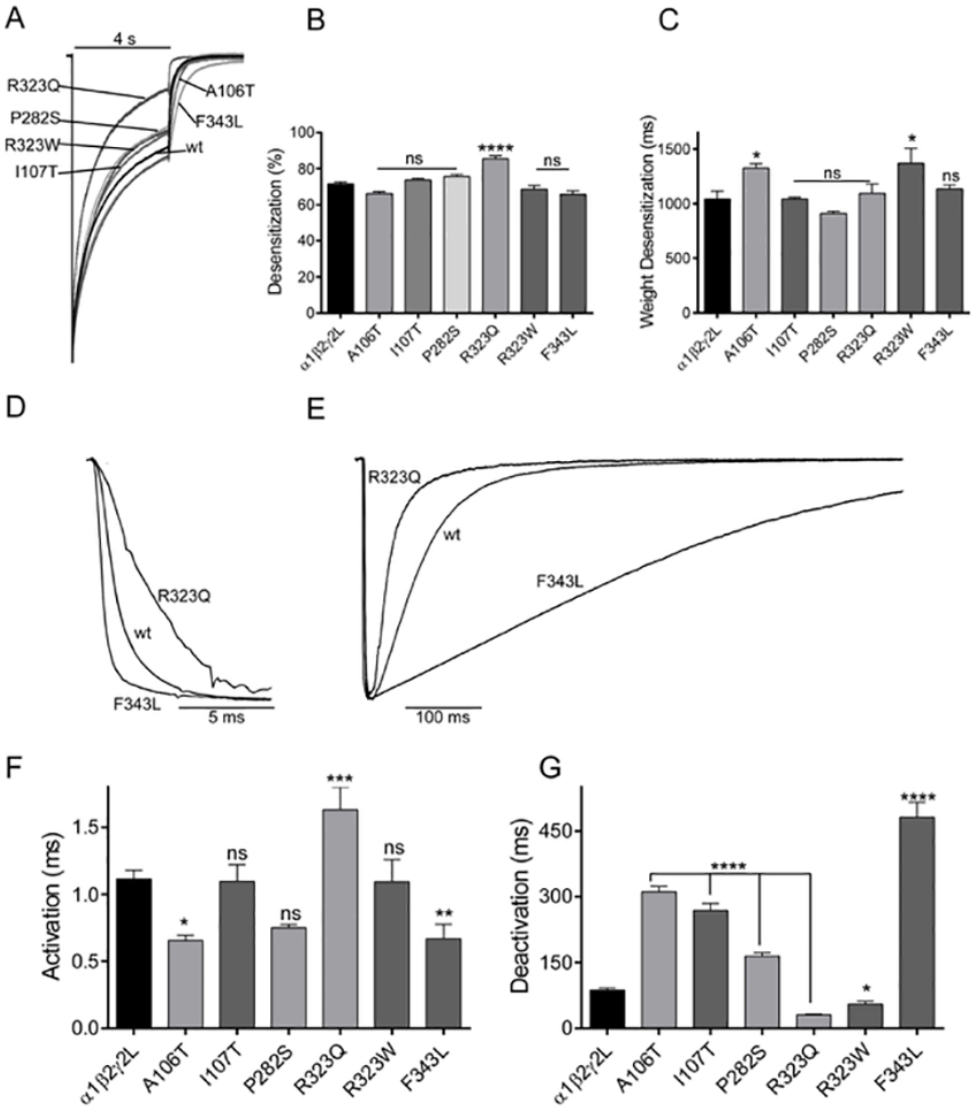

Figure 2-8: Mutant γ2 subunits altered the kinetic properties of $GABA_A$ receptor currents.
(A) Superimposed representative traces show the desensitization of GABA-evoked currents produced by 4s applications of 1 mM GABA to wild-type (wt) and mutant receptors. Traces were normalized to wt currents for clarity. **(B)** Bar graphs show average extent of desensitization measured at the end of the application of GABA, and **(C)** the weighted desensitization time constant during 4s applications of GABA were determined. Representative current traces show activation **(D)** and deactivation (**E**) of currents produced by 10 ms GABA (1 mM) applications to wt and mutant receptors containing the γ2(R323Q) and γ2(F343L) subunits. Traces were normalized for clarity. Bar graphs show **(F)** average activation time constant and (**G**) weighted deactivation time constant from the cells co-expressing α1β2 subunits with mutant or wt γ2L subunits. Values were expressed as mean ± S.E.M. (see Supplementary Table 1). One-way ANOVA with Dunnett's post-test was used to determine significance. ****$p < 0.0001$, ***$p < 0.001$, **$p < 0.01$, *$p < 0.05$, and $^{ns}p > 0.05$, respectively, relative to wt condition.

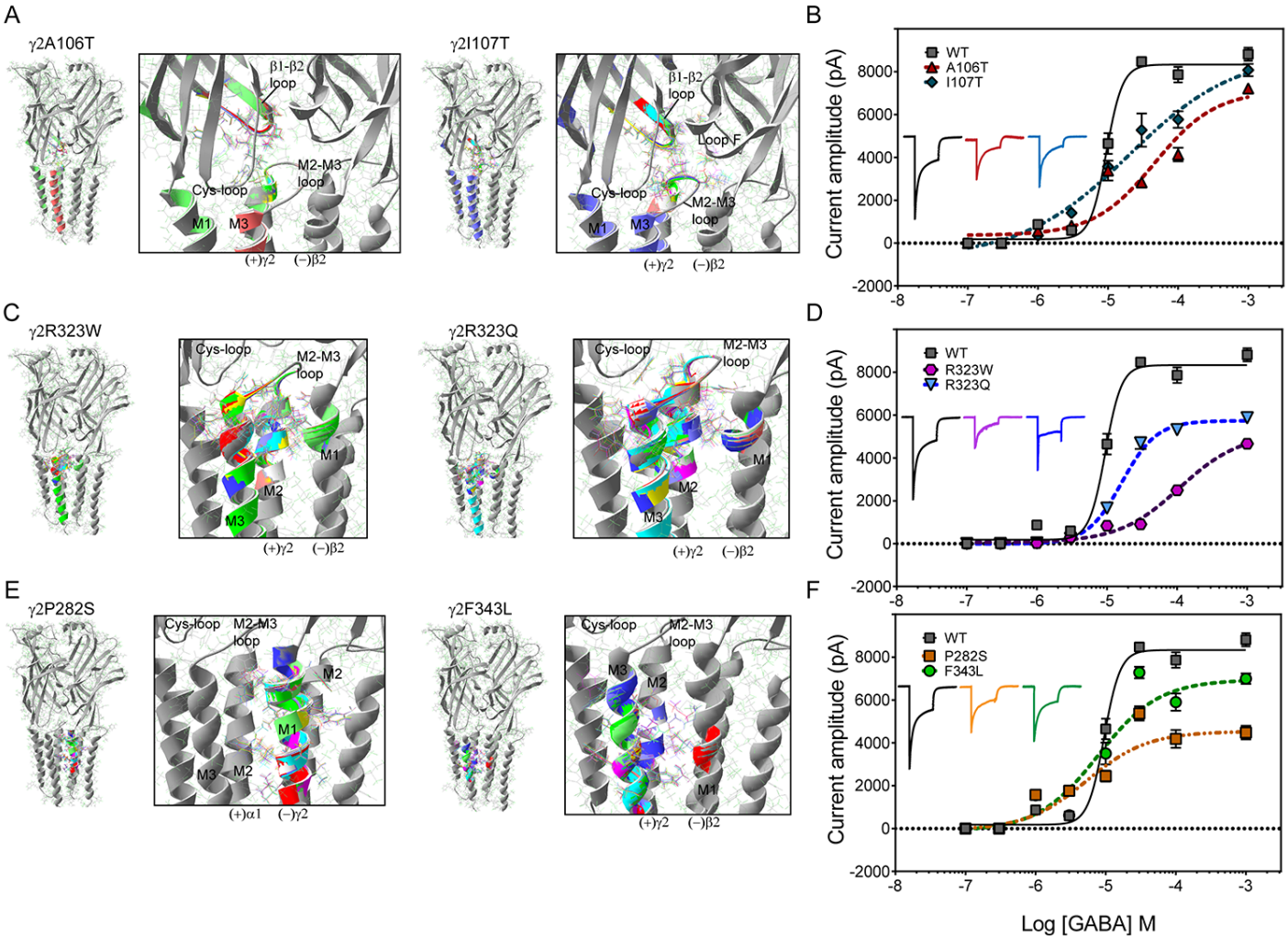

Figure 2-9: *De novo* γ2 mutations decreased GABA potency by disrupting structural domains important for $GABA_A$ receptor function.

(**A**), (**C**), and (**E**). On the right are represented two neighboring subunits where the mutations are located in relation to the γ+/β- and α+/γ- interfaces. Enlarged views of structural domains showing structural rearrangements caused by the γ2(A106T) and γ2(I107T) (**A**), γ2(R323W) and γ2(R323Q) (**C**), and γ2(P282S) and γ2(F343L) (**E**) mutations were shown in black boxes. The structural perturbations in the secondary structure and side chain residues that differed among the wild-type (in gray) and the mutant simulation (RMS deviation ≥ 0.5 Å) were indicated in a different color from the wild-type simulation. The principal (+) and complementary (-) interfaces of each subunit were shown, and structural domains along the interface of the N-terminal (C loop, β1-β2 loop, Cys-loop, loop F) and transmembrane domains (M2-M3 loop, M1, M2, M3) were indicated. (**B**), (**D**), and (**F**). GABA concentration-response curves for receptors containing γ2(A106T) and γ2(I107T) (**B**), γ2(R323W) and γ2(R323Q) (**D**), and γ2(P282S) and γ2(F343L) (**F**) mutant subunits (dashed lines) and for wild type (wt) receptors (solid lines) were obtained. Inside the panels, representative peak currents evoked by a 4 s application of GABA (100 μM) were shown. The color of the traces indicated the experimental condition as represented in the GABA-concentration response curves. The Peak current traces obtained from receptors containing mutant γ2 subunits were normalized with respect to wild-type receptors for comparison. Values were expressed as mean ± S.E.M (n = 5-6 cells for each experimental condition). The data represented the summary of 37 cells with comparable capacitances (8-12 pF) recorded from three independent transfections.

Table 2-1. Clinical features of all individuals with *GABRG2* variants identified in this study.

	Patient 1	Patient 2	Patient 3	Patient 4	Patient 5	Patient 6	Patient 7	Patient 8
Variant	c.316G>A	c.316G>A	c.320T>C	c.844C>T	c.968G>A	c.968G>A	c.967C>T	c.1027 T>C
Origin	*De novo*	*De novo*	*De novo*	*De novo*	*De novo*	*De novo*	*De novo*	*De novo*
Protein Change	p.A106T	p.A106T	p.I107T	p.P282S	p.R323Q	p.R323Q	p.R323W	p.F343L
Sex	Female	Male	Female	Female	Female	Female	Female	Female
Age at inclusion	7 years	9 years	3 years	10 years	4 years	3 2/12 years	9 years	6 years
Age at seizure onset	Day of Life 1	3 months	1.5 months	1 year	10 months	1 year	11 months	1 year
Seizure type at onset	GTCS	Tonic	Tonic	Secondary generalized	FS, GTCS, myoclonic	FS, myoclonic	GTCS	Tonic
Seizure frequency at onset	Daily	Unknown	Daily	Unknown	Sporadic GTCS	Daily	Weekly	Daily
Further seizure types	Tonic, CPS	CPS, secondary generalized, atonic	Infantile spasms, tonic	Atypical absences	Myoclonic, absences, GTCS, CPS	Atonic, myoclonias during sleep, atypical absences, GTCS	Absences	None
AED responses	Seizure free for 2 years on LEV	No clear response	No clear response	Slight improvement with LTG	No clear response	No clear response	VPA and TPM best combination	Some improvement on LEV
Seizure outcome	Seizure free for 3 years (1 year seizure free off AED)	Remains intractable	Remains intractable	Remains intractable	Remains intractable	Remains intractable	Seizure free for 3 years	Seizures Persist
EEG at onset	Normal	Normal	High voltage, slowing of background, sharp transients on the right side	Generalized and multifocal spikes	Normal	Generalized spikes, irregular spike-wave-complexes	Normal background, rare generalized spike waves	Excess diffuse beta and intermittent left temporal slowing.
Other EEG	No epileptiform activity seen	Diffuse xs beta, multifocal sharps	Background slowing, rare sharp transients right more than left	Generalized spike-wave nearly continuous	Generalized irregular spike wave	Generalized spikes irregular spike-wave-complexes	Normal background frequencies, rare single generalized or hemispheric accentuated spike waves	poor organization, diffuse xs beta, frequent sharps maximal at the central vertex
Development	Severe global delay	Severe global delay	Severe global delay	Severe global delay	Severe global delay	Severe global delay	Severe global delay	Severe global delay
Language	Non verbal	Non verbal	Non verbal	Non verbal	Non verbal	Non verbal	Non verbal	Non verbal
Neurological exam	Hypotonia, nystagmus	Hypotonia, nystagmus, hyperkinetic movements with some choreoathetotic components	Hypotonia, nystagmus, hand stereotypies, choreoathetosis	Hypotonia, roving eye movements	Normal	Hypotonia, mild ataxia	Normal	Hypotonia, intermittent hand posturing
MRI Findings	Delayed myelination	Volume loss	Normal	Normal	Normal	Normal	Normal	Falx hypoplasia

GTCS, generalized tonic-clonic seizures; FS, febrile seizures; CPS, complex partial seizures; AED, antiepileptic drug; LEV, levetiracetam; LTG, lamotrigine; VPA, valproic acid; TPM, topiramate

Information presented in table is the Variant; Origin of mutation; Protein Change; Sex of patient; Age at inclusion of study; Age at seizure onset; Seizure type at onset; Seizure frequency at onset; Seizure types that evolved with age; Responses to AEDs; Seizure outcome at last follow up; predominant EEG patterns at onset; Other patterns that were found on any EEG; Developmental outcome (best functioning); Language function (at best); Neurological exam and MRI findings. Abbreviations are presented at bottom.

Table 2-2. Effects of $GABA_A$ receptor γ2 subunit mutations on α1β2γ2L receptor channel function.

	α1β2γ2L	***A106T***	***I107T***	***P282S***	***R323Q***	***R323W***	***F343L***
Current amplitude, pA	6389 ± 157 (n = 45)	4620 ± 190[b] (n = 12)	3833 ± 253[a] (n = 14)	4076 ± 428[a] (n = 21)	3159 ± 195[a] (n = 32)	3402 ± 267[a] (n = 30)	4453 ± 202[a] (n = 22)
Desensitization extent, %	72 ± 1 (n = 51)	66 ± 1 (n = 12)	74± 1 (n = 14)	76 ± 1 (n = 25)	85 ± 2[a] (n = 15)	69 ± 2 (n = 22)	66 ± 2 (n = 11)
Desensitization τ, ms	1042 ± 72[d] (n = 32)	1324 ± 42 (n = 12)	1042 ± 15 (n = 7)	911 ± 17 (n = 17)	1094 ± 84 (n = 15)	1369 ± 134[d] (n = 12)	1134 ± 37 (n = 11)
Zinc inhibition, %	10 ± 1 (n = 51)	11 ± 1 (n = 12)	24 ± 1[a] (n = 14)	20 ± 2[a] (n = 24)	32 ± 2[a] (n = 15)	26 ± 2[a] (n = 21)	10 ± 1 (n = 11)
Activation τ, ms	1.11 ± 0.07[d] (n = 36)	0.65 ± 0.04 (n = 12)	1.10 ± 0.12 (n = 7)	0.75 ± 0.02 (n = 14)	1.63 ± 0.17[b] (n = 18)	1.09 ± 0.17 (n = 12)	0.67 ± 0.11[c] (n = 17)
Deactivation τ, ms	87 ± 5 (n = 32)	312 ± 12[a] (n = 8)	268 ± 16[a] (n = 6)	165 ± 7[a] (n = 12)	31 ± 2[a] (n = 18)	55± 6[d] (n = 13)	482 ± 33[a] (n = 7)

Kinetic parameters were obtained from macroscopic currents recorded from lifted cells, which were voltage-clamped at -20 mV. Current amplitude, desensitization extent and desensitization τ refer to peak current and residual current amplitudes at the end of 1 mM GABA applications for 4 s, and weighted desensitization time constant, respectively. Activation and deactivation τ refer to weighted activation and deactivation time constant respectively, when applying 1 mM GABA for 10 ms. Values reported are mean ± S.E.M. One-way ANOVA with Dunnett's multiple comparisons test was used to determine significance. [a]$p < 0.0001$, [b]$p < 0.001$, [c]$p < 0.01$ and [d]$p < 0.05$, respectively, relative to α1β2γ2L.

Table 2-3. Summary of *in vitro* characterization of *GABRG2* mutations identified in this study

	Macroscopic properties						Cellular localization	
GABRG2 mutations	Current	GABA potency	Kinetics				Intracellular	Surface
			Desensitization extent	Desensitization τ	Activation τ	Deactivation τ		
A106T	↓	↓	→	↑	↓	↓	→	↓
I107T	↓	↓	→	→	→	↓	↑	↓
P282S	↓	→	→	→	→	↓	↑	↓
R323Q	↓	↓	↑	→	↑	↓	→	↓
R323W	↓	↓	→	↑	→	↓	→	↓
F343L	↓	→	→	→	↓	↑	→	↓

References

1. A. T. Berg, S. F. Berkovic, M. J. Brodie, J. Buchhalter, J. H. Cross, W. van Emde Boas, J. Engel, J. French, T. A. Glauser, G. W. Mathern, S. L. Moshe, D. Nordli, P. Plouin, I. E. Scheffer, Revised terminology and concepts for organization of seizures and epilepsies: report of the ILAE Commission on Classification and Terminology, 2005-2009. *Epilepsia* **51**, 676-685 (2010).

2. A. Katsnelson, G. Buzsaki, J. W. Swann, Catastrophic childhood epilepsy: a recent convergence of basic and clinical neuroscience. *Sci Transl Med* **6**, 262ps213 (2014).

3. R. H. Thomas, S. F. Berkovic, The hidden genetics of epilepsy-a clinically important new paradigm. *Nat Rev Neurol* **10**, 283-292 (2014).

4. P. M. C. Epi, A roadmap for precision medicine in the epilepsies. *Lancet Neurol* **14**, 1219-1228 (2015).

5. G. L. Carvill, S. B. Heavin, S. C. Yendle, J. M. McMahon, B. J. O'Roak, J. Cook, A. Khan, M. O. Dorschner, M. Weaver, S. Calvert, S. Malone, G. Wallace, T. Stanley, A. M. Bye, A. Bleasel, K. B. Howell, S. Kivity, M. T. Mackay, V. Rodriguez-Casero, R. Webster, A. Korczyn, Z. Afawi, N. Zelnick, T. Lerman-Sagie, D. Lev, R. S. Moller, D. Gill, D. M. Andrade, J. L. Freeman, L. G. Sadleir, J. Shendure, S. F. Berkovic, I. E. Scheffer, H. C. Mefford, Targeted resequencing in epileptic encephalopathies identifies de novo mutations in CHD2 and SYNGAP1. *Nat Genet* **45**, 825-830 (2013).

6. A. McTague, K. B. Howell, J. H. Cross, M. A. Kurian, I. E. Scheffer, The genetic landscape of the epileptic encephalopathies of infancy and childhood. *Lancet Neurol* **15**, 304-316 (2016).

7. E.-R. E. S. C. Euro, P. Epilepsy Phenome/Genome, K. C. Epi, De novo mutations in synaptic transmission genes including DNM1 cause epileptic encephalopathies. *Am J Hum Genet* **95**, 360-370 (2014).

8. M. Farrant, Z. Nusser, Variations on an inhibitory theme: phasic and tonic activation of GABA(A) receptors. *Nat Rev Neurosci* **6**, 215-229 (2005).

9. C. Essrich, M. Lorez, J. A. Benson, J. M. Fritschy, B. Luscher, Postsynaptic clustering of major GABAA receptor subtypes requires the gamma 2 subunit and gephyrin. *Nat Neurosci* **1**, 563-571 (1998).

10. C. Schweizer, S. Balsiger, H. Bluethmann, I. M. Mansuy, J. M. Fritschy, H. Mohler, B. Luscher, The gamma 2 subunit of GABA(A) receptors is required for maintenance of receptors at mature synapses. *Mol Cell Neurosci* **24**, 442-450 (2003).

11. K. F. Haas, R. L. Macdonald, $GABA_A$ receptor subunit gamma2 and delta subtypes confer unique kinetic properties on recombinant $GABA_A$ receptor currents in mouse fibroblasts. *J Physiol* **514 (Pt 1)**, 27-45 (1999).

12. R. L. Macdonald, J. Q. Kang, Molecular pathology of genetic epilepsies associated with $GABA_A$ receptor subunit mutations. *Epilepsy Curr* **9**, 18-23 (2009).

13. J. Q. Kang, W. Shen, C. Zhou, D. Xu, R. L. Macdonald, The human epilepsy mutation GABRG2(Q390X) causes chronic subunit accumulation and neurodegeneration. *Nat Neurosci* **18**, 988-996 (2015).

14. R. L. Macdonald, J. Q. Kang, mRNA surveillance and endoplasmic reticulum quality control processes alter biogenesis of mutant $GABA_A$ receptor subunits associated with genetic epilepsies. *Epilepsia* **53 Suppl 9**, 59-70 (2012).

15. H. O. Tan, C. A. Reid, F. N. Single, P. J. Davies, C. Chiu, S. Murphy, A. L. Clarke, L. Dibbens, H. Krestel, J. C. Mulley, M. V. Jones, P. H. Seeburg, B. Sakmann, S. F. Berkovic, R. Sprengel, S. Petrou, Reduced cortical inhibition in a mouse model of familial childhood absence epilepsy. *Proc Natl Acad Sci U S A* **104**, 17536-17541 (2007).

16. C. A. Reid, T. Kim, A. M. Phillips, J. Low, S. F. Berkovic, B. Luscher, S. Petrou, Multiple molecular mechanisms for a single $GABA_A$ mutation in epilepsy. *Neurology* **80**, 1003-1008 (2013).

17. A. Poduri, E. L. Heinzen, V. Chitsazzadeh, F. M. Lasorsa, P. C. Elhosary, C. M. LaCoursiere, E. Martin, C. J. Yuskaitis, R. S. Hill, K. D. Atabay, B. Barry, J. N. Partlow, F. A. Bashiri, R. M. Zeidan, S. A. Elmalik, M. M. Kabiraj, S. Kothare, T. Stodberg, A. McTague, M. A. Kurian, I. E. Scheffer, A. J. Barkovich, F. Palmieri, M. A. Salih, C. A. Walsh, SLC25A22 is a novel gene for migrating partial seizures in infancy. *Ann Neurol* **74**, 873-882 (2013).

18. S. Richards, N. Aziz, S. Bale, D. Bick, S. Das, J. Gastier-Foster, W. W. Grody, M. Hegde, E. Lyon, E. Spector, K. Voelkerding, H. L. Rehm, A. L. Q. A. Committee, Standards and guidelines for the interpretation of sequence variants: a joint consensus recommendation of the American College of Medical Genetics and Genomics and the Association for Molecular Pathology. *Genet Med* **17**, 405-424 (2015).

19. J. R. Lemke, E. Riesch, T. Scheurenbrand, M. Schubach, C. Wilhelm, I. Steiner, J. Hansen, C. Courage, S. Gallati, S. Burki, S. Strozzi, B. G. Simonetti, S. Grunt, M. Steinlin, M. Alber, M. Wolff, T. Klopstock, E. C. Prott, R. Lorenz, C. Spaich, S. Rona, M. Lakshminarasimhan, J. Kroll, T. Dorn, G. Kramer, M. Synofzik, F. Becker, Y. G. Weber, H. Lerche, D. Bohm, S. Biskup, Targeted next generation sequencing as a diagnostic tool in epileptic disorders. *Epilepsia* **53**, 1387-1398 (2012).

20. C. N. Connolly, B. J. Krishek, B. J. McDonald, T. G. Smart, S. J. Moss, Assembly and cell surface expression of heteromeric and homomeric-aminobutyric acid type A receptors. *Journal of Biological Chemistry* **271**, 89-96 (1996).

21. X. Huang, C. C. Hernandez, N. Hu, R. L. Macdonald, Three epilepsy-associated *GABRG2* missense mutations at the gamma+/beta- interface disrupt GABAA receptor assembly and trafficking by similar mechanisms but to different extents. *Neurobiol Dis* **68**, 167-179 (2014).

22. J. Schindelin, I. Arganda-Carreras, E. Frise, V. Kaynig, M. Longair, T. Pietzsch, S. Preibisch, C. Rueden, S. Saalfeld, B. Schmid, J. Y. Tinevez, D. J. White, V. Hartenstein, K. Eliceiri, P. Tomancak, A. Cardona, Fiji: an open-source platform for biological-image analysis. *Nat Methods* **9**, 676-682 (2012).

23. C. C. Hernandez, K. N. Gurba, N. Hu, R. L. Macdonald, The GABRA6 mutation, R46W, associated with childhood absence epilepsy, alters 6beta22 and 6beta2 GABA(A) receptor channel gating and expression. *The Journal of physiology* **589**, 5857-5878 (2011).

24. M. T. Bianchi, R. L. Macdonald, Slow phases of GABA(A) receptor desensitization: structural determinants and possible relevance for synaptic function. *J Physiol* **544**, 3-18 (2002).

25. T. Schwede, J. Kopp, N. Guex, M. C. Peitsch, SWISS-MODEL: An automated protein homology-modeling server. *Nucleic acids research* **31**, 3381-3385 (2003).

26. C. A. Smith, T. Kortemme, Backrub-like backbone simulation recapitulates natural protein conformational variability and improves mutant side-chain prediction. *J Mol Biol* **380**, 742-756 (2008).

27. E. F. Pettersen, T. D. Goddard, C. C. Huang, G. S. Couch, D. M. Greenblatt, E. C. Meng, T. E. Ferrin, UCSF Chimera--a visualization system for exploratory research and analysis. *J Comput Chem* **25**, 1605-1612 (2004).

28. R. L. Macdonald, R. W. Olsen, $GABA_A$ receptor channels. *Annu Rev Neurosci* **17**, 569-602 (1994).

29. P. S. Miller, A. R. Aricescu, Crystal structure of a human $GABA_A$ receptor. *Nature* **512**, 270-275 (2014).

30. I. A. Adzhubei, S. Schmidt, L. Peshkin, V. E. Ramensky, A. Gerasimova, P. Bork, A. S. Kondrashov, S. R. Sunyaev, A method and server for predicting damaging missense mutations. *Nat Methods* **7**, 248-249 (2010).

31. P. Kumar, S. Henikoff, P. C. Ng, Predicting the effects of coding non-synonymous variants on protein function using the SIFT algorithm. *Nat Protoc* **4**, 1073-1081 (2009).

32. J. Q. Kang, W. Shen, M. Lee, M. J. Gallagher, R. L. Macdonald, Slow degradation and aggregation in vitro of mutant $GABA_A$ receptor gamma2(Q351X) subunits associated with epilepsy. *J Neurosci* **30**, 13895-13905 (2010).

33. E. Manders, F. Verbeek, J. Aten, Measurement of co-localization of objects in dual-colour confocal images. *Journal of microscopy* **169**, 375-382 (1993).

34. S. V. Costes, D. Daelemans, E. H. Cho, Z. Dobbin, G. Pavlakis, S. Lockett, Automatic and quantitative measurement of protein-protein colocalization in live cells. *Biophys J* **86**, 3993-4003 (2004).

35. T. Klausberger, K. Fuchs, B. Mayer, N. Ehya, W. Sieghart, GABA(A) receptor assembly. Identification and structure of gamma(2) sequences forming the intersubunit contacts with alpha(1) and beta(3) subunits. *J Biol Chem* **275**, 8921-8928 (2000).

36. I. Sarto, L. Wabnegger, E. Dogl, W. Sieghart, Homologous sites of GABA(A) receptor alpha(1), beta(3) and gamma(2) subunits are important for assembly. *Neuropharmacology* **43**, 482-491 (2002).

37. M. T. Bianchi, K. F. Haas, R. L. Macdonald, Structural determinants of fast desensitization and desensitization-deactivation coupling in $GABA_A$ receptors. *J Neurosci* **21**, 1127-1136 (2001).

38. S. P. Venkatachalan, C. Czajkowski, Structural link between gamma-aminobutyric acid type A (GABAA) receptor agonist binding site and inner beta-sheet governs channel activation and allosteric drug modulation. *The Journal of biological chemistry* **287**, 6714-6724 (2012).

39. T. Althoff, R. E. Hibbs, S. Banerjee, E. Gouaux, X-ray structures of GluCl in apo states reveal a gating mechanism of Cys-loop receptors. *Nature* **512**, 333-337 (2014).

40. W. Y. Lo, A. H. Lagrange, C. C. Hernandez, K. N. Gurba, R. L. Macdonald, Co-expression of gamma2 subunits hinders processing of N-linked glycans attached to the N104 glycosylation sites of $GABA_A$ receptor beta2 subunits. *Neurochemical research* **39**, 1088-1103 (2014).

41. V. S. Janve, C. C. Hernandez, K. M. Verdier, N. Hu, R. L. Macdonald, Epileptic encephalopathy de novo *GABRB* mutations impair GABA receptor function. *Annals of neurology*, (2016).

42. J. Q. Kang, R. L. Macdonald, Molecular Pathogenic Basis for *GABRG2* Mutations Associated With a Spectrum of Epilepsy Syndromes, From Generalized Absence Epilepsy to Dravet Syndrome. *JAMA Neurol*, (2016).

43. E. Todd, K. N. Gurba, E. J. Botzolakis, A. K. Stanic, R. L. Macdonald, GABAA receptor biogenesis is impaired by the gamma2 subunit febrile seizure-associated mutation, *GABRG2(R177G)*. *Neurobiol Dis* **69**, 215-224 (2014).

44. J. Q. Kang, W. Shen, R. L. Macdonald, Trafficking-deficient mutant *GABRG2* subunit amount may modify epilepsy phenotype. *Ann Neurol* **74**, 547-559 (2013).

45. E. M. Reinthaler, B. Dejanovic, D. Lal, M. Semtner, Y. Merkler, A. Reinhold, D. A. Pittrich, C. Hotzy, M. Feucht, H. Steinbock, U. Gruber-Sedlmayr, G. M. Ronen, B. Neophytou, J. Geldner, E. Haberlandt, H. Muhle, M. A. Ikram, C. M. van Duijn, A. G. Uitterlinden, A. Hofman, J. Altmuller, A. Kawalia, M. R. Toliat, E. C. Euro, P. Nurnberg, H. Lerche, M. Nothnagel, H. Thiele, T. Sander, J. C. Meier, G. Schwarz, B. A. Neubauer, F. Zimprich, Rare variants in gamma-aminobutyric acid type A receptor genes in rolandic epilepsy and related syndromes. *Ann Neurol* **77**, 972-986 (2015).

46. H. Kodera, C. Ohba, M. Kato, T. Maeda, K. Araki, D. Tajima, M. Matsuo, N. Hino-Fukuyo, K. Kohashi, A. Ishiyama, S. Takeshita, H. Motoi, T. Kitamura, A. Kikuchi, Y. Tsurusaki, M. Nakashima, N. Miyake, M. Sasaki, S. Kure, K. Haginoya, H. Saitsu, N. Matsumoto, De novo *GABRA1* mutations in Ohtahara and West syndromes. *Epilepsia* **57**, 566-573 (2016).

47. S. Baulac, G. Huberfeld, I. Gourfinkel-An, G. Mitropoulou, A. Beranger, J. F. Prud'homme, M. Baulac, A. Brice, R. Bruzzone, E. LeGuern, First genetic evidence of GABA(A) receptor dysfunction in epilepsy: a mutation in the gamma2-subunit gene. *Nat Genet* **28**, 46-48 (2001).

48. R. H. Wallace, C. Marini, S. Petrou, L. A. Harkin, D. N. Bowser, R. G. Panchal, D. A. Williams, G. R. Sutherland, J. C. Mulley, I. E. Scheffer, S. F. Berkovic, Mutant GABA(A) receptor gamma2-subunit in childhood absence epilepsy and febrile seizures. *Nat Genet* **28**, 49-52 (2001).

49. M. Boillot, M. Morin-Brureau, F. Picard, S. Weckhuysen, V. Lambrecq, C. Minetti, P. Striano, F. Zara, M. Iacomino, S. Ishida, I. An-Gourfinkel, M. Daniau, K. Hardies, M. Baulac, O. Dulac, E. Leguern, R. Nabbout, S. Baulac, Novel *GABRG2* mutations cause familial febrile seizures. *Neurol Genet* **1**, e35 (2015).

50. D. Audenaert, E. Schwartz, K. G. Claeys, L. Claes, L. Deprez, A. Suls, T. Van Dyck, L. Lagae, C. Van Broeckhoven, R. L. Macdonald, P. De Jonghe, A novel *GABRG2* mutation associated with febrile seizures. *Neurology* **67**, 687-690 (2006).

51. X. Shi, M. C. Huang, A. Ishii, S. Yoshida, M. Okada, K. Morita, H. Nagafuji, S. Yasumoto, S. Kaneko, T. Kojima, S. Hirose, Mutational analysis of *GABRG2* in a Japanese cohort with childhood epilepsies. *J Hum Genet* **55**, 375-378 (2010).

52. L. A. Harkin, D. N. Bowser, L. M. Dibbens, R. Singh, F. Phillips, R. H. Wallace, M. C. Richards, D. A. Williams, J. C. Mulley, S. F. Berkovic, I. E. Scheffer, S. Petrou, Truncation of the GABA(A)-receptor gamma2 subunit in a family with generalized epilepsy with febrile seizures plus. *Am J Hum Genet* **70**, 530-536 (2002).

53. X. Huang, M. Tian, C. C. Hernandez, N. Hu, R. L. Macdonald, The *GABRG2* nonsense mutation, Q40X, associated with Dravet syndrome activated NMD and generated a truncated subunit that was partially rescued by aminoglycoside-induced stop codon read-through. *Neurobiol Dis* **48**, 115-123 (2012).

54. A. J. Johnston, J. Q. Kang, W. Shen, W. O. Pickrell, T. D. Cushion, J. S. Davies, K. Baer, J. G. Mullins, C. L. Hammond, S. K. Chung, R. H. Thomas, C. White, P. E. Smith, R. L. Macdonald, M. I. Rees, A novel *GABRG2* mutation, p.R136*, in a family with GEFS+ and extended phenotypes. *Neurobiol Dis* **64**, 131-141 (2014).

55. S. Braat, R. F. Kooy, The $GABA_A$ Receptor as a Therapeutic Target for Neurodevelopmental Disorders. *Neuron* **86**, 1119-1130 (2015).

Chapter 3: Differential protein structural disturbances and suppression of assembly partners produced by nonsense *GABRG2* epilepsy mutations: implications for disease phenotypic heterogeneity

Juexin Wang[*], Dingding Shen[*], Geqing Xia, Wangzhen Shen, Robert L. Macdonald, Dong Xu, Jing-Qiong Kang

[*] Both authors contributed equally

This work has been published in Sci Rep. 2016 Oct 20; 6:35294.

1. Abstract

Mutations in $GABA_A$ receptor subunit genes are frequently associated with epilepsy, and nonsense mutations in *GABRG2* are associated with several epilepsy syndromes including childhood absence epilepsy, generalized tonic clonic seizures and the epileptic encephalopathy, Dravet syndrome. The molecular basis for the phenotypic heterogeneity of mutations is unclear. Here we focused on three nonsense mutations in *GABRG2* (*GABRG2(R136**), *GABRG2(Q390**) and *GABRG2(W429**)) associated with epilepsies of different severities. Structural modeling and structure-based analysis indicated that the surface of the wild-type γ2 subunit was naturally hydrophobic, which is suitable to be buried in the cell membrane. Different mutant γ2 subunits had different stabilities and different interactions with their wild-type subunit binding partners because they adopted different conformations and had different surface hydrophobicities and different tendency to dimerize. We utilized flow cytometry and biochemical approaches in combination with lifted whole cell patch-clamp recordings. We demonstrated that the truncated subunits had no to minimal surface expression and unchanged or reduced surface expression of wild-type partnering subunits. The amplitudes of GABA-evoked currents from the mutant α1β2γ2(R136*), α1β2γ2(Q390*) and α1β2γ2(W429*) receptors were reduced compared to the currents from α1β2γ2 receptors but with differentially reduced levels. This thus suggests differential protein structure disturbances are correlated with disease severity.

Key words: $GABA_A$ receptors, genetic epilepsy, mutation, *GABRG2(R136*)*, *GABRG2(Q390*)*, *GABRG2(W429*),* protein structure prediction, dimer, hydrophobicity

2. Introduction

Mutations in *GABRG2* are associated with epilepsies of varying severities. However, the basis for the mutant γ2 subunits structure and the correlation between structural disturbances and disease phenotypes has not been reported. We have demonstrated that nonsense *GABRG2* mutations result in loss-of-function but different nonsense mutations are associated with epilepsy phenotypes with different severities. Thus, understanding the structural alterations of mutant γ2 subunits may provide novel insights into epilepsy phenotypic heterogeneity. *GABRG2(R136*)* is a mutation associated with febrile seizures (FS) (*1*), *GABRG2(Q390*)* is a mutation associated with the severe epilepsy Dravet syndrome (*2*), and *GABRG2(W429*)* is a mutation associated with FS and the moderately severe genetic epilepsy with FS plus (GEFS+) (*3*). We have demonstrated that protein degradation rate is associated with steady state protein expression of the mutant $GABA_A$ receptor γ2 subunit (*4*). However, the structural basis for the mutant protein's stability, and the correlating biochemistry and function of the mutant subunits has not been reported.

Although the $GABA_A$ receptor is a major mediator of fast inhibitory neurotransmission in the CNS, and the assembly and current kinetic properties of $GABA_A$ receptors have been well characterized, the structure of the receptor is less known. Among $GABA_A$ receptor subunits, the first three-dimensional structure of the $GABA_A$ receptor β3 homopentamer was resolved by X-ray diffraction and has revealed many architectural details of the homopentamer and its role as a pentamer in channel signal transduction (*5*). However, other unsolved subunits of $GABA_A$ receptors could also oligomerize and produce different pentamers with various functional roles and their structures remain unknown. In addition, missense mutations and nonsense mutations with truncations of different lengths of these subunits still lack structure-based explanation of their properties. Protein structure prediction provides a powerful tool to infer tertiary structure from protein amino

acid sequence (*6*). With structural modeling and protein docking, there are already several successes in predicting function-related structural conformational differences between mutant/truncated and wild-type structures (*7-11*).

In the present study, we characterized the properties of the three FS and epilepsy associated truncated mutant γ2 subunits based on structural modeling. Based on the predicted $GABA_A$ receptor subunit structural models and a series of computational analyses, we quantitatively inferred the protein-protein interaction stabilities among these subunits in the complexes. Our computations are mainly rooted in one widely accepted hypothesis on stability of protein complexes: if the predicted binding affinity is higher, then the proposed protein-protein complex is likely more stable and has a higher probability to exist *in vivo* (*10, 12*). In particular, we have demonstrated that differences in protein stability are due mainly to the differentially accessible surface area (*ASA*) and surface hydrophobicity (*13*). ASA is protein surface area accessible to a solvent from solvent probe radius 1.4 Å as calculated by nACCESS. With various protein docking processes, we have determined that different mutant subunits have different interactions with the remaining wild-type partnering subunits, like α1 subunits, and the stabilities of the dimers of different mutant subunits are different.

We have used biochemistry and flow cytometry to further validate the results of protein structural modeling. We have determined total and surface expression of the three mutant γ2 subunits. We have determined the propensity of the mutant subunits to form high molecular mass protein aggregates. With a de-glycosylation study, we have demonstrated the differential glycosylation arrest of the wild-type subunits when co-expressed with the different mutant γ2 subunits and ER retention of the wild-type partnering subunits. With whole-cell patch clamp recordings, we have identified different extents of preservation of wild-type channel function.

3. Methods

Structural modeling of the wild-type and the mutant $GABA_A$ receptor subunits

We mainly used our in-house protein structure prediction tool MUFOLD (*6*) to construct protein models of $GABA_A$ receptor α1, β2, β3, γ2, and δ subunits. We also carefully modeled mutant $GABA_A$ receptor γ2 subunits including: (1) the γ2(R136*) subunit, with all transmembrane regions deleted and only part of the N-terminal domain remains; (2) the γ2(Q390*) subunit, with the fourth hydrophobic transmembrane α-helix (YARIFFPTAFCLFNLVYWVSYLYL) deleted and a new α-helix with many charged amino acids (KDKDKKKKNPAPTIDIRPRSATI) found to assume its location; and (3) the γ2(W429*) subunit, with the fourth hydrophobic transmembrane α-helix truncated. In the MUFOLD protocol, several experimental protein structures in PDB were identified based on homology as templates (PDB id: 4cof and 2bg9). Then multidimensional scaling (MDS) was used to reconstruct multiple protein decoys based on these templates, and these decoys were clustered and evaluated. With several iterations of model generation and evaluation, one decoy was chosen as the predicted protein model and then refined by Rosetta (*14*). For mutant $GABA_A$ receptor γ2 subunits, the original input subunits were split into different domains, and each domain was modeled individually and then assembled together.

To further understand the stability of the wild-type and mutant subunits, a dimer structure was constructed between two subunits in symmetric docking by SymmDock (*15*). SymmDock used a priori restriction on its transformational search space only to symmetric transformations, which makes it gains both in efficiency and performance on cyclically symmetric homo-multimers. Because $GABA_A$ receptor subunits are membrane proteins, special filtering on dimer models was applied to make sure the intracellular, transmembrane, and extracellular domains interacting correspondingly between the γ2 monomers. General docking was performed in conjunction with template-based docking (*16*) between γ2 and α subunits by mapping their corresponding positions to the $GABA_A$ receptor β3 homopentamer template (PDB id: 4cof). Heteropentamers

and hypothetical homopentamers were also constructed by template-based docking. Chimera (*17*) and Pymol (*18*) were used to display the protein structural models.

Quantitatively inferring stability of dimer and pentamer models

We used several quantitative methods to calculate buried surface area and force field to computationally infer the binding affinities of the proposed docking protein complexes (Table 3-6). Buried accessible surface area (*ASA*) and buried hydrophobic accessible surface area (*hydroASA*) dominate binding affinity (*19*), and we treat them as the *hydrophobicity score*. *ASA* is calculated as sum of the surface areas of two proteins monomers minus the surface of protein complex dimer. We used nACCESS [15] software to get solvent *ASA* with solvent probe radius 1.4 Å. Between two proteins and the protein complex, buried surface area caused by carbon and sulfur atoms are defined as the Hydrophobic Buried Surface Area (S_{pho}), buried surface area caused by oxygen and nitrogen atoms as the Hydrophilic Buried Surface Area (S_{phi}). An empirical score (*EmpiricalValue)* was used to obtain the binding affinity by incorporating buried surface area and the hydrophobicity in empirical linear combination. *EmpiricalValue* incorporates buried hydrophobic surface area, and the weights came from previous work (*13*) (Eq. (1). For a given protein complex, *EmpiricalValue* is calculated as (1):

$$\text{EmpiricalValue} = 0.0134 * S_{pho} + 0.0043 * S_{phi} \quad (1)$$

To incorporate the solvent characteristics in transmembrane domain and the extracellular/intracellular domains, we calculated *EmpiricalValue* from three individual domains:

$$\textit{EmpiricalValue'} = (0.0134 * S^{\text{extracellular}}_{pho} + 0.0043 * S^{\text{extracellular}}_{phi}) + (0.0043 * S^{\text{transmembrane}}_{pho} + 0.0134 * S^{\text{transmembrane}}_{phi}) + (0.0134 * S^{\text{intracellular}}_{pho} + 0.0043 * S^{\text{intracellular}}_{phi}) \quad (2)$$

We also used *Choi's dG_est,* which is another empirical based binding affinity calculation (*18*). Its predicted binding energy *dG_est* value is obtained by estimating the contribution of the solvation factor in protein binding by a minimalistic solvation-based model. In addition, force field-based method Rosetta interface analyzer (*20-22*) was applied to examine the quality and stability of protein-protein interaction interface. We

chose the widely accepted binding energy per unit area (*dG_separated/dSASAx100*) and *packstat* (value from poor 0.0 to good 1.0) to illustrate the quality of the interface. In general, the value of *dG_separated/dSASAx100* below -1.5 and value of *packstat* above 0.65 are considered to be good. These two structure-based values are both from Rosetta interface analyzer of Rosetta Buddle 3.4.

Expression vectors with $GABA_A$ receptor subunits

The cDNAs encoding human α1, β2, and γ2 subunits in the pcDNA(3.1) vector with the cytomegalovirus (CMV) promoter were as described previously (*23, 24*). All the truncation mutations were generated using the QuikChange site-directed mutagenesis kit (Stratagene, La Jolla, CA) and confirmed by DNA sequencing in the Vanderbilt DNA Core. The short form of the γ2 subunit was used in this study, and numbering of γ2 subunit amino acids was based on the immature peptide that includes the 39 amino acids of the signal peptide.

Cell culture and transfection

HEK 293T cells were replenished with DMEM supplemented with 10% FBS and 1% antibiotics. HEK 293-T cells for immunoblots were transfected with Fugene (Invitrogen, Carlsbad, CA). Cells were co-transfected with 1 μg of each subunit or 3 μg of single subunit plasmid for each 60 mm^2 dish, and the total lysates were harvested 48 hr later.

Western blot and protein digestion

Transfected HEK293T cells were collected in modified RIPA buffer (50 mM Tris (pH = 7.4), 150 mM NaCl, 1% NP-40, 0.2% sodium deoxycholate, 1 mM EDTA) and 1% protease inhibitor cocktail (Sigma). Collected samples were subjected to gel electrophoresis using 4-12% BisTris NuPAGE precast gels (Invitrogen) and transferred to PVDF-FL membranes (Millipore). Monoclonal anti-α1 subunit antibodies (NeuroMab) and polyclonal anti-γ2 subunit antibodies (Alomone or Millipore) were used to detect $GABA_A$ receptor subunits. Anti-Na+/K+ ATPase antibody (Abcam) was used as a loading control. IRDye® (LI-COR Biosciences)

conjugated secondary antibody was used at a 1:10,000 dilution in all cases. Membranes were scanned using the Odyssey Infrared Imaging System (LI-COR Biosciences). The integrated intensity value of bands was determined using the Odyssey Image Studio software (LI-COR Biosciences).

For protein digestion, cell lysates were incubated with enzyme Endo H or PNGase F in G7 or G5 reaction buffer, respectively (New England BioLabs). Digestion proceeded for 3 h at 37°C and was stopped with 5% β-mercaptoethanol (Sigma). Treated samples were then subjected to SDS-page electrophoresis and western blot.

Measurement of surface $GABA_A$ receptor subunit expression using flow cytometry

Measurement of surface expression of $GABA_A$ receptor α1 and HA-tagged γ2 subunits using flow cytometry has been described previously (*25*). Briefly, transfected HEK 293T cells were removed from the dishes by trypsinization and then resuspended in FACS buffer (phosphate buffered saline, PBS supplemented with 2% FBS and 0.05% sodium azide). Following washes with FACS buffer and permeabilization with Cytofix/cytoperm (BD Biosciences) for 15 min, cells were incubated with mouse monoclonal anti-HA antibody (1:200) or anti-α1 subunit antibody for 2 hours and then incubated with fluorophore Alexa-647 conjugated goat anti-mouse 2^{nd} antibody (1:2000) for 1 hour at 4^{o} C. Cells were then washed with FACS buffer and fixed with 2% paraformaldehyde. The acquired data were analyzed using FlowJo 7.1 (Treestar).

Electrophysiology

HEK 293T cells were co-transfected with 2 µg of each subunit plasmid and 1 µg of the pHook-1 cDNA (Invitrogen, Carlsbad, CA) using a modified calcium phosphate precipitation method and selected 24 hours after transfection by magnetic hapten coated beads (*26*). For each recording, the external bathing solution consisted of (in mM) NaCl 142, KCl 8, $MgCl_2$ 6, $CaCl_2$ 1, HEPES 10, glucose 10, pH 7.4 and 325-330 mOsm. The pipette solution consisted of (in mM) KCl 153, $MgCl_2$ 1 MgATP 2, HEPES 10, EGTA 5, pH 7.3 and

310-320 mOsm. Recording pipettes were made of thin-walled borosilicate glass (World Precision Instruments, Pittsburgh, PA) pulled with a P-2000 laser puller (Sutter Instruments, San Rafael, CA) and fire polished with a microforge (Narishige, East Meadow, NY) to resistances between 1.2-1.8 MΩ when filled with internal solution. Lifted whole cells were voltage clamped at -50 mV (*23, 27*).

Data analysis

Protein IDVs were quantified by using Odyssey fluorescence imaging system (Li-Cor). Macroscopic currents were low pass filtered at 2 kHz, digitized at 10 kHz, and analyzed using the pClamp9 software suite (Axon Instruments, Union City, CA). Statistical significance of immunoblot flow cytometry and electrophysiology data was determined by ANOVA with Bonferroni posttests, a Student's unpaired t test or, if appropriate, single-value t test (GraphPad Prism, La Jolla, CA). All analyses used an alpha level of 0.05 to determine statistical significance.

4. Results

Wild-type and mutant $GABA_A$ receptor γ2 subunits had different surface hydrophobicity scores

We determined structural alterations of the three mutant γ2 subunits based on protein homology modeling (Figure 3-1A). The *GABRG2(R136*)* mutation resulted in a loss of a portion of the N-terminus, all four transmembrane domains and all extracellular and intracellular loops with the only the short upstream N-terminal peptide remaining. The *GABRG2(Q390*)* mutation resulted in the loss of the downstream 78 amino acids in the middle of the intracellular TM3-TM4 loop towards the C-terminus while the *GABRG2(W429*)* mutation resulted in loss of the downstream 39 amino acids in the middle of the TM3-TM4 intracellular loop towards the C-terminus. With MUFOLD, structural homology modeling of wild-type and three mutant γ2 subunits was illustrated (Figure 3-1B). It is of note that all the mutant γ2 subunits we presented here are whole proteins including sequences of N-terminus, transmembrane domain to intracellular loop while only

part of the γ2(Q390*) protein model was reported in our previous study (*8*). The hydrophobicity of the protein surface was presented in Figure 3-1C. We measured the whole *ASA* and *hydroASA* of the wild-type and mutant subunits as hydrophobicity scores. At monomer level, compared with the wild-type γ2 subunit (17701.32 for *hydroASA* and 26892.48 for whole *ASA*), the mutant γ2(W429*) subunit had similar areas in *hydroASA* (163641 for *hydroASA*; 24877.64 for whole *ASA*). The mutant γ2(Q390*) subunit had reduced values in whole *ASA* and *hydroASA* (13372.87 *hydroASA*; 20332.57 for whole *ASA*) while the mutant γ2(R136*) subunit protein had the most reduced values in whole *ASA* and *hydroASA* (3580.68 *hydroASA*; 5823.09 for whole *ASA*) and (Figure 3-1D, Table 3-1, Table 3-2).

Different mutant γ2 subunits formed homodimers with different stabilities

After obtaining structural models of wild-type γ2 and mutant subunits, the homodimers were obtained by symmetrical docking and template-based docking on the corresponding models individually. Using the same procedures as previously described by Yu (*28*) and Tsigelny (*29, 30*), we demonstrated that the γ2 subunit homodimers could adopt three different possible conformations. The first conformation was a non-propagating dimer (head-to-tail), which could be obtained by symmetric docking. The second conformation was a propagating dimer that may propagate to a fibril and this dimer could also be obtained by symmetric docking but with membrane constraints, i.e. choosing symmetric docking head-to-head results in both membrane regions located in the membrane. The third conformation was also a propagating dimer that could propagate to a ring structure. We constructed γ2 subunit dimers by adopting the experimentally resolved homo-pentamer as the template.

We present the γ2 subunit homodimers predicted by SymmDock were shown by PyMOL. The two γ2 subunit chains were shown in red and green (Figure 3-2A). Alpha-beta-alpha-beta-gamma pentamer ribbons of the wild-type and the mutant γ2 subunit containing receptors were also presented (Figure 3-2B). We modeled all three possible conformations of mutant γ2 and wild-type γ2 dimers, and calculated the energies which were

represented by buried surface values for each of these hypothetically propagating dimers to rings or annular structures (Figure 3-2C). A larger buried surface values could represent a larger binding affinity and a more stability of the dimers and a higher likelihood of forming ring or annular structures. The wild-type and mutant γ2(W429*) dimers had similar energy (3647.423 for wt and 3650.25 for W429*) propagating to rings. The mutant γ2(Q390X) dimer had the highest energy (5015.323) while the mutant γ2(R136*) dimer had the lowest energy propagating to rings (482) among all the four γ2 subunit dimers (Figure 3-2C). This suggests that γ2(Q390*) subunit dimers are more stable and more likely to form ring or annular structures. We also calculated the energies for propagating fibrils (Figure 3-2D) and nonpropagating dimers (Figure 3-2E) for the wild-type and mutant γ2 subunits. The energy of the γ2(W429*) dimers propagating to fibrils (2697.394) is similar to the wild-type γ2 subunit dimer (2342.576). The energy of the γ2(Q390*) dimers propagating to fibrils (2475.417) is similar to that of γ2 (R136*) subunit dimers (2513.002) (Figure 3-2D). The energies of nonpropagating dimers for the wild-type γ2 subunit (6021.28) were higher than all the mutant γ2 subunits (2513 for γ2 (R136*), 4217.18 for γ2 (Q390*) and 5457.34 for γ2(W429*)) (Figure 3-2E).

Different mutant γ2 subunits had different levels of total protein, and all mutant γ2 subunits were more likely to form dimers and higher oligomers

We utilized a biochemical approach to determine expression levels of mutant γ2 subunits and their propensity to dimerize. We co-expressed mutant γ2 subunits with α1 and β2 subunits and determined the total γ2 subunit protein level. We separately analyzed the γ2(R136*) subunit because of its much smaller molecular mass compared with the other mutant subunits. We demonstrated previously that γ2(R136*) subunits migrated in multiple bands, but with reduced amounts, while wild-type γ2 subunits only migrated in one band. In contrast, mutant γ2(Q390*) and γ2(W429*) subunits migrated with multiple bands at higher oligomers and with one band at monomer level with increased protein amount (Figure 3-3A). We demonstrated previously that the bands of higher oligomers in γ2(Q390*) and γ2(W429*) subunits are dimers and higher oligomers (*4, 23*) by pulse chase radio labeling. The dimers as well as the higher oligomers are resistant to detergent as evidenced

on SDS gels. It is likely that the multiple bands observed in γ2(R136*) subunits are the different glycosylation forms of the mutant protein dimers as the subunits only migrated in two bands after either Endo H (H) digestion, which removes the ER glycosylation, or PNGase F (F) digestion, which removes all glycans. We observed the identical pattern after H and F digestion, indicating the mutant γ2(R136*) subunits only had ER glycosylation (Figure 3-3B). We quantified the total subunit protein amount and demonstrated that the γ2(R136*) subunit had reduced total amount of protein (0.65 ± 0.032, n = 4), γ2(Q390*) subunits had increased total amount of protein (3.175 ± 0.125, n = 4) while the γ2(W429*) subunits (1.025 ± 0.086) had a total amount of protein that was similar to that of wild-type subunit, which was arbitrarily taken as 1 (Figure 3-3C). We also determined the relative amount of dimers/higher oligomers compared to monomers in each condition. The dimers/higher oligomers or monomers were normalized to loading control and the ratio of dimers/higher oligomers over monomers was measured. We demonstrated that all three mutant γ2 subunits (1.72 ± 0.13 for R136*, 2.68 ± 0.29 for Q390*, 1.575 ± 0.085 for W429*, n = 4) were more likely to form dimers or higher oligomers compared with wild-type γ2 subunits (0.385 ± 0.06 for wt) (Figure 3-3D). Highest steady state amount of higher oligomers and total protein of γ2(Q390*) subunits among all γ2 subunits suggested that the γ2(Q390*) subunits were most stable and were not easily disposed of by the cellular degradation machinery. In summary, compared to wild-type γ2 subunits, γ2(R136*) subunit levels were reduced, γ2(Q390*) subunits had increased total protein, and total γ2(W429*) subunits were unaltered.

Surface hydrophobicity of γ2 subunits was the highest among $GABA_A$ receptor subunits, and the γ2-γ2 dimer was the most stable dimer among all $GABA_A$ receptor subunit homodimers

We previously demonstrated that wild-type γ2 subunits also have a tendency to dimerize when there is no partnering subunit (*23*). We modeled wild-type γ2 subunits and compared them with other wild-type subunits including α1, β2 and δ subunits (Figure 3-4A). We demonstrated that the hydrophobicity score and the ratio of *hydroASA* over the whole *ASA* of the γ2 subunits were the highest among all the $GABA_A$ receptor subunits (Figure 3-4B, C and Table 3-3). For all structural models, α, β2, β3, γ2, and δ subunits were treated as

monomers, and the homodimers were obtained by symmetric docking on these corresponding models individually. The binding affinities were predicted by these quantitative criteria listed in Table 3-4 Binding affinities obtained from *Hydrophobic Buried Surface Area*, *EmpiricalValue*, *Choi's dG_est* and *dG_separated/dSASAx100* could explain the phenomenon that wild-type γ2 dimers had the highest binding affinity among all wild-type $GABA_A$ receptor subunit dimers, even larger than α1, β3, and δ subunit dimers. *Buried Area ASA* of the wild-type γ2 dimer was a little smaller than the wild-type β2 dimer, which is inconsistent with the observation, while *Packstat* failed to explain the protein stability ranking among these dimers. From these results, we concluded that the wild-type γ2 dimer had the largest buried surface area and the largest hydrophobic buried surface area compared with all other wild-type subunit dimers. The large C-terminus in the intracellular region of γ2 dimers may make it the most stable dimer among all the wild-type dimers.

There was differential interaction of mutant γ2 subunits with wild-type partnering subunits

Instead of directly symmetrical docking in constructing dimers, mutant β-α-β-α-γ2(R136*), β-α-β-α-γ2(Q390*), β-α-β-α-γ2(W429*) and wild-type β-α-β-α-γ2 pentameric receptors were constructed by template-based docking from the solved β3 homopentamer structure (Figure 3-5A). Since the mutant γ2 subunit was the only difference among these pentamers, we only considered the α-γ2 and γ2-β binding affinity variants between the wild-type and mutant pentamers in the template-based docking pentamer. The average of these two binding affinities was assumed to determine the stability of the whole pentamer. The average interface affinities in wild-type α-γ2/γ2-β, mutant α-γ2(R136*)/β-γ2(R136*), mutant α-γ2(Q390*)/β-γ2(Q390X) and mutant α-γ2(W429*)/β-γ2(W429*) subunits illustrate the stability of these pentamers (Table 3-4, 3-5). The binding affinities of all the protein-protein interfaces were detailed in Table 3-5. Binding affinities obtained from buried surface area and empirical score (*Buried Surface Area*, *Hydrophobic Surface Area*, *EmpiricalValue*, *EmpiricalValue'*, and *Choi's dG_est*) were all consistent with the observation that the mutant pentamer β-α-β-α-γ2(R136*) was less stable than the wild-type pentamer β-α-β-α-γ2, and the wild-type

pentamer β-α-β-α-γ2 was less stable than the mutant pentamer β-α-β-α-γ2(Q390*). Only structure-based criterion *dG_separated/dSASAx100* and *Packstat* could not explain the stability rankings.

The structural interpretation from the modeling results was similar to hydrophobicity analysis in mutant subunit dimers. The large truncation in the γ2(R136*) subunit made the binding affinity reduced by the buried surface area shrinking in both interfaces of neighboring α and β subunits. While the truncation in the γ2(Q390*) subunit increased buried surface area in adjacent subunits of the pentamer, the different interactions among the wild-type and mutant γ2 subunits may have different impacts on the biogenesis of wild-type partnering subunits. We have compared the total α1 subunit expression when it was co-expressed with the wild-type β2 subunit and different γ2 subunits. Compared with the α1 subunit co-expressed with the wild-type γ2 subunit, the α1 subunit expression was not changed in the γ2(R136*) subunit condition. In contrast, the α1 subunit expression was reduced when co-expressed with γ2(Q390*) and γ2(W429*) subunits (Figure 3-5B). When normalized to the α1 subunit in the wild-type γ2 subunit condition which was arbitrarily taken as 1, the α1 subunit was reduced almost by half when co-expressed with the γ2(Q390*) subunit (0.53 ± 0.04, n = 4) while the α1 subunit was reduced by ~25% when co-expressed with the γ2(W429*) subunit (0.76 ± 0.08, n = 4) (Figure 3-5C).

There was different surface expression of mutant γ2 subunits and their wild-type partnering subunits

Because γ2 subunits have to be co-assembled with α and β subunits to form pentamers before they can traffick to the cell surface and synapses, we co-expressed γ2 subunits with α1 and β2 subunits. We determined the surface expression of the wild-type and mutant γ2 subunits and the wild-type α1 subunit with flow cytometry. When co-expressed with α1 and β2 subunits, surface expression of all three mutant γ2 subunits were reduced substantially (2.25 ± 0.95 for R136*; 4.63 ± 0.69 for Q390*; 13 ± 2.04 for W429*, n = 4) relative to wild-type

γ2 subunits (taken as 100) (Figure 3-6A and C). However, the surface expression of the γ2(W429*) subunit was higher than that of the γ2(R136*) and γ2(Q390*) subunits.

We then determined surface expression of α1 subunits. The α1 subunit surface expression with co-expression of γ2(R136*) subunits (103 ± 7, n = 4) was not reduced compared with the wild-type. The α1 subunit surface expression was substantially reduced with co-expression of γ2(Q390*) subunits (44 ± 4, n = 4) and reduced to a lesser extent with co-expression of γ2(W429*) subunits (70 ± 9, n = 4) (Figure 3-6D).

Wild-type α1 subunits had different glycosylation and ER retention when co-expressed with mutant γ2 subunits.

Endoplasmic reticulum (ER) retention and ER associated degradation (ERAD) are common pathways for disposal of misfolded mutant proteins. The ERAD quality control pathway is conserved for all the glycoproteins including $GABA_A$ receptor subunits (*31*). We have demonstrated that both wild-type and mutant $GABA_A$ receptor subunits are subject to ERAD. We co-expressed α1 and β2 subunits with wild-type or mutant γ2 subunits in HEK cells, obtained total cell lysates for each transfection condition, and treated them with Endo H or PNGase F followed by analysis with SD-PAGE. With Endo H digestion, the α1 subunit migrated at 48.4 and 46 KDa, and the 48.4 KDa band contained the mature form while the 46 KDa band contained the immature form (Figure 3-7A), as previously reported (*32*). Total α1 subunit levels were not changed with co-expression of mutant γ2(R136*) subunits (1.05 ± 0.05 for U, 1.03 ± 0.07 for H, 1.07 ± 0.04 for F, n = 4); but were reduced with co-expression of either γ2(Q390*) subunits (0.48 ± 0.02 for U, 0.51 ± 0.05 for H, 0.46 ± 0.07 for F, n = 4) or γ2(W429*) subunits (0.79 ± 0.03 for U, 0.82 ± 0.14 for H, 0.78 ± 0.05 for F) (Figure 3-7B). The α1 subunit was more reduced with co-expression of γ2(Q390*) subunits than of γ2(W429*) subunits. We then compared the relative ratio of the mature or the immature form to the total α1 subunit protein. The mature form of α1 subunits are trafficked beyond the ER and reach the cell surface while the immature form resides in the ER. There were no differences in the ratios of mature and immature α1

subunit to the total α1 subunit for the γ2(R136*) subunit (0.76 ± 0.11 for mature wt vs 0.81 ± 0.09 for mature R136*; 0.27 ± 0.08 for immature wt vs 0.21 ± 0.06 for immature R136*). However, the ratio of the mature to total α1 subunit was reduced with coexpression of γ2(Q390*) (0.25 ± 0.05 for mature Q390*; and γ2(W429*) (0.44 ± 0.08 for mature γ2(W429*) subunits. In contrast, the ratio of the immature band to the total α1 subunit was increased with co-expression of the two mutant subunits (0.73 ± 0.15 for the immature γ2(Q390*) subunit; 0.61 ± 0.14 for the immature γ2(W429*) subunit) (n = 4) (Figure 3-7C). The increased presence of the immature α1 subunit and glycosylation arrest was likely due to the oligomerization of α1 and γ2 subunits and stable interactions between these subunits. Consequently, thee immature subunits would be degraded by ERAD, resulting in decreased surface expression of the α1 subunits and reduced total current.

Different γ2 mutant subunits co-expressed with α1 and β2 subunits produced receptors with different channel functions

Co-expression of the different mutant γ2 subunits resulted in different levels of surface expression of the wild-type partnering subunits. To confirm this, we compared the peak current amplitude and zinc sensitivity of currents recorded from cells co-expressing α1 and β2 subunits with γ2, γ2(R136*), γ2(Q390*) or γ2(W429*) subunits. The peak currents from cells expressing the α1β2γ2(R136*) (724.8 ± 88.05, n = 10), α1β2γ2(Q390*) (214.4 ± 83.15, n = 8) or α1β2γ2(W429*) (1029 ± 95.48, n = 7) subunits were smaller than those recorded from cells co-expressing wild-type γ2 subunits (3502 ± 493.3, n = 6) (Figure 3-8A). Compared to currents from cells co-expressing α1 and β2 subunits with wild-type γ2 subunits, currents recorded from cells co-expressing mutant γ2 subunits had enhanced zinc sensitivity, suggesting surface expression of α1β2 receptors with co-expression of all of the mutant subunits (Figures 3-8A, 8C). Zinc (10 μM) application minimally reduced wild-type receptor currents (8.33± 1.29, n = 6) but reduced currents from cells co-expressing mutant γ2 subunits by ~80-90% (Figure 3-8C).

5. Discussion

We propose that differential protein structural disturbances in mutant $GABA_A$ receptor γ2 subunits result in differential mutant γ2 subunit protein biogenesis, maturation, surface expression and ultimately total GABA-evoked current. The mutant γ2 subunits resulting from different mutations that produce different structural disturbances may be phenotype modifiers of their associated genetic epilepsies.

We have demonstrated that different mutant subunits are predicted to adopt different conformations. Consequently, these structurally altered mutant subunits had different protein surface hydrophobicities. The γ2(R136*) subunits only retained a short N-terminal upstream sequence, which were efficiently degraded inside cells. Based on the structure modeling and biological data, it is likely that γ2(R136*) subunits were not incorporated into the pentamer as the wild-type receptor. Therefore, the α1β2γ2(R136*) receptor current had a high sensitivity to zinc inhibition which suggests γ2 subunit was absent and the current was likely produced by α1β2 receptors. The γ2(Q390*) subunits adopted a new α-helix, became very aggregation-prone, were stable and inefficiently degraded while the γ2(W429*) subunits had a stability that was similar to wild-type γ2 subunits. Based on the buried surface area, mutant γ2(Q390*) subunit dimers had the highest energies while γ2(R136*) subunits had the lowest energies. Consequently, the γ2(R136*) subunit dimer was the least stable, the γ2(Q390*) subunit dimer was the most stable, and the γ2(W429*) subunit dimer had stability similar to wild-type γ2 subunit dimers. The γ2(R136*) subunit could not form heterodimers with binding partners like the α1 subunit while both γ2(Q390*) and γ2(W429*) subunits could form heterodimers with binding partners. The mutant γ2(Q390*) subunit is the most stable protein and formed the most higher oligomers compared with γ2(R136*) and γ2(Q390*) subunits. Although both wild-type γ2 subunit and mutant γ2(Q390*) subunits could dimerize, the mutant γ2(Q390*) subunit formed the most higher oligomers compared to wild-type γ2 and mutant γ2(R136*) and γ2(W429*) subunits. Interestingly, although to a different degree, all mutant γ2 subunits were more likely to dimerize than wild-type γ2 subunits. It is likely that the hydrophobicity surface in the wild-type γ2 subunits that promote dimerization is somehow masked by co-assembly with other

partnering subunits such as α1 and β2 subunits, while the hydrophobicity surface of mutant γ2 subunits could not be masked during subunit folding and assembly. Thus, mutant γ2 subunits are available to dimerize or to form the higher oligomers.

The interaction of γ2 subunits and wild-type partnering subunits like α1 or β2 subunits are different. The mutant γ2 subunits suppressed biogenesis of their partnering wild-type subunits. The docking study indicated that γ2(R136*) subunits had minimal interaction with wild-type α1 subunits. As the *ASA* located at the interface of proteins dominates their stability, γ2(R136*) subunits with only small remnant of the extracellular domain had minimal interaction with wild-type α1 subunits, consistent with the experimental biochemical observations. We demonstrated that the α1 subunit surface expression levels were unaltered when α1 subunits were co-expressed with β2 and γ2(R136*) subunits. In contrast, α1 subunit levels were most reduced when α1 subunits were co-expressed with γ2(Q390*) subunits and were reduced, but to a lesser extent, when co-expressed with γ2(W429*) subunits. The increased buried surface area or the high energies to form propagating dimers in γ2(Q390*) subunits may explain the strong dominant negative suppression of the partnering subunits like α1 subunits.

Reduced surface expression of mutant protein is a common observation among all $GABA_A$ receptor subunit mutations (*33*). The nonsense mutations in $GABA_A$ receptor subunits results in loss of function of the subunit. We demonstrated that all of the mutant γ2 subunits had minimal surface expression, although the γ2(W429*) subunit had a small but significant increase of surface expression compared to the γ2(R136*) and γ2(Q390*) subunits. However, the significance of this small increase is unknown *in vivo* with a much crowded cellular environment and during development. As to the partnering α1 subunit, its surface expression was consistent with the total protein expression for each mutation. The surface expression of α1 subunits was unaltered when co-expressed with β2 and γ2(R136*) subunits but was reduced when co-expressed with β2 and γ2(Q390*) subunits or γ2(W429*) subunits. $GABA_A$ receptors must traffick to the cell surface to conduct

chloride ions. Those mutant subunits that are retained intracellularly are nonfunctional and may cause cellular toxicity like ER stress (*4*).

Since only receptors trafficked to the cell surface are functional, and different mutant γ2 subunits result in differential surface expression of partnering subunits, we determined the total GABA-evoked current produced for receptors formed in the presence of each mutant γ2 subunit. When mutant γ2 subunits were co-expressed with α1 and β2 subunits, all of the currents were substantially reduced. However, the mutant α1β2γ2(Q390*) receptor channel current was the most reduced while the α1β2γ2(W429*) receptor current was the least reduced. With the zinc sensitivity test, it is likely that all the mutant currents were largely due to α1β2 receptor currents. This is consistent with the notion that β subunits compensate for γ subunits when they are lacking, and that the γ subunit is not essential for receptor assembly (*34*) but is critical for receptor clustering at synapses (*35*). In patients heterozygously harboring these *GABRG2* mutations, it is likely the mutant γ2 subunits are not present on the cell surface. Only the wild-type subunits will traffick to the cell surface and synapses.

In this study, homology modeling provides a promising method to obtain a high accuracy tertiary protein model, which could reveal substantial structural detail. This homology modelling can help to explain protein functions and molecular mechanisms. Once the structure was predicted, it could be treated as a monomer for docking predictions. In our study, the challenge in constructing dimers mostly comes from the membrane region, which restricts intracellular, transmembrane, and extracellular domains to bind accordingly to its counter part of the monomer. In this work, we filtered all the unqualified models in dimer construction. We used the structurally solved β3 homopentamer and hypothetical homopentamer structures to model $GABA_A$ receptor subunits by aligning a monomer to corresponding position to the β3 template. Because our docking prediction of all of the wild-type and mutant $GABA_A$ receptor subunits was template-based, the prediction is more accurate than with general docking.

In protein-protein interactions, many factors could influence the binding affinity, including hot spots, anchor residues, allosteric regulators and non-interface affinity modifiers. Hence, we used multiple quantitative criteria to infer the binding affinities of the protein complexes constructed from docking on structure prediction components. Compared with the experimental results, buried surface area based and empirical based methods are consistent with most biochemical and electrophysiological observations, while Rosetta based predictions succeed only in one observation. The limitation of structure based methods may come from Rosetta's sensitive energy function, where small errors in structural conformation may produce large fluctuations in energy values.

In summary, as shown in Table 3-7, we demonstrated that different *GABRG2* mutations may result in mutant subunits with different protein conformations due to different structural disturbances and different functional consequences. This could be applied to other mutations associated with many human diseases. In this study, all the three *GABRG2* mutations (R136*, Q390*, W429*) resulted in a loss-of-function of the mutant subunits, which could not traffick to the cell surface and were retained inside ER with glycosylation arrest. However, the *GABRG2* R136* mutation resulted in a mutant subunit that had the least impact on partnering subunits due to its unstable binding with the partnering subunits, while the γ2(Q390*) subunits had the most dominant negative suppression of the wild-type partnering subunits due to the stable binding with partners during protein-protein interactions. The γ2(W429*) subunits had a mild dominant negative suppression on the wild-type partnering subunits. Therefore, the *GABRG2(Q390*)* mutation should result in a more severe phenotype compared with *GABRG2(R136*)* and *GABRG2(Q390*)* mutations.

Acknowledgements: Research was supported by grants from Citizen United for Research in Epilepsy (CURE), Dravet syndrome foundation (DSF), Dravet.org which is previously named IDEAleague, Vanderbilt Clinical and Translation Science Award and NINDS R01 NS082635 to J.Q.K., NINDS R01 NS51590 to R.L.M and R01 GM100701 to D.X., NICHD Grant No. P30 HD15052 to Vanderbilt Kennedy Center.

Table 3-1. Summary of the binding affinity of *GABRG2* mutant subunits.

Index	Binding Affinity of homo-dimer	Binding Affinity of pentamer α-β-α-β-γ2 pentamer
Wide-type γ2	stable	stable
Mutant γ2(R136*)	least stable	least stable
Mutant γ2(Q390*)	most stable	most stable
Mutant γ2(W429*)	same as wild-type	same as wild-type

Table 3-2. Binding affinity quantitative criteria on different mutant γ2 subunits form homo-dimers with different stabilities

Name	Buried Surface Area	Hydrophobic Buried Surface ASA	Empirical Value	Empricial Value'	Choi's dG_est	dG_separated/dSASAx100	Packstat
Wide-type γ2	2342.576	1675.349	25.319	NA	-13.26	104.139	0.464
Mutant γ2(R136*)	2513.002	1556.015	24.966	NA	-9.09	474.118	0.558
Mutant γ2(Q390*)	2475.417	1796.585	26.993	NA	-9.13	233.474	0.482
Mutant γ2(W429*)	2697.394	1679.967	26.886	NA	-9.70	17.501	0.423

Table 3-3. Binding affinity quantitative criteria on wide-type GABAR subunits

Name	Buried Surface Area	Hydrophobic Buried Surface ASA	EmpiricalValue	EmpiricalValue'	Choi's dG_est	dG_separated /dSASAx100	Packstat
$GABA_AR$-α	2247.564	1372.385	22.153	NA	-11.12	341.663	0.461
$GABA_AR$-β2	2358.566	1558.47	24.324	NA	-12.48	456.072	0.534
$GABA_AR$-β3	2300.280	1487.457	23.428	NA	-10.39	278.083	0.645
$GABA_AR$-δ	2150.594	1214.823	20.302	NA	-10.03	129.653	0.575
$GABA_AR$-γ2	2342.576	1675.349	25.319	NA	-13.26	104.139	0.464

Table 3-4. Binding affinity quantitative criteria on interaction of the mutant γ2 subunits with the wild-type partnering subunits

Name	Buried Surface Area	Hydrophobic Buried Surface ASA	EmpiricalValue	EmpiricalValue'	Choi's dG_est	dG_separated/dSASAx100	Packstat
pentamer α-β-α-β-γ2(R136*)	1123.039	654.1	10.781	10.781	-9.37	351.0895	0.508
pentamer α-β-α-β-γ2(Q390*)	4725.071	3229.327	49.705	31.983	-12.76	326.311	0.516
pentamer α-β-α-β-γ2(W429*)	4120.845	2734.375	42.602	33.753	-12.41	315.1405	0.5805
pentamer α-β-α-β-γ2	4149.771	2744.97	42.823	46.491	-12.41	310.7	0.5445

Table 3-5. Details in interface binding affinities by quantitative criteria on interaction of the mutant γ2 subunits with the wild-type partnering subunits

Name	Buried Surface Area	Hydrophobic Buried Surface ASA	EmpiricalValue	EmpiricalValue'	Choi's dG_est	dG_separated/dSASAx100	Packstat
γ2(R136*)_α	487.011	268.335	4.536	4.5359958	-9.86	0.43	0.272
γ2(R136*)_β3	1759.066	1039.865	17.0268	17.0267553	-8.88	701.749	0.744
γ2(Q390*)_α	4729.686	3315.521	50.5089	27.1772649	-13.22	477.717	0.503
γ2(Q390*)_α	2642.559	1586.729	25.802		-10.7	527.193	0.564
γ2(Q390*)_α	257.206	227.641	1.3753		-8.47	8.585	0.462
γ2(Q390*)_β3	4720.455	3143.133	48.900	36.7894956	-12.3	174.905	0.529
γ2(Q390*)_β3_p1	2857.863	1696.21	27.724		-10.49	144.395	0.634
γ2(Q390*)_β3_p2	1344.309	983.359	9.0652		-9.61	96.252	0.494
γ2(W429*)_α	5063.039	3507.032	53.685	36.4813397	-13.48	484.282	0.494
γ2(W429*)_α_p1	2598.362	1571.929	25.478		-10.7	519.845	0.486
γ2(W429*)_α_p2	1735.684	1403.024	10.491		-9.6	463.565	0.418
γ2(W429*)_α_p3	43.366	35.902	0.513		-8.47	0	NA
γ2(W429*)_β3	3178.651	1961.717	31.520	31.0254521	-11.34	145.999	0.667
γ2(W429*)_β3_p1	2812.69	1656.06	27.165		-10.48	135.046	0.611
γ2(W429*)_β3_p2	328.803	263.077	2.0120		-8.93	97.793	0.471
γ2(W429*)_β3_p3	271.486	74.878	1.849		-8.47	NA	NA
γ2_α1	5134.923	3535.588	54.254	36.912574	-13.48	475.399	0.467
γ2_α1_p1	2598.364	1571.923	25.477		-10.7	519.845	0.533
γ2_α1_p2	1720.879	1393.051	10.383		-9.6	463.332	0.452
γ2_α1_p3	111.936	62.722	1.052		-8.47	0.466	0.355
γ2_β3	3164.619	1954.351	31.392	56.0689895	-11.34	146.001	0.622
γ2_β3_p1	2812.692	1656.054	27.165		-10.48	135.046	0.619
γ2_β3_p2	313.997	253.103	1.904		-8.93	97.792	0.462
γ2_β3_p3	272.842	76.138	1.866		-8.47	Infinity	NA

P1, P2, P3 are different domains of the dimer. P1 is extracellular part, P2 is transmembrane part and P3 is intracellular

Table 3-6. Assessments criteria of protein-protein binding affinity

No	Name	Category	Absolute Value/ Relative Value	Short Description	Tool	Correlate with stability
1	Buried Surface Area	Buried Area	Absolute Value	(Solvent) Accessible Surface Area as the difference between surface area of the complex and the sum of the surface areas of the two proteins	nACCESS	Positive
2	Hydrophobic Buried Surface ASA	Buried Area	Absolute Value	ASA Buried Area caused by Carbon and Sulfur atoms	nACCESS	Positive
3	EmpiricalValue	Empirical Score	Relative Value	Linear combination of Empirical weights on Hydrophobic ASA and Hydrophilic ASA	nACCESS	Positive
4	EmpiricalValue	Empirical Score	Relative Value	Different weights on Hydrophobic ASA and Hydrophilic ASA of transmembrane and extracellular/intracellular domains	nACCESS	Positive
5	Choi's dG_est	Empirical Score	Absolute Value	Linear combination of buried surface areas according to amino-acid types	minipredictor	Positive
6	dG_separated/dSASAx100	Force Field	Absolute Value	Binding energy per unit area, the dG_separated binding energy divided by the total interface surface area	Rosetta Interface Analyzer	Negative
7	Analyzer's Packstat	Force Field	Absolute Value	How well packed the interface is with 0.0 being as poor as possible and 1.0 being perfect shape complementarity	Rosetta Interface Analyzer	Positive

Seven criteria to quantitatively infer the binding affinity and they can be grouped into three categories. The calculated value can be either absolute or relative and they are positively or negatively correlated with the stability.

Table 3-7. The structural disturbances and molecular defects of *GABRG2* nonsense mutations

	R136*	Q390*	W429*
Dimer hydrophobicity	low	high	moderate
Homodimer	yes	yes	yes
Heterodimer	no	yes	yes
Higher oligomer	yes	yes	yes
Surface expression	no	no	No
Suppression of Binding partners	no	yes	yes/moderate
Glycosylation arrest	yes	yes	yes
Channel function	reduced	reduced	reduced

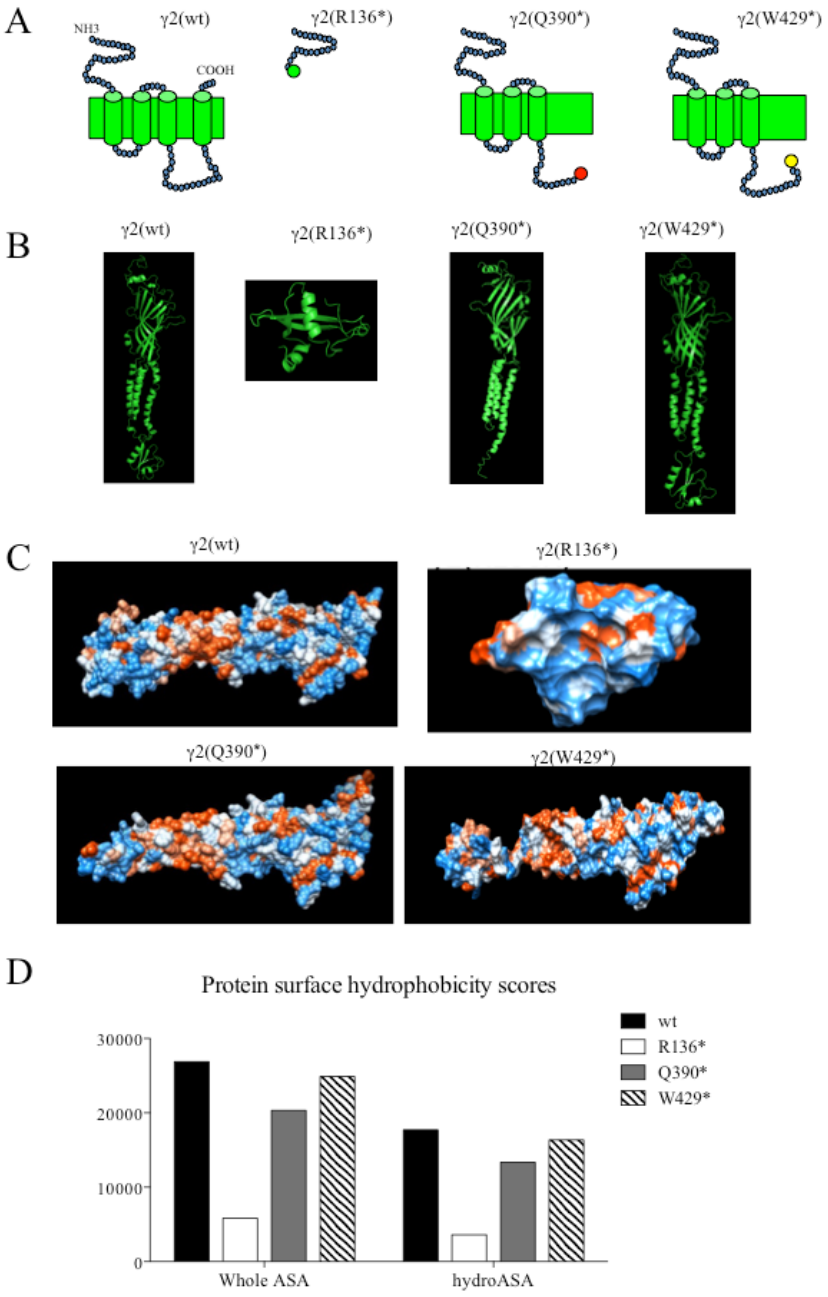

Figure 3-1. Differential protein surface hydrophobicities of mutant γ2 subunits.
A. The schematic illustration of the wild-type γ2 and the mutant γ2(R136*), γ2(Q390*) and γ2(W429*) subunits. **B.** Predicted protein structural models of the wild-type γ2 and the mutant γ2(R136*), γ2(Q390*) and γ2(W429*) subunits. All structural models were predicted by MUFOLD and presented by Pymol. **C.** Predicted protein surface hydrophobicity. Orange stands for hydrophobic residues and blue stands for hydrophilic residues. The protein surfaces were shown by Chimera. **D**. Histogram showing the whole accessible surface area (whole ASA) and hydrophobicity surface accessible area (hydroASA).

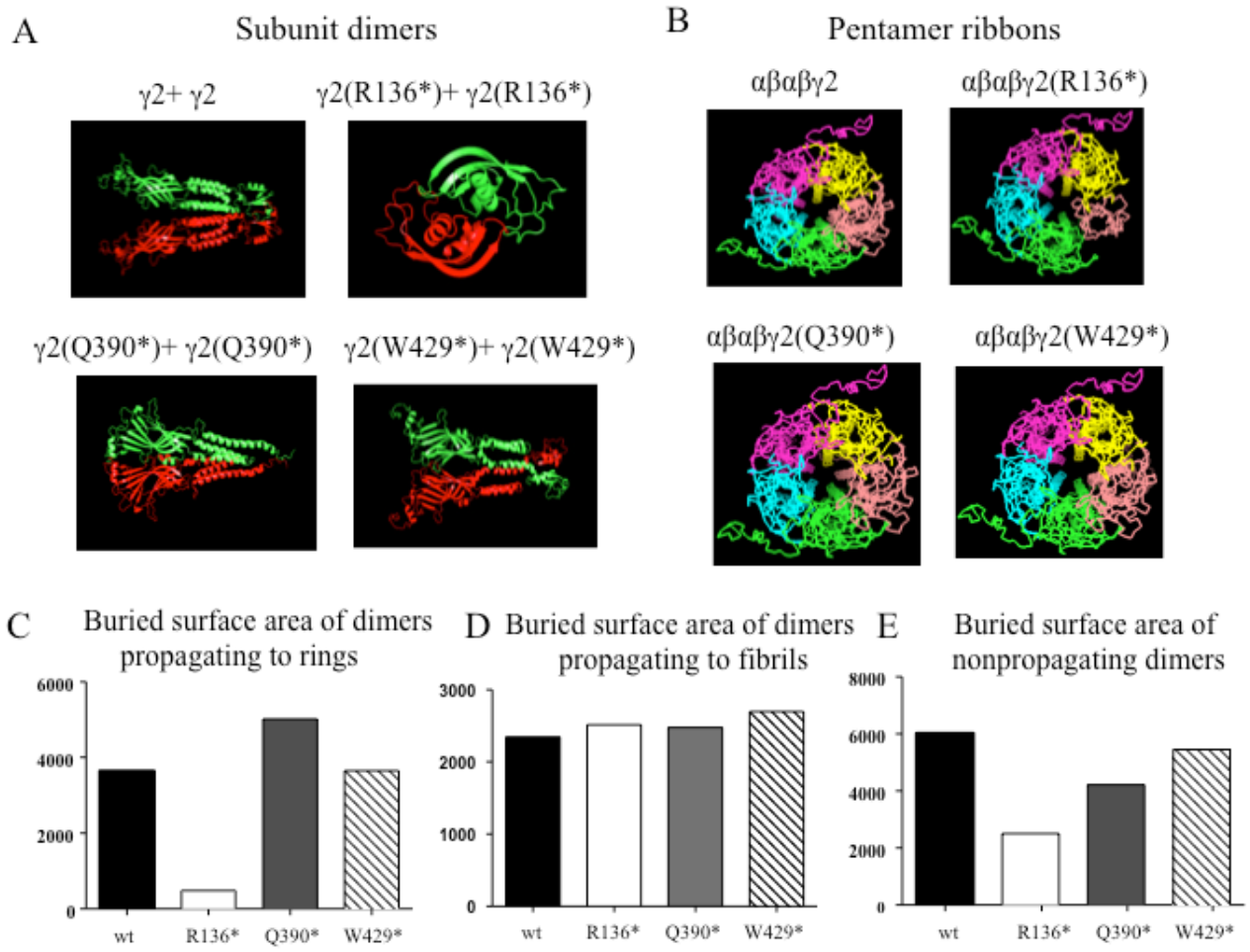

Figure 3-2. Differential potential mutant γ2 subunit homodimers and oligomers.
A. Top docking models for potential mutant γ2 subunit homodimers predicted by SymmDock were shown by PyMOL. In each panel, the two γ2 subunit chains were shown in red and green. **B.** Alpha-beta-alpha-beta-gamma pentamer ribbons of the wild-type and the mutant γ2 subunit containing receptors. Yellow stands alpha subunit, purple for beta subunit, cyan for alpha subunit, green for beta subunit while red stands for the wild-type or the mutant γ2 subunits. **C.** The values of buried surface area of the wild-type or the mutant γ2 subunit dimers which could propagate to ring or annular structures. **D, E.** The values of buried surface area of dimers which could propagate to fibrils (**D**) or nonpropagating dimers (**E**) for the wild-type or the mutant γ2 subunits.

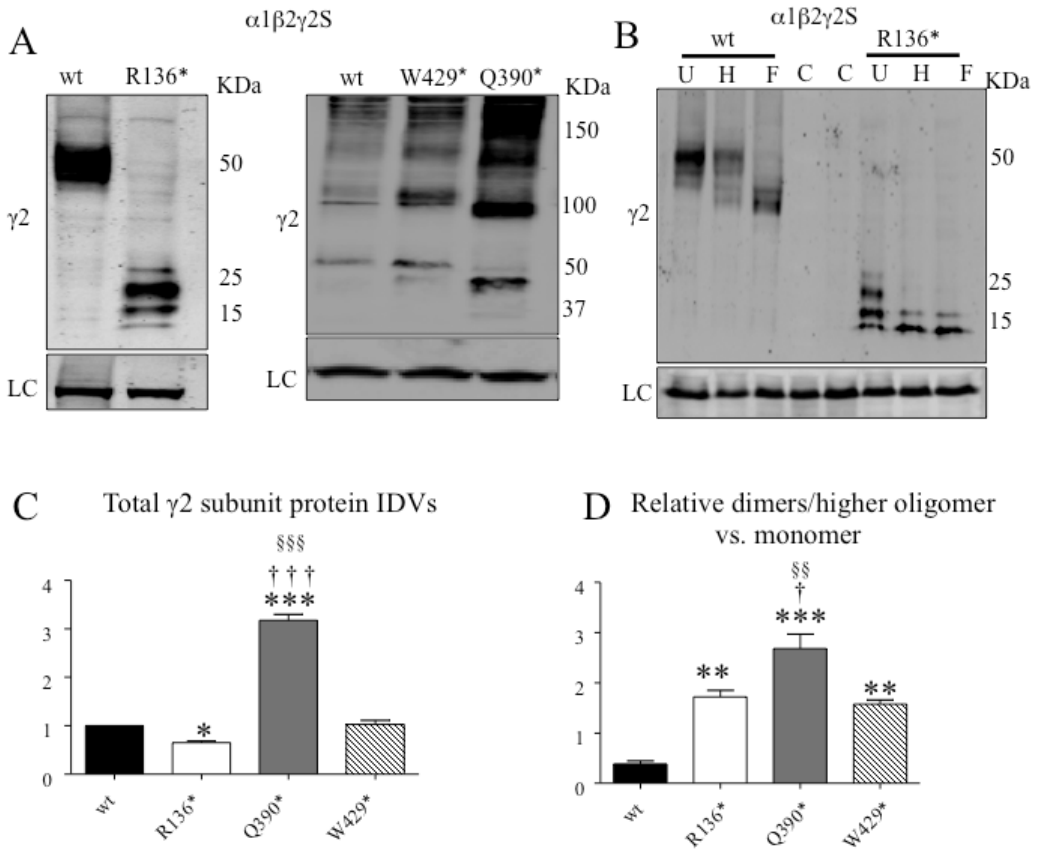

Figure 3-3. Differential propensity of dimerization/formation of higher oligomers of mutant γ2 subunits.
A, B. HEK293T cells were cotransfected with α1, β2 and γ2, γ2(R136*), γ2(Q390*), and γ2(W429*) subunits for 2 days. Total lysates containing γ2 subunits were fractionated by SDS-PAGE and immunoblotted by anti-γ2 subunit antibody. **A.** The gels for γ2(R136*) subunits were run separately because of the small protein mass of the mutant γ2(R136*) subunits. **B.** Total lysates from HEK293T cells were cotransfected with α1, β2 and γ2, γ2(R136*) were either untreated or treated with Endo-H (H) or PNGase F (F) and were then fractionated by SDS-PAGE. **C.** Total mutant subunit band IDVs were normalized to the wild-type γ2 subunits. **D.** The relative ratio of dimer/high molecular mass complexes normalized to the monomer IDVs. In C and D, (* < 0.05, * * <0.01, vs; ***<0.001 vs wt, †< 0.05, †††< 0.001 vs R136*, §§ <0.01, §§§ <0.001 vs W429*). ANOVA with Bonferroni post hoc test was used.

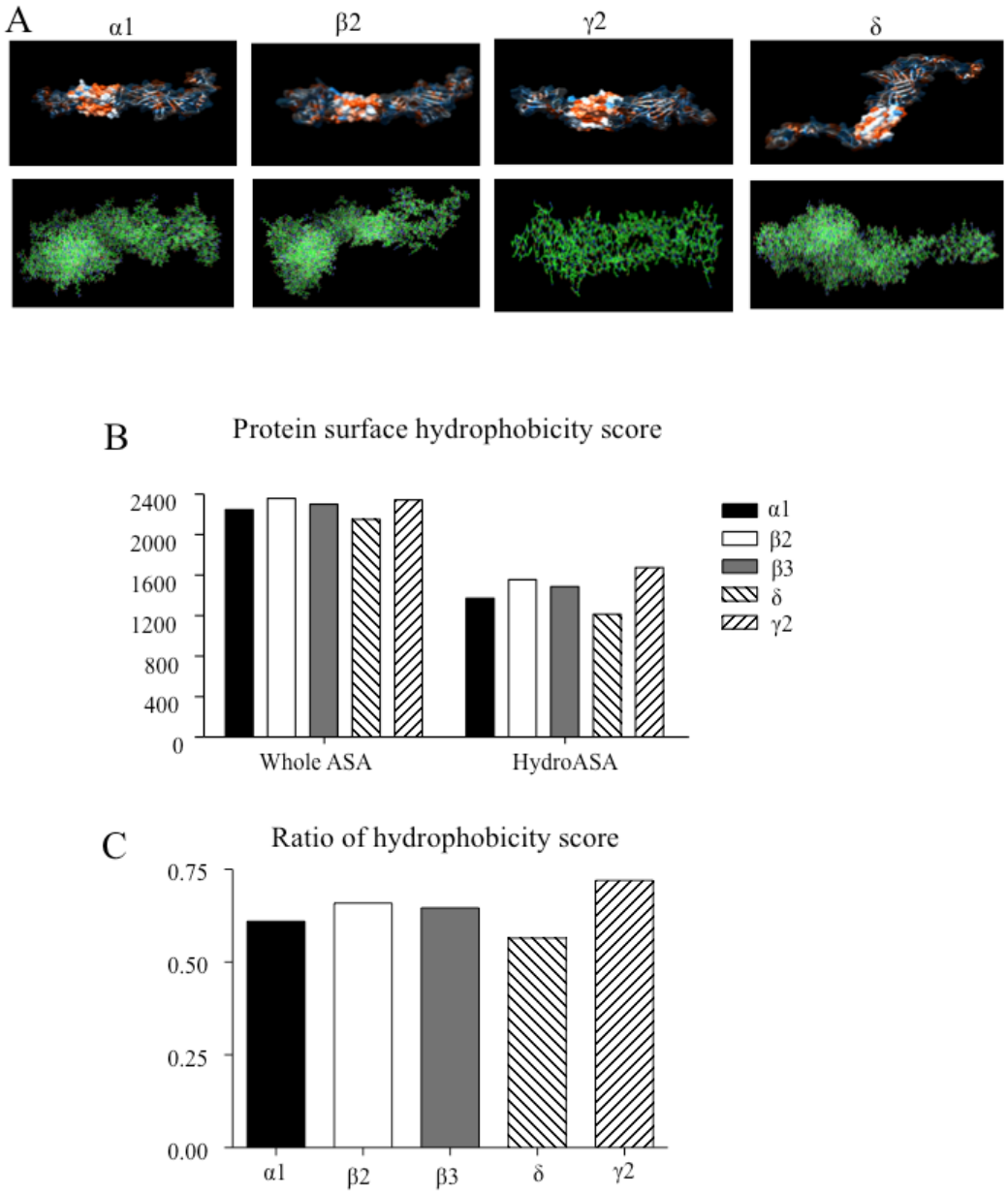

Figure 3-4. Structural modeling of $GABA_A$ receptor subunits and their hydrophobicities.
A. Natural hydrophobic surface (upper panel) and atom (lower panel) presentation of GABRA1, GABRB2, GABRG2, and GABRD (from left to right). Hydrophobicity of the residues was presented by different colors. Orange represents hydrophobic residues and blue hydrophilic residues. The transmembrane domain was presented in solid, while other parts were transparent. These figures are presented by Chimera. **B.** Surface hydrophobicity score of $GABA_A$ receptor subunits. **C.** The ratio of surface hydrophobicity score (*hydroASA/whole ASA*) was plotted.

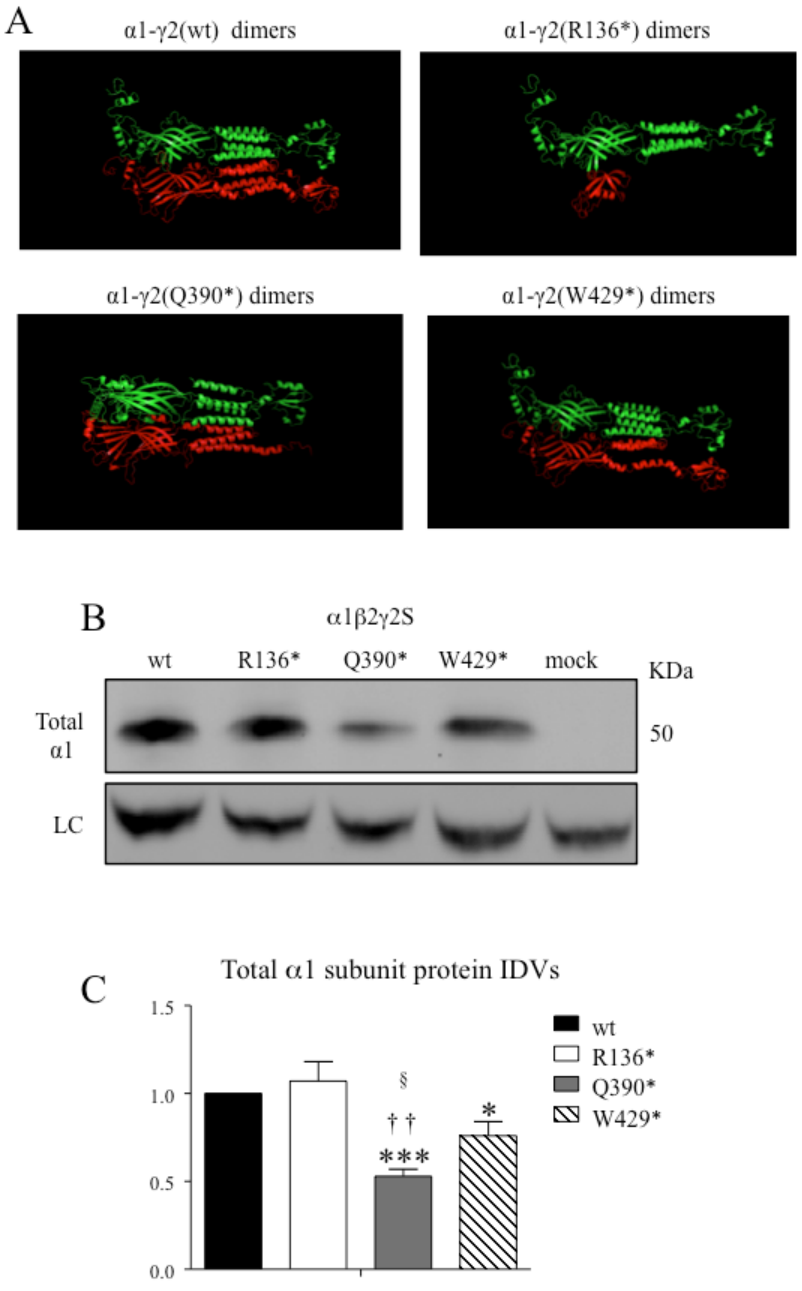

Figure 3-5. Differential interactions of mutant γ2 subunit with partnering subunits.
A. Top docking models of potential complexes between the mutant γ2 subunit (shown in green) and its wild-type partnering α1 subunit (shown in red) predicted by template-based docking were shown by PyMOL. **B.** Total lysates from HEK293T cells cotransfected with α1, β2 and γ2, γ2(R136*), γ2(Q390*), and γ2(W429*) subunits for 2 days were fractionated by SDS-PAGE and immunoblotted by anti-α1 subunit antibody. The gels were run under the same experimental conditions and were cropped around 50 KDa. The full-length gel for B was presented in Supplementary Figure 1. **C.** Total mutant subunit band IDVs were normalized to the wild-type γ2 subunits (* < 0.05 vs wt; ***<0.001 vs wt) ††< 0.01 vs R136*, § <0.05 vs W429*). One sample t test and unpaired student t test were used.

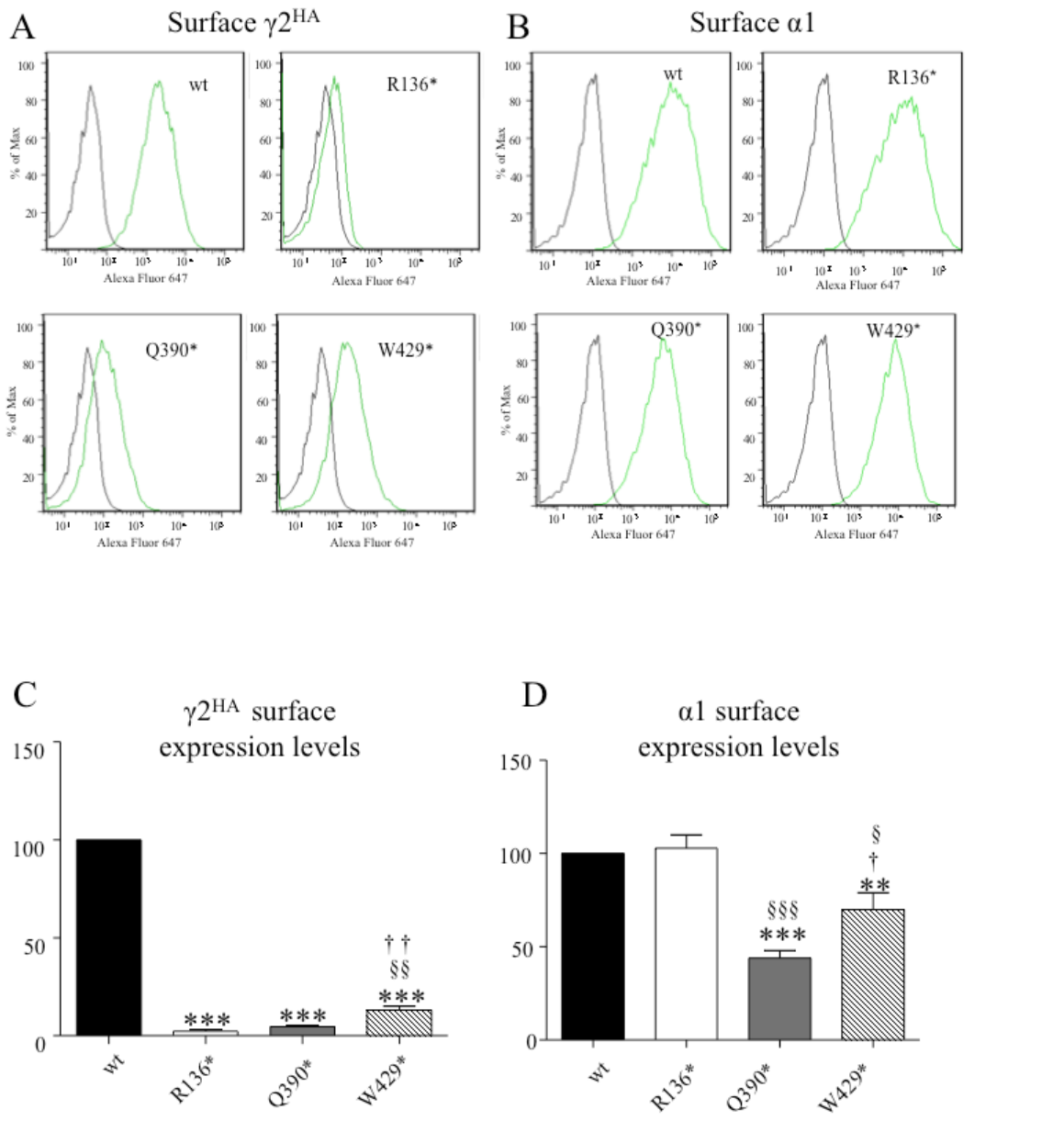

Figure 3-6. Differential cell surface expression of the mutant γ2 subunits and the partnering α1 subunits

A, B. The flow cytometry histograms depict surface HA levels detected with HA-Alexa 647 (**A**) or α1-Alexa 647 (**B**) With coexpression of $\gamma2^{HA}$, $\gamma2(R136*)^{HA}$, $\gamma2(Q390*)^{HA}$ and $\gamma2(W429*)^{HA}$ subunits with α1 and β2 subunits in HEK293T cells. **C.** The relative fluorescence intensities of HA signals from cells expressing the mutant $\gamma2^{HA}$ subunits were normalized to those from wild-type $\gamma2^{HA}$ subunits which were arbitrarily taken as 100. **D**. Relative fluorescence intensities of α1 subunit signals from cells expressing the mutant $\gamma2^{HA}$ subunits normalized to those from wild-type α1 subunits which were arbitrarily taken as 100. In **C** and **D**, ***p < 0.001 vs. wt; † p<0.05, †† p<0.01 vs Q390*, § p < 0.05, §§P<0.01 vs. W429*. One sample t test and unpaired student t test were used.

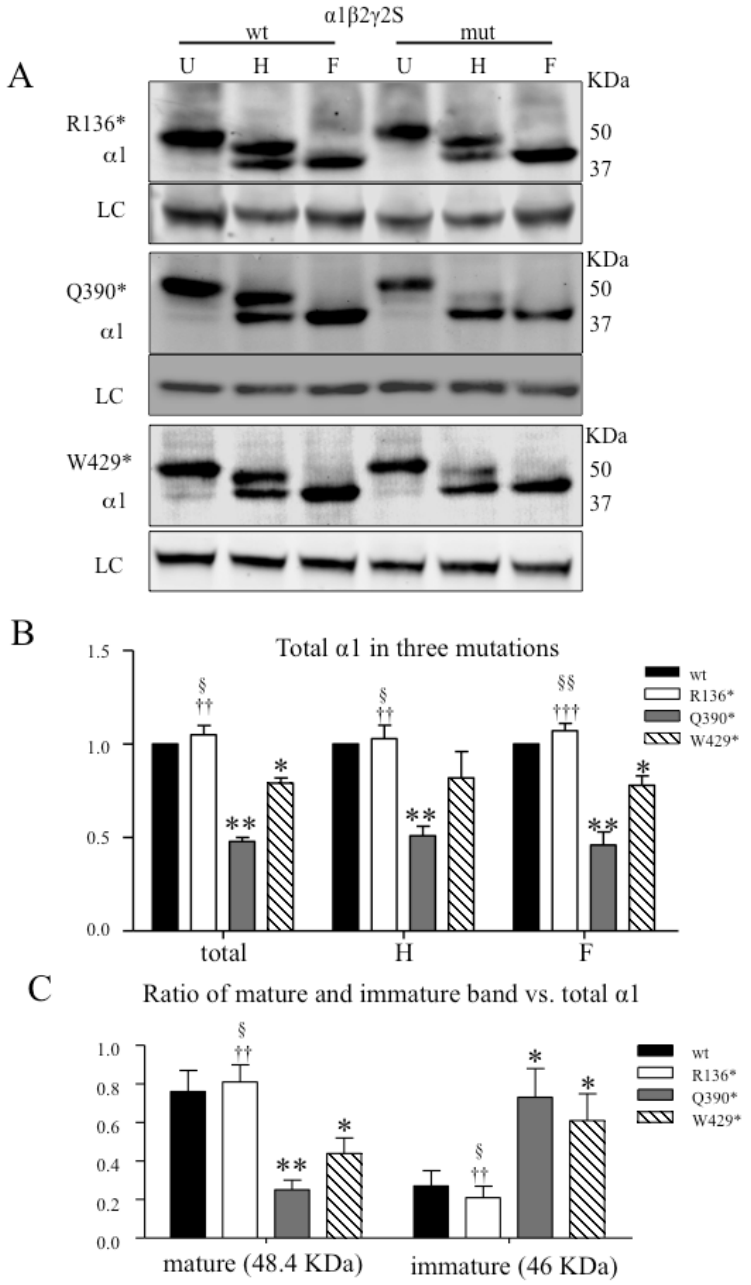

Figure 3-7. The wild-type partnering α1 subunits had glycosylation arrest when coexpressed with γ2(Q390*) and γ2(W429*) subunits but not with γ2(R136*) subunits.

A. HEK293T cells were cotransfected with α1 and β2 subunits and γ2 (wt), γ2(R136*), γ2(Q390*), or γ2(W429*) subunits. Total lysates of these HEK293T cells were undigested (U) or digested with Endo H (H) or PNGase F (F) followed by SDS-PAGE and probed with anti-α1 subunit antibody. After Endo-H digestion, α1 subunits migrated in 48.4 KDa and 46 KDa. The gels were run under the same experimental conditions and were cropped around 50KDa. The full-length gel for A was presented in Supplementary Figure 1. **B.** The total α1 subunit protein in U, H and F condition for the wild-type and the mutant α1β2γ2 receptors was quantified and normalized to the wild-type α1 subunit. In H, the IDVs of 48.4 KDa and 46 KDa bands were added. **C**. The ratios of the mature (48.4 KDa) or the immature (46 KDa) band vs total α1 subunit in untreated condition (U) were plotted. In **B** and **C**, *p < 0.01, **p < 0.01 vs wt; † p<0.05, †† p<0.01 vs Q390*, § p < 0.05, §§P<0.01 vs W429*. ANOVA with Bonferroni post hoc test was used.

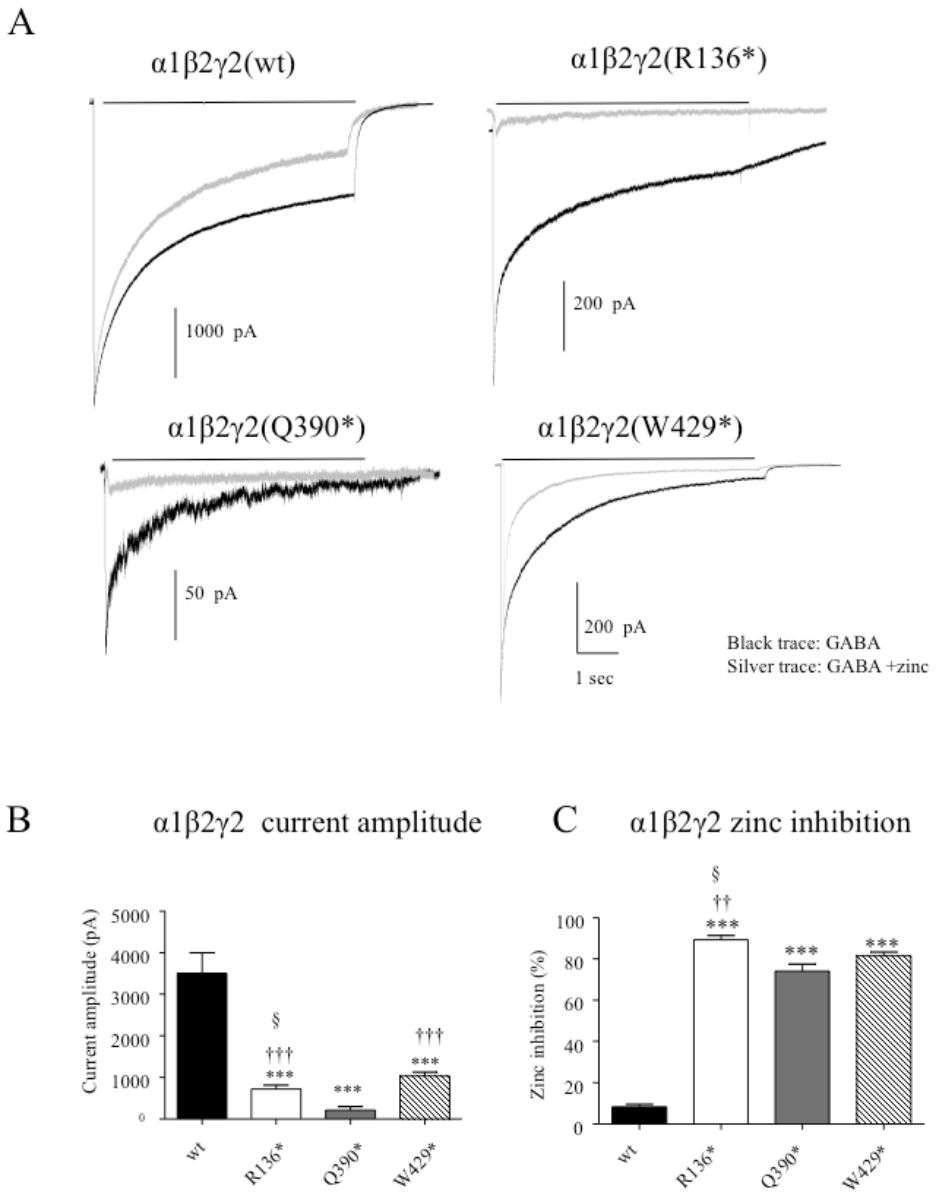

Figure 3-8. Currents recorded from cells expressing all the mutant γ2 subunits in combination with α1 and β2 subunits had reduced peak current amplitudes and were more sensitive to zinc inhibition.

A. $GABA_A$ receptor currents were obtained from HEK293T cells co-expressing α1 and β2 subunits with wild-type γ2, mutant γ2(R136*), γ2(Q390*) or γ2(W429*) (1:1:1 cDNA ratio), subunits with application of 1 mM GABA for 6 sec (black trace). **B.** The amplitudes of $GABA_A$ receptor currents from (A) were plotted. Values were mean ± SEM (n = 8-15 patches from 4 different transfections) (***p < 0.001 vs. wt, †††p < 0.001vs Q390*, § p < 0.05 vs W429*). C. $GABA_A$ receptor currents were obtained with 1 mM GABA applied for 6 sec (black trace) and co-application of 1 mM GABA with 10 μM zinc after pre-application of 10 μM zinc (silver traces). The cells were pre-applied with zinc (10 μM) for 6 sec before co-application. The percent reduction of peak amplitude of $GABA_A$ receptor currents after GABA and zinc co-application were plotted. (***p < 0.001 vs wt; ††p < 0.001vs Q390*, § p < 0.05 vs W429*). ANOVA with Bonferroni post hoc test was used.

References

1. A. J. Johnston, J. Q. Kang, W. Shen, W. O. Pickrell, T. D. Cushion, J. S. Davies, K. Baer, J. G. L. Mullins, C. L. Hammond, S. K. Chung, R. H. Thomas, C. White, P. E. M. Smith, R. L. Macdonald, M. I. Rees, A novel GABRG2 mutation, p.R136*, in a family with GEFS+ and extended phenotypes. *Neurobiol Dis* **64**, 131-141 (2014).

2. L. A. Harkin, D. N. Bowser, L. M. Dibbens, R. Singh, F. Phillips, R. H. Wallace, M. C. Richards, D. A. Williams, J. C. Mulley, S. F. Berkovic, I. E. Scheffer, S. Petrou, Truncation of the GABA(A)-receptor gamma2 subunit in a family with generalized epilepsy with febrile seizures plus. *Am J Hum Genet* **70**, 530-536 (2002).

3. H. Sun, Y. Zhang, J. Liang, X. Liu, X. Ma, H. Wu, K. Xu, J. Qin, Y. Qi, X. Wu, SCN1A, SCN1B, and GABRG2 gene mutation analysis in Chinese families with generalized epilepsy with febrile seizures plus. *J Hum Genet* **53**, 769-774 (2008).

4. J. Q. Kang, W. Shen, R. L. Macdonald, Trafficking-deficient mutant GABRG2 subunit amount may modify epilepsy phenotype. *Ann Neurol* **74**, 547-559 (2013).

5. P. S. Miller, A. R. Aricescu, Crystal structure of a human GABAA receptor. *Nature* **512**, 270-275 (2014).

6. J. Zhang, Q. Wang, B. Barz, Z. He, I. Kosztin, Y. Shang, D. Xu, MUFOLD: A new solution for protein 3D structure prediction. *Proteins* **78**, 1137-1152 (2010).

7. C. Chothia, Hydrophobic bonding and accessible surface area in proteins. *Nature* **248**, 338-339 (1974).

8. J. Q. Kang, W. Shen, C. Zhou, D. Xu, R. L. Macdonald, The human epilepsy mutation GABRG2(Q390X) causes chronic subunit accumulation and neurodegeneration. *Nat Neurosci* **18**, 988-996 (2015).

9. S. Miller, A. M. Lesk, J. Janin, C. Chothia, The accessible surface area and stability of oligomeric proteins. *Nature* **328**, 834-836 (1987).

10. N. Tuncbag, A. Gursoy, R. Nussinov, O. Keskin, Predicting protein-protein interactions on a proteome scale by matching evolutionary and structural similarities at interfaces using PRISM. *Nat Protoc* **6**, 1341-1354 (2011).

11. J. Wang, L. Chen, Y. Wang, J. Zhang, Y. Liang, D. Xu, A computational systems biology study for understanding salt tolerance mechanism in rice. *PLoS One* **8**, e64929 (2013).

12. J. Chen, N. Sawyer, L. Regan, Protein-protein interactions: general trends in the relationship between binding affinity and interfacial buried surface area. *Protein Sci* **22**, 510-515 (2013).

13. D. Xu, S. L. Lin, R. Nussinov, Protein binding versus protein folding: the role of hydrophilic bridges in protein associations. *J Mol Biol* **265**, 68-84 (1997).

14. A. Leaver-Fay, M. Tyka, S. M. Lewis, O. F. Lange, J. Thompson, R. Jacak, K. Kaufman, P. D. Renfrew, C. A. Smith, W. Sheffler, I. W. Davis, S. Cooper, A. Treuille, D. J. Mandell, F. Richter, Y. E. Ban, S. J. Fleishman, J. E. Corn, D. E. Kim, S. Lyskov, M. Berrondo, S. Mentzer, Z. Popovic, J. J. Havranek, J. Karanicolas, R. Das, J. Meiler, T. Kortemme, J. J. Gray, B. Kuhlman, D. Baker, P. Bradley, ROSETTA3: an

object-oriented software suite for the simulation and design of macromolecules. *Methods Enzymol* **487**, 545-574 (2011).

15. D. Schneidman-Duhovny, Y. Inbar, R. Nussinov, H. J. Wolfson, Geometry-based flexible and symmetric protein docking. *Proteins* **60**, 224-231 (2005).

16. A. Szilagyi, Y. Zhang, Template-based structure modeling of protein-protein interactions. *Curr Opin Struct Biol* **24**, 10-23 (2014).

17. E. F. Pettersen, T. D. Goddard, C. C. Huang, G. S. Couch, D. M. Greenblatt, E. C. Meng, T. E. Ferrin, UCSF Chimera--a visualization system for exploratory research and analysis. *J Comput Chem* **25**, 1605-1612 (2004).

18. J. M. Choi, A. W. Serohijos, S. Murphy, D. Lucarelli, L. L. Lofranco, A. Feldman, E. I. Shakhnovich, Minimalistic predictor of protein binding energy: contribution of solvation factor to protein binding. *Biophys J* **108**, 795-798 (2015).

19. T. Kajander, P. C. Kahn, S. H. Passila, D. C. Cohen, L. Lehtio, W. Adolfsen, J. Warwicker, U. Schell, A. Goldman, Buried charged surface in proteins. *Structure* **8**, 1203-1214 (2000).

20. J. Adolf-Bryfogle, R. L. Dunbrack, Jr., The PyRosetta Toolkit: a graphical user interface for the Rosetta software suite. *PLoS One* **8**, e66856 (2013).

21. S. M. Lewis, B. A. Kuhlman, Anchored design of protein-protein interfaces. *PLoS One* **6**, e20872 (2011).

22. Y. Song, M. Tyka, A. Leaver-Fay, J. Thompson, D. Baker, Structure-guided forcefield optimization. *Proteins* **79**, 1898-1909 (2011).

23. J. Q. Kang, W. Shen, M. Lee, M. J. Gallagher, R. L. Macdonald, Slow degradation and aggregation in vitro of mutant GABAA receptor gamma2(Q351X) subunits associated with epilepsy. *J Neurosci* **30**, 13895-13905 (2010).

24. J. Q. Kang, W. Shen, R. L. Macdonald, The GABRG2 mutation, Q351X, associated with generalized epilepsy with febrile seizures plus, has both loss of function and dominant-negative suppression. *J Neurosci* **29**, 2845-2856 (2009).

25. W. Y. Lo, E. J. Botzolakis, X. Tang, R. L. Macdonald, A conserved Cys-loop receptor aspartate residue in the M3-M4 cytoplasmic loop is required for GABAA receptor assembly. *J Biol Chem* **283**, 29740-29752 (2008).

26. L. J. Greenfield, Jr., F. Sun, T. R. Neelands, E. C. Burgard, J. L. Donnelly, R. L. MacDonald, Expression of functional GABAA receptors in transfected L929 cells isolated by immunomagnetic bead separation. *Neuropharmacology* **36**, 63-73 (1997).

27. J. Q. Kang, R. L. Macdonald, The GABAA receptor gamma2 subunit R43Q mutation linked to childhood absence epilepsy and febrile seizures causes retention of alpha1beta2gamma2S receptors in the endoplasmic reticulum. *J Neurosci* **24**, 8672-8677 (2004).

28. X. Yu, J. Zheng, Polymorphic structures of Alzheimer's beta-amyloid globulomers. *PLoS One* **6**, e20575 (2011).

29. I. F. Tsigelny, P. Bar-On, Y. Sharikov, L. Crews, M. Hashimoto, M. A. Miller, S. H. Keller, O. Platoshyn, J. X. Yuan, E. Masliah, Dynamics of alpha-synuclein aggregation and inhibition of pore-like oligomer development by beta-synuclein. *FEBS J* **274**, 1862-1877 (2007).

30. I. F. Tsigelny, Y. Sharikov, V. L. Kouznetsova, J. P. Greenberg, W. Wrasidlo, T. Gonzalez, P. Desplats, S. E. Michael, M. Trejo-Morales, C. R. Overk, E. Masliah, Structural diversity of Alzheimer's disease amyloid-beta dimers and their role in oligomerization and fibril formation. *J Alzheimers Dis* **39**, 583-600 (2014).

31. R. L. Macdonald, J. Q. Kang, M. J. Gallagher, in *Jasper's Basic Mechanisms of the Epilepsies,* J. L. Noebels, M. Avoli, M. A. Rogawski, R. W. Olsen, A. V. Delgado-Escueta, Eds. (Bethesda (MD), 2012).

32. J. Q. Kang, W. Shen, R. L. Macdonald, Two molecular pathways (NMD and ERAD) contribute to a genetic epilepsy associated with the GABA(A) receptor GABRA1 PTC mutation, 975delC, S326fs328X. *J Neurosci* **29**, 2833-2844 (2009).

33. J. Q. Kang, R. L. Macdonald, Making sense of nonsense GABA(A) receptor mutations associated with genetic epilepsies. *Trends Mol Med* **15**, 430-438 (2009).

34. C. N. Connolly, B. J. Krishek, B. J. McDonald, T. G. Smart, S. J. Moss, Assembly and cell surface expression of heteromeric and homomeric gamma-aminobutyric acid type A receptors. *J Biol Chem* **271**, 89-96 (1996).

35. M. J. Alldred, J. Mulder-Rosi, S. E. Lingenfelter, G. Chen, B. Luscher, Distinct gamma2 subunit domains mediate clustering and synaptic function of postsynaptic GABAA receptors and gephyrin. *J Neurosci* **25**, 594-603 (2005).

Chapter 4: Neurobehavioral comorbidities in the *Gabrb3*$^{+/N110D}$ KI mouse model of infantile spasms

1. Abstract

Genetic epilepsies vary in severity from relatively mild childhood absence epilepsy to very severe epileptic encephalopathies (EEs) such as infantile spasms (IS). EEs are often associated with mutations in genes mediating synaptic transmission, including $GABA_A$ receptor ($GABA_AR$) channel subunit genes (*GABR*s). *GABR*s code for the major inhibitory receptors in the brain, and recently the single nucleotide *de novo* mutation N110D in the $GABA_AR$ β3 subunit gene (*GABRB3*) has been shown to be associated with IS. This mutation disrupted $GABA_AR$ current kinetic properties *in vitro*, which may contribute to the epilepsy phenotype. Compared with *in vitro* models, genetically modified mice preserve the complexity of the nervous system and better recapitulate real pathophysiological conditions. Therefore, to have a complete understanding of IS epileptogenesis, our laboratory generated a knock in (KI) mouse carrying this human IS mutation, the heterozygous (het) *Gabrb3*$^{+/N110D}$ KI mice. We have shown that that this animal had epilepsy with multiple seizure types consistent with IS. Here, we hypothesized that the KI mice would have neurodevelopmental consequences that extend beyond epileptogenesis, influencing the realm of cognition and behavior. In this study, I performed a suite of behavioral tests in adult *Gabrb3*$^{+/N110D}$ KI mice to assess activity, anxiety, social interaction and memory. In these tests, the *Gabrb3*$^{+/N110D}$ KI mice displayed hyperactivity and increased anxiety, exhibited social deficits, and had impaired spatial learning and memory, all of which were consistent with cognitive impairment and autistic-like behaviors seen in IS patients. The *Gabrb3*$^{+/N110D}$ KI mice described in this study can serve as a valuable model to unravel the underlying neural mechanisms of and to test drugs designed to ameliorate the neurobehavioral abnormalities of IS.

Childhood epilepsies vary in severity from relatively benign childhood absence epilepsy (CAE) to devastating epileptic encephalopathies (EEs). Infantile Spasms (IS) is one of the classical and catastrophic EEs usually occurring in children younger than 1 year of age and having a peak incidence around 6 months of age (*1*). IS are characterized by intractable epileptic spasms occurring in clusters, often accompanied by a severely abnormal interictal hypsarrhythmia pattern on EEG (*2*). In addition to spasms, most IS patients develop other refractory seizure types in the course of their disease, including partial, myoclonic, tonic and generalized tonic-clonic (GTC) seizures (*3*). Children with IS often manifest long-term neurological impairment beyond epilepsy, including developmental delay, autism spectrum disorders (ASD) and cognitive impairment (*4*). Unfortunately, current treatments for IS are inadequate with severe adverse effects and the outcome of IS is usually poor. Because of the severity of the seizures and the associated intellectual and behavioral disabilities, IS patients and their families often suffer from substantial economic, social, and emotional burdens (*5*). Therefore, understanding the mechanisms underlying IS and developing novel therapies remain critical scientific and clinical priorities.

IS can present with a wide range (over 200) of symptomatic etiologies including neonatal infections, structural brain malformations and hypoxic ischemic or metabolic damage (*6*). Recently, a significant proportion of IS patient's etiologies have been shown to be genetic in nature and pathogenic variants typically arise *de novo (7)*. Due to increased efficiency and reduced cost of next generation sequencing technology, mutations in a growing list of genes essential for the establishment of proper neural networks during development have been statistically associated with IS (*4, 8*). In 2013, the National Institutes of Health funded Epi4K consortium performed whole exome sequencing of IS trios (proband and unaffected parents) and found a *de novo* mutation in the $GABA_A$ receptor ($GABA_AR$) β3 subunit gene (*GABRB3*) (*9*). The patient (female) with the *GABRB3(N110D)* mutation had IS onset at 5 months of age, followed by development of myoclonic spells. Her EEG had a typical hypsarrhythmia pattern. The identification of this

genetic cause of an isolated IS patient provides a possible inroad, through understanding the consequence of *GABRB3(N110D)* mutation in the brain, to defining the underlying pathophysiology of IS.

$GABA_A$Rs are pentameric chloride ion channels that mediate the majority of fast inhibitory transmission in the central nervous system. Most receptors in the brain are composed of 2α, 2β, and 1γ subunit(s) (*10*). Given the critical role of $GABA_A$Rs, it is not surprising that a number of mutations in the *GABR* genes have been associated with a broad spectrum of epilepsy syndromes (*11*). The β3 subunits are widespread and abundant in prenatal and neonatal brain. In adults, the β3 subunit is expressed at a lower level, but remains one of the most essential components of $GABA_A$Rs in many brain regions involved in seizure generation such as cerebral cortex, thalamus and hippocampus (*12, 13*). *GABRB3,* therefore, plays a critical role in neurodevelopment as well as adult brain function. Previously, *GABRB3* mutations (P11S, S15F and G32R) have been associated with CAE (*14, 15*), and P11S has been linked with maternal transmission in autism disorders (*16*). Moreover, the heterozygous $Gabrb3^{+/-}$ mice exhibit absence-like seizures (*17, 18*).

Although many genetic animal models of epilepsy have been created, only a few have been used to explore the mechanisms underlying epilepsy-associated *GABR* mutations (*19-21*). Until recently, there has been only one genetic knock-in (KI) mouse model of IS, the Aristaless-related homeobox mutation model (ARX spasms model) (*22*). The frustrating absence of good genetic mouse models for IS prevented full understanding of disease pathophysiology and limited the development of novel therapies aimed at reducing epileptic and cognitive consequences. Recently, our laboratory generated the first KI mouse line bearing a human IS-associated *GABR* mutation, the het $Gabrb3^{+/N110D}$ KI mouse. We have characterized the cellular deficits produced by this *GABRB3* mutation *in vitro* in transfected HEK293T cells, demonstrating that this IS mutation changed current kinetic properties (*23*). Our initial characterization of the $Gabrb3^{+/N110D}$ KI mice showed frequent epileptic extensor spasms occurring in clusters in P14-P15 young IS mice, and frequent myoclonic seizures and occasional GTCSs with EEG abnormalities in adult 4-6 mo. IS mice.

In this study, I investigated the performance of these *Gabrb3*$^{+/N110D}$ KI mice in a battery of behavioral tasks, showing that they had significantly abnormal neurobehavioral profiles persisting into adulthood. First, *Gabrb3*$^{+/N110D}$ KI mice were hyperactive, evidenced by significant increases in the distance traveled and vertical counts during the open field test. Second, *Gabrb3*$^{+/N110D}$ KI mice displayed anxiety-like behaviors in both the open field and elevated zero maze tests. Additionally, use of the Barnes maze test revealed impaired spatial learning and memory in *Gabrb3*$^{+/N110D}$ KI mice. Lastly, in the three-chamber social interaction test, *Gabrb3*$^{+/N110D}$ KI mice were shown to have impaired sociability and social novelty, indicating that they have social deficits. In contrast, the mice exhibited intact motor coordination in the rotarod test, and normal depression level in the tail suspension test. These initial behavioral analyses are intended as a preliminary assessment of *Gabrb3*$^{+/N110D}$ KI mice. Further work is needed to fully characterize these behavioral changes during development and the underlying biological mechanisms.

2. Materials and methods

1) Mice

Five-six months old *Gabrb3*$^{+/N110D}$ KI mice and their corresponding wild-type littermates were housed in a 12-h light/dark cycle with standard rodent food and water ad libitum. Mice were extensively handled for at least one week prior to the beginning of the experiments. The investigator performing each experiment was blinded to genotype. Both male and female mice were included. Experiments were performed in the Vanderbilt University Medical Center (VUMC) Murine Neurobehavioral Core Laboratory (MNBCL). All experimental procedures were approved by Vanderbilt University Division of Animal Care.

2) Open field test

The open field test was performed as previously described (*21*), using the standard protocol in the MNBCL. Briefly, each individual mouse was placed for 60 min in an open field activity chamber (Med Associates, 27 x

27 x 20.3 cm), which was contained within a light- and air-controlled environmental box. Mice were not previously habituated to the locomotor activity chamber. Location and movement were detected by interruption of infrared beams by the body of the mouse (16 photocells in each horizontal direction, as well as 16 photocells elevated by 4 cm to measure vertical counts) and were measured by the Med Associates Activity Monitoring program. Data analyzed include total distance traveled, rearing activity (vertical counts), and time resting in the center (50% of area) and the peripheral zone, as measures of locomotion activity and anxiety. The open field arena was cleaned with MB-10® (Quip Laboratories) and wiped with paper towels between each trial.

3) Elevated zero maze test

The elevated zero maze was a modification of the elevated plus maze used for assessing anxiety-related behaviors. The elevated circular platform (40 cm off the ground, 50 cm in diameter) was divided into four equal-sized arenas, with two enclosed arms opposite each other (5 cm wide with 15 cm high walls) and two open arms (5 cm wide) between the enclosed arenas. Lumens in each of the four arenas were recorded and maintained constant across all mice. Briefly, each mouse was lowered by its tail into an open arena of the maze and allowed to explore for 300 s. The whole circular platform was cleaned with MB-10® and wiped with paper towels between each animal. Mouse activity was monitored via an overhead camera connected to a computer in a separate room using video acquisition and ANY-maze analysis software (Stoelting, Wood Dale, IL). Data analyzed include time spent and distance traveled in open versus closed arms, and number of entries into open arms.

4) Rotarod test

Motor coordination and balance were tested using a commercially available accelerating rotarod (Ugo Basile model 7650; Stoelting Co., Wood Dale, IL, USA). The rotarod began at four rotations per minute (rpm) and accelerated to 40 rpm at a smooth rate over the course of a 300-s trial. Mice were placed on the rotating

cylinder while it was rotating slowly at 4 rpm. The time taken for the mouse to fall off the rotating rod was recorded with a maximal trial duration of 300 s. Occasionally, mice clung to the rod and the whole animal rotated along with it without regaining control. This behavior was classified as a 'rotation'. Thus, the "latency to fall" was recorded either when the mouse fell from the rod or when the mouse made the first rotation, whichever occurred first. Three sessions were conducted on consecutive days, with three trials per session.

5) Tail suspension test

The tail of a mouse was taped to a vertical aluminum bar connected to a strain gauge inside a commercial tail suspension test chamber (Med Associates). Mice were hung directly vertically to minimize chances of injury and to decrease the propensity for mice to climb their tail during the test. Mice were allowed to hang for 6 min. Force transducers and automated software (Med Associates) were used to measure immobility. Settings utilized were a lower threshold of 7, upper threshold of 20, gain of 8, and resolution of 220 ms (*24*) . The duration of immobility was scored as time below the lower threshold.

6) Three-chamber social interaction test

The three-chamber social interaction test was based on a previous study (*25*) and is briefly outlined here. The apparatus was divided into 3 equal-sized polycarbonate chambers separated by high walls, each with a sliding door. All mice were socially isolated in the morning prior to the start of the task and were left for several hours to acclimate to their new housing environment, ensuring that all mice had the same social starting point regardless of how many cage-mates each animal had. Additionally, mice should be more prone to engaging in social behaviors after isolation. At the start of the task, the subject mouse was placed in the middle chamber, and was moved back to this chamber between each stage but was not removed from the apparatus until the entire protocol were complete. Additional mice and objects were placed in the two side chambers. The three-chamber social interaction test had three stages: 1) Habituation: the test mouse was allowed to

freely explore all three chambers for 10 min to acclimate to the apparatus. 2) Sociability: the test mouse was allowed to freely explore a stranger mouse (novel mouse) and an empty transparent pencil cup (novel object) for 10 min. 3) Social Novelty: the test mouse was allowed to freely explore a novel mouse and the familiar mouse (from the sociability trial) for 10 min. Mice, excluding the subject mouse, were contained in inverted transparent pencil cups in the apparatus. Time the test mouse spent actively investigating each stimulus was recorded by hand using ANY-maze software.

7) Barnes maze test

The Barnes maze consists of a white circular platform with 12 holes equally spaced around the perimeter. A black escape tunnel was placed under one hole. Distal cues were placed around the room. The Barnes maze test was based on the protocol described in the previous studies (*26, 27*). The procedure includes three components: pretraining, training, and memory probe, and each is briefly outlined. 1) Pretraining: the mouse was placed in a black start box for 30 s and was then guided to the target hole where the mouse was able to descend into the escape box. The target hole was one of 12 on the table, with the other 11 being blocked from below. From the surface of the maze, the open escape hole looks identical to the closed holes so that the mice can locate the target box only with the spatial extra cues surrounding the maze. After 30 s, the mouse was removed from the escape box and placed back in the start box for three additional trials. The pretraining session only occurred on the first day of Barnes maze testing. The maze was not cleaned between pertaining trials. 2) Training: similar to pretraining, the mouse was placed in the start box for 30 s, and was then allowed to freely explore the maze to find the target hole using extra-maze cues. Mice that failed to find the target box within 5 min were gently guided to its location. For those mice, 300 s were recorded as the escape latency. Mice were exposed to 4 training trials per day for 5 consecutive days. The maze was cleaned with MB-10® between each mouse and each trial and was rotated 90° between each trial to prevent the mice from utilizing intra-maze cues when locating the target hole. The target hole did not move in relation to the room. 3) Probe: A 300 s probe test was conducted 1 hr after the final training trial on the fifth day using the same parameters

described during the training session, except that all 12 holes were now blocked. All sessions were recorded by a camera and analyzed using ANY-maze software.

8) Statistical analysis

All behavioral data were analyzed with GraphPad Prism software. Independent-sample t tests were used in the analyses of locomotor activity, elevated zero maze, and probe trials of Barnes maze test. A two-way ANOVA was used for three-chamber test of sociability and social novelty. A repeated-measures ANOVA were used to analyze training trials of the Barnes maze test. Post hoc and a priori Bonferroni comparisons were used to evaluate individual mean comparisons where appropriate. All analyses used an α level of 0.05 for statistical significance.

3. Results

1) *Gabrb3*$^{+/N110D}$ KI mice displayed hyperactivity and increased anxiety

To evaluate IS behavioral comorbidities in *Gabrb3*$^{+/N110D}$ KI mice, we first assessed their locomotor activity using open field test (Figure 4-1). Throughout the entire 60 min testing duration, KI mice (11573 ± 1271 cm, n = 19) travelled a significantly greater distance than wild-type littermates (5355 ± 522.5 cm, n = 19). In addition, KI mice (575.4 ± 72.05, n = 19) had significantly more vertical counts compared with their corresponding controls (375.4 ± 41.48 n = 19). These findings indicated that *Gabrb3*$^{+/N110D}$ KI mice had hyperactivity in a novel environment.

Analysis of thigmotaxis revealed that heterozygous KI mice had reduced time spent in the center relative to wild-type mice (10.26 ± 1.76 min versus 24.24 ± 1.77 min, n = 19 for heterozygous and wild type mice, $p < 0.0001$, unpaired t test) and decreased percent of distance travelled in the center (0.31 ± 0.03 versus 0.57 ± 0.03, n = 19 for heterozygous and wild type mice, $p < 0.0001$, unpaired t test) during the 60 min test, suggesting possible increases in anxiety in *Gabrb3*$^{+/N110D}$ KI mice (Figure 4-2A, B).

We next attempted to confirm an anxiety phenotype in KI mice using elevated zero maze test (Figure 4-2C). In the elevated zero maze, rodents were placed on an elevated circular maze with two open arms and two arms enclosed by walls. Rodents normally make fewer entries onto the open arms of the maze, and anxious animals avoid the open arms even more. In this context, anxiety-related behavior was measured by the degree to which the mouse avoided the unenclosed areas of the maze. As expected, KI mice spent substantially less time in the open arm than wild-type mice (80.46 ± 7.481 s versus 123.4 ± 8.801 s, n = 20 for heterozygous KI and wild type mice, unpaired t test, $p < 0.0005$), confirming the anxiety-related behaviors in *Gabrb3*$^{+/N110D}$ KI mice.

2) *Gabrb3*$^{+/N110D}$ *KI* mice exhibited social behavioral abnormalities

In addition to hyperactivity, impaired social interaction is common among patients with IS. To test for social deficits, wild-type and *Gabrb3*$^{+/N110D}$ KI mice were subjected to a three-chamber social interaction test. After habituation, mice were allowed to choose between a chamber containing an age-matched mouse (novel mouse) and a chamber containing an empty container (novel object) (Figure 4-3A). For sociability, a preference for exploring the novel mouse was shown by control wild-type mice, but such a social motivation and interaction was not found in *Gabrb3*$^{+/N110D}$ KI mice. Compared with wild-type mice, pairwise comparisons confirmed that *Gabrb3*$^{+/N110D}$ KI mice spent a substantially decreased time exploring novel mice ($p < 0.0001$) (Figure 4-3B). After the socialization stage, the test mice were exposed to a familiar mouse (from the sociability trial) versus a novel mouse (Figure 4-3C). For social novelty, wild-type control mice interacted more extensively with the novel mouse than the familiar one. In contrast, KI mice did not show a significant preference for the stranger mouse. In addition, mutant mice displayed significantly less interaction with the novel target mouse compared to controls (Figure 4-3D). Thus, the *Gabrb3*$^{+/N110D}$ KI mice displayed social interaction deficits.

3) *Gabrb3*$^{+/N110D}$ KI mice had deficits in spatial learning and memory

To assess spatial learning and memory, we performed the Barnes maze test in which mice were trained to rapidly escape a brightly lighted circular field by finding a specific dark hole at its periphery using spatial cues (Figure 4-4). The Barnes maze was a circular white platform with 12 holes. One of the holes (target hole) exited into a dark box. Indeed, an overall decrease in the primary latency (latency to first reach the target hole) was observed during the 5 training days in both groups. However, in the KI mice, the escape latency was prolonged in the first three days compared to the respective wild-type littermates, but this disparity between groups was no longer present after the third day (Figure 4-4A). In addition, KI mice committed a greater number of errors on day 2-4 (Figure 4-4B). This indicated a slower acquisition in spatial learning for *Gabrb3*$^{+/N110D}$ KI mice. During the probe trial, the KI mice (29.46 ± 2.23 s, n = 17) had reduced time spent in the target hole area compared with their wild-type littermates (40.06 ± 2.45 s, n = 17). In addition, the KI mice (78.65 ± 7.33, n = 17) showed increased number of entries into the non-target holes than their corresponding controls (51.94 ± 2.432, n = 17). This suggested that the *Gabrb3*$^{+/N110D}$ mice had impaired spatial memory.

4) *Gabrb3*$^{+/N110D}$ KI mice had no motor deficits or depression-like behavior

We next assessed procedural learning and neuromuscular ability using the rotarod test, with 3 trials conducted on each of 3 consecutive days (Figure 4-5A). No significant difference was found in the rotarod fall latency between the wild-type and *Gabrb3*$^{+/N110D}$ KI mice when the rod was rotating at an accelerating rate ($p = 0.88$). This indicated that the *Gabrb3*$^{+/N110D}$ KI mice had intact motor coordination.

To examine the emotional aspects of *Gabrb3*$^{+/N110D}$ KI mice, we employed the tail suspension test. Immobility in the tail suspension test is considered a model of despair in a stressful situation; administration of an antidepressant drug decreases the immobility in rodents (*28*). In this test, the mice were hung on a bar by the tail for 6 min and immobility behavior was scored. The *Gabrb3*$^{+/N110D}$ KI mice did not show increased

duration of immobility compared with wild-type mice (p = 0.23) (Figure 4-5B), indicating normal level of behavioral despair.

4. Discussion

1) *Gabrb3*$^{+/N110D}$ KI mice model core neurobehavioral comorbidities of IS

Despite their adverse impacts on quality of life, the cognitive deficits and neuropsychiatric comorbidities in IS have rarely been addressed systematically in an animal model. In this study, we performed a thorough behavioral assessment of adult *Gabrb3*$^{+/N110D}$ KI mice and revealed several abnormal behavioral phenotypes including hyperactivity, increased anxiety, social interaction deficits, and impaired spatial learning and memory, which were consistent with cognitive impairment and autistic-like behaviors (Table 1). These results suggested that *Gabrb3*$^{+/N110D}$ KI mice phenocopy major neurobehavioral comorbidities of IS.

Developmental outcome is poor in a majority of patients with IS, and ~80% of patients with a diagnosis of IS had some form of cognitive impairment (*29, 30*). In the Barnes maze test, *Gabrb3*$^{+/N110D}$ KI mice showed deficits in hippocampus-dependent spatial learning and memory, as manifested by prolonged latency to the target hole and increased errors in the learning trial, as well as decreased time investigating the target hole and increased errors in the probe trial. Given the multiple forms of learning and memory, additional behavioral paradigms that allow investigation of different memory systems measuring short-term episodic memory (novel object recognition test) and associative memory (contextual fear-conditioning task) will strength findings of fundamental cognitive abnormalities in the *Gabrb3*$^{+/N110D}$ KI mice.

IS has a very strong and specific association with ASD (*31*): the prevalence of ASD is 30–46% in IS (*32-34*). ASD is a neurodevelopmental disorder characterized by impaired social interaction and communication, as well as a markedly restricted repertoire of repetitive interests and behaviors (*35*) . Studying these features in mice is problematic, but an easy test is available to measure social interaction, which is one of the core

symptoms of ASD (*36*). In the three-chamber social interaction test, *Gabrb3*$^{+/N110D}$ KI mice were observed to have a lack of preference for both sociability and social novelty. In addition, *Gabrb3*$^{+/N110D}$ KI mice demonstrated other autistic-like abnormalities including hyperactivity in the open field test and anxiety-like behavior in both open field and elevated zero maze tests. It should be noted that the hyperactivity and anxiety-like behaviors might contribute to the impaired social interaction in KI mice by limiting target exploration or evoking anxiety-like responses. Further investigations of communication skills such as the ultrasonic vocalization test, as well as stereotyped and repetitive behaviors such as self-grooming and digging, will support the ASD features of *Gabrb3*$^{+/N110D}$ KI mice.

2) Mechanisms underlying the neurobehavioral abnormalities in *Gabrb3*$^{+/N110D}$ KI mice

The exact neural mechanisms underlying the neurocognitive impairment in *Gabrb3*$^{+/N110D}$ KI mice are to be deciphered in future studies. It is important to understand the nature and extent of the contribution of the seizures themselves, versus the developmental and functional effects of the *GABRB3(N11D)* mutation, towards the neurobehavioral phenotypes in this mouse model of IS.

In theory, epileptiform activity itself can disrupt brain development through multiple mechanisms such as alteration of neurotransmitter systems and neuronal properties. The observation that individuals with EEs who are successfully treated with surgery can show improvement in cognitive function demonstrates that seizures play an important role in the neuropsychiatric deficits (*37*). A critical issue is whether the epilepsy independently worsens the development of cognitive and behavioral deficits in the *Gabrb3*$^{+/N110D}$ KI mice. Thus, it is important to examine the impact of the epilepsy itself on neurocognitive features in *Gabrb3*$^{+/N110D}$ KI mice with respect to other mouse models of IS. Is seizure severity related to neurocognitive severity? Does the age of seizure onset predict neurodevelopmental outcomes? After all, if epileptic activity does in fact exacerbate the neurobehavioral phenotypes, then the emergence of seizures at an earlier age—especially during the period of rapid brain growth could portend worse developmental outcomes.

It is also conceivable that the *GABRB3(N110D)* mutation may directly contribute to cognitive and behavioral abnormalities through mechanisms other than seizures. In other words, from a mechanistic standpoint, neurobehavioral deficits and spasms may be two separate end-results of the underlying gene defect in the *Gabrb3*$^{+/N110D}$ mouse model. Both animal and human data suggest that individuals predisposed to epilepsy manifest increased rates of comorbidities even before seizure onset. Studies of *Scn1a* knockout mice have demonstrated cognitive impairment independent of seizures *(38)*. Studies of *Arx*$^{-/Y}$ *Emx1*^{Cre} mice demonstrated that at least some behaviors (altered anxiety, hyperactivity, and social deficits) were unrelated to the on-going seizures (*39*). Thus, the underlying genetic defect may be the predominant contribution to the clinical presentation, overshadowing the possible impact of epilepsy seizure severity on the cognitive and behavioral phenotypes. There might be common pathways shared between epileptogenesis and cognitive/behavioral disturbance in the *Gabrb3*$^{+/N110D}$ mouse model. The impaired GABAergic signaling and excitatory-inhibitory imbalance in neurodevelopmental functioning serves as one illustrative example.

3) Comparison of *Gabrb3*$^{+/N110D}$ KI mouse model with other rodent models of IS

Until recently, several pharmacological models of epileptic spasms that express varying degrees of the full phenotypic spectrum have been developed in rats. In addition, a growing list of genetic mouse models with altered IS risk genes manifest some, but not all, aspects of human IS phenotypes (Table 4-2). Among them, the *Arx*$^{(GCG)10+7}$ mouse model is the only currently available mouse KI developmental model of IS carrying a human mutation (*22*). Together, these models suggest roles for neuroinflammation, aberrant interneuron migration and differentiation, impaired excitatory/inhibitory balance, and neuroendocrine systems in the etiology of IS.

The *Gabrb3*$^{+/N110D}$ mouse model in this study is the first genetic mouse model bearing a human IS-associated *GABR* mutation and recapitulates major features of the human disease, in particular, abnormal infantile motor

spasms, ictal EEG abnormalities, chronic seizures persisting into adulthood, and neurobehavioral deficits. A limitation of the model is that drug-testing studies have not been done yet. The extent to which the prior spasms and the underlying genetic defect contribute to these neurobehavioral comorbidities will be best determined when effective antiepileptic therapies are identified in the *Gabrb3*$^{+/N110D}$ model. Additional molecular analysis of this mouse model may be helpful in unraveling the downstream changes in the cellular basis of IS.

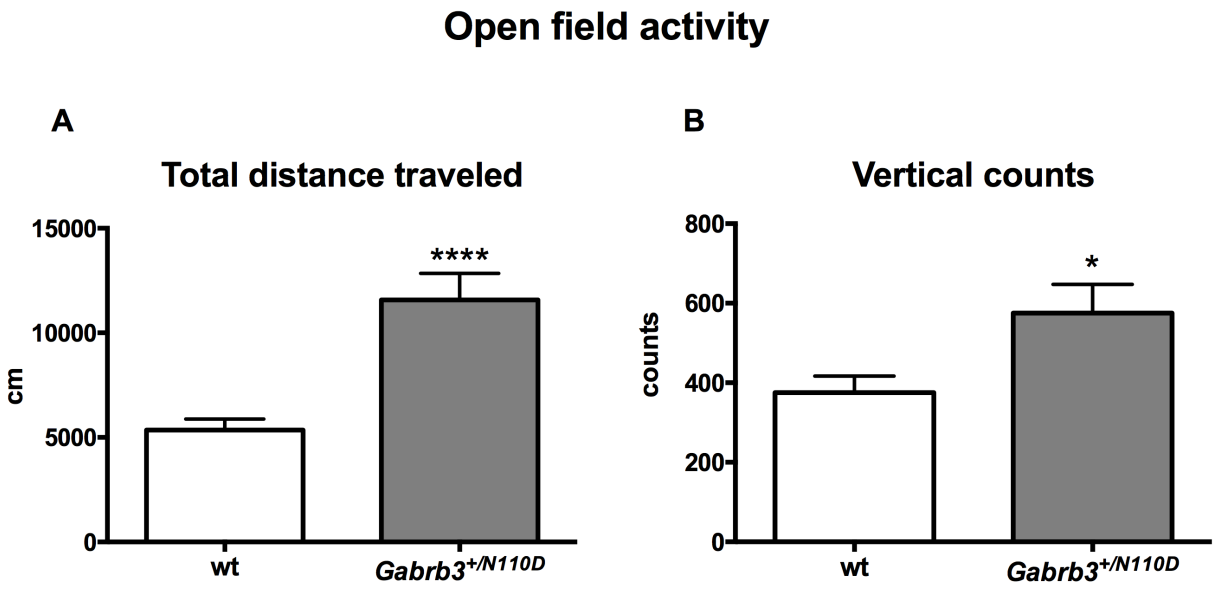

Figure 4-1: *Gabrb3*$^{+/N110D}$ KI mice had a hyperactive phenotype.
Data shown was collected from 60 minutes in the locomotor activity chambers. Panel **(A)** showed the total distance traveled (center and surround included) in the locomotor activity chambers. Panel **(B)** showed vertical counts, or the number of rearings detected. Unpaired two-tailed Student's *t* test, *p < 0.05, ****p < 0.0001, n = 19.

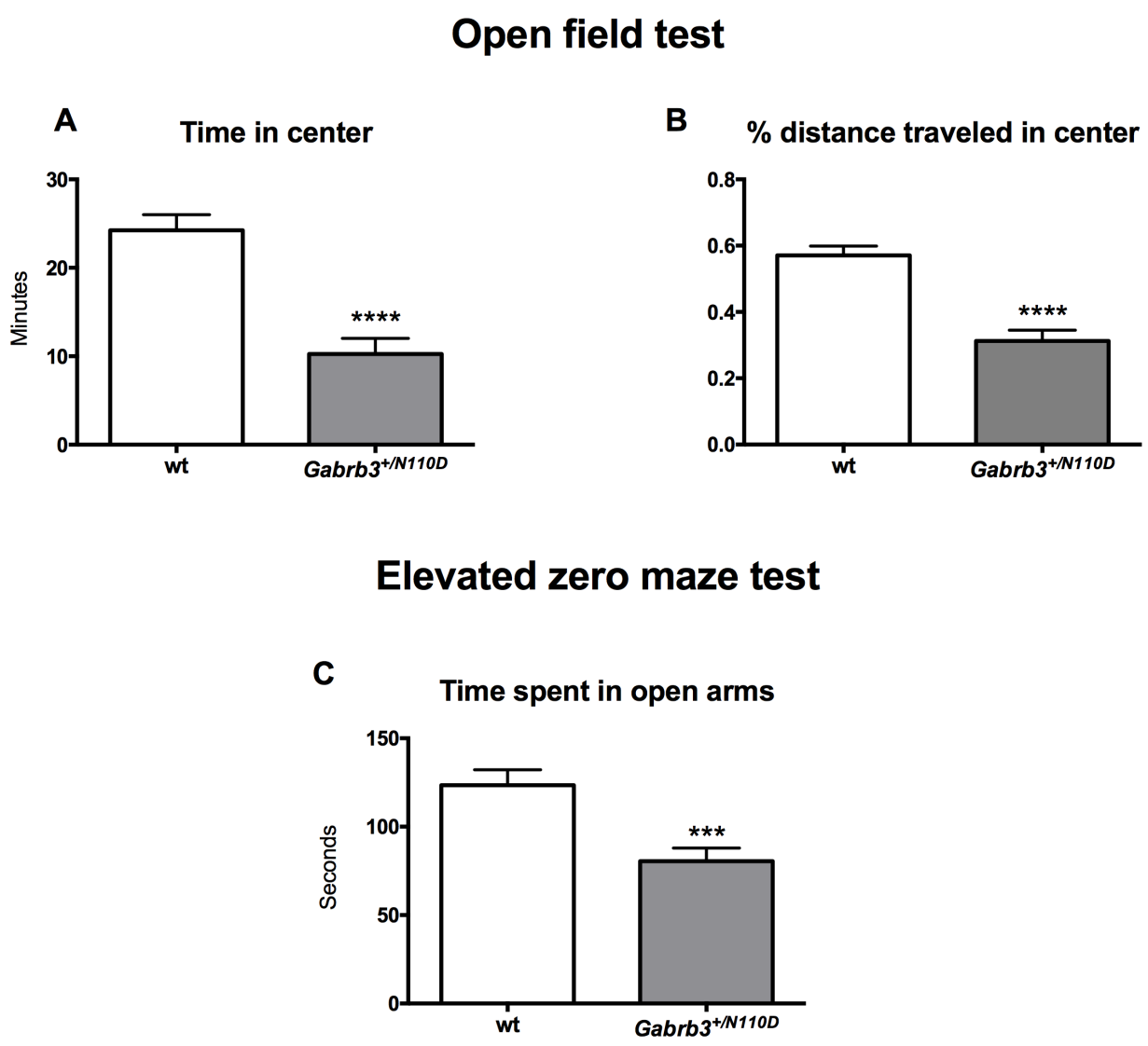

Figure 4-2: *Gabrb3*$^{+N110D}$ KI mice displayed elevated anxiety in both the locomotor activity chambers and the elevated zero maze test.

(**A, B**) Two components of the 60-minute trial in the locomotor activity chambers were shown. The chamber was divided into two 50% sections by area: the center, and the surround. Time spent in the center area was shown on the left, percent of distance traveled within the center area was show on the right. (**C**) During the elevated zero maze test (5-minute trial), *GABRB3*$^{+N110D}$ KI mice spent significantly less time in the open arms. Unpaired two-tailed Student's t test, ***$p < 0.005$, ****$p < 0.0001$, n = 19-20.

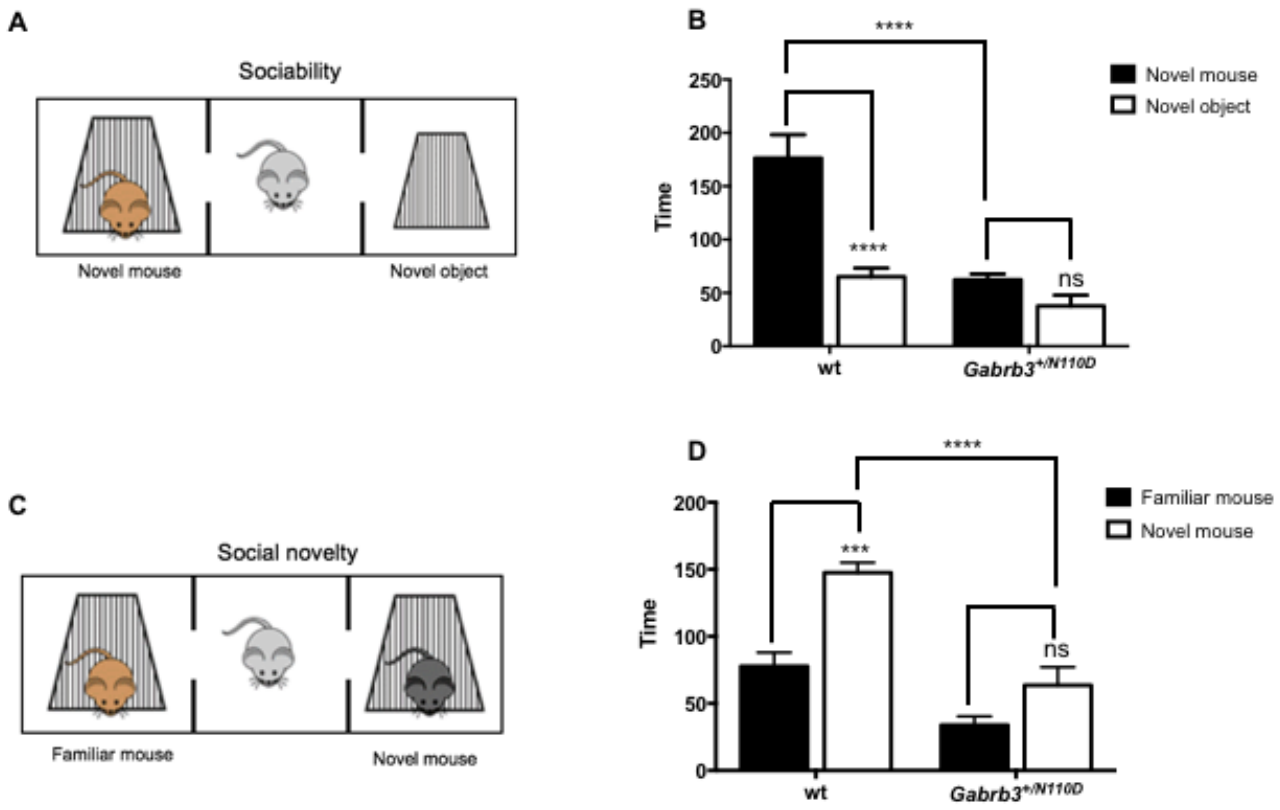

Figure 4-3: In the three-chamber social interaction test, *Gabrb3*$^{+N110D}$ KI mice displayed social abnormalities.

Not shown was Stage 1, a 10-minute familiarization stage for the test mouse to acclimate to the set up. (**A**) Stage 2 of the test (sociability stage) was a 10-minute trial in which the test mice had two socialization options: 1) an empty inverted pencil cup in one side chamber (novel object), or 2) an inverted pencil cup containing a novel age-matched mouse in the other side chamber (novel mouse). (**B**) Whereas wild-type mice spent more time actively investigating the novel mouse than the novel object, *Gabrb3*$^{+N110D}$ KI mice had no preference for the novel mouse. (**C**) Stage 3 of the test (social novelty stage) was a 10-minute trial in which the test mice had two options: 1) familiar socialization, in which the novel mouse from stage 2 remains where it was, or 2) novel socialization, in which a new novel mouse was placed under the previously empty pencil cup. (**D**) Whereas wild-type mice spent more time actively investigating the novel mouse than the familiar mouse, *Gabrb3*$^{+N110D}$ KI mice had no preference for the novel mouse. Bonferroni post-tests from the two-way ANOVA. Four comparisons were made in each group. ***$p < 0.001$, ****$p < 0.0001$, $n = 10$.

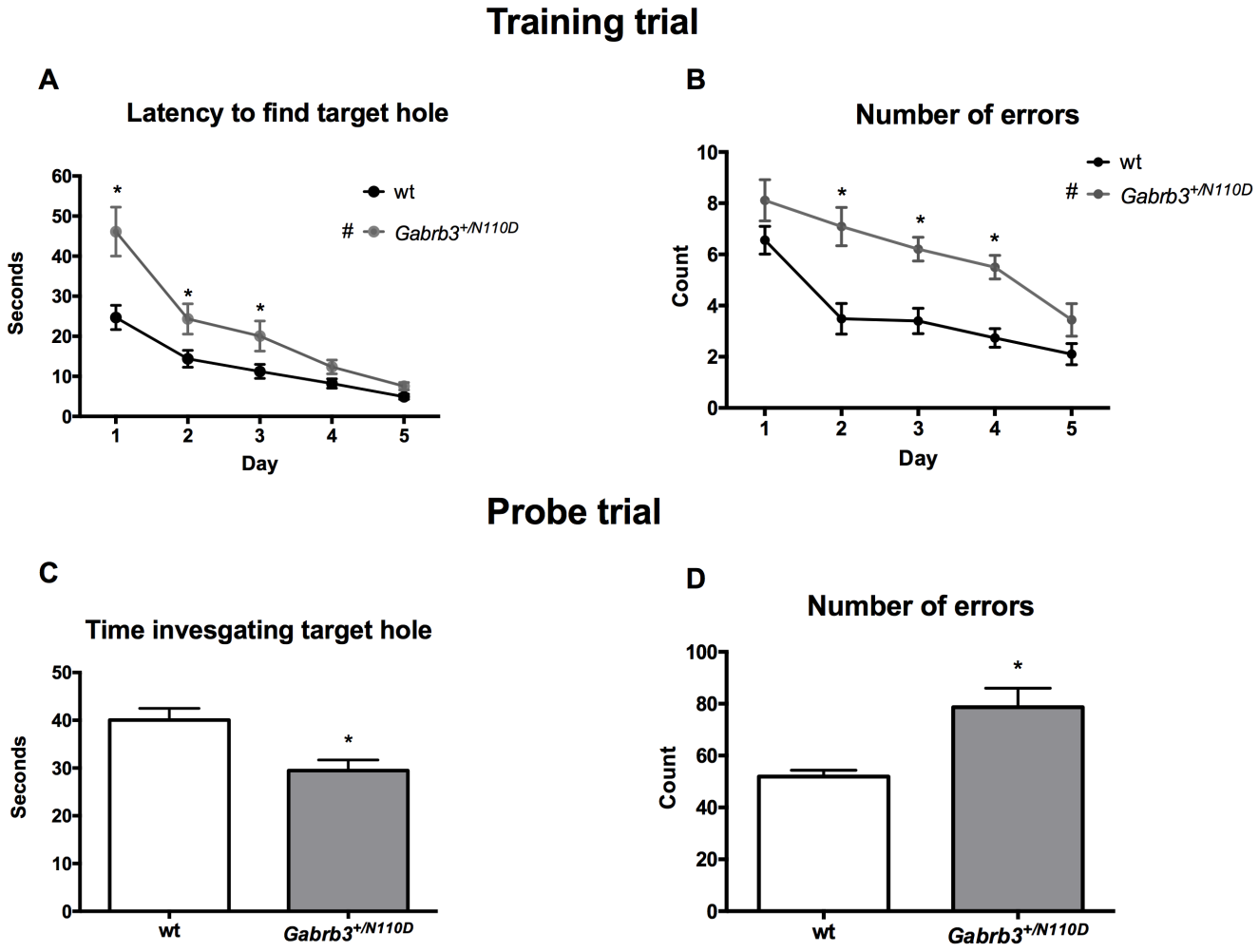

Figure 4-4: Barnes maze test demonstrated that *Gabrb3*$^{+N110D}$ KI mice had slowed spatial learning and impaired spatial memory.

(A, B) 5 days of learning trials depicted a profound spatial learning deficit in *GABRB3*$^{+N110D}$ KI mice. The time it took each animal (latency) to find the target hole **(A)**, and the number of non-target hole zones entered (errors) **(B)** were recorded and quantified for each day in each mouse genotype. Two-way ANOVA for repeated measures, #$p < 0.05$ for genotype effect, *$p < 0.05$, $n = 17$. **(C, D)** 5-minute probe trial for spatial memory performed on day 5 after the learning trials. The target hole was now covered and appeared identical to the other 11 holes. Time spent in the vicinity of the target hole **(C)** and the number of non-target hole zones entered (errors) **(D)** were displayed. Unpaired two-tailed Student's t test, *$p < 0.05$, $n = 17$.

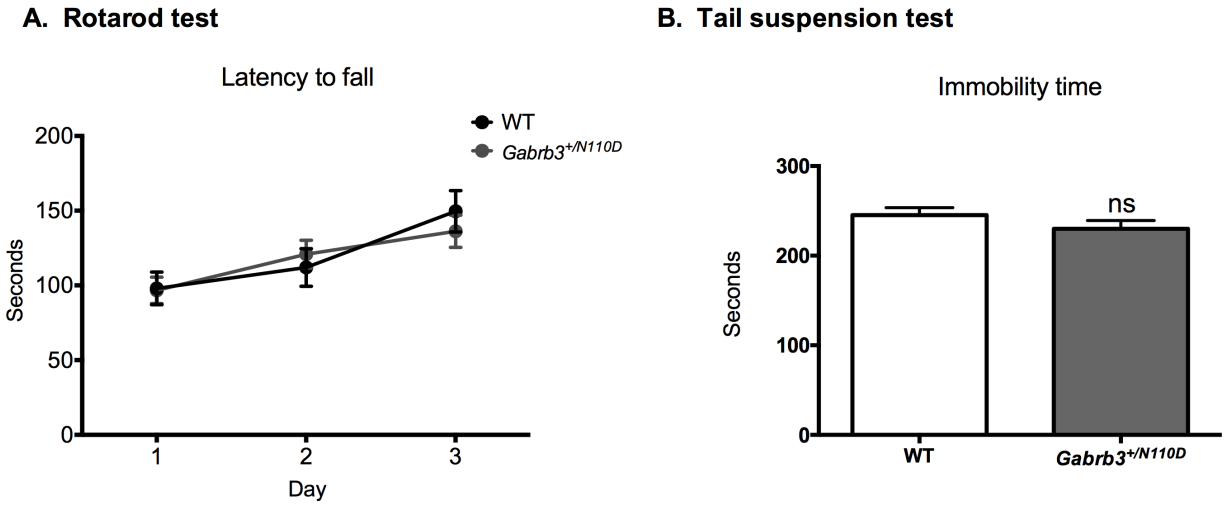

Figure 4-5: *Gabrb3*$^{+N110D}$ KI mice displayed no motor dysfunction and no increased despair behavior. **(A)** In the rotarod test, the latency to fall from the rotarod was significantly decreased in both wild-type and *Gabrb3*$^{+N110D}$ KI mice while there was no difference between two genotypes. Two-way ANOVA for repeated measures, n = 10. (B) In a tail suspension test, duration of immobility was indistinguishable between wild-type and *Gabrb3*$^{+N110D}$ KI mice. Unpaired two-tailed Student's t test, n = 16.

Table 4-1: Summary of behavioral phenotypes in *Gabrb3*$^{+/N110D}$ KI mice

Behavioral Paradigm	Parameter	*Gabrb3*$^{+/N110D}$ mice	Phenotype	Figure
Open field	Distance traveled	↑	Hyperactive	Fig. 4-1A
	Vertical counts	↑		Fig. 4-1B
Open field	Time in center	↓	Anxious	Fig. 4-2A
	% distance traveled in center	↓		Fig. 4-2B
Elevated zero maze	Time in open arms	↓		Fig. 4-2C
Three chamber test	Sociability: time with novel mouse	↓	Social deficits	Fig. 4-3B
	Social novelty: time with novel mouse	↓		Fig. 4-3D
Barnes maze (Learning trial)	Latency to escape	↑	Impaired spatial learning	Fig. 4-4A
	Total errors	↑		Fig. 4-4B
Barnes maze (Probe trial)	Time in target hole	↓	Impaired spatial memory	Fig. 4-4C
	Total errors	↑		Fig. 4-4D
Rotarod	Latency to fall	→	Normal motor function	Fig. 4-5A
Tail suspension	Immobility time	→	Not depressed	Fig. 4-5B

Table 4-2: Rodent models of IS

Model	Spasms	EEG features	Therapeutic effects on spasms	Neurobehavioral comorbidities
Gabrb3$^{+/N110D}$ KI mice (This study)	Frequent epileptic extensor spasms occurring in clusters in P14-P15 mice	Ictal EEG electrodecrement	N.R.	Hyperactivity, decreased anxiety, cognitive deficits, social deficits
TTX (rat) (*40-42*)	Spontaneous spasms after P21	Hypsarrhythmia Ictal EEG electrodecrement	N.R.	N.R.
NMDA (rat) (*43-45*)	Chemically-induced spasms No spontaneous spasms	Ictal EEG electrodecrement	Both Vigabatrin and ACTH were effective	Cognitive deficits
NMDA/ betamethasone (rat) (*46-50*)	Chemically-induced spasms No spontaneous spasms	Ictal EEG electrodecrement	Vigabatrin, ACTH, the neurosteroid ganaxolone, and the ketone body β-hydroxybutyrate were effective	Hyperactivity, decreased anxiety
CRH (rat) (*51, 52*)	Limbic seizures without spasms	Focal sharp waves without hypsarrhythmia or ictal electrodecrement	Phenytoin was effective. ACTH did not affect spasms.	Cognitive deficits
Multiple hit (rat) (*53*)	Spasms between P4 -P13	Ictal EEG electrodecrement	ACTH did not affect spasms. Vigabatrin transiently suppressed spasms at P5.	Cognitive deficits, autistic-like behaviors
Down syndrome/GBL (Ts65Dn mouse) (*54*)	Spasms between 1 week and 2 months	Ictal EEG electrodecrement	Both Vigabatrin and ACTH were effective	N.R.
ARX cKO (mouse) (*55*)	Limbic seizures around P14–17 and epileptic spasms in adulthood	Ictal EEG electrodecrement	N.R.	N.R.
ARX KI (mouse) (*22, 56*)	Spasms between P7 –P20	Ictal EEG electrodecrement	N.R.	Decreased anxiety, impaired learning and sociability
APC cKO (mouse) (*57*)	Spasms between P5 –P14	Ictal EEG electrodecrement	N.R.	N.R.

TTX: tetrodotoxin; CRH: Corticotropin-releasing hormone; NMDA: N-methyl-D-aspartate; ACTH: adrenocorticotropic hormone; GBL: γ-butyrolactone; N.R.: not reported; cKO: conditional knockout; ARX: aristaless related homeobox gene; APC: adenomatous polyposis coli gene

References

1. J. M. Pellock, R. Hrachovy, S. Shinnar, T. Z. Baram, D. Bettis, D. J. Dlugos, W. D. Gaillard, P. A. Gibson, G. L. Holmes, D. R. Nordl, C. O'Dell, W. D. Shields, E. Trevathan, J. W. Wheless, Infantile spasms: a U.S. consensus report. *Epilepsia* **51**, 2175-2189 (2010).

2. P. Pavone, P. Striano, R. Falsaperla, L. Pavone, M. Ruggieri, Infantile spasms syndrome, West syndrome and related phenotypes: what we know in 2013. *Brain Dev* **36**, 739-751 (2014).

3. W. D. Shields, Infantile spasms: little seizures, BIG consequences. *Epilepsy Curr* **6**, 63-69 (2006).

4. A. R. Paciorkowski, L. L. Thio, W. B. Dobyns, Genetic and biologic classification of infantile spasms. *Pediatr Neurol* **45**, 355-367 (2011).

5. A. Katsnelson, G. Buzsaki, J. W. Swann, Catastrophic childhood epilepsy: a recent convergence of basic and clinical neuroscience. *Sci Transl Med* **6**, 262ps213 (2014).

6. J. P. Osborne, A. L. Lux, S. W. Edwards, E. Hancock, A. L. Johnson, C. R. Kennedy, R. W. Newton, C. M. Verity, F. J. O'Callaghan, The underlying etiology of infantile spasms (West syndrome): information from the United Kingdom Infantile Spasms Study (UKISS) on contemporary causes and their classification. *Epilepsia* **51**, 2168-2174 (2010).

7. R. H. Thomas, S. F. Berkovic, The hidden genetics of epilepsy-a clinically important new paradigm. *Nat Rev Neurol* **10**, 283-292 (2014).

8. A. McTague, K. B. Howell, J. H. Cross, M. A. Kurian, I. E. Scheffer, The genetic landscape of the epileptic encephalopathies of infancy and childhood. *Lancet Neurol* **15**, 304-316 (2016).

9. K. C. Epi, P. Epilepsy Phenome/Genome, A. S. Allen, S. F. Berkovic, P. Cossette, N. Delanty, D. Dlugos, E. E. Eichler, M. P. Epstein, T. Glauser, D. B. Goldstein, Y. Han, E. L. Heinzen, Y. Hitomi, K. B. Howell, M. R. Johnson, R. Kuzniecky, D. H. Lowenstein, Y. F. Lu, M. R. Madou, A. G. Marson, H. C. Mefford, S. Esmaeeli Nieh, T. J. O'Brien, R. Ottman, S. Petrovski, A. Poduri, E. K. Ruzzo, I. E. Scheffer, E. H. Sherr, C. J. Yuskaitis, B. Abou-Khalil, B. K. Alldredge, J. F. Bautista, S. F. Berkovic, A. Boro, G. D. Cascino, D. Consalvo, P. Crumrine, O. Devinsky, D. Dlugos, M. P. Epstein, M. Fiol, N. B. Fountain, J. French, D. Friedman, E. B. Geller, T. Glauser, S. Glynn, S. R. Haut, J. Hayward, S. L. Helmers, S. Joshi, A. Kanner, H. E. Kirsch, R. C. Knowlton, E. H. Kossoff, R. Kuperman, R. Kuzniecky, D. H. Lowenstein, S. M. McGuire, P. V. Motika, E. J. Novotny, R. Ottman, J. M. Paolicchi, J. M. Parent, K. Park, A. Poduri, I. E. Scheffer, R. A. Shellhaas, E. H. Sherr, J. J. Shih, R. Singh, J. Sirven, M. C. Smith, J. Sullivan, L. Lin Thio, A. Venkat, E. P. Vining, G. K. Von Allmen, J. L. Weisenberg, P. Widdess-Walsh, M. R. Winawer, De novo mutations in epileptic encephalopathies. *Nature* **501**, 217-221 (2013).

10. M. Farrant, Z. Nusser, Variations on an inhibitory theme: phasic and tonic activation of GABA(A) receptors. *Nat Rev Neurosci* **6**, 215-229 (2005).

11. J. Q. Kang, W. Shen, M. Lee, M. J. Gallagher, R. L. Macdonald, Slow degradation and aggregation in vitro of mutant $GABA_A$ receptor gamma2(Q351X) subunits associated with epilepsy. *J Neurosci* **30**, 13895-13905 (2010).

12. S. G. Fillman, C. E. Duncan, M. J. Webster, M. Elashoff, C. S. Weickert, Developmental co-regulation of the beta and gamma $GABA_A$ receptor subunits with distinct alpha subunits in the human dorsolateral prefrontal cortex. *Int J Dev Neurosci* **28**, 513-519 (2010).

13. D. J. Laurie, W. Wisden, P. H. Seeburg, The distribution of thirteen $GABA_A$ receptor subunit mRNAs in the rat brain. III. Embryonic and postnatal development. *J Neurosci* **12**, 4151-4172 (1992).

14. K. N. Gurba, C. C. Hernandez, N. Hu, R. L. Macdonald, *GABRB3* mutation, G32R, associated with childhood absence epilepsy alters alpha1beta3gamma2L gamma-aminobutyric acid type A (GABAA) receptor expression and channel gating. *J Biol Chem* **287**, 12083-12097 (2012).

15. M. Tanaka, R. W. Olsen, M. T. Medina, E. Schwartz, M. E. Alonso, R. M. Duron, R. Castro-Ortega, I. E. Martinez-Juarez, I. Pascual-Castroviejo, J. Machado-Salas, R. Silva, J. N. Bailey, D. Bai, A. Ochoa, A. Jara-Prado, G. Pineda, R. L. Macdonald, A. V. Delgado-Escueta, Hyperglycosylation and reduced GABA currents of mutated *GABRB3* polypeptide in remitting childhood absence epilepsy. *Am J Hum Genet* **82**, 1249-1261 (2008).

16. R. J. Delahanty, J. Q. Kang, C. W. Brune, E. O. Kistner, E. Courchesne, N. J. Cox, E. H. Cook, Jr., R. L. Macdonald, J. S. Sutcliffe, Maternal transmission of a rare *GABRB3* signal peptide variant is associated with autism. *Mol Psychiatry* **16**, 86-96 (2011).

17. T. M. DeLorey, A. Handforth, S. G. Anagnostaras, G. E. Homanics, B. A. Minassian, A. Asatourian, M. S. Fanselow, A. Delgado-Escueta, G. D. Ellison, R. W. Olsen, Mice lacking the beta3 subunit of the $GABA_A$ receptor have the epilepsy phenotype and many of the behavioral characteristics of Angelman syndrome. *J Neurosci* **18**, 8505-8514 (1998).

18. G. E. Homanics, T. M. DeLorey, L. L. Firestone, J. J. Quinlan, A. Handforth, N. L. Harrison, M. D. Krasowski, C. E. Rick, E. R. Korpi, R. Makela, M. H. Brilliant, N. Hagiwara, C. Ferguson, K. Snyder, R. W. Olsen, Mice devoid of gamma-aminobutyrate type A receptor beta3 subunit have epilepsy, cleft palate, and hypersensitive behavior. *Proc Natl Acad Sci U S A* **94**, 4143-4148 (1997).

19. H. O. Tan, C. A. Reid, F. N. Single, P. J. Davies, C. Chiu, S. Murphy, A. L. Clarke, L. Dibbens, H. Krestel, J. C. Mulley, M. V. Jones, P. H. Seeburg, B. Sakmann, S. F. Berkovic, R. Sprengel, S. Petrou, Reduced cortical inhibition in a mouse model of familial childhood absence epilepsy. *Proc Natl Acad Sci U S A* **104**, 17536-17541 (2007).

20. C. Zhou, L. Ding, M. E. Deel, E. A. Ferrick, R. B. Emeson, M. J. Gallagher, Altered intrathalamic $GABA_A$ neurotransmission in a mouse model of a human genetic absence epilepsy syndrome. *Neurobiol Dis* **73**, 407-417 (2015).

21. J. Q. Kang, W. Shen, C. Zhou, D. Xu, R. L. Macdonald, The human epilepsy mutation *GABRG2(Q390X)* causes chronic subunit accumulation and neurodegeneration. *Nat Neurosci* **18**, 988-996 (2015).

22. M. G. Price, J. W. Yoo, D. L. Burgess, F. Deng, R. A. Hrachovy, J. D. Frost, Jr., J. L. Noebels, A triplet repeat expansion genetic mouse model of infantile spasms syndrome, Arx(GCG)10+7, with interneuronopathy, spasms in infancy, persistent seizures, and adult cognitive and behavioral impairment. *J Neurosci* **29**, 8752-8763 (2009).

23. V. S. Janve, C. C. Hernandez, K. M. Verdier, N. Hu, R. L. Macdonald, Epileptic encephalopathy de novo GABRB mutations impair $GABA_A$ receptor function. *Ann Neurol*, (2016).

24. B. McLaughlin, M. A. Buendia, T. P. Saborido, A. M. Palubinsky, J. N. Stankowski, G. D. Stanwood, Haploinsufficiency of the E3 ubiquitin ligase C-terminus of heat shock cognate 70 interacting protein (CHIP) produces specific behavioral impairments. *PLoS One* **7**, e36340 (2012).

25. M. D. Carter, C. R. Shah, C. L. Muller, J. N. Crawley, A. M. Carneiro, J. Veenstra-VanderWeele, Absence of preference for social novelty and increased grooming in integrin beta3 knockout mice: initial studies and future directions. *Autism Res* **4**, 57-67 (2011).

26. F. E. Harrison, R. S. Reiserer, A. J. Tomarken, M. P. McDonald, Spatial and nonspatial escape strategies in the Barnes maze. *Learn Mem* **13**, 809-819 (2006).

27. T. A. Warner, W. Shen, X. Huang, Z. Liu, R. L. Macdonald, J. Q. Kang, Differential molecular and behavioural alterations in mouse models of *GABRG2* haploinsufficiency versus dominant negative mutations associated with human epilepsy. *Hum Mol Genet* **25**, 3192-3207 (2016).

28. J. F. Cryan, C. Mombereau, A. Vassout, The tail suspension test as a model for assessing antidepressant activity: review of pharmacological and genetic studies in mice. *Neurosci Biobehav Rev* **29**, 571-625 (2005).

29. E. Trevathan, C. C. Murphy, M. Yeargin-Allsopp, The descriptive epidemiology of infantile spasms among Atlanta children. *Epilepsia* **40**, 748-751 (1999).

30. F. Guzzetta, Cognitive and behavioral outcome in West syndrome. *Epilepsia* **47 Suppl 2**, 49-52 (2006).

31. K. C. Nickels, M. J. Zaccariello, L. D. Hamiwka, E. C. Wirrell, Cognitive and neurodevelopmental comorbidities in paediatric epilepsy. *Nat Rev Neurol* **12**, 465-476 (2016).

32. E. Saemundsen, P. Ludvigsson, V. Rafnsson, Autism spectrum disorders in children with a history of infantile spasms: a population-based study. *J Child Neurol* **22**, 1102-1107 (2007).

33. E. Saemundsen, P. Ludvigsson, V. Rafnsson, Risk of autism spectrum disorders after infantile spasms: a population-based study nested in a cohort with seizures in the first year of life. *Epilepsia* **49**, 1865-1870 (2008).

34. A. T. Berg, S. Plioplys, R. Tuchman, Risk and correlates of autism spectrum disorder in children with epilepsy: a community-based study. *J Child Neurol* **26**, 540-547 (2011).

35. B. S. Abrahams, D. H. Geschwind, Advances in autism genetics: on the threshold of a new neurobiology. *Nat Rev Genet* **9**, 341-355 (2008).

36. J. L. Silverman, M. Yang, C. Lord, J. N. Crawley, Behavioural phenotyping assays for mouse models of autism. *Nat Rev Neurosci* **11**, 490-502 (2010).

37. Y. J. Lee, J. S. Lee, H. C. Kang, D. S. Kim, K. W. Shim, S. Eom, H. D. Kim, Outcomes of epilepsy surgery in childhood-onset epileptic encephalopathy. *Brain Dev* **36**, 496-504 (2014).

38. A. C. Bender, H. Natola, C. Ndong, G. L. Holmes, R. C. Scott, P. P. Lenck-Santini, Focal Scn1a knockdown induces cognitive impairment without seizures. *Neurobiol Dis* **54**, 297-307 (2013).

39. J. C. Simonet, C. N. Sunnen, J. Wu, J. A. Golden, E. D. Marsh, Conditional Loss of Arx From the Developing Dorsal Telencephalon Results in Behavioral Phenotypes Resembling Mild Human ARX Mutations. *Cereb Cortex* **25**, 2939-2950 (2015).
40. J. D. Frost, Jr., C. L. Lee, R. A. Hrachovy, J. W. Swann, High frequency EEG activity associated with ictal events in an animal model of infantile spasms. *Epilepsia* **52**, 53-62 (2011).

41. J. D. Frost, Jr., C. L. Lee, J. T. Le, R. A. Hrachovy, J. W. Swann, Interictal high frequency oscillations in an animal model of infantile spasms. *Neurobiol Dis* **46**, 377-388 (2012).

42. C. L. Lee, J. D. Frost, Jr., J. W. Swann, R. A. Hrachovy, A new animal model of infantile spasms with unprovoked persistent seizures. *Epilepsia* **49**, 298-307 (2008).

43. R. Kabova, S. Liptakova, R. Slamberova, M. Pometlova, L. Velisek, Age-specific N-methyl-D-aspartate-induced seizures: perspectives for the West syndrome model. *Epilepsia* **40**, 1357-1369 (1999).

44. C. E. Stafstrom, D. M. Sasaki-Adams, NMDA-induced seizures in developing rats cause long-term learning impairment and increased seizure susceptibility. *Epilepsy Res* **53**, 129-137 (2003).

45. Y. J. Wang, Y. Zhang, X. H. Liang, G. Yang, L. P. Zou, Effects of adrenal dysfunction and high-dose adrenocorticotropic hormone on NMDA-induced spasm seizures in young Wistar rats. *Epilepsy Res* **100**, 125-131 (2012).

46. L. Velisek, K. Jehle, S. Asche, J. Veliskova, Model of infantile spasms induced by N-methyl-D-aspartic acid in prenatally impaired brain. *Ann Neurol* **61**, 109-119 (2007).

47. T. Chachua, M. S. Yum, J. Veliskova, L. Velisek, Validation of the rat model of cryptogenic infantile spasms. *Epilepsia* **52**, 1666-1677 (2011).

48. M. S. Yum, T. Chachua, J. Veliskova, L. Velisek, Prenatal stress promotes development of spasms in infant rats. *Epilepsia* **53**, e46-49 (2012).

49. M. S. Yum, M. Lee, T. S. Ko, L. Velisek, A potential effect of ganaxolone in an animal model of infantile spasms. *Epilepsy Res* **108**, 1492-1500 (2014).

50. M. S. Yum, M. Lee, D. C. Woo, D. W. Kim, T. S. Ko, L. Velisek, beta-Hydroxybutyrate attenuates NMDA-induced spasms in rats with evidence of neuronal stabilization on MR spectroscopy. *Epilepsy Res* **117**, 125-132 (2015).

51. T. Z. Baram, L. Schultz, Corticotropin-releasing hormone is a rapid and potent convulsant in the infant rat. *Brain Res Dev Brain Res* **61**, 97-101 (1991).

52. T. Z. Baram, L. Schultz, ACTH does not control neonatal seizures induced by administration of exogenous corticotropin-releasing hormone. *Epilepsia* **36**, 174-178 (1995).

53. M. H. Scantlebury, A. S. Galanopoulou, L. Chudomelova, E. Raffo, D. Betancourth, S. L. Moshe, A model of symptomatic infantile spasms syndrome. *Neurobiol Dis* **37**, 604-612 (2010).

54. M. A. Cortez, L. Shen, Y. Wu, I. S. Aleem, C. H. Trepanier, H. R. Sadeghnia, A. Ashraf, A. Kanawaty, C. C. Liu, L. Stewart, O. C. Snead, 3rd, Infantile spasms and Down syndrome: a new animal model. *Pediatr Res* **65**, 499-503 (2009).

55. E. Marsh, C. Fulp, E. Gomez, I. Nasrallah, J. Minarcik, J. Sudi, S. L. Christian, G. Mancini, P. Labosky, W. Dobyns, A. Brooks-Kayal, J. A. Golden, Targeted loss of Arx results in a developmental epilepsy mouse model and recapitulates the human phenotype in heterozygous females. *Brain* **132**, 1563-1576 (2009).

56. P. R. Olivetti, J. L. Noebels, Interneuron, interrupted: molecular pathogenesis of ARX mutations and X-linked infantile spasms. *Curr Opin Neurobiol* **22**, 859-865 (2012).

57. A. Pirone, J. Alexander, L. A. Lau, D. Hampton, A. Zayachkivsky, A. Yee, A. Yee, M. H. Jacob, C. G. Dulla, APC conditional knock-out mouse is a model of infantile spasms with elevated neuronal beta-catenin levels, neonatal spasms, and chronic seizures. *Neurobiol Dis* **98**, 149-157 (2017).

Chapter 5: Discussion and future directions

1. Summary of experimental chapters

Genetics plays an important etiological role in human epilepsy. With the revolution of molecular techniques, a rapid growth in the number of known monogenic determinants underlying GEs has occurred in recent years. To date, dozens of mutations in *GABRs* have been identified in different epilepsy syndromes (Table 1-2). In this dissertation, I present my work on three projects that characterize epilepsy-associated *GABR* mutations *in vitro* and *in vivo*.

In **chapter II,** I described the results of performing next-generation sequencing in parent-offspring trios with EE, leading to the discovery of 6 different *de novo GABRG2* mutations. The functional effects of these *GABRG2* mutations were studied *in vitro* in HEK293T cells expressing recombinant wild-type or mutant α1β2γ2L $GABA_AR$ subunits. Our clinical genetic information and functional investigation established *GABRG2* as a new genetic risk factor for early onset EE. This broadened the *GABRG2* phenotypic spectrum and complemented the prevailing GABAergic channelopathy paradigm in epilepsy. Our findings showed the power of massively parallel sequencing in detecting genetic defects in patients with EE. This approach is critical to identify additional EE–related *GABR* mutations. This study also created a paradigm for future studies of the genotype-phenotype relationships in *GABRG2*-encephalopathy. In **chapter III**, we extensively characterized three nonsense *GABRG2* mutations associated with epilepsy syndromes with different severities, *GABRG2(R136X), GABRG2(Q390X)* and *GABRG2(W429X*). We compared changes among mutant γ2 subunits in protein surface hydrophobicity, tendency for dimerization and subunit-subunit interactions. In addition, we determined the total and surface expression of the mutant subunits and their propensity to aggregate and characterized the properties of mutant receptor channels. We concluded that despite having loss-of-function in common, different nonsense *GABRG2* mutations resulted in different structural disturbance and different suppression of wild-type partnering subunits, leading to different epilepsy severities.

The characterization of the structural basis for the different mutant γ2 subunits in this study may provide novel insights into epilepsy phenotype heterogeneity. To our knowledge, this is the first attempt to correlate mutant protein structural disturbances, biochemical properties and function of the mutant proteins resulting from different mutations associated with a spectrum of disease phenotypes in the same gene. The technical simplicity of a transfected heterologous model cell to determine alterations of $GABA_AR$ structure and function, an efficient first step, cannot accurately reflect the dynamic effects of a *GABR* mutation on brain circuitry and disease development and can only suggest rather than explain why, where, or when altered cellular excitability in a given network can cause seizures. In **chapter IV,** we studied the IS-associated *GABRB3(N110D)* mutation *in vivo*. We demonstrated that *Gabrb3*$^{+/N110D}$ mice have increased anxiety-like behaviors, hyperactivity, abnormal social behaviors, spatial learning delay, and spatial memory deficits.

In the following sections, I will speculate on future genomic medicine of epilepsy using *GABR* mutations as examples.

2. Advances in the discovery of epilepsy genes: emerging complexity of genotype-phenotype architecture

Early gene discovery in epilepsy was limited to using linkage analysis in large families with relatively mild dominantly inherited epilepsies. The field of epilepsy genetics is now expanding rapidly. A strategic shift towards NGS studies including gene panels, WES and WGS, underlie the past decade's virtual explosion of genetic findings, with new mutations emerging as being implicated in epilepsy on almost a weekly basis. Many epilepsies previously considered idiopathic are now known to have a genetic basis. Arguably the most important discovery, based on the global collaboration of several research groups, was the recognition that *de novo* mutations contribute to a substantial proportion of patients with noninherited, severe EEs.

Gene discovery has reinforced the complex genetic architecture of epilepsy. NGS studies have revealed how mutations in the same gene can give rise to a spectrum of epilepsy phenotypes and severities (*1*) and have highlighted that a specific epilepsy phenotype can be caused by mutations in different genes (*2*). Thus it is now increasingly clear that etiological heterogeneity, variable penetrance and a broad phenotypic pleiotropy are pervasive characteristics of epilepsy genetics. Epilepsy-associated *GABR* mutations are prime examples of this insight (Table 1-2). Generally, monogenic cases of GEs are associated primarily with mutations in *GABRA1*, *GABRB3* and *GABRG2*. These three traditional *GABR* hEP genes previously associated with milder epilepsy syndromes have been shown to cause more severe phenotypes in some patients. *GABRA1* mutations originally reported in a family with JME *(7)* were also described in DS and other severe infantile onset EEs *(8-10)*. While the first *GABRB3* mutations were identified in families with CAE prior to the exome era *(11)*, their role in EEs became obvious with the publication of the initial Epi4K study *(12)*. A recent publication reviewed the phenotypic data of 22 patients with *GABRB3* variants and found a wide spectrum ranging from simple FSs, GEFS+, myoclonic-astatic epilepsy (MAE), west syndrome (WS) and other severe EEs *(13)*. For *GABRG2* mutations, it has been generally accepted that missense mutations are associated with relatively mild phenotypes including FS and CAE, while nonsense *GABRG2* mutations lead to more severe phenotypes ranging from GEFS + to DS *(14)*. In one of my projects, we used a combination of massively parallel sequencing and *in vitro* functional assays and first established that missense mutations in *GABRG2* are genetic risk factors for EEs *(15)*. A recent study in our laboratory also revealed that a novel *GABRG2* missense mutation P302L contributes to the pathogenesis of DS, further expanding the phenotypic spectrum of *GABRG2* mutations *(16)*. Another important point is that additional *GABR*s are emerging as hEP genes. For example, a new entity, *GABRB1* encephalopathy, presenting with epileptic seizures and developmental regression in infancy has been described *(12, 17)*. In addition, *de novo GABRB2* mutations were discovered in a patient with intellectual disability and epilepsy *(18)* and an in an infant with EME *(19)*. As well as facilitating the discovery of new epilepsy genes, the ability of NGS to screen for genetic variants in multiple genes in parallel has revealed the potential for so-called blended phenotypes –patients whose disorder might

be explained by more than one large-effect genetic variant (*3*). A patient with 7q11.23 deletion (Williams syndrome) plus a *de novo GABRA1* variant presenting with severe drug-resistant epilepsy was reported recently (*4*). There are nineteen *GABR* genes, however, so far only a few of them have been reported to be implicated in GEs. What other *GABR* genes will be recognized to have a role in the epilepsies and the associated phenotypes remains to be seen. Interestingly, mutations in *GABRG2* are more frequently associated with FS than other *GABR* genes (*5*). Whether or not the presence of this correlation is due only to chance or to fundamental differences in the loss of function of specific subunits requires further investigation.

We are now living in an unprecedented era of genome-wide studies in epilepsy gene discovery. As analysis of epilepsy gene panels and clinical WES become mainstream, genetic findings in epilepsies in the coming years will continue to advance at a dramatic rate. However, the discovery of genetic variants contributing to the disorder is not as straightforward as we might have predicted. There are many genetic mysteries that need to be unraveled in order to gain a broad insight into the complex genotype-phenotype architecture of genetic epilepsies.

First of all, while the clinical validity of many epilepsy genes is beyond doubt, the factors contributing to the broad phenotypic spectrum remain to be investigated. Previous studies from our laboratory suggested that the epilepsy phenotypic heterogeneity associated with *GABR* mutations may be related to the extent of the reduction of $GABA_AR$ channel function and the differential dominant negative suppression, as well to toxicity related to the metabolism of mutant subunit proteins (*6*). In one of my projects, we utilized structural modeling and structure-based analysis, and demonstrated that differential protein structure disturbances may serve as the molecular basis for the disease heterogeneity (*7*). Given that hEP gene mutations are rarely 100% penetrant and family members with the same mutation sometimes exhibit phenotypes with different severities, it is likely that the genetic background or modifying genes also play a role in the epileptogenesis of GEs. In addition, stochastic events in cellular and developmental processes, epigenetics and environmental factors are

typically implicated in the extensive variability of phenotypic expression. However, the degree to which phenotypic penetrance is influenced by these factors is yet to be determined.

Secondly, there is an emerging number of major epilepsy genes implicated in both benign and severe phenotypes, raising the question whether various conditions represent distinct entities or a fluid continuum (*8*). For instance, there are only two main categories of patients with *KCNQ2* mutations, 1) patients with benign (familial) neonatal epilepsy, and 2) patients with neonatal EE, also called *KCNQ2* encephalopathy (*9*). Both syndromes make up the two ends of a spectrum, providing the impression that the phenotypes associated with *KCNQ2* gene may represent distinct entities at both ends of the spectrum. In contrast, the example of *GABRG2* highlights the "fluid continuum" point. As discussed above, *GABRG2* mutations have been associated with a spectrum of phenotypes ranging from simple FS to GEFS+ and severe EEs, arguing for a fluid continuum rather than distinct entities that do not overlap. This gradient is somewhat reflected in the functional alterations of *GABRG2* mutations with different severities, ranging from simple loss of function to mild or strong dominant negative effect. Although it will be challenging, identifying detailed delineation of the phenotypic spectrum that is affected by a genetic variant is crucial. With more genetic studies in common epilepsies, the middle ground between the extremes of mild familial epilepsies and severe EEs will be increasingly associated with many major epilepsy genes. It will be interesting to see to what extent the *GABRG2* example also holds true for other genetic etiologies in epilepsies.

Thirdly, how divergent genetic etiologies result in the same clinical and electrographic features still remains obscure. For example, IS has been associated with a very large number of gene mutations, including but not limited to *ARX*, *CDKL5, SCL25A2, DNM1* and *STXBP1*. For *ARX*-encephalopathy, it has been shown that interneurons loss and abnormal segregation due to disruption in tangential migration (interneuronopathy) results in epilepsy (*10*). There is growing evidence that dysfunction of various genes can lead to disruption of common pathways or mechanisms that converge to produce a given phenotype. One of my projects is

focused on the *Gabrb3*$^{+/N110D}$ model of IS. Additional work remains to understand whether interneuronopathy is shared in this mouse model or there is something unique about this *Gabrb3* gene leading to IS.

Finally, there is increasing recognition of the importance of comorbidities in GEs, especially the neurodevelopmental disabilities such as motor dysfunction or cognitive impairment (*11*). Are these disorders caused directly by the mutations or secondary to uncontrolled seizures? The pathophysiological connection between epilepsies and these associated disorders is yet to be elucidated.

3. Challenges in understanding the building blocks of epilepsy genetics: paradigm shift from gene discovery to data interpretation

As mentioned in the last section, we have seen unprecedented success in defining the genetic etiology of epilepsy by NGS and hundreds of new genes have been discovered. However, the field of epilepsy genetics is still in its infancy. The ability to assess pathogenicity of variants, provide functional analysis, and develop targeted therapies (a topic I will elaborate on later) has not kept pace with rapid progress in sequencing technology. Although clinical genetic testing may provide a specific molecular diagnosis for some epilepsy patients, test results often lead to more questions than answers. While genetics has traditionally been a relatively resource-scarce field, the flood of genomic data generated by NGS studies in the past several years threatens to create an opposite problem: a bewildering constellation of contributing genes (*12*). The genetic deluge has made it painfully clear that the prior bottleneck of limited data generation has been overcome at the expense of a new interpretation bottleneck-we are generating more data than we can interpret (*8*). Thus, it is far from certain that identifying more mutations will be useful to epilepsy researchers and clinicians in the near future. Making sense of this ever expanding amount of data, i.e. the interpretation of detected variants and the prediction of their pathogenicity, is currently a major project in the field of epilepsy genetics and remains challenging given our current knowledge.

Currently, the epilepsy genetics community is fairly good at detecting variants that are deleterious in an evolutionary sense but is not nearly as good at connecting this information with whether variants are pathogenic. As 22000 single-nucleotide variants are identified on WES, and 5 million variants on WGS of an individual, whether a nonsynonymous variant is epilepsy-associated and of major effect should always be questioned, even if it occurs in known epilepsy genes. Although valid biological explanations exist for much of the genetic heterogeneity and phenotypic pleiotropy, there is a risk that a variant claimed to be pathogenic is benign and not causative. Now there is a growing sense of caution in asserting that a particular variant is harmful in the absence of strong supporting evidence (*13*). Thus, the current wave of epilepsy gene discovery has been accompanied by a wave of gene retirement, constantly refining the list of possible hEP genes. For example, in 2016, the *EFHC1* gene previously implicated in JME was no longer considered the causative gene after careful assessment of the available evidence linking this gene to epilepsy (*14, 15*).

Achieving confidence in the determination of causality between a variant and epilepsy is a complex task that requires various types of supportive data. Pathogenic rare variants should be interpreted according to a combination of population genetic data, computational (in silico) data, *de novo* or family segregation data and biologic foundations (*16*). Publicly available databases such as the 1,000 Genomes Project [www.1000genomes.org] and the Exome Variant Server [NHLBI Exome Sequencing Project (ESP), Seattle, Washington, http://evs.gs.washington.edu/EVS/] enable laboratories to evaluate whether a newly identified variant in a patient with epilepsy has also been seen in populations of individuals who are not known to have diseases. New methods to assess a gene's tolerance of variation have been described in the research setting (*17*). In addition, software including such as PolyPhen-2 *(18)* and SIFT *(19)* provides very useful platforms to predict whether or not a given missense variant would adversely affect protein function based heavily upon sequence conservation. However, it is by no means certain that mutations located in structured domains will be deleterious or that those located in unstructured domains will be benign. The gold standard would be for all newly identified variants, even in known genes, to undergo functional assessment in a model system (*2*).

Functional characterizations are essential for us to clearly understand the structure-function relationship of mutant subunits/receptors and to make predictions how mutations/variants disrupt receptor function. In one of my projects, we studied six *de novo GABRG2* variants identified in EE patients. In silico analysis using PolyPhen-2 and SIFT predicted that the substitutions P282S, R323Q, R323W and F343L would not be tolerated and might damage protein structure. In contrast, the variants A106T and I107T, which were in a non-conserved residue location were predicted to be tolerated. In contrast, our functional analysis demonstrated that all of these variants impaired $GABA_AR$ biogenesis and/or channel function, providing strong evidence for their causal role in EE.

Despite remarkable progress in epilepsy gene discovery, a large proportion of affected individuals with presumed GEs remain without a genetic diagnosis, even when high-resolution gene panels or WES are applied (*20*). Improved coverage of candidate genes and copy number variants may decrease the number of unexplained cases, but only to a small degree. However, the total amount of genetic information in an individual is much greater than is typically evaluated by most currently available clinical or research tests. First, postzygotic, somatic mosaic mutations are increasingly recognized as an important cause of epilepsy that deserve special mention. Detection of somatic mosaic mutations is technically difficult, depending on the level of mosaicism and which lineages of cells carry the mutation. In some cases, somatic mosaic mutations may be present only in the brain (or with the part of the brain responsible for seizures), which are not always detectable in DNA from patient's blood (*21*). For example, somatic mosaicism for *SCN1A* mutations has been identified in mildly affected parents of children with Dravet syndrome (*22, 23*). For this reason, single-cell and ultra-deep sequencing are needed to detect and measure the somatic mutation rates in different cell types and lineages (*24*). In addition, a largely unexplored area is the impact of variants in nonexonic DNA. Rare non-coding mutations have been identified in some human diseases and are likely to play a role in epilepsy as well. For example, *GABRG2(IVS6+2T→G)* is a splice donor site mutation in intron 6 identified in a GEFS+ family *(25)*. The ability to inexpensively sequence entire genomes will facilitate the transition

from WES to WGS and readily allow analysis of noncoding variation, something that has only been studied on a limited basis to date. Finally, assessment of epigenetic factors and systematic analysis of noncoding regulatory RNAs (including microRNA and long noncoding RNA) may hold the key to further explaining a significant proportion of cases and may represent promising areas for future research (*26*).

We are now transitioning into a phase of epilepsy genetics in which the rate-limiting step is no longer gene discovery. Instead, the future will concentrate more on the biological and clinical interpretations of the torrent of specific risk variants identified through NGS.

4. Investigating mechanisms of *GABR*-associated GEs beyond *in vitro* systems: what can we learn from genetically engineered mouse models *in vivo*?

After identifying epilepsy-causing mutations, researchers still need to determine the role of these mutations that are central to epileptogenesis. Study of associated molecular/cellular mechanisms *in vitro* reveals how a mutation affects channel function and cell excitability. However, epilepsy is a circuit-based disorder and there is still lack of understanding of the impact of these mutations in a complex neuronal milieu during development. Animal models are essential to study the complex network effects not evident in the study of cultured cell systems and will help to more accurately describe the relationship between genotype and phenotype.

In one of my projects, I studied the behavioral phenotypes of the *Gabrb3*$^{+/N110D}$ KI mouse, which is a model of IS. Our laboratory also generated the *Gabrb3*$^{+/D120N}$ KI mouse, which is a model of LGS and the *Gabrb3*$^{+/P11S}$ KI mouse, which is a model of CAE and ASD. The different epilepsy syndromes caused by different mutations in the same *GABRB3* gene are likely due to mutation effects that vary in type and severity. We have developed a mechanistic understanding of the cellular/molecular deficits produced by these mutations *in*

vitro. To bridge the known cellular/molecular dysfunction with clinical phenotypes, we propose several future studies *in vivo*.

First of all, a promising avenue of investigation is to identify specific brain regions underlying seizure generation/spread and analyze the detailed circuitry of neuronal networks hyperexcitability in these models. These three mutations/mouse models are associated with three different epilepsy syndromes; what are the circuitry deficits for these clinical syndromes? We have performed video-EEG recordings from these three mouse models and observed different seizure semiologies and EEG abnormalities, which are consistent with the patients' phenotypes. Surface EEG recording could provide some general information, but its spatial resolution is low. Thus, it cannot show if specific brain regions are involved. Comparing the altered thalamocortical or limbic system network oscillations in these three types of epilepsy model using multiunit recordings may be worth trying. In addition, new techniques such as large-scale multielectrode arrays, calcium imaging of network activity in awake-behaving animals, and functional magnetic resonance imaging (fMRI) can be applied to KI mice to study circuit dynamics during and between seizures in intact systems. Shedding light on these issues is important for identifying specific network activities and brain regions that are particularly implicated in different epilepsy syndromes, which may be potentially used as targets in screening for the development of antiepileptic approaches.

Second, studying abnormal brain network development/structure in these mouse models should be revealing. It has long been established that even extremely small changes during neural development can trigger a cascade of drastic effects that define long-term network stability. In contrast to mature brain, GABA is excitatory in the developing brain as a result of an initially higher intracellular chloride concentration (*27*). There is now growing evidence demonstrating that excitatory GABAergic neurotransmission plays a fundamental role in many aspects of brain development, such as neuronal migration, synapse formation and shaping of dendritic trees (*28*). Thus, it would be expected that these *GABRB3* mutations would alter the

course of neuronal network development, which could contribute to seizure and neurobehavioral comorbidities. Imaging study including fluorescence microscopy and electron microscopy to compare morphology and connections of neurons and synapses at different developmental stages may reveal some general structural abnormalities. It has been demonstrated in animal models that the epileptogenic effects of the *GABRG2(R82Q)* mutation associated with GEFS+ occur mainly during key windows in development (*29*). Thus, in our KI mice carrying different *GABRB3* mutations, we are also hoping to identify early pre-epileptic periods in which specific abnormalities of neuronal network are present without generating behavioral seizures. These age-related periods may suggest specific developmental roles of these *GABRB3* mutations, and might provide a critical time window for therapeutic approaches that prevent seizures and the associated developmental defects.

Third, is there any abnormality of synaptic plasticity in these mouse models? Synaptic plasticity is the ability of synapses to strengthen or weaken over time, in response to changes in both amplitude and temporal dynamics of neuronal activity. The epileptic brain shows hyperexcitability, and patterns of neuronal firing will change brain plasticity, which could in turn be one cause of the excitation/inhibition imbalances. Experimental evidence suggests that the start, progress, and consolidation of epileptic stage could overlap with the mechanisms underlying long-term plasticity, which could be explained by an alteration of the factors that regulate the synaptic plasticity of excitatory and inhibitory circuits (*30*). Sensory inputs and intrinsic brain activity can effect long-term changes in synaptic efficacy and eventually increase or decrease neuronal connectivity by modulating the number of synapses. These changes in synaptic plasticity can be measured as long-term potentiation (LTP) or long-term depression (LTD). Electrophysiological recordings can be used to compare different types of synaptic plasticity. I will perform field excitatory postsynaptic potentials (EPSPs) recordings in transverse hippocampal slices and determine LTP/LTD at the Schaffer collateral-pyramidal synapses within the CA1 region. Briefly, an extracellular recording electrode is placed among apical dendrites of CA1 pyramidal cells, and stimulating electrodes are positioned in the Schaffer collaterals. LTP is

induced by tetanic high-frequency stimulation (HFS) of Schaffer collaterals comprising delivery of trains of pulses at 100 Hz for 1 sec. LTD is induced by low-frequency stimulation (LFS) of Schaffer collaterals comprising delivery of 900 pulses at 1 Hz for 15 min. I will decide whether these mouse models display defective LTP/LTD compared to wild-type controls.

Fourth, how do these *GABRB3* mutations induce adaptive cellular plasticity? Individuals with each *GABR* mutation manifest two competing processes during epileptogenesis, loss of inhibition due to the mutant *GABR* allele and compensatory mechanisms such as adaptive neuronal plasticity in response to loss of inhibition. To understand the process of GE epileptogenesis, both processes must be understood for each mutation. Whole transcriptome analysis using RNAseq allows quantitative characterization of mouse brain whole transcriptomes that demonstrate cellular plasticity associated with *GABR* mutations. We will primarily focus our analysis on somatosensory cortex and nRT nucleus of thalamus. Transcriptome alterations of these mouse models between WT littermates can be compared using RNAseq. We want to know how gene expression in different types of neurons and non neurons including astrocytes and oligodendrocytes is altered to cause a series of changes. Expression levels of all transcriptomes in mouse cortex and thalamus will demonstrate if one mutant *GABRB3* allele is sufficient to induce adaptive cellular responses, alter cortical and thalamic neuronal activity, and produce a generalized epilepsy. Comparison of results among these mouse models would suggest if the responses were associated with loss of one normal β3 allele or with a specific mutation effect. Transcripts will be grouped into functional modules based on gene involvement in Gene Ontology (GO) or KEGG pathway. The Allen brain atlas will be referenced to demonstrate the *in situ* pattern of each gene. Functional modules that are significantly over-represented or under-represented in different brain regions and in different neuron types will demonstrate the molecular and cellular plasticity in adaption to *GABRB3* mutations. The whole transcriptome analysis data will be verified using *in situ* hybridization and immunohistochemistry.

Although genetic mouse models carrying human epilepsy mutations allow epileptologists to probe the effect of a single molecule on the development of epilepsy, one must be mindful that the phenotype may not be directly attributable to the mutated gene. Rather, the mutation may cause downstream effects or compensatory changes that are directly associated with the production of seizures. For example, It has been shown that several genetic models of generalized epilepsy all caused a similar downstream effect: the augmentation of tonic GABAergic currents in the thalamus (*31*).

Every epilepsy mutation discovered has a complex underlying biological mechanism that will take some time to unravel. It is unreasonable to create KI or transgenic mice for each newly discovered epilepsy mutation. With luck, the large numbers of discovered epilepsy mutations can be exploited to develop categories of genetic etiologies. Take the known monogenic *GABR* mutations as an example: studies from our laboratory suggest that mutations in the same category usually share similar molecular mechanisms, although the severities of these effects vary mutation by mutation. Thus, it is useful to generate KI mice for at least one mutation in each category. Work in our laboratory has permitted classification of these *GABR* mutations into 6 classes based on their location and effects: those that reduce subunit expression due to: 1) impaired transcription, 2) impaired translation, 3) truncation and ER retention with or without a dominant negative effect on other subunits, 4) misfolding and degradation, 5) ER retention of functional receptors, and a final class of mutations 6) reduces surface receptor function. Those categories are very helpful in focusing our pathophysiological investigations. In addition, identification of shared mechanisms among different *GABR* mutations should accelerate the development of new treatments, a topic I will elaborate on later. Besides these three *GABRB3* KI mouse models mentioned in this section, we have made a class 2 *GABRG2(IVS6+2T→G)* transgenic mouse, a class 3 $Gabrg2^{+/Q390X}$ KI mouse, a class 4 $Gabra1^{+/A322D}$ KI mouse, and a class 6 $Gabrg2^{+/K328M}$ KI mouse. The class 5 $Gabrg2^{+/R82Q}$ KI mouse model is already available (*32*).

5. Therapeutic strategies: precision medicine in GEs

The ultimate goal of epilepsy genetic research is to aid the development of effective antiepileptic treatments. Despite the various mechanisms of action of currently available antiepileptic drugs (AEDs), many of them have undesirable side effects, and about one third of epilepsy patients fail to achieve complete freedom from seizures (*33*). Importantly, all conventional AEDs only have purely symptomatic effects: they just suppress seizures but they do not target the underlying mechanism of epileptogenesis (*34*).

In this new era of genomic medicine, our understanding of genetics and neurobiology of epilepsies has led to optimism that antiepileptic treatments could be targeted to a person's specific genetic diagnosis (precision medicine) *(35)*. This allows improvement in treatment options for individual patients, both in terms of effectiveness and minimization of side effects. The success of precision medicine in epilepsy relies on establishing an accurate genetic diagnosis, analyzing functional consequences of specific variants, evaluating candidate therapeutic drugs in the laboratory setting, and initiating targeted therapy trials back into clinic (*36*). Here we narrowly define precision medicine as a specific therapy targeting a precisely established genetic etiology, rather than the use of genetic diagnosis to inform a relatively nonspecific treatment approach, such as prescription of stiripentol and avoidance of sodium channel blockers in epilepsy patients with *SCN1A* mutations and the ketogenic diet in glucose transporter 1 (GLUT) deficiency syndrome due to *SLC2A1* mutations (*3*). Precision medicine is now a major focus of the epilepsy research community. Looking to the future, the aim of precision medicine is to improve not only seizure control, but also associated neurodevelopmental comorbidities.

To date, more than a dozen precision therapies are used in a small number of patients with GEs, some with substantial success. A remarkable example is the administration of memantine, an N-methyl-D-aspartate (NMDA) receptor antagonist, in a patient with EOEE caused by a *de novo GRIN2A* missense mutation (*37*). *GRIN2A* encodes a subunit of the NMDA receptor, which is an excitatory ion channel that is activated by

glutamate. *In vitro* experiments testing for activity of the receptor were performed prior to use of the drug, demonstrating that this mutation resulted in increased activation of NMDA receptor, leading to neuronal excitation and seizures. Similarly, quinidine reverses large potassium currents emanating from gain-of-function *KCNT1* mutations, suggesting that it could led to rational intervention in patients with epilepsy of infancy with migrating focal seizures (*38*) and severe autosomal dominant nocturnal frontal lobe epilepsy (*39*).

Recent studies of *GABR* mutations provide molecular targets for potential new therapeutic strategies for the treatment of GEs. As mentioned before, epilepsy-associated *GABR* mutations can cause multiple consequences including elimination of the mutant mRNA through NMD, misfolding and degradation of the nascent polypeptides, impaired receptor oligomerization, dominant negative suppression of wild-type $GABA_AR$ expression, formation of insoluble protein aggregates, and altered electrophysiological properties. Specific potential therapies for each of these molecular consequences have been proposed (Table 5-1). (*40*) Potential therapeutic approaches would include increasing $GABA_AR$ channel function or decreasing the disturbance of cellular homeostasis by the presence of mutant $GABA_AR$ subunits. Here, I will summarize several categories of future therapy based on our understanding of GEs caused by monogenic *GABR* mutations.

1) Upregulate wild-type $GABA_ARs$ using gene therapy

Loss of function or haploinsufficiency is a key mechanism of GE-associated *GABR* mutations. Thus, we can increase the activity of the wild-type allele to compensate for the loss of one normal allele. This approach is ideal for mutations like *GABRG2(R136X)* causing only haploinsufficiency. This strategy also works for other mutations like *GABRG2(Q390X)* with dominant negative effects, as extra wild-type subunit protein could compete with mutant subunit protein, thus increasing the function of wild-type subunit protein while reducing dominant negative effects of mutant subunit protein. A recent study from our laboratory has reported that overexpression of wild-type $\gamma2^{HA}$ subunits using a BAC transgenic mouse, the Tg $^{(hGABRG2HA)}$ mouse, could

increase expression of cortical and thalamic γ2 subunits, rescue reduced GABAergic inhibition, raise PTZ seizure threshold and reduce spontaneous seizures in *Gabrg2*$^{+/Q390X}$ KI mouse model of Dravet syndrome/GEFS+ (*41*). This is proof of principle that increasing expression of wild-type subunits could become a future direction to treat severe GEs caused by *GABR* and by extension to other ion channel gene mutations.

In the future, gene delivery strategies upregulating the gene expression of wild-type subunits will have more promising clinical application for the treatment of GEs (*42*). As the gold standard for delivery of exogenous genetic material, lentiviruses or adeno-associated viruses (AAV) can be used. They elicit relatively low immune and inflammatory responses and have been used in clinical trials (*43*). Besides, non-viral delivery strategies such as nanoparticles are gaining interest due to lower safety concerns, an ease in manufacturing and greater customizability (*44*) . It would be important to test whether there is a critical time window during development for therapeutic intervention, as we are hoping to prevent or arrest epileptogenesis before the disease onset, rather than treat already-manifest seizures. In addition, it would be interesting to investigate how many copies of wildtype allele are sufficient to attenuate seizures.

However, the translation of gene therapy approaches into the clinic still face many obstacles (*42*). First, delivery of large molecules and transcripts across the blood–brain barrier and into cells is challenging. A second concern is the constitutive nature of the therapy. Once a gene is introduced, the effect is permanent and might produce undesirable side effects, which cannot simply be switched off. This issue of potential off-target effects might be mitigated by locally delivered gene therapy that is targeted to a specific epileptogenic zone or population of neurons.

2) Promote read-through of nonsense *GABR* mutations

For mutant $GABA_AR$ subunit mRNAs with PTCs that cause epilepsy due to loss of function of one allele, nonsense suppression therapy aimed at increasing translational read-through and generating a full-length protein may restore deficient protein function (*45*). In addition, this approach would reduce expression of nonfunctional truncated protein that might have cellular toxicity.

Generally, two types of drug are used to promote read-through at PTCs: aminoglycosides and PTC124 (Ataluren) (*46*). Aminoglycosides are a class of antibiotics that bind to the ribosome decoding center. Gentamicin, the aminoglycoside most commonly used to suppress translation termination at PTCs, has been shown to restore physiologically relevant levels of functional protein *in vitro*, *in vivo* and in patients with nonsense mutations (*47*). Our laboratory has demonstrated that gentamicin could partially restore the synthesis of full-length functional γ2 subunits from subunits containing the *GABRG2(Q40X)* mutation *(48)*. This strategy may also be useful to prevent the production of toxic mutant protein like γ2(Q390X) subunits. However, aminoglycosides are known to have toxic side effects with long-term administration, including hearing loss and kidney damage (*49*). If additional promising compounds with reduced toxicity and enhanced efficiency of PTC suppression are identified in future, it will be very interesting to test them in *Gabrg2*$^{+/Q390X}$ KI mice. PTC124, also known as ataluren, is an oxadiazole compound identified by PTC Therapeutics that suppresses termination at PTCs in mammalian cells without affecting translation termination at natural stop codons. Comprehensive preclinical studies showed that advantages of ataluren over the clinically used aminoglycosides include minimal off-target side effects, no antibacterial activity, and orally bioavailability (*50*). Promising safety and efficacy data from phase 1 and phase 2 clinical trials with Duchenne Muscular Dystrophy (DMD) and cystic fibrosis (CF) patients carrying nonsense mutations led to the initiation phase 3 clinical trials for both diseases (*51, 52*). The same strategy with PTC124 might be useful for GE patients who harbor PTC-generating mutations.

3) Maintain proteostasis of trafficking-deficient $GABA_AR$s

Problems in any step during the biogenesis of $GABA_AR$s will affect the normal surface expression level of the receptors. Many *GABR* mutations lead to epilepsy by abolishing the folding, assembly, and trafficking of the mutant receptors. One emerging therapeutic strategy for such deficiencies is to adapt the proteostasis network to restore the function of trafficking-deficient $GABA_AR$s *(53, 54)*.

Two classes of small molecules are employed: proteostasis regulators (*55*) and pharmacological chaperones (*56*). Proteostasis regulators operate on the proteostasis network components to correct folding and trafficking deficiencies. For example, SAHA, acting as a proteostasis regulator, enhances the functional cell surface expression of the A322D α1 subunit of $GABA_AR$s partially by increasing the BiP protein level and the interaction between the calnexin and the mutant α1 subunit in the ER (*57*). Verapamil, an L-type calcium channel blocker, acting as a proteostasis regulator, enhances the function of the D219N α1 subunit of $GABA_AR$s by promoting calnexin-assisted folding (*58*). Recently, a chemical corrector, 4-phenylbutyrate (4PBA), restored the function of trafficking-defective $LGI1^{E383A}$ function and ameliorated the increased seizure susceptibility of the $LGI1^{E383A}$ mice *in vivo*, which is a model of autosomal dominant lateral temporal lobe epilepsy (ADLTE) (*59*). Pharmacological chaperones directly bind to the receptors in the ER, stabilize a correct folding conformation, increase the successful rate of folding, and promote protein delivery to the cell surface (*60*). A pharmacological chaperone (VX-809 or lumacaftor) that targets specific cystic fibrosis transmembrane conductance regulator (CFTR) folding defective mutants, has been recently approved for clinical use in patients affected by CF (*61*). Different proof-of-principle strategies have been applied to restore *in vitro* functioning of trafficking-deficient mutant sodium channels, such as incubation at low temperature, molecular interactions with different co-expressed proteins, exposure to sodium channel blockers such as phenytoin (*62-64*). Agonists and antagonists are candidates of pharmacological chaperones for $GABA_AR$s. $GABA_AR$ agonists and a competitive antagonist bicuculline enhance the surface expression level

of $GABA_ARs$ by acting as pharmacological chaperones (*65, 66*). Previous studies in our laboratory demonstrated that lower incubation temperature (30°C) increased stability and trafficking of mutant γ2 subunits, but failed to identify significant chaperone effects of either GABA or diazepam (*67*). With more thorough drug screening, chemicals with specific chaperone effects on $GABA_ARs$ may be identified or developed in the future. Combining proteostasis regulators and pharmacological chaperones is expected to achieve better therapeutic effects on GEs.

4) Eliminate production of dominant-negative mutant protein using allele-specific RNA interference

Recent studies suggest that in addition to impairing inhibitory neurotransmission, the pathology of *GABR* mutations is likely to be due to the presence of mutant toxic protein. For example, mutant γ2(Q390X) subunits formed substantial protein aggregates, produced dominant-negative suppression of wild-type subunits, disturbed cellular homeostasis and caused widespread neurodegeneration, which can contribute to epilepsy *(68)*. In this context, a therapeutic strategy using allele-specific RNA interference (RNAi) of the mutant transcripts to suppress or eliminate the detrimental effect of mutant protein might be a useful approach *(69)*.

The development of RNAi-based CNS-related therapeutics such as small interfering RNA (siRNA) or short hairpin RNA (shRNA) has largely focused on neurodegenerative diseases, such as Alzheimer's disease (*70*), Huntington's disease (*71*), Parkinson's disease (*72*), and Machado-Joseph disease (*73*). Similar strategies might be beneficial for treating *GABR* mutations with dominant-negative effects, although it is difficult to quantify how much RNAi-mediated reduction in mutant protein will be required for the treatment of the pathology of GEs. More importantly, little is known about duration of effect, the optimal delivery route, and risk of off-target effects.

5) Correct *GABR* mutations using genome editing technology

Ideally, the treatment for GEs would be to edit the faulty gene and correct the disease-causing mutations(s) permanently. Genome editing technologies, especially the CRISPR/Cas (clustered regularly interspaced short palindromic repeat (CRISPR)–CRISPR-associated protein) systems represent exciting and promising approaches that have been developed to achieve this goal (*74*).

CRISPR functions as an innate immune mechanism in bacteria and archaea that protects them against phage infection (*75*). The engineered CRISPR system is composed of two distinct parts: a nuclease (e.g. Cas9) which is able to cut the double DNA strand, and a small guide RNA (sgRNA) which drives the nuclease in a precise genome location (*76*). This results in a precise double strand break of the DNA in a defined genome region and permits gene editing in mammalian cells. Some groups have already successfully used *in vivo* genome editing based on the CRISPR platform to correct disease mutations in mouse models of several genetic diseases, such as hereditary tyrosinemia (*77, 78*) and DMD (*79, 80*). However, homology-directed repair (HDR) is much less active than non-homologous end joining (NHEJ) in post-mitotic neurons (*81*). For this reason, using HDR as an editing tool to treat neurological genetic diseases is challenging. A recent study demonstrated for the first time that using homology-independent targeted integration (HITI) based on NHEJ, it is possible to precisely insert a DNA sequence in a genome location in mature neurons *in vivo* using CRISPR/Cas9 (*82*). This opens new possibilities for gene editing in neurons to treat monogenic GEs.

However, *in vivo* clinical use of genome editing technologies to rescue GEs is in its infancy because many methodological and social/ethical challenges still remain today. (*83, 84*). The big challenge is to precisely correct mutations in highly structured ion channels in neurons. With current methodology, additional amino nucleotides may be introduced. In this context it is important to make sure that the coding sequence will not be affected (*85*). Other limitations include low viral transduction efficiency, the possibility of off-target recognition by sequences of the sgRNA, safety and ethical concerns and etc. Continued development of viral

vectors and new CRISPR systems are helping to overcome these limitations (*86*). We believe that novel genome-editing technologies based on CRISPR–Cas systems holds potential for personalized therapeutic applications for GEs.

6. Conclusions

The handful of known *GABR* mutations are just the tip of the iceberg among epilepsy-related genes-an area where genetic and phenotypic heterogeneity is an emerging theme. Our understanding of *GABR* mutations *in vitro* and *in vivo*, while promising, only marked the start of a long road ahead for unraveling complex developmental relationships bridging a single mutation and human physiology during epileptogenesis. We anticipate that streamlined approaches to functional studies of *GABR* mutations, and other epilepsy-associated mutations in the future, will move the field of GEs closer to translating genetic discoveries to directed therapies as we enter the era of precision medicine.

Table 5-1 Mutation specific therapies for GEs associated with *GABR* mutations

Classification	Example	Mechanism	Therapy strategies
Class I **Promoter mutations**	*GABRB3(-897 T/C)*	Reduced subunit due to impaired transcription	• Use transcriptional activators to increase mutant gene transcription. • Up regulate wild type subunits.
Class II **Early exon nonsense mutations**	*GABRG2(Q40X)* *GABRG2 (IVS6+2T->G)* *GABRG2 (R136X)* *GABRA1 (975delC, S326fs328X)*	Impaired translation (NMD) of truncated subunits	• Use aminoglycosides or other drugs, to suppress PTCs by enabling amino acid read-through, thus permitting complete translation of the mutant transcript. • Up regulate wild type subunits.
Class III **Last exon nonsense mutations**	*GABRG2(Q390X)* *GABRG2(W429X)* *GABRG2(S443delC)* *GABRA1(K353delins18X)*	ER retention of truncated subunits, with or without dominant negative effect	• Use aminoglycosides or other drugs, to suppress PTCs by enabling amino acid read-through, thus permitting complete translation of the mutant transcript. • Down regulate mutant subunits with toxic effects – allele-specific RNA interference • Up regulate wild type subunits.
Class IV **Missense mutations**	*GABRA1(A322D)*	Subunit misfolded and degraded (ERAD)	• Administration of proteostasis regulators or pharmacological chaperones to maintain proteostasis of mutant receptors. • Up regulate wild type subunits.
Class V Missense mutations	*GABRG2 (R82Q)* *GABRG2 (P83S)* *GABRA1 (D219N)* *GABRG2 (R177G)* *GABRB3(P11S, S15F, G32R)*	ER retention with impaired oligomerization with wild-type subunits	• Administration of proteostasis regulators or pharmacological chaperones to maintain proteostasis of mutant receptors. • Up regulate wild type subunits.
Class VI Missense mutations	*GABRG2(K328M)* *GABRD(E177A)* *GABRD(R220H)*	Impaired surface receptor function	• Use specific or nonspecific $GABA_A$ receptor positive allosteric modulators to enhance current (channel 'potentiators'). • Up regulate wild type subunits.

References

1. X. Zhu, A. C. Need, S. Petrovski, D. B. Goldstein, One gene, many neuropsychiatric disorders: lessons from Mendelian diseases. *Nat Neurosci* **17**, 773-781 (2014).

2. A. McTague, K. B. Howell, J. H. Cross, M. A. Kurian, I. E. Scheffer, The genetic landscape of the epileptic encephalopathies of infancy and childhood. *Lancet Neurol* **15**, 304-316 (2016).

3. J. D. Symonds, S. M. Zuberi, M. R. Johnson, Advances in epilepsy gene discovery and implications for epilepsy diagnosis and treatment. *Curr Opin Neurol* **30**, 193-199 (2017).

4. B. Popp, R. Trollmann, C. Buttner, A. Caliebe, C. T. Thiel, U. Huffmeier, A. Reis, C. Zweier, Do the exome: A case of Williams-Beuren syndrome with severe epilepsy due to a truncating *de novo* variant in *GABRA1*. *Eur J Med Genet* **59**, 549-553 (2016).

5. M. Boillot, M. Morin-Brureau, F. Picard, S. Weckhuysen, V. Lambrecq, C. Minetti, P. Striano, F. Zara, M. Iacomino, S. Ishida, I. An-Gourfinkel, M. Daniau, K. Hardies, M. Baulac, O. Dulac, E. Leguern, R. Nabbout, S. Baulac, Novel *GABRG2* mutations cause familial febrile seizures. *Neurol Genet* **1**, e35 (2015).

6. J. Q. Kang, R. L. Macdonald, Molecular Pathogenic Basis for *GABRG2* Mutations Associated With a Spectrum of Epilepsy Syndromes, From Generalized Absence Epilepsy to Dravet Syndrome. *JAMA Neurol* **73**, 1009-1016 (2016).

7. J. Wang, D. Shen, G. Xia, W. Shen, R. L. Macdonald, D. Xu, J. Q. Kang, Differential protein structural disturbances and suppression of assembly partners produced by nonsense *GABRG2* epilepsy mutations: implications for disease phenotypic heterogeneity. *Sci Rep* **6**, 35294 (2016).

8. I. Helbig, A. A. Tayoun, Understanding Genotypes and Phenotypes in Epileptic Encephalopathies. *Mol Syndromol* **7**, 172-181 (2016).

9. S. Weckhuysen, S. Mandelstam, A. Suls, D. Audenaert, T. Deconinck, L. R. Claes, L. Deprez, K. Smets, D. Hristova, I. Yordanova, A. Jordanova, B. Ceulemans, A. Jansen, D. Hasaerts, F. Roelens, L. Lagae, S. Yendle, T. Stanley, S. E. Heron, J. C. Mulley, S. F. Berkovic, I. E. Scheffer, P. de Jonghe, KCNQ2 encephalopathy: emerging phenotype of a neonatal epileptic encephalopathy. *Ann Neurol* **71**, 15-25 (2012).

10. M. G. Price, J. W. Yoo, D. L. Burgess, F. Deng, R. A. Hrachovy, J. D. Frost, Jr., J. L. Noebels, A triplet repeat expansion genetic mouse model of infantile spasms syndrome, Arx(GCG)10+7, with interneuronopathy, spasms in infancy, persistent seizures, and adult cognitive and behavioral impairment. *J Neurosci* **29**, 8752-8763 (2009).

11. M. R. Keezer, S. M. Sisodiya, J. W. Sander, Comorbidities of epilepsy: current concepts and future perspectives. *Lancet Neurol* **15**, 106-115 (2016).

12. E. L. Heinzen, B. M. Neale, S. F. Traynelis, A. S. Allen, D. B. Goldstein, The genetics of neuropsychiatric diseases: looking in and beyond the exome. *Annu Rev Neurosci* **38**, 47-68 (2015).

13. M. Lek, K. J. Karczewski, E. V. Minikel, K. E. Samocha, E. Banks, T. Fennell, A. H. O'Donnell-Luria, J. S. Ware, A. J. Hill, B. B. Cummings, T. Tukiainen, D. P. Birnbaum, J. A. Kosmicki, L. E. Duncan, K. Estrada, F. Zhao, J. Zou, E. Pierce-Hoffman, J. Berghout, D. N. Cooper, N. Deflaux, M. DePristo, R. Do, J. Flannick,

M. Fromer, L. Gauthier, J. Goldstein, N. Gupta, D. Howrigan, A. Kiezun, M. I. Kurki, A. L. Moonshine, P. Natarajan, L. Orozco, G. M. Peloso, R. Poplin, M. A. Rivas, V. Ruano-Rubio, S. A. Rose, D. M. Ruderfer, K. Shakir, P. D. Stenson, C. Stevens, B. P. Thomas, G. Tiao, M. T. Tusie-Luna, B. Weisburd, H. H. Won, D. Yu, D. M. Altshuler, D. Ardissino, M. Boehnke, J. Danesh, S. Donnelly, R. Elosua, J. C. Florez, S. B. Gabriel, G. Getz, S. J. Glatt, C. M. Hultman, S. Kathiresan, M. Laakso, S. McCarroll, M. I. McCarthy, D. McGovern, R. McPherson, B. M. Neale, A. Palotie, S. M. Purcell, D. Saleheen, J. M. Scharf, P. Sklar, P. F. Sullivan, J. Tuomilehto, M. T. Tsuang, H. C. Watkins, J. G. Wilson, M. J. Daly, D. G. MacArthur, C. Exome Aggregation, Analysis of protein-coding genetic variation in 60,706 humans. *Nature* **536**, 285-291 (2016).

14. D. Pal, I. Helbig, Commentary: Pathogenic EFHC1 mutations are tolerated in healthy individuals dependent on reported ancestry. *Epilepsia* **56**, 195-196 (2015).

15. R. L. Subaran, J. M. Conte, W. C. Stewart, D. A. Greenberg, Pathogenic EFHC1 mutations are tolerated in healthy individuals dependent on reported ancestry. *Epilepsia* **56**, 188-194 (2015).

16. S. Richards, N. Aziz, S. Bale, D. Bick, S. Das, J. Gastier-Foster, W. W. Grody, M. Hegde, E. Lyon, E. Spector, K. Voelkerding, H. L. Rehm, A. L. Q. A. Committee, Standards and guidelines for the interpretation of sequence variants: a joint consensus recommendation of the American College of Medical Genetics and Genomics and the Association for Molecular Pathology. *Genet Med* **17**, 405-424 (2015).

17. S. Petrovski, Q. Wang, E. L. Heinzen, A. S. Allen, D. B. Goldstein, Genic intolerance to functional variation and the interpretation of personal genomes. *PLoS Genet* **9**, e1003709 (2013).

18. I. A. Adzhubei, S. Schmidt, L. Peshkin, V. E. Ramensky, A. Gerasimova, P. Bork, A. S. Kondrashov, S. R. Sunyaev, A method and server for predicting damaging missense mutations. *Nat Methods* **7**, 248-249 (2010).

19. P. C. Ng, S. Henikoff, Predicting deleterious amino acid substitutions. *Genome Res* **11**, 863-874 (2001).
20. R. S. Moller, H. A. Dahl, I. Helbig, The contribution of next generation sequencing to epilepsy genetics. *Expert Rev Mol Diagn* **15**, 1531-1538 (2015).

21. C. T. Myers, H. C. Mefford, Advancing epilepsy genetics in the genomic era. *Genome Med* **7**, 91 (2015).
22. A. Y. Huang, X. Xu, A. Y. Ye, Q. Wu, L. Yan, B. Zhao, X. Yang, Y. He, S. Wang, Z. Zhang, B. Gu, H. Q. Zhao, M. Wang, H. Gao, G. Gao, Z. Zhang, X. Yang, X. Wu, Y. Zhang, L. Wei, Postzygotic single-nucleotide mosaicisms in whole-genome sequences of clinically unremarkable individuals. *Cell Res* **24**, 1311-1327 (2014).

23. X. Xu, X. Yang, Q. Wu, A. Liu, X. Yang, A. Y. Ye, A. Y. Huang, J. Li, M. Wang, Z. Yu, S. Wang, Z. Zhang, X. Wu, L. Wei, Y. Zhang, Amplicon Resequencing Identified Parental Mosaicism for Approximately 10% of "de novo" SCN1A Mutations in Children with Dravet Syndrome. *Hum Mutat* **36**, 861-872 (2015).

24. A. Poduri, G. D. Evrony, X. Cai, C. A. Walsh, Somatic mutation, genomic variation, and neurological disease. *Science* **341**, 1237758 (2013).

25. C. Kananura, K. Haug, T. Sander, U. Runge, W. Gu, K. Hallmann, J. Rebstock, A. Heils, O. K. Steinlein, A splice-site mutation in GABRG2 associated with childhood absence epilepsy and febrile convulsions. *Arch Neurol* **59**, 1137-1141 (2002).

26. K. Kobow, I. Blumcke, Epigenetics in epilepsy. *Neurosci Lett*, (2017).

27. Y. Ben-Ari, Excitatory actions of gaba during development: the nature of the nurture. *Nat Rev Neurosci* **3**, 728-739 (2002).

28. E. Sernagor, F. Chabrol, G. Bony, L. Cancedda, GABAergic control of neurite outgrowth and remodeling during development and adult neurogenesis: general rules and differences in diverse systems. *Front Cell Neurosci* **4**, 11 (2010).

29. C. Chiu, C. A. Reid, H. O. Tan, P. J. Davies, F. N. Single, I. Koukoulas, S. F. Berkovic, S. S. Tan, R. Sprengel, M. V. Jones, S. Petrou, Developmental impact of a familial GABAA receptor epilepsy mutation. *Ann Neurol* **64**, 284-293 (2008).

30. K. Staley, Molecular mechanisms of epilepsy. *Nat Neurosci* **18**, 367-372 (2015).

31. D. W. Cope, G. Di Giovanni, S. J. Fyson, G. Orban, A. C. Errington, M. L. Lorincz, T. M. Gould, D. A. Carter, V. Crunelli, Enhanced tonic GABAA inhibition in typical absence epilepsy. *Nat Med* **15**, 1392-1398 (2009).

32. H. O. Tan, C. A. Reid, F. N. Single, P. J. Davies, C. Chiu, S. Murphy, A. L. Clarke, L. Dibbens, H. Krestel, J. C. Mulley, M. V. Jones, P. H. Seeburg, B. Sakmann, S. F. Berkovic, R. Sprengel, S. Petrou, Reduced cortical inhibition in a mouse model of familial childhood absence epilepsy. *Proc Natl Acad Sci U S A* **104**, 17536-17541 (2007).

33. S. L. Moshe, E. Perucca, P. Ryvlin, T. Tomson, Epilepsy: new advances. *Lancet* **385**, 884-898 (2015).

34. E. Trinka, F. Brigo, Antiepileptogenesis in humans: disappointing clinical evidence and ways to move forward. *Curr Opin Neurol* **27**, 227-235 (2014).

35. P. M. C. Epi, A roadmap for precision medicine in the epilepsies. *Lancet Neurol* **14**, 1219-1228 (2015).

36. L. A. Smith, J. F. Ullmann, H. E. Olson, C. M. Achkar, G. Truglio, M. Kelly, B. Rosen-Sheidley, A. Poduri, A Model Program for Translational Medicine in Epilepsy Genetics. *J Child Neurol* **32**, 429-436 (2017).

37. T. M. Pierson, H. Yuan, E. D. Marsh, K. Fuentes-Fajardo, D. R. Adams, T. Markello, G. Golas, D. R. Simeonov, C. Holloman, A. Tankovic, M. M. Karamchandani, J. M. Schreiber, J. C. Mullikin, D. f. t. N. C. S. P. Ph, C. J. Tifft, C. Toro, C. F. Boerkoel, S. F. Traynelis, W. A. Gahl, GRIN2A mutation and early-onset epileptic encephalopathy: personalized therapy with memantine. *Ann Clin Transl Neurol* **1**, 190-198 (2014).

38. D. Bearden, A. Strong, J. Ehnot, M. DiGiovine, D. Dlugos, E. M. Goldberg, Targeted treatment of migrating partial seizures of infancy with quinidine. *Ann Neurol* **76**, 457-461 (2014).

39. M. A. Mikati, Y. H. Jiang, M. Carboni, V. Shashi, S. Petrovski, R. Spillmann, C. J. Milligan, M. Li, A. Grefe, A. McConkie, S. Berkovic, I. Scheffer, S. Mullen, M. Bonner, S. Petrou, D. Goldstein, Quinidine in the treatment of KCNT1-positive epilepsies. *Ann Neurol* **78**, 995-999 (2015).

40. R. B. Daroff, W. G. Bradley, *Bradley's neurology in clinical practice / [edited by] Robert B. Daroff ... [et al.]*. (Elsevier/Saunders, Philadelphia, PA, ed. 6th, 2012).

41. X. Huang, C. Zhou, M. Tian, J. Q. Kang, W. Shen, K. Verdier, A. Pimenta, R. L. MacDonald, Overexpressing wild-type gamma2 subunits rescued the seizure phenotype in *Gabrg2*$^{+/Q390X}$ Dravet syndrome mice. *Epilepsia*, (2017).

42. D. M. Kullmann, S. Schorge, M. C. Walker, R. C. Wykes, Gene therapy in epilepsy-is it time for clinical trials? *Nat Rev Neurol* **10**, 300-304 (2014).

43. A. Snowball, S. Schorge, Changing channels in pain and epilepsy: Exploiting ion channel gene therapy for disorders of neuronal hyperexcitability. *FEBS Lett* **589**, 1620-1634 (2015).

44. J. Y. Tan, D. L. Sellers, B. Pham, S. H. Pun, P. J. Horner, Non-Viral Nucleic Acid Delivery Strategies to the Central Nervous System. *Front Mol Neurosci* **9**, 108 (2016).

45. J. Q. Kang, R. L. Macdonald, Making sense of nonsense GABA(A) receptor mutations associated with genetic epilepsies. *Trends Mol Med* **15**, 430-438 (2009).

46. K. M. Keeling, X. Xue, G. Gunn, D. M. Bedwell, Therapeutics based on stop codon readthrough. *Annu Rev Genomics Hum Genet* **15**, 371-394 (2014).

47. H. L. Lee, J. P. Dougherty, Pharmaceutical therapies to recode nonsense mutations in inherited diseases. *Pharmacol Ther* **136**, 227-266 (2012).

48. X. Huang, M. Tian, C. C. Hernandez, N. Hu, R. L. Macdonald, The GABRG2 nonsense mutation, Q40X, associated with Dravet syndrome activated NMD and generated a truncated subunit that was partially rescued by aminoglycoside-induced stop codon read-through. *Neurobiol Dis* **48**, 115-123 (2012).

49. L. Linde, B. Kerem, Introducing sense into nonsense in treatments of human genetic diseases. *Trends Genet* **24**, 552-563 (2008).

50. E. M. Welch, E. R. Barton, J. Zhuo, Y. Tomizawa, W. J. Friesen, P. Trifillis, S. Paushkin, M. Patel, C. R. Trotta, S. Hwang, R. G. Wilde, G. Karp, J. Takasugi, G. Chen, S. Jones, H. Ren, Y. C. Moon, D. Corson, A. A. Turpoff, J. A. Campbell, M. M. Conn, A. Khan, N. G. Almstead, J. Hedrick, A. Mollin, N. Risher, M. Weetall, S. Yeh, A. A. Branstrom, J. M. Colacino, J. Babiak, W. D. Ju, S. Hirawat, V. J. Northcutt, L. L. Miller, P. Spatrick, F. He, M. Kawana, H. Feng, A. Jacobson, S. W. Peltz, H. L. Sweeney, PTC124 targets genetic disorders caused by nonsense mutations. *Nature* **447**, 87-91 (2007).

51. E. Kerem, M. W. Konstan, K. De Boeck, F. J. Accurso, I. Sermet-Gaudelus, M. Wilschanski, J. S. Elborn, P. Melotti, I. Bronsveld, I. Fajac, A. Malfroot, D. B. Rosenbluth, P. A. Walker, S. A. McColley, C. Knoop, S. Quattrucci, E. Rietschel, P. L. Zeitlin, J. Barth, G. L. Elfring, E. M. Welch, A. Branstrom, R. J. Spiegel, S. W. Peltz, T. Ajayi, S. M. Rowe, G. Cystic Fibrosis Ataluren Study, Ataluren for the treatment of nonsense-mutation cystic fibrosis: a randomised, double-blind, placebo-controlled phase 3 trial. *Lancet Respir Med* **2**, 539-547 (2014).

52. Y. Shimizu-Motohashi, S. Miyatake, H. Komaki, S. Takeda, Y. Aoki, Recent advances in innovative therapeutic approaches for Duchenne muscular dystrophy: from discovery to clinical trials. *Am J Transl Res* **8**, 2471-2489 (2016).

53. Y. L. Fu, Y. J. Wang, T. W. Mu, Proteostasis Maintenance of Cys-Loop Receptors. *Adv Protein Chem Struct Biol* **103**, 1-23 (2016).

54. W. E. Balch, R. I. Morimoto, A. Dillin, J. W. Kelly, Adapting proteostasis for disease intervention. *Science* **319**, 916-919 (2008).

55. T. W. Mu, D. S. Ong, Y. J. Wang, W. E. Balch, J. R. Yates, 3rd, L. Segatori, J. W. Kelly, Chemical and biological approaches synergize to ameliorate protein-folding diseases. *Cell* **134**, 769-781 (2008).

56. Y. J. Wang, X. J. Di, T. W. Mu, Using pharmacological chaperones to restore proteostasis. *Pharmacol Res* **83**, 3-9 (2014).

57. X. J. Di, D. Y. Han, Y. J. Wang, M. R. Chance, T. W. Mu, SAHA enhances Proteostasis of epilepsy-associated alpha1(A322D)beta2gamma2 GABA(A) receptors. *Chem Biol* **20**, 1456-1468 (2013).

58. D. Y. Han, B. J. Guan, Y. J. Wang, M. Hatzoglou, T. W. Mu, L-type Calcium Channel Blockers Enhance Trafficking and Function of Epilepsy-associated alpha1(D219N) Subunits of GABA(A) Receptors. *ACS Chem Biol* **10**, 2135-2148 (2015).

59. N. Yokoi, Y. Fukata, D. Kase, T. Miyazaki, M. Jaegle, T. Ohkawa, N. Takahashi, H. Iwanari, Y. Mochizuki, T. Hamakubo, K. Imoto, D. Meijer, M. Watanabe, M. Fukata, Chemical corrector treatment ameliorates increased seizure susceptibility in a mouse model of familial epilepsy. *Nat Med* **21**, 19-26 (2015).

60. A. Ulloa-Aguirre, P. M. Conn, Pharmacoperones as a New Therapeutic Approach: In Vitro Identification and In vivo Validation of Bioactive Molecules. *Curr Drug Targets* **17**, 1471-1481 (2016).

61. C. M. Farinha, M. Sousa, S. Canato, A. Schmidt, I. Uliyakina, M. D. Amaral, Increased efficacy of VX-809 in different cellular systems results from an early stabilization effect of F508del-CFTR. *Pharmacol Res Perspect* **3**, e00152 (2015).

62. R. Rusconi, P. Scalmani, R. R. Cassulini, G. Giunti, A. Gambardella, S. Franceschetti, G. Annesi, E. Wanke, M. Mantegazza, Modulatory proteins can rescue a trafficking defective epileptogenic Nav1.1 Na+ channel mutant. *J Neurosci* **27**, 11037-11046 (2007).

63. S. Cestele, E. Schiavon, R. Rusconi, S. Franceschetti, M. Mantegazza, Nonfunctional NaV1.1 familial hemiplegic migraine mutant transformed into gain of function by partial rescue of folding defects. *Proc Natl Acad Sci U S A* **110**, 17546-17551 (2013).

64. G. Bechi, R. Rusconi, S. Cestele, P. Striano, S. Franceschetti, M. Mantegazza, Rescuable folding defective NaV1.1 (SCN1A) mutants in epilepsy: properties, occurrence, and novel rescuing strategy with peptides targeted to the endoplasmic reticulum. *Neurobiol Dis* **75**, 100-114 (2015).

65. R. S. Eshaq, L. D. Stahl, R. Stone, 2nd, S. S. Smith, L. C. Robinson, N. J. Leidenheimer, GABA acts as a ligand chaperone in the early secretory pathway to promote cell surface expression of GABAA receptors. *Brain Res* **1346**, 1-13 (2010).

66. P. Wang, R. S. Eshaq, C. K. Meshul, C. Moore, R. L. Hood, N. J. Leidenheimer, Neuronal gamma-aminobutyric acid (GABA) type A receptors undergo cognate ligand chaperoning in the endoplasmic reticulum by endogenous GABA. *Front Cell Neurosci* **9**, 188 (2015).

67. X. Huang, C. C. Hernandez, N. Hu, R. L. Macdonald, Three epilepsy-associated GABRG2 missense mutations at the gamma+/beta- interface disrupt GABAA receptor assembly and trafficking by similar mechanisms but to different extents. *Neurobiol Dis* **68**, 167-179 (2014).

68. J. Q. Kang, W. Shen, C. Zhou, D. Xu, R. L. Macdonald, The human epilepsy mutation *GABRG2(Q390X)* causes chronic subunit accumulation and neurodegeneration. *Nat Neurosci* **18**, 988-996 (2015).

69. D. Boison, Inhibitory RNA in epilepsy: research tools and therapeutic perspectives. *Epilepsia* **51**, 1659-1668 (2010).

70. X. Feng, P. Zhao, Y. He, Z. Zuo, Allele-specific silencing of Alzheimer's disease genes: the amyloid precursor protein genes with Swedish or London mutations. *Gene* **371**, 68-74 (2006).

71. J. B. Carroll, S. C. Warby, A. L. Southwell, C. N. Doty, S. Greenlee, N. Skotte, G. Hung, C. F. Bennett, S. M. Freier, M. R. Hayden, Potent and selective antisense oligonucleotides targeting single-nucleotide polymorphisms in the Huntington disease gene / allele-specific silencing of mutant huntingtin. *Mol Ther* **19**, 2178-2185 (2011).

72. M. Takahashi, M. Suzuki, M. Fukuoka, N. Fujikake, S. Watanabe, M. Murata, K. Wada, Y. Nagai, H. Hohjoh, Normalization of Overexpressed alpha-Synuclein Causing Parkinson's Disease By a Moderate Gene Silencing With RNA Interference. *Mol Ther Nucleic Acids* **4**, e241 (2015).

73. C. Nobrega, I. Nascimento-Ferreira, I. Onofre, D. Albuquerque, H. Hirai, N. Deglon, L. P. de Almeida, Silencing mutant ataxin-3 rescues motor deficits and neuropathology in Machado-Joseph disease transgenic mice. *PLoS One* **8**, e52396 (2013).

74. J. D. Sander, J. K. Joung, CRISPR-Cas systems for editing, regulating and targeting genomes. *Nat Biotechnol* **32**, 347-355 (2014).

75. P. Horvath, R. Barrangou, CRISPR/Cas, the immune system of bacteria and archaea. *Science* **327**, 167-170 (2010).

76. A. V. Wright, J. K. Nunez, J. A. Doudna, Biology and Applications of CRISPR Systems: Harnessing Nature's Toolbox for Genome Engineering. *Cell* **164**, 29-44 (2016).

77. H. Yin, W. Xue, S. Chen, R. L. Bogorad, E. Benedetti, M. Grompe, V. Koteliansky, P. A. Sharp, T. Jacks, D. G. Anderson, Genome editing with Cas9 in adult mice corrects a disease mutation and phenotype. *Nat Biotechnol* **32**, 551-553 (2014).

78. Q. Ding, A. Strong, K. M. Patel, S. L. Ng, B. S. Gosis, S. N. Regan, C. A. Cowan, D. J. Rader, K. Musunuru, Permanent alteration of PCSK9 with in vivo CRISPR-Cas9 genome editing. *Circ Res* **115**, 488-492 (2014).

79. L. Xu, K. H. Park, L. Zhao, J. Xu, M. El Refaey, Y. Gao, H. Zhu, J. Ma, R. Han, CRISPR-mediated Genome Editing Restores Dystrophin Expression and Function in mdx Mice. *Mol Ther* **24**, 564-569 (2016).

80. Y. Zhang, C. Long, H. Li, J. R. McAnally, K. K. Baskin, J. M. Shelton, R. Bassel-Duby, E. N. Olson, CRISPR-Cpf1 correction of muscular dystrophy mutations in human cardiomyocytes and mice. *Sci Adv* **3**, e1602814 (2017).

81. D. B. Cox, R. J. Platt, F. Zhang, Therapeutic genome editing: prospects and challenges. *Nat Med* **21**, 121-131 (2015).

82. K. Suzuki, Y. Tsunekawa, R. Hernandez-Benitez, J. Wu, J. Zhu, E. J. Kim, F. Hatanaka, M. Yamamoto, T. Araoka, Z. Li, M. Kurita, T. Hishida, M. Li, E. Aizawa, S. Guo, S. Chen, A. Goebl, R. D. Soligalla, J. Qu, T. Jiang, X. Fu, M. Jafari, C. R. Esteban, W. T. Berggren, J. Lajara, E. Nunez-Delicado, P. Guillen, J. M. Campistol, F. Matsuzaki, G. H. Liu, P. Magistretti, K. Zhang, E. M. Callaway, K. Zhang, J. C. Belmonte, *In*

vivo genome editing via CRISPR/Cas9 mediated homology-independent targeted integration. *Nature* **540**, 144-149 (2016).

83. M. Heidenreich, F. Zhang, Applications of CRISPR-Cas systems in neuroscience. *Nat Rev Neurosci* **17**, 36-44 (2016).

84. H. B. Lee, B. N. Sundberg, A. N. Sigafoos, K. J. Clark, Genome Engineering with TALE and CRISPR Systems in Neuroscience. *Front Genet* **7**, 47 (2016).

85. R. C. Wykes, G. Lignani, Gene therapy and editing: Novel potential treatments for neuronal channelopathies. *Neuropharmacology*, (2017).

86. B. P. Kleinstiver, V. Pattanayak, M. S. Prew, S. Q. Tsai, N. T. Nguyen, Z. Zheng, J. K. Joung, High-fidelity CRISPR-Cas9 nucleases with no detectable genome-wide off-target effects. *Nature* **529**, 490-495 (2016).